NATURAL PRODUCT TREATMENT OF GASTROINTESTINAL DISEASES, 2nd Edition

EDITED BY: Mingyu Sun, Hailian Shi and Hemant Goyal
PUBLISHED IN: Frontiers in Pharmacology

frontiers Research Topics

ISSN 1664-8714
ISBN 978-2-8325-3049-8
DOI 10.3389/978-2-8325-3049-8

About Frontiers

Frontiers is more than just an open-access publisher of scholarly articles: it is a pioneering approach to the world of academia, radically improving the way scholarly research is managed. The grand vision of Frontiers is a world where all people have an equal opportunity to seek, share and generate knowledge. Frontiers provides immediate and permanent online open access to all its publications, but this alone is not enough to realize our grand goals.

Frontiers Journal Series

The Frontiers Journal Series is a multi-tier and interdisciplinary set of open-access, online journals, promising a paradigm shift from the current review, selection and dissemination processes in academic publishing. All Frontiers journals are driven by researchers for researchers; therefore, they constitute a service to the scholarly community. At the same time, the Frontiers Journal Series operates on a revolutionary invention, the tiered publishing system, initially addressing specific communities of scholars, and gradually climbing up to broader public understanding, thus serving the interests of the lay society, too.

Dedication to Quality

Each Frontiers article is a landmark of the highest quality, thanks to genuinely collaborative interactions between authors and review editors, who include some of the world's best academicians. Research must be certified by peers before entering a stream of knowledge that may eventually reach the public - and shape society; therefore, Frontiers only applies the most rigorous and unbiased reviews.
Frontiers revolutionizes research publishing by freely delivering the most outstanding research, evaluated with no bias from both the academic and social point of view. By applying the most advanced information technologies, Frontiers is catapulting scholarly publishing into a new generation.

What are Frontiers Research Topics?

Frontiers Research Topics are very popular trademarks of the Frontiers Journals Series: they are collections of at least ten articles, all centered on a particular subject. With their unique mix of varied contributions from Original Research to Review Articles, Frontiers Research Topics unify the most influential researchers, the latest key findings and historical advances in a hot research area! Find out more on how to host your own Frontiers Research Topic or contribute to one as an author by contacting the Frontiers Editorial Office: frontiersin.org/about/contact

NATURAL PRODUCT TREATMENT OF GASTROINTESTINAL DISEASES, 2nd Edition

Topic Editors:
Mingyu Sun, Shanghai University of Traditional Chinese Medicine, China
Hailian Shi, Shanghai University of Traditional Chinese Medicine, China
Hemant Goyal, University of Texas Health Science Center at Houston, United States

Publisher's note: This is a 2nd edition due to an article retraction.

Citation: Sun, M., Shi, H., Goyal, H., eds. (2023). Natural Product Treatment of Gastrointestinal Diseases, 2nd Edition. Lausanne: Frontiers Media SA.
doi: 10.3389/978-2-8325-3049-8

Table of Contents

frontiers | Frontiers in Pharmacology

TYPE Editorial
PUBLISHED 09 November 2022
DOI 10.3389/fphar.2022.1074528

OPEN ACCESS

EDITED AND REVIEWED BY
Angelo A. Izzo,
University of Naples Federico II, Italy

*CORRESPONDENCE
Mingyu Sun,
mysun248@hotmail.com

SPECIALTY SECTION
This article was submitted to Gastrointestinal and Hepatic Pharmacology, a section of the journal Frontiers in Pharmacology

RECEIVED 19 October 2022
ACCEPTED 31 October 2022
PUBLISHED 09 November 2022

CITATION
Sun M, Shi H and Goyal H (2022), Editorial: Natural product treatment of gastrointestinal diseases.
Front. Pharmacol. 13:1074528.
doi: 10.3389/fphar.2022.1074528

Editorial: Natural product treatment of gastrointestinal diseases

Mingyu Sun[1]*, Hailian Shi[2] and Hemant Goyal[3]

[1]Institute of Liver Diseases, Shuguang Hospital Affiliated to Shanghai University of Traditional Chinese Medicine, Shanghai, China, [2]Shanghai University of Traditional Chinese Medicine, Shanghai, China, [3]University of Texas Health Science Center at Houston, Houston, TX, United States

KEYWORDS

natural product, intestinal flora, inflammation and immunity, gastrointestinal diseases, herbal formulae

Editorial on the Research Topic
Natural product treatment of gastrointestinal diseases

Gastrointestinal (GI) cancers, including esophageal, gastric, and colorectal cancers, are one of the major malignant diseases detrimental to health and account for almost 20% of all cancers worldwide. Besides their high incidence, GI cancers are related to high mortality rates, placing these malignancies among the most prominent public health issues of our time. Gastrointestinal diseases are prevalent, especially functional gastrointestinal disorders. Natural product has been used for thousands of years in the treatment of gastrointestinal diseases including cancer. To discover and develop the natural product with therapeutic selectivity and without toxicity are very important steps in the treatment of GI diseases. Because of their wide range of pharmacologic activities and low toxicity in animal models, many natural products have been used as alternative treatments for gastrointestinal diseases and cancers.

This Research Topic aimed at widening the knowledges on natural product treatment of Gastrointestinal Diseases. The articles received by the journal were carefully reviewed, thus offering a high-quality Research Topic. We summarize the main findings and perspectives detailed within each of the nine accepted articles.

Colorectal cancer (CRC) is the third most common cancer worldwide. Despite the improved knowledge on CRC heterogeneity and advances in the medical sciences, it is still urgent to cope with the challenges and side effects of common treatments for the disease. Actinobacteria are known to be prolific producers of a wide range of bioactive natural products against CRC. This review by Bahrami et al. is a holistic picture on actinobacter-derived cytotoxic compounds against CRC. This review describes the chemical structure of 232 natural products presenting anti-CRC activity with the being majority of quinones, lactones, alkaloids, peptides, and glycosides. Most of these natural products are derived from marine actinobacteria followed by terrestrial and endophytic actinobacteria, respectively. The high diversity of actinobacterial strains and their natural products

derivatives, described here provides a new perspective and direction for the production of new anti-CRC drugs and paves the way to innovation for drugs discovery in the future.

Previous researches proved the inhibitory effect of quercetin on breast cancer, ovarian cancer and gastric cancer, but the inhibitory effect of quercetin on colorectal cancer still needs to be clarified. Chen et al. proved that quercetin inhibited the tumorigenesis of CRC cells through downregulating hsa_circ_0006990. Quercetin induced the differentiation of M2-TAMs into M1-TAMs by inhibiting autophagy and then downregulated hsa_circ_0006990 in CRC cells co-cultured with M2-TAMs, finally inhibiting the proliferation and metastasis of CRC cells.

More and more research evidences have proved that gut microbiota plays a very important role both in the pathological process of gastrointestinal diseases and gastrointestinal cancers. Researchers are increasingly concerned about the role of gut bacteria in natural products to treat gastrointestinal diseases. How to regulate the intestinal flora and the advantages of the action of natural products is a growing topic of interest. Lu et al. review paper summarizes the role of gut microbiota in colorectal tumorigenesis and the mechanism by which natural products reduce tumorigenesis and improve therapeutic response.

However, gut microbiota also affected the serum metabolism of natural products. Cai et al. found that antineoplastic Fufangchangtai (FFCT) showed no significant effect on the tumor volume of colorectal tumor-bearing nude mice, but could increase the levels of $CD4^+$ and CD8+T lymphocytes. Furthermore, the tumor induced dysbiosis of gut bacteria could affect the absorption and metabolism of FFCT, evidenced by the decreased levels of Matrine, Isogingerenone B and Armillaripin in tumor-bearing mice after FFCT intervention. And, FFCT could increase abundance of Roseburia, Turicibacter and Flexispira, indicating that FFCT might improve the intestinal microenvironment by modulating gut microbiota in colorectal tumor-bearing mice.

Esophageal squamous cell carcinoma (ESCC) is one of the deadliest digestive system cancers worldwide lacking effective therapeutic strategies. Chen et al. explored that the natural product celastrol coordinatively triggered extrinsic and intrinsic apoptosis pathways to diminish the tumor growth of ESCC *in vivo* and *in vitro*, by synergistically triggering DR5-dependent extrinsic apoptosis and Noxa-dependent intrinsic apoptosis through transactivation of ATF4 in ESCC cells. Furthermore, FoxO3a-Bim pathway was also involved in the intrinsic apoptosis of ESCC cells induced by celastrol. The findings highlighted celastrol as a promising apoptosis-inducing therapeutic strategy for ESCC.

Irritable bowel syndrome (IBS) is characterized by recurrent abdominal pain associated with disordered defecation. Jiang et al. revealed Wenshen-Jianpi prescription can alleviate the visceral hypersensitivity in IBS-D model rats, mainly accompanied by down regulating the expression of TNF-α, p-MEK1/2, p-ERK1 and p-ERK2 in the colon tissue.

Inflammatory bowel diseases (IBDs) are systemic diseases and not only impair the gut functions but also influence extraintestinal organs, such as the liver, kidney, and eyes. Yu et al. contributed their research paper that Cao-Xiang-Wei-Kang capsule alleviates the progression of murine experimental colitis induced by dextran sodium sulfate (DSS) by suppressing inflammation, promoting mucosal healing, and re-establishing a microbiome profile that favors re-epithelization.

Pterostilbene (PTE) is a natural polyphenol compound that has been proven to improve intestinal inflammation, but its laxative effect on slow transit constipation (STC) has never been studied. Yao et al. presented a research paper that PTE might alleviate constipation by inhibiting oxidative stress-induced apoptosis of interstitial Cajal cells through modulating PI3K/AKT/Nrf2 signaling pathway. PTE also attenuated the dysbiosis of gut microbiota in STC mice.

Acute pancreatitis (AP) is one kind of inflammatory diseases of the pancreas with early local symptoms and followed by systemic inflammatory response. Progression of AP into severe acute pancreatitis (SAP) usually leads to a life-threatening condition with multiple organ dysfunction, particularly acute lung injury (ALI), which is the cause of most deaths during the early phase of AP. A study by Wu et al. explored that Emodin has a therapeutic effect on AP-associated lung injury, which is at least partially due to the inhibition of NLRP3/Caspase1/GSDMD-mediated AMs pyroptosis signaling ways.

Author contributions

All authors listed have made a substantial, direct, and intellectual contribution to the work and approved it for publication.

Conflict of interest

The authors declare that the research was conducted in the absence of any commercial or financial relationships that could be construed as a potential conflict of interest.

Publisher's note

frontiers | Frontiers in Pharmacology

ORIGINAL RESEARCH
published: 16 May 2022
doi: 10.3389/fphar.2022.913420

Based on Network Pharmacology and Gut Microbiota Analysis to Investigate the Mechanism of the Laxative Effect of Pterostilbene on Loperamide-Induced Slow Transit Constipation in Mice

Zhiwei Yao[†], *Siqi Fu*[†], *Bingbing Ren, Lushun Ma and Daqing Sun* *

Department of Pediatric Surgery, Tianjin Medical University General Hospital, Tianjin, China

OPEN ACCESS

Edited by:
Hailian Shi,
Shanghai University of Traditional Chinese Medicine, China

Reviewed by:
Wen-Xie Xu,
Shanghai Jiao Tong University, China
Qiyi Chen,
Tongji University, China

***Correspondence:**
Daqing Sun
sdqchris2019@tmu.edu.cn

[†]*These authors have contributed equally to this work and share first authorship*

Specialty section:
This article was submitted to Gastrointestinal and Hepatic Pharmacology, a section of the journal Frontiers in Pharmacology

Received: *05 April 2022*
Accepted: *02 May 2022*
Published: *16 May 2022*

Citation:
Yao Z, Fu S, Ren B, Ma L and Sun D (2022) Based on Network Pharmacology and Gut Microbiota Analysis to Investigate the Mechanism of the Laxative Effect of Pterostilbene on Loperamide-Induced Slow Transit Constipation in Mice. Front. Pharmacol. 13:913420. doi: 10.3389/fphar.2022.913420

Background: Pterostilbene (PTE) is a natural polyphenol compound that has been proven to improve intestinal inflammation, but its laxative effect on slow transit constipation (STC) has never been studied. This study aims to investigate the laxative effect of PTE on loperamide (LOP)-induced STC mice and its influence on intestinal microbes through a combination of network pharmacological analysis and experimental verification.

Material and Methods: PTE was used to treat LOP-exposed mice, and the laxative effect of PTE was evaluated by the total intestinal transit time and stool parameters. The apoptosis of Cajal interstitial cells (ICCs) was detected by immunofluorescence. The mechanism of PTE's laxative effect was predicted by network pharmacology analysis. We used western blot technology to verify the predicted hub genes and pathways. Malondialdehyde (MDA) and GSH-Px were tested to reflect oxidative stress levels and the changes of gut microbiota were detected by 16S rDNA high-throughput sequencing.

Results: PTE treatment could significantly improve the intestinal motility disorder caused by LOP. Apoptosis of ICCs increased in the STC group, but decreased significantly in the PTE intervention group. Through network pharmacological analysis, PTE might reduce the apoptosis of ICCs by enhancing PI3K/AKT and Nrf2/HO-1 signaling, and improve constipation caused by LOP. In colon tissues, PTE improved the Nrf2/HO-1 pathway and upregulated the phosphorylation of AKT. The level of MDA increased and GSH-Px decreased in the STC group, while the level of oxidative stress was significantly reduced in the PTE treatment groups. PTE also promoted the secretion of intestinal hormone and restored the microbial diversity caused by LOP.

Conclusion: Pterostilbene ameliorated the intestinal motility disorder induced by LOP, this effect might be achieved by inhibiting oxidative stress-induced apoptosis of ICCs through the PI3K/AKT/Nrf2 signaling pathway.

Keywords: pterostilbene, slow transit constipation, network pharmacology, gut microbiota, oxidative stress, interstitial cells of cajal

1 INTRODUCTION

Functional constipation (FC) is a common gastrointestinal dysfunction symptom around the world. In recent years, the incidence has been rising rapidly (Shin et al., 2019) (van Mill et al., 2019). Epidemiological data showed that the percentage of FC in adults is as high as 15.3% (Barberio et al., 2021). Slow transit constipation (STC), which accounts for about 55% of FC (Tanner et al., 2021), It is main clinical features are slowing of intestinal motility and delayed passage of intestinal contents. Senna and other laxatives often appear in the treatment of STC. However, long-term administration of these agents does not provide satisfactory efficacy and severe adverse effects including drug dependence and melanosis are noted in patients (Bassotti and Blandizzi, 2014) (Lim et al., 2019). Therefore, it is necessary to explore safe and effective alternative treatment options.

Interstitial cells of Cajal (ICCs) are pacemaker cells for many rhythmic movements in the gastrointestinal tract (Horváth et al., 2006). The number of ICCs in the colon of STC patients is significantly reduced (He et al., 2000) (Serra et al., 2020), and ICCs defects have also been consistently found in animal models of STC (He et al., 2000) (Zhu et al., 2016). Further research found that the network of ICCs also undergoes periodic changes under normal physiological conditions (Gibbons et al., 2009). Apoptosis can lead to loss of ICCs, and was observed in a large proportion of STC patient colons (Zheng et al., 2021) (Faussone-Pellegrini, 2005). Therefore, maintenance of ICCs function has been regarded as an important therapeutic method for STC.

Elevated levels of oxidative stress have been found in both constipated patients and animal models (Wang et al., 2004) (Lee et al., 2020). At the same time, some studies have found that the increased apoptosis of ICCs in diabetic gastroparesis mice is related to oxidative stress (Tian et al., 2018) (Wang et al., 2021c). However, the relationship between ICCs apoptosis and oxidative stress in STC animal models has not been reported.

Pterostilbene (PTE) is a natural derivative of resveratrol, mainly derived from berries and grapes (chemical structure of PTE was shown in **Figure 1B**). It has been found to have a protective effect in colitis caused by high-fat diet and dextran sulfate sodium (Chen et al., 2021) (Fan-Jiang et al., 2021). Previous studies also found that polyphenol compounds had the effect of promoting the motility of the gut (Koh et al., 2021). In addition, PTE has also been shown to improve the disordered intestinal microflora of rats fed high-fat (Milton-Laskibar et al., 2021). However, the laxative effect and the influence of the intestinal microflora of PTE on STC mice have not been studied, and whether the apoptosis of ICCs is involved in the effect of PTE on colonic transit is also unclear.

The aim of this study was to verify the laxative effect of PTE in loperamide (LOP)-induced STC model mice and whether these therapeutic effects might be mediated by improving oxidative stress, apoptosis of ICCs and intestinal flora. We predicted the potential targets and mechanisms of PTE in the treatment of STC

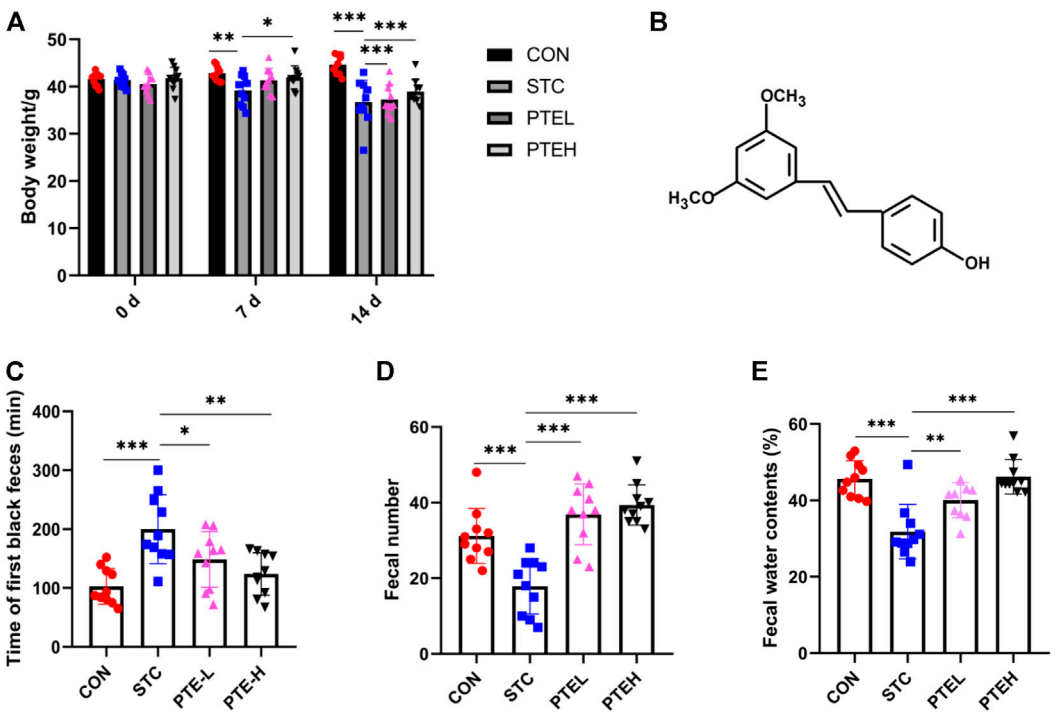

FIGURE 1 | PTE alleviated LOP-induced constipation symptoms. **(A)** Body weight. **(B)** Chemical structure of PTE. Fecal parameters: **(C)** The whole gut transit time. **(D)** Fecal number. **(E)** Water contents. (n = 10). *p < 0.05, **p < 0.01, ***p < 0.001. (LOP, loperamide; STC, slow transit constipation; PTE, pterostilbene).

by network analysis, and validated the predicted results by *in vivo* experiments.

2 MATERIAL AND METHODS

2.1 Animals

Forty Kunming male mice (Specific Pathogen Free), 8 weeks old, weighing 41.32 ± 1.837 g, were purchased from Vital River Co., Ltd (Beijing). All animals were raised in the experimental animal center of Tianjin Medical University (constant temperature 25°C, 12 h light/dark cycle). All experimental protocols involving animals were approved by the Animal Ethics Committee of Tianjin Medical University.

2.2 Experiment Grouping and Model Preparation

Before the experiment, mice were randomly divided into four groups: CON (control group), STC (STC model group), PTEL (PTE low-dose group), and PTEH (PTE high-dose group). n = 10. Except for the CON group, the other groups were given 5 mg/kg LOP (34,014, Sigma) by gavage to replicate the mice constipation model for 7 days. The LOP suspension was prepared with physiological saline, and the administration volume was 10 ml/kg, twice daily. The CON group was given normal saline by intragastric administration with the same volume, twice a day, for 7 days. Starting from day 8, the dose of LOP was doubled to 10 mg/kg, and PTE (Macklin Biochemical Co., Ltd, P815984, Shanghai) was given 1 h after administration of LOP. PTE was prepared as a suspension with 0.5% carboxymethylcellulose sodium (CMC-Na) (C299502, Aladdin, Shanghai); the CON group and STC group were given 0.5% CMC-Na by gavage, 10 ml/kg, once a day, for 7 days. PTE groups were administered intragastrically in the low-dose group (30 mg/kg) and the high-dose group (60 mg/kg) for 7 days (**Supplementary Figure S1**).

2.3 Determination of Defecation Parameters

During the period from modeling to sampling, the mental state, fur, eating situation, stool quality, and quantity of each group of mice were observed every day. After the last dose, the mice in each group were fasted with water for 12 h and were fed with 0.2 ml India ink (S30881, Yuanye Bio-Technology, Shanghai, China). Then, all animals returned to normal food intake and were reared in a single cage. From the end of the gavage ink, recorded the time (min) to discharge the first black stool, collected the feces within 6 h, recorded the number of pellets, and weighed (wet weight A). The fecal pellets were placed in an oven at 70°C and continuously dried for 24 h and weighed (dry weight B), and the moisture content of the feces was calculated = (A-B)/A × 100%.

2.4 Network Pharmacology Analysis

2.4.1 Screening of Pterostilbene Treatment Slow Transit Constipation Targets

PharmMapper, STITCH, SwissTargetPrediction and Chembl database were used to predict the potential target genes of PTE (Yang et al., 2020). After merging the above four database targets, the PTE-related targets was uniformly transformed by the UniPort database (Zhang Y. et al., 2021). "slow transit constipation" was used as the key words in the PharmGkb, OMIM, GeneCards, Drugbank, and TTD databases to search for STC-related targets (Yu et al., 2021). The detailed information about databases and platforms was shown in **Supplementary Table S1**.

PTE and STC disease target data were imported together to R software (3.6.3) and got the intersection of the drug and disease targets, the intersection genes were the potential target of PTE to treat STC, then output the venn diagram. According to the article of Liu (Zhang W. et al., 2021), the intersection genes were imported into the STRING database online to build a PPI network, set the confidence score:≥0.9, after the protein interaction analysis, the resulting file was exported by Cytoscape software (CytoNCA plug-in), and the core target map of the protein interaction network was made (Zhang W. et al., 2021).

2.4.2 GO Function and Kyoto Encyclopedia of Genes and Genomes Pathway Enrichment Analysis

The common targets of disease and drug were calculated by ClusterProfiler package in R software (v3.6.3) to execute GO (gene ontology-biological process) function and KEGG (Kyoto encyclopedia of genes and genomes) pathway enrichment analysis, and $p < 0.05$ for target Gene screening, analysis of the biological processes and main signal pathways of PTE's pharmacological effects (Li XM. et al., 2021).

2.5 Detection of Gut Hormones and Oxidative Stress-Related Indicators

After the last experiment, all mice were anesthetized and then blood was taken from the eyeballs, the upper serum was centrifuged (3,500 r/min, 10 min) to determine the level of motilin (MTL) and gastrin (Gas) by ELISA kit (Mlbio, Shanghai, China) and the levels of malondialdehyde (MDA) and GSH-Px were detected by available kits (A001-3 and A003-1, Nanjing Jiancheng, China).

2.6 Immunofluorescence

Immunofluorescence staining was performed as previously reported (Wang et al., 2021c). For Immunofluorescence staining, colon tissue paraffin sections (5 μm) were used. The slides were deparaffinized in xylene, subsequently hydrated in different concentrations of ethanol and antigen unmasked using sodium citrate buffer for 20 min. The samples were then treated with 0.2% Triton-X (Sigma) for 30 min at room temperature. Next, the sections were incubated with anti-c-kit antibody (R & D, AF1356, 1:200) overnight at 4°C. After washing three times in PBS, the slides were incubated with secondary antibodies (1:200) for 1 h at 37°C. In order to detect the apoptosis of ICCs, the TUNEL kit (Roche, Germany) was used to continue to incubate the slices at 37°C for 10 min; then the apoptotic ICCs were observed under a fluorescence microscope (Olympus, BX53).

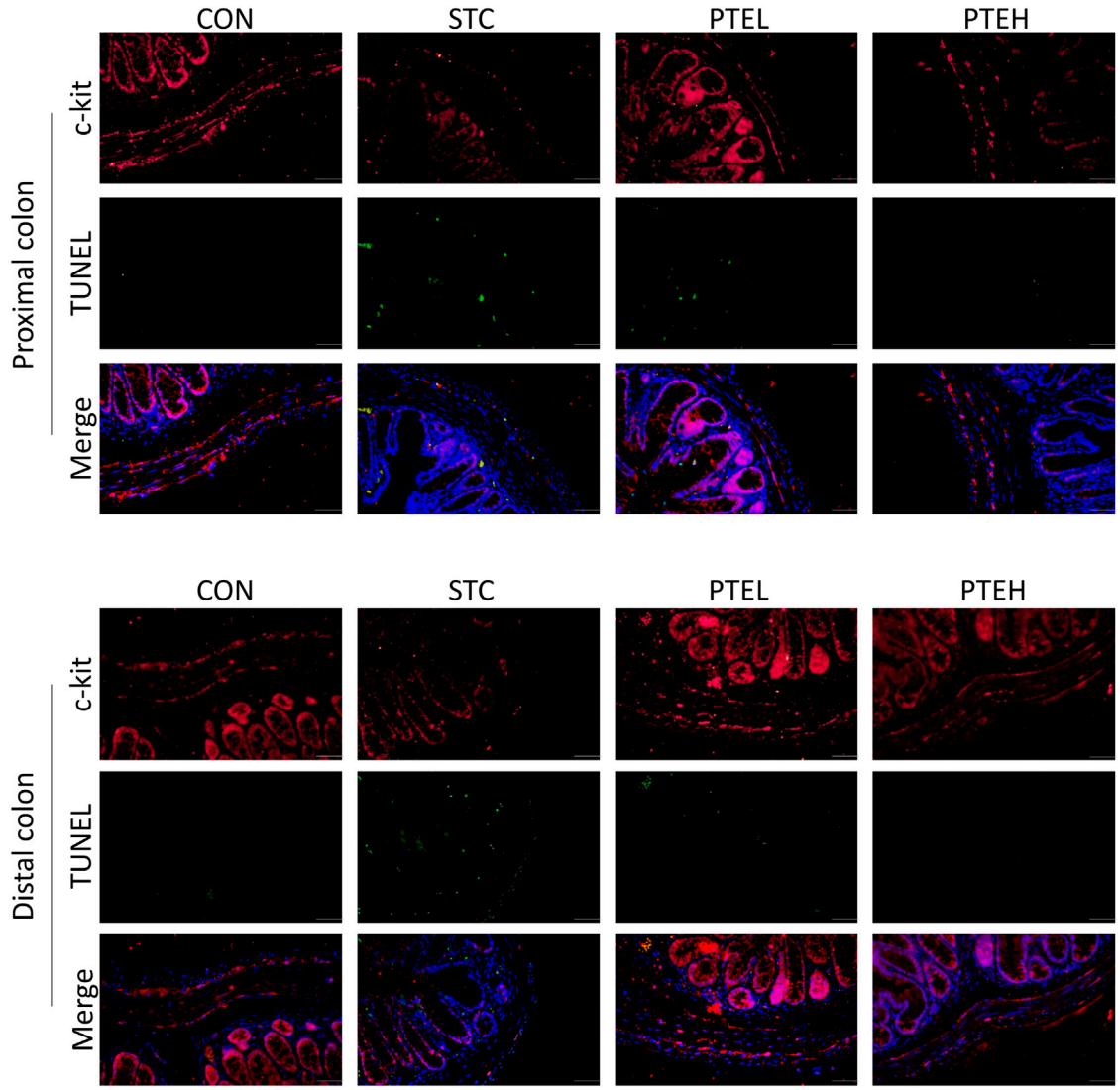

FIGURE 2 | Images of cross-sections showing the alteration of the apoptosis of interstitial cells of Cajal (ICCs) in the colon. c-kit positive ICCs were stained in red and TUNEL positive ICCs were stained in green, cell nuclei were labeled with DAPI (blue). (n = 3 in each group). Scale bar = 100 μm.

2.7 Western Blot Analysis

The total protein of colon tissues was extracted and quantified by BCA kit (Biotechnology) as described previously (Zhu et al., 2017), the protein was separated with 10% SDS-PAGE gel. After blocking the PVDF membrane with the skimmed milk powder, added the primary antibody c-kit (#3074, CST), SCF antibody (bs-0545R, BIOSS), p-AKT (#4060; CST), AKT (#9272; CST), Nrf2 (bs-1074R, BIOSS), HO-1 (bs-23397R, BIOSS), β-actin antibody (#4970, CST), GAPDH (1:5,000; Sangon Biotech, Shanghai, China) overnight at 4°C. After that, the secondary antibody was added to incubate for 1 h. Finally, all membranes were visualized by Tanon 5,200 automatic chemiluminescence imaging analysis system. Image J software (ImageJ, 1.52v) was used to analyze the gray value of the band.

2.8 16S rDNA Extraction and Sequencing

All DNA samples are extracted with reference to Young's method (Yang et al., 2021). The total DNA was measured in the PCR by LC-Bio Co., Ltd (Hang Zhou, China. The primers were shown in **Supplementary Table S2**). All samples were sequenced on an Illumina NovaSeq platform provided by LC-Bio.

2.9 Statistical Processing

All data analysis and processing used GraphPad Prism 8.0.1 software and represented the mean ± SD. To compare the difference between the groups, one-way ANOVA and Student's t-test were used. $p < 0.05$ was accepted as statistically significant.

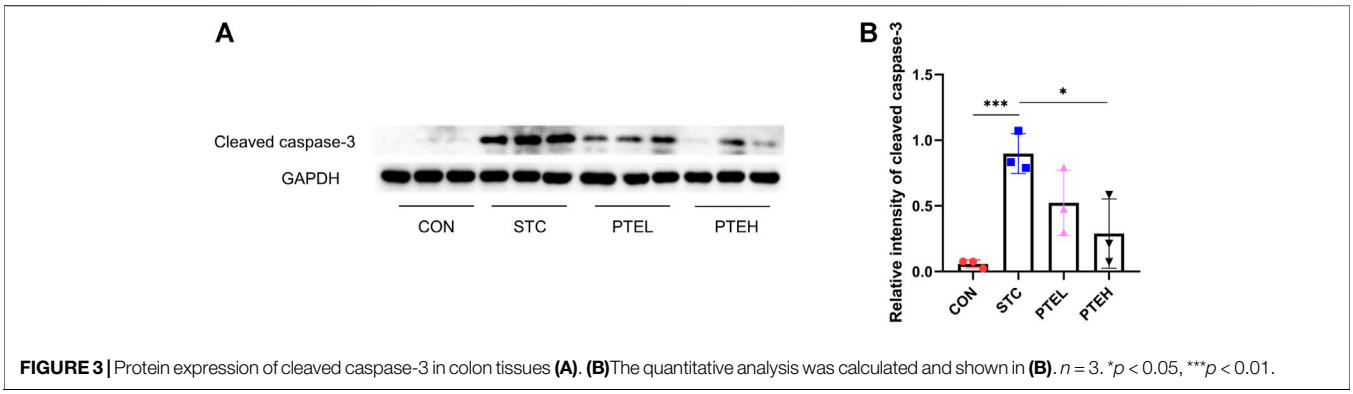

FIGURE 3 | Protein expression of cleaved caspase-3 in colon tissues **(A)**. **(B)**The quantitative analysis was calculated and shown in **(B)**. $n = 3$. $^{*}p < 0.05$, $^{***}p < 0.01$.

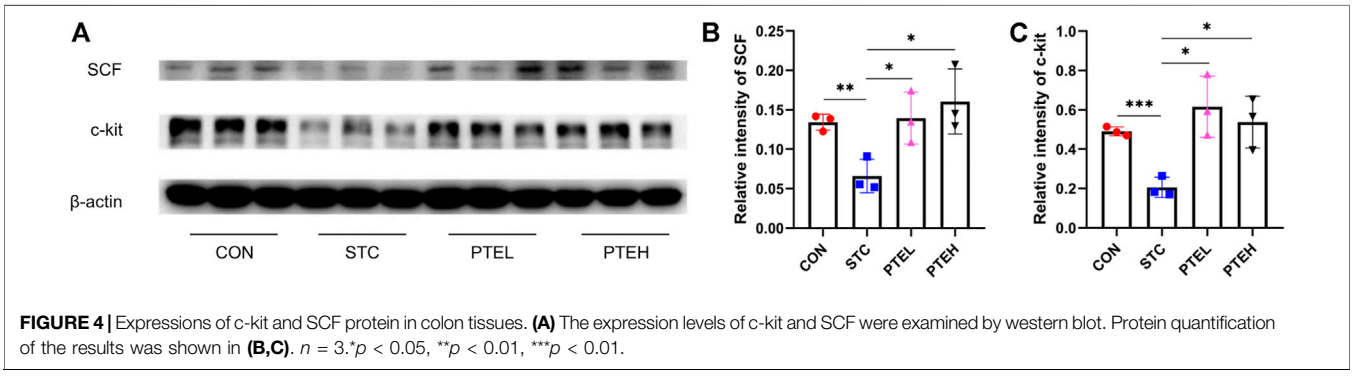

FIGURE 4 | Expressions of c-kit and SCF protein in colon tissues. **(A)** The expression levels of c-kit and SCF were examined by western blot. Protein quantification of the results was shown in **(B,C)**. $n = 3$.$^{*}p < 0.05$, $^{**}p < 0.01$, $^{***}p < 0.01$.

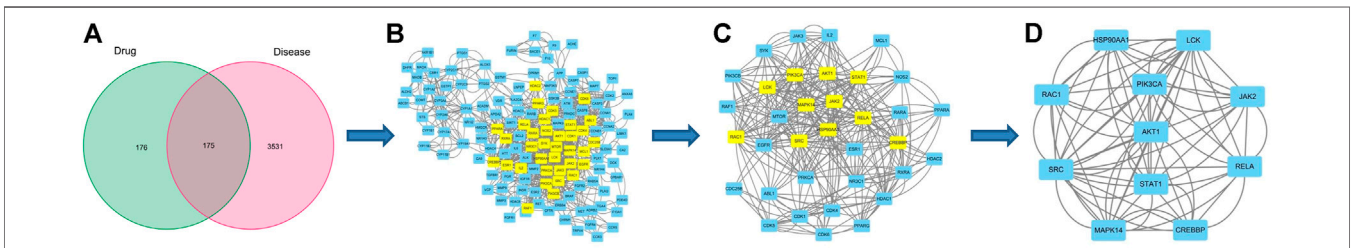

FIGURE 5 | Identification of PTE-STC target genes and construction of the PPI network. **(A)** PTE target gene prediction for STC treatment. The 175 genes were considered the molecular targets of PTE against STC. **(B)** The PPI network of PTE-STC targets constructed by Cytoscape. **(C)** The PPI network of significant proteins extracted from **(B)**; **(D)** The PPI network of core targets for STC treatment obteined from **(C)**.

3 RESULTS

3.1 Pterostilbene Alleviated Loperamide-Induced Constipation Symptoms

No mouse died during the entire experiment. Since the 7th day, we found the weight in the STC group was slightly lower than normal ($p < 0.01$), but the PTE treatment group was relieved ($p < 0.05$) (**Figure 1A**). According to previous studies, the time of the first black stool was used to access the whole gut transit ability (Li T. et al., 2021). Compared with the CON group, the whole gut transit time was longer in the STC group ($p < 0.05$), the number of defecation particles and the water content was reduced ($p < 0.05$); In addition, the above indicators after PTE administration could be restored to the level of the CON group ($p < 0.05$) (**Figures 1C–E**). These results suggested that PTE had a pronounced laxative effect on LOP-induced STC mice.

3.2 Pterostilbene Reduced Interstitial Cells Apoptosis and Activated the Stem Cell Factor/C-Kit Pathway

TUNEL and cleaved caspase three are often used as markers of apoptosis (Wang D. et al., 2021). Therefore, TUNEL and the expressions of cleaved caspase three in each group were detected by immunofluorescence staining and western blot, respectively. There were a large number of TUNEL + cells and

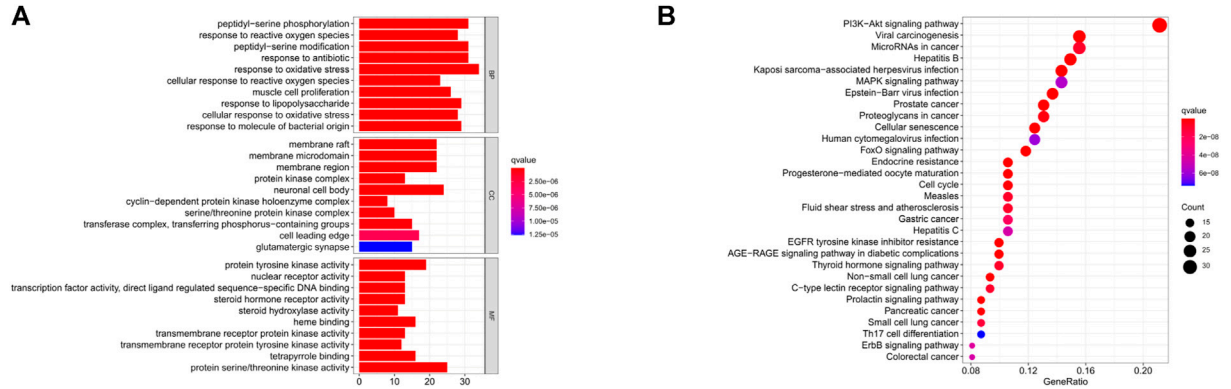

FIGURE 6 | GO functional enrichment analysis **(A)** and KEGG enrichment analysis of the PTE-STC intersection target gene **(B)**.

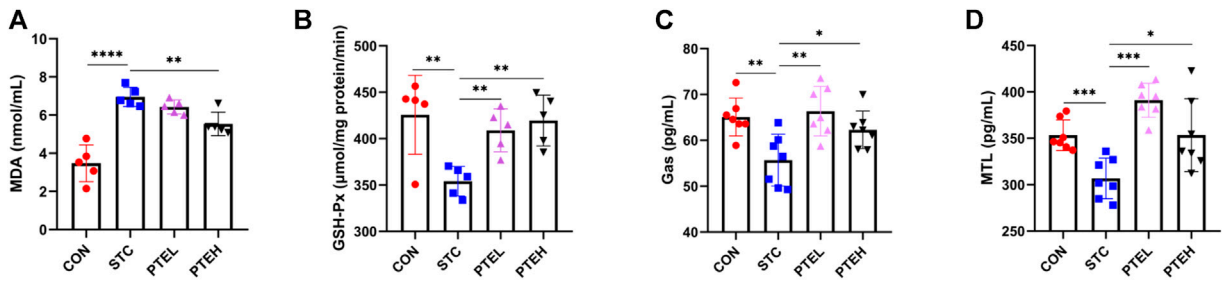

FIGURE 7 | Effects of PTE on oxidative stress-related parameters and gastrointestinal hormones in serum of STC mice. **(A,B)** The malonaldehyde (MDA) level and GSH-Px were elevated in each group (n = 5). **(C,D)** Gas and MTL levels in serum (n = 7). $^{*}p < 0.05$, $^{**}p < 0.01$, $^{***}p < 0.001$ (Gas, Gastrin; MTL, Motilin).

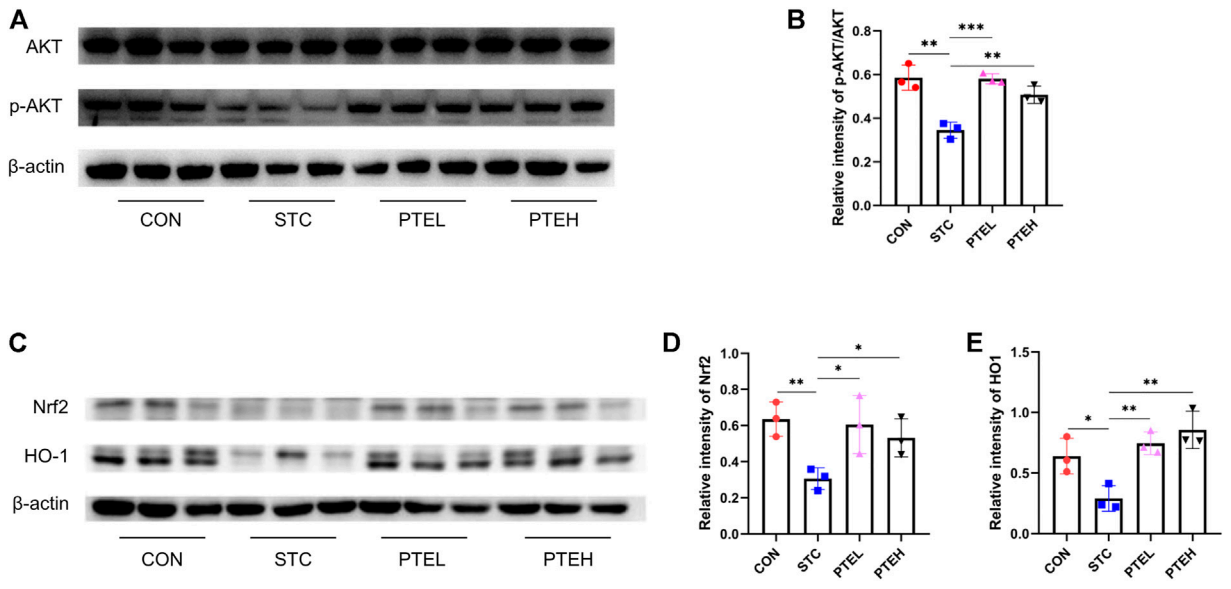

FIGURE 8 | Protein expressions of Nrf2, HO-1, p-AKT, and AKT in the colon. **(A,C)** Expression levels of p-AKT, AKT, and Nrf2/HO-1 protein in the colon and the quantification analysis was calculated in **(B,D–E)**. n = 3. $^{*}p < 0.05$, $^{**}p < 0.01$, $^{***}p < 0.001$.

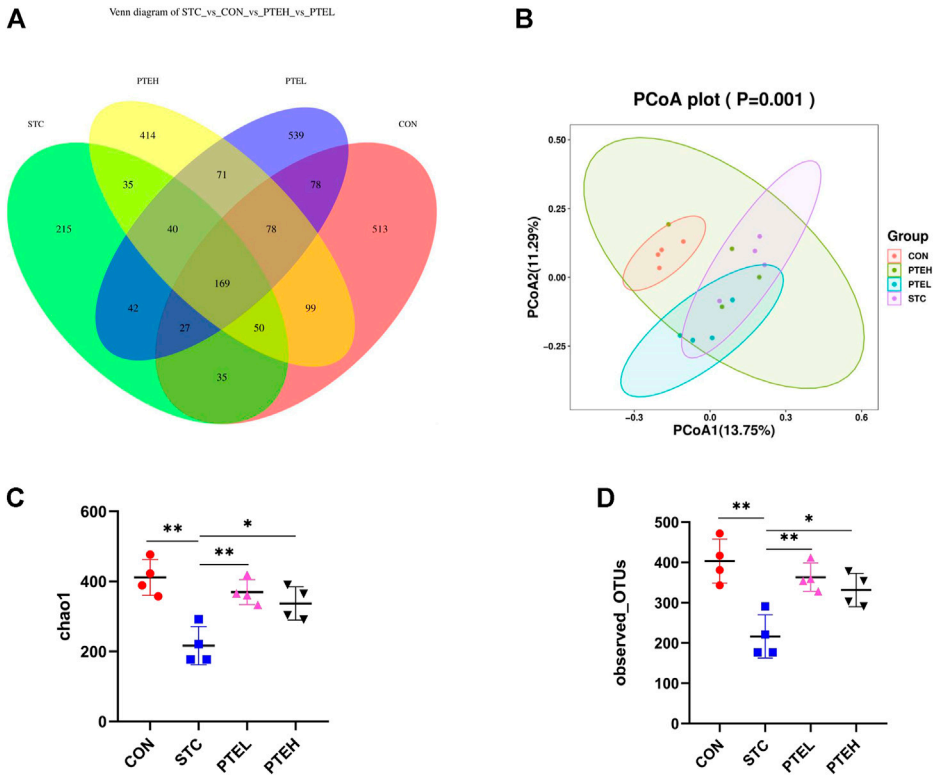

FIGURE 9 | Regulation of gut microbiota structure by PTE. **(A)** The Venn diagram of different mice microflora; **(B)** The beta diversity of microbiomes in different samples, which were based on unweighted UniFrac metrics; **(C,D)** Alpha diversity indexes: **(C)** chao1 index, **(D)** Observed OTUs. ($n = 4$). *$p < 0.05$, **$p < 0.01$. (OTUs, operational taxonomic units; PCoA, principal co-ordinates analysis).

a small amount of c-kit + cells in both the distal and proximal colon tissues of the STC group. However, the PTE treated groups showed significantly lower numbers of TUNEL-positive cells and more c-kit + cells than the STC group (**Figure 2**). Furthermore, the western blot results showed that cleaved caspase-3 protein expression was significantly higher in the STC group than in the PTE treated groups. In summary, these results show that PTE reduced LOP-induced slow bowel movements by inhibiting ICCs apoptosis (**Figure 3**). Western blot results also showed that the expression of c-kit and SCF in the colon tissue of the STC group was significantly lower than that in the CON group ($p < 0.01$); PTE treatment could restore the expression levels of the above proteins ($p < 0.05$) (**Figure 4**).

3.3 Pterostilbene Targets the Anti-oxidative Stress Effect

We found 351 potential targets for PTE and 3706 STC disease target genes (**Figure 5A**); As shown in **Figure 5A**, the 175 target genes were the intersection of STC and PTE targets. Next, we constructed a PPI network of possible target genes involved in the protective effect of PTE against STC through STRING and the network was further visualized with Cytoscape software (**Figure 5B**). Among these potential protein targets, we found that hub genes, such as PIK3CA, SRC, AKT1, CREBBP, RELA, HSP90AA1, RAC1, LCK, JAK2, STAT1, and MAPK14 might play a critical role in the biological activity in the PTE treatment process (**Figures 5C,D**).

In order to further clarify the potential mechanism of the influence of PTE on STC, a total of 175 candidate targets were analyzed by GO and KEGG pathway enrichment analysis. GO analysis indicated that PTE might improve the intestinal motility damage induced by LOP through response to reactive oxygen species and oxidative stress (**Figure 6A**). KEGG pathway enrichment analysis was shown in **Figure 6B**, which mainly involved cell proliferation-related pathways, such as PI3K/AKT signaling pathway.

The results of GO and KEGG analysis indicated that the underlying molecular mechanisms of PTE against STC were closely related to oxidative stress and PI3K/AKT signaling. Likewise, PPI analysis revealed that core target proteins of PTE were involved in the PI3K/AKT pathway, such as PIK3CA and AKT1. More and more studies have shown that PI3K/AKT exerts anti-oxidative stress effects by regulating Nrf2 (Fu et al., 2021) (Liu et al., 2022). Meanwhile, the PI3K/AKT signaling pathway also plays an important role in cell apoptosis and proliferation (Wang et al., 2018). Briefly, it was suggested that PTE might exert anti-STC effects by inhibiting oxidative stress and reducing ICCs

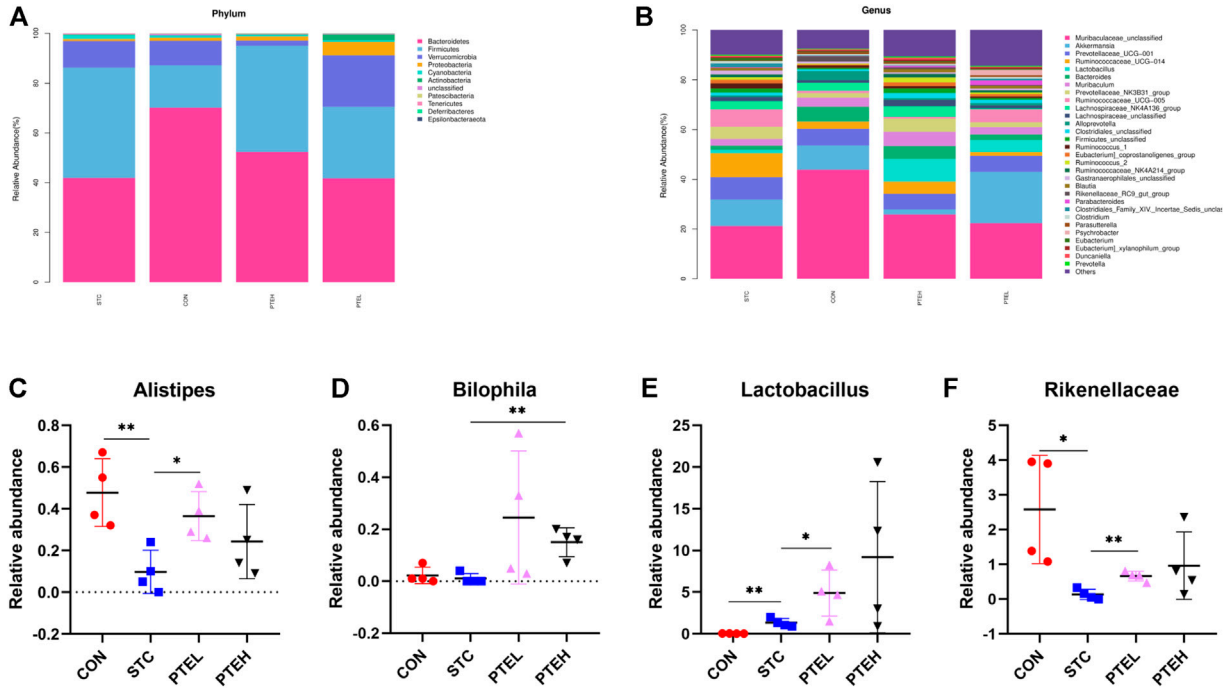

FIGURE 10 | The taxonomic composition of gut microbiota in mouse feces between different groups. **(A,B)** Relative abundance of microbial communities. **(C–F)** Relative abundance of main genus in different groups: **(C)** Alipipes; **(D)** Bilophila; **(E)** Lactobacillus; **(F)** Rikenellaceae. (n = 4). *p < 0.05, **p < 0.01.

apoptosis through the PI3K/AKT pathway. To test this hypothesis, *in vivo* experiments were performed to validate network analysis predictions.

Next, we measured the levels of oxidative stress marker MDA and GSH-Px, and found that LOP treatment increased oxidative product MDA in the constipated mice and depletion of antioxidant enzyme activities such as GSH-Px. To the opposite, PTE induced a significant decrease in the activity of MDA and effectively increased the activity of GSH-Px (**Figures 7A,B**). This indicated that LOP-induced STC mice have obvious oxidative stress, and PTE might play a laxative effect by reducing the level of oxidative stress.

3.4 Effects of Pterostilbene on the Expression of PI3K/AKT and Nrf2/HO-1 Pathways

To further verify the downstream mechanism of PTE in STC mice, the expressions of PI3K/AKT and Nrf2/HO-1 were detected by western blot. The results showed that LOP reduced the phosphorylation of AKT and attenuated Nrf2/HO-1 expression. Compared with the STC group, PTE treatment could significantly increase p-AKT expression (**Figures 8A,B**). With the same trend as p-AKT, the protein expression of Nrf2/HO-1 was significantly increased in PTE treated groups. These results were consistent with predictions from network pharmacology (**Figures 8C–E**).

3.5 Pterostilbene Elevated the Levels of the Intestinal Hormone in Serum

Compared with the control group, the serum levels of motilin (MTL) and gastrin (Gas) in the STC group were significantly reduced ($p < 0.01$); However, the levels of the hormone in the PTE groups significantly increased ($p < 0.05$), indicating that PTE could alleviate constipation by regulating the level of gastrointestinal hormones (**Figures 7C,D**).

3.6 Pterostilbene Altered Diversity of Gut Microbiota in Loperamide-Induced Slow Transit Constipation Mice

Based on the operational taxonomic units (OTUs) number, the results of the Venn diagram showed that a total of 2,405 OTUs were observed. The overlapping parts of the four groups represented the common OTUs between the groups, a total of 169 OUTs (**Figure 9A**).

In ecology, Alpha diversity was usually used to measure the diversity of flora within an individual (Ren et al., 2017). The fecal microbial community chao1 and observed OTUs index of mice in the STC group were lower than those in the CON group. After PTE treatment, the microbial diversity of STC mice was restored ($p < 0.05$) (**Figures 9C,D**). By analyzing the Beta diversity index to compare the similarity of microbial composition between groups, principal coordinate analysis (PCoA) was used. Compared with the CON group, the species composition in the STC model group was quite different, the composition of

that restored in the PTE groups. The results showed that PTE could improve the diversity of intestinal microflora in mice with STC (**Figure 9B**).

Figure 10A showed a columnar cluster diagram of the species composition classification of each group at the phylum level. Comparing the changes in abundance between the groups, it was found that due to the intervention of LOP, the relative abundance of Firmicutes in the STC group was higher than that in the CON group, while the relative abundance of Bacteroidetes was significantly reduced; Compared with the CON group, the relative abundance of Firmicutes in the PTE low-dose group and the PTE high-dose group increased to varying degrees, and the relative abundance of Bacteroidetes decreased, but the difference was not significant ($p > 0.05$).

At the genus level, we observed that Muribaculaceae, Akkermansia, and Prevotellaceae were the dominant bacteria (**Figure 10B**). Compared with the CON group, PTE intervention could increase the abundance of Lactobacillus and Bilophila ($p < 0.05$) (**Figures 10D,E**). Alipipes and Rikenellaceae was found higher abundance in the STC group than that in the CON group, but restored after PTE treatment (**Figures 10C,F**). These results indicated that the changes in the intestinal microbial structure caused by LOP in the pathogenesis of STC in mice might be reversed by PTE treatment.

4 DISCUSSION

In this study, our data evaluated the laxative effect of PTE on LOP-induced constipation in mice. Next, the mechanism was predicted by network pharmacology, and PTE might play an anti-oxidative stress role through the PI3K/AKT pathway, regulate the apoptosis of ICCs, thereby improving the symptoms of constipation. *In vivo* experiments, we verified the above speculation.

Stool parameters, including stool volume, water content, and total intestinal transit time, were considered to be important factors in evaluating constipation symptoms and drug efficacy (Ren et al., 2017). We found that the stool parameters and total intestinal transit time were significantly reduced after taking LOP. Moreover, these changes could be significantly restored by PTE treatment. Our study demonstrated that PTE had a laxative effect on LOP-induced STC mice. MTL and Gas are important hormones that regulate intestinal motility (Suo et al., 2014). In this study, LOP decreased the release of MTL and Gas, but PTE treatment increased the production of hormone in a dose-dependent manner. It was suggested that PTE may alleviate the symptoms of constipation by increasing the levels of MTL and Gas.

The role of ICCs in the development of STC is increasingly appreciated, and colonic motility is significantly slowed in the absence of ICCs (Yin et al., 2018). Apoptosis is a common method of cell reduction. There is evidence that ICCs apoptosis is observed in the colon of a majority of STC patients (Zheng et al., 2021), and apoptotic ICCs can be identified by TUNEL immunostaining. In this experiment, we used c-kit immunolabeled colon sections and TUNEL staining to detect apoptotic ICCs, and found that apoptotic ICCs increased in STC group, while the number of apoptotic ICCs decreased in PTE groups. The SCF/c-kit pathway is the basic guarantee to maintain the number of ICCs (Wang et al., 2021b). PTE administration could enhance the expression of SCF/c-kit pathway and reduce the apoptosis of ICCs. It was suggested that PTE had an anti-apoptotic effect on ICCs in mouse colon and further promoted intestinal transit.

So what is the mechanism that causes PTE to reduce ICCs apoptosis? We further found that PI3K/AKT signaling might reduce ICCs apoptosis by mediating downstream Nrf2/HO-1 signaling to play an anti-oxidative stress role through network pharmacology analysis.

The breakdown of the oxidative-antioxidant balance will lead to mitochondrial dysfunction, lipid peroxidation, or apoptosis. Previous studies have shown that oxidative stress has an important role in ICCs apoptosis (Wang et al., 2021b). Meanwhile, elevated levels of oxidative stress and significant ICCs loss were observed in both STC patients and LOP-induced constipation animal models (Gibbons et al., 2009) (Lee et al., 2020). Therefore, reducing oxidative stress-induced ICCs apoptosis may be a therapeutic target for STC. MDA is a biomarker of oxidative stress, and GSH-Px is an important reactive oxygen species scavenging enzyme that maintains redox balance in the body (Hajji et al., 2020). According to our results, in the STC group, the MDA content increased, while the GSH-Px activity decreased. In contrast, treatment with PTE reversed the above changes. In addition, LOP-induced apoptosis of ICCs in colon was significantly alleviated after PTE intervention treatment. These results suggested that PTE may protect ICCs from oxidative stress-induced apoptosis.

More and more studies have found that the PI3K/AKT pathway regulates cellular oxidative stress by enhancing the expression of Nrf2/HO-1 and exerts cytoprotective effects (Koundouros and Poulogiannis, 2018) (Gao et al., 2020). Nrf2 is a transcription factor that regulates the expression of oxidative stress-related proteins and enzymes involved in metabolism and detoxification, such as HO-1 (Loboda et al., 2016). Under conditions of oxidative stress, Nrf2 activates transcription to generate various antioxidant enzymes in the cytoplasm, including HO-1, CAT, and GSH-Px (Zhuang et al., 2019) (Wen et al., 2018). Previous studies have elucidated that Nrf2 plays a key role in protecting ICCs from oxidative stress (Wang et al., 2021c). Activation of Nrf2 can reduce oxidative stress and reduce apoptosis in ICCs. In our study, apoptosis of ICCs in the colon of STC mice and reduction of Nrf2/HO-1 pathway were observed, resulting in slower colonic transit in mice. Consistent with our data, PI3K/AKT signaling was significantly reduced in STC mice with a large number of apoptotic ICCs, whereas PTE treatment upregulated AKT phosphorylation levels, promoted Nrf2/HO-1 expression, and reduced the number of apoptotic ICCs. These results suggested that PTE could enhance the Nrf2/HO-1 pathway through the PI3K/AKT pathway to protect ICCs from oxidative stress injury and reduce apoptosis, thereby alleviating intestinal motility disorders.

In recent years, many studies pointed out that intestinal flora was closely related to the occurrence and development of STC (De Vadder et al., 2018) (Müller et al., 2020). In our study, the diversity of microbiota in constipated mice was reduced, and PTE had a greater impact on the richness and diversity of

the intestinal microbial community in STC mice, especially in the PTEH group. PTE intervention could increase the abundance of Lactobacillus and Bilophila. Lactobacillus is a well-known beneficial intestinal bacteria and Bilophila is essential for the production of hydrogen sulfide in the intestine (Hanson et al., 2021). The gaseous transmitter hydrogen sulfide promoted the proliferation of ICCs through phosphorylation of AKT protein kinase (Huang et al., 2010). The abundance of Alipipes and Rikenellaceae in the STC group was much lower, but recovered after PTE treatment. According to reports, Alisipes and Rikenellaceae are all butyric acid-producing bacteria, butyric acid and other SCFAs have obvious laxative activity and stimulate ICCs proliferation (Wu et al., 2020) (Xu et al., 2020). Thus, the laxative effect of PTE may be co-regulated by all these mechanisms. On the other hand, this study also has some limitations. We did not further explore the relationship between ICCs and colonic contractile activity, and will be the focus of future research.

5 CONCLUSION

In this study, a combination of network pharmacology predictive analysis and experimental verification was used to explore the laxative effect of PTE on LOP-induced STC and its possible mechanism. PTE might play a laxative effect by inhibiting oxidative stress-induced apoptosis of ICCs through the PI3K/AKT/Nrf2 signaling pathway. The results of animal experiments also verified the results predicted by network analysis. In addition, PTE treatment restored the disordered gut microbes in STC mice. Our results provided experimental and theoretical evidence and suggested PTE as a promising drug for STC therapy.

DATA AVAILABILITY STATEMENT

The datasets presented in this study can be found in online repositories. The names of the repository/repositories and accession number(s) can be found below: https://www.ncbi.nlm.nih.gov/sra/PRJNA820465.

ETHICS STATEMENT

The animal study was reviewed and approved by Experimental Animal Welfare Ethics Committee of Tianjin Medical University General Hospital.

AUTHOR CONTRIBUTIONS

ZY and SF designed and wrote the whole study. BR carried out target analysis. LM analyzed the data and animal testing with the help from ZY and SF. DS reviewed and wrote the manuscript.

FUNDING

This work was supported by the National Natural Science Foundation of China (No. 81770537 and 82070554).

SUPPLEMENTARY MATERIAL

The Supplementary Material for this article can be found online at: https://www.frontiersin.org/articles/10.3389/fphar.2022.913420/full#supplementary-material

REFERENCES

Barberio, B., Judge, C., Savarino, E. V., and Ford, A. C. (2021). Global Prevalence of Functional Constipation According to the Rome Criteria: a Systematic Review and Meta-Analysis. *lancet. Gastroenterology hepatology* 6, 638–648. doi:10.1016/S2468-1253(21)00111-4

Bassotti, G., and Blandizzi, C. (2014). Understanding and Treating Refractory Constipation. *World J. Gastrointest. Pharmacol. Ther.* 5, 77–85. doi:10.4292/wjgpt.v5.i2.77

Chen, L. Z., Zhang, X. X., Liu, M. M., Wu, J., Ma, D., Diao, L. Z., et al. (2021). Discovery of Novel Pterostilbene-Based Derivatives as Potent and Orally Active NLRP3 Inflammasome Inhibitors with Inflammatory Activity for Colitis. *J. Med. Chem.* 64, 13633–13657. doi:10.1021/acs.jmedchem.1c01007

De Vadder, F., Grasset, E., Mannerås Holm, L., Karsenty, G., Macpherson, A. J., Olofsson, L. E., et al. (2018). Gut Microbiota Regulates Maturation of the Adult Enteric Nervous System via Enteric Serotonin Networks. *Proc. Natl. Acad. Sci. U. S. A.* 115, 6458–6463. doi:10.1073/pnas.1720017115

Fan-Jiang, P. Y., Lee, P. S., Nagabhushanam, K., Ho, C. T., and Pan, M. H. (2021). Pterostilbene Attenuates High-Fat Diet and Dextran Sulfate Sodium-Induced Colitis via Suppressing Inflammation and Intestinal Fibrosis in Mice. *J. Agric. Food Chem.* 69, 7093–7103. doi:10.1021/acs.jafc.1c02783

Faussone-Pellegrini, M. S. (2005). Interstitial Cells of Cajal: once Negligible Players, Now Blazing Protagonists. *Ital. J. Anat. Embryol.* 110, 11–31.

Fu, Z., Jiang, Z., Guo, G., Liao, X., Liu, M., and Xiong, Z. (2021). rhKGF-2 Attenuates Smoke Inhalation Lung Injury of Rats via Activating PI3K/Akt/Nrf2 and Repressing FoxO1-NLRP3 Inflammasome. *Front. Pharmacol.* 12, 641308. doi:10.3389/fphar.2021.641308

Gao, X., He, D., Liu, D., Hu, G., Zhang, Y., Meng, T., et al. (2020). Beta-naphthoflavone Inhibits LPS-Induced Inflammation in BV-2 Cells via AKT/Nrf-2/HO-1-NF-κB Signaling axis. *Immunobiology* 225, 151965. doi:10.1016/j.imbio.2020.151965

Gibbons, S. J., De Giorgio, R., Faussone Pellegrini, M. S., Garrity-Park, M. M., Miller, S. M., Schmalz, P. F., et al. (2009). Apoptotic Cell Death of Human Interstitial Cells of Cajal. *Neurogastroenterol. Motil.* 21, 85–93. doi:10.1111/j.1365-2982.2008.01185.x

Hajji, N., Wannes, D., Jabri, M. A., Rtibi, K., Tounsi, H., Abdellaoui, A., et al. (2020). Purgative/laxative Actions of Globularia Alypum Aqueous Extract on Gastrointestinal-Physiological Function and against Loperamide-Induced Constipation Coupled to Oxidative Stress and Inflammation in Rats. *Neurogastroenterol. Motil.* 32, e13858. doi:10.1111/nmo.13858

Hanson, B. T., Dimitri Kits, K., Löffler, J., Burrichter, A. G., Fiedler, A., Denger, K., et al. (2021). Sulfoquinovose Is a Select Nutrient of Prominent Bacteria and a Source of Hydrogen Sulfide in the Human Gut. *ISME J.* 15, 2779–2791. doi:10.1038/s41396-021-00968-0

He, C. L., Burgart, L., Wang, L., Pemberton, J., Young-Fadok, T., Szurszewski, J., et al. (2000). Decreased Interstitial Cell of Cajal Volume in Patients with Slow-Transit Constipation. *Gastroenterology* 118, 14–21. doi:10.1016/s0016-5085(00)70409-4

Horváth, V. J., Vittal, H., Lörincz, A., Chen, H., Almeida-Porada, G., Redelman, D., et al. (2006). Reduced Stem Cell Factor Links Smooth Myopathy and Loss of

Interstitial Cells of Cajal in Murine Diabetic Gastroparesis. *Gastroenterology* 130, 759–770. doi:10.1053/j.gastro.2005.12.027

Huang, Y., Li, F., Tong, W., Zhang, A., He, Y., Fu, T., et al. (2010). Hydrogen Sulfide, a Gaseous Transmitter, Stimulates Proliferation of Interstitial Cells of Cajal via Phosphorylation of AKT Protein Kinase. *Tohoku J. Exp. Med.* 221, 125–132. doi:10.1620/tjem.221.125

Koh, Y. C., Ho, C. T., and Pan, M. H. (2021). Recent Advances in Health Benefits of Stilbenoids. *J. Agric. Food Chem.* 69, 10036–10057. doi:10.1021/acs.jafc.1c03699

Koundouros, N., and Poulogiannis, G. (2018). Phosphoinositide 3-Kinase/Akt Signaling and Redox Metabolism in Cancer. *Front. Oncol.* 8, 160. doi:10.3389/fonc.2018.00160

Lee, H. J., Choi, E. J., Park, S., and Lee, J. J. (2020). Laxative and Antioxidant Effects of Ramie (Boehmeria Nivea L.) Leaf Extract in Experimental Constipated Rats. *Food Sci. Nutr.* 8, 3389–3401. doi:10.1002/fsn3.1619

Li, T., Yan, Q., Wen, Y., Liu, J., Sun, J., and Jiang, Z. (2021a). Synbiotic Yogurt Containing Konjac Mannan Oligosaccharides and Bifidobacterium Animalis Ssp. Lactis BB12 Alleviates Constipation in Mice by Modulating the Stem Cell Factor (SCF)/c-Kit Pathway and Gut Microbiota. *J. Dairy Sci.* 104, 5239–5255. doi:10.3168/jds.2020-19449

Li, X. M., Li, M. T., Jiang, N., Si, Y. C., Zhu, M. M., Wu, Q. Y., et al. (2021b). Network Pharmacology-Based Approach to Investigate the Molecular Targets of Sinomenine for Treating Breast Cancer. *Cancer Manag. Res.* 13, 1189–1204. doi:10.2147/CMAR.S282684

Lim, J. M., Kim, Y. D., Song, C. H., Park, S. J., Park, D. C., Cho, H. R., et al. (2019). Laxative Effects of Triple Fermented Barley Extracts (FBe) on Loperamide (LP)-induced Constipation in Rats. *BMC Complement. Altern. Med.* 19, 143. doi:10.1186/s12906-019-2557-x

Liu, S., Jin, Z., Xia, R., Zheng, Z., Zha, Y., Wang, Q., et al. (2022). Protection of Human Lens Epithelial Cells from Oxidative Stress Damage and Cell Apoptosis by KGF-2 through the Akt/Nrf2/HO-1 Pathway. *Oxid. Med. Cell. Longev.* 2022, 6933812. doi:10.1155/2022/6933812

Loboda, A., Damulewicz, M., Pyza, E., Jozkowicz, A., and Dulak, J. (2016). Role of Nrf2/HO-1 System in Development, Oxidative Stress Response and Diseases: an Evolutionarily Conserved Mechanism. *Cell. Mol. Life Sci.* 73, 3221–3247. doi:10.1007/s00018-016-2223-0

Milton-Laskibar, I., Marcos-Zambrano, L. J., Gómez-Zorita, S., Fernández-Quintela, A., Carrillo de Santa Pau, E., Martínez, J. A., et al. (2021). Gut Microbiota Induced by Pterostilbene and Resveratrol in High-Fat-High-Fructose Fed Rats: Putative Role in Steatohepatitis Onset. *Nutrients* 13, 1738. doi:10.3390/nu13051738

Müller, M., Hermes, G. D. A., Canfora, E. E., Smidt, H., Masclee, A. A. M., Zoetendal, E. G., et al. (2020). Distal Colonic Transit Is Linked to Gut Microbiota Diversity and Microbial Fermentation in Humans with Slow Colonic Transit. *Am. J. Physiol. Gastrointest. Liver Physiol.* 318, G361–G369. doi:10.1152/ajpgi.00283.2019

Ren, X., Liu, L., Gamallat, Y., Zhang, B., and Xin, Y. (2017). Enteromorpha and Polysaccharides from Enteromorpha Ameliorate Loperamide-Induced Constipation in Mice. *Biomed. Pharmacother.* 96, 1075–1081. doi:10.1016/j.biopha.2017.11.119

Serra, J., Pohl, D., Azpiroz, F., Chiarioni, G., Ducrotté, P., Gourcerol, G., et al. (2020). European Society of Neurogastroenterology and Motility Guidelines on Functional Constipation in Adults. *Neurogastroenterol. Motil.* 32, e13762. doi:10.1111/nmo.13762

Shin, J. E., Park, K. S., and Nam, K. (2019). Chronic Functional Constipation. *Korean J. Gastroenterol.* 73, 92–98. doi:10.4166/kjg.2019.73.2.92

Suo, H., Zhao, X., Qian, Y., Li, G., Liu, Z., Xie, J., et al. (2014). Therapeutic Effect of Activated Carbon-Induced Constipation Mice with Lactobacillus Fermentum Suo on Treatment. *Int. J. Mol. Sci.* 15, 21875–21895. doi:10.3390/ijms151221875

Tanner, S., Chaudhry, A., Goraya, N., Badlani, R., Jehangir, A., Shahsavari, D., et al. (2021). Prevalence and Clinical Characteristics of Dyssynergic Defecation and Slow Transit Constipation in Patients with Chronic Constipation. *J. Clin. Med.* 10, 2027. doi:10.3390/jcm10092027

Tian, L., Song, S., Zhu, B., and Liu, S. (2018). Electroacupuncture at ST-36 Protects Interstitial Cells of Cajal via Sustaining Heme Oxygenase-1 Positive M2 Macrophages in the Stomach of Diabetic Mice. *Oxid. Med. Cell. Longev.* 2018, 3987134. doi:10.1155/2018/3987134

van Mill, M. J., Koppen, I. J. N., and Benninga, M. A. (2019). Controversies in the Management of Functional Constipation in Children. *Curr. Gastroenterol. Rep.* 21, 23. doi:10.1007/s11894-019-0690-9

Wang, D., Shi, S., Ren, T., Zhang, Y., Guo, P., Wang, J., et al. (2021a). U0126 Pretreatment Inhibits Cisplatin-Induced Apoptosis and Autophagy in HEI-OC1 Cells and Cochlear Hair Cells. *Toxicol. Appl. Pharmacol.* 415, 115447. doi:10.1016/j.taap.2021.115447

Wang, H., Zhao, K., Ba, Y., Gao, T., Shi, N., Niu, Q., et al. (2021b). Gastric Electrical Pacing Reduces Apoptosis of Interstitial Cells of Cajal via Antioxidative Stress Effect Attributing to Phenotypic Polarization of M2 Macrophages in Diabetic Rats. *Oxid. Med. Cell. Longev.* 2021, 1298657. doi:10.1155/2021/1298657

Wang, H., Zhao, K., Shi, N., Niu, Q., Liu, C., and Chen, Y. (2021c). Electroacupuncture Regularizes Gastric Contraction and Reduces Apoptosis of Interstitial Cells of Cajal in Diabetic Rats. *Front. Physiol.* 12, 560738. doi:10.3389/fphys.2021.560738

Wang, J. Y., Wang, Y. L., Zhou, S. L., and Zhou, J. F. (2004). May Chronic Childhood Constipation Cause Oxidative Stress and Potential Free Radical Damage to Children? *Biomed. Environ. Sci.* 17, 266–272.

Wang, X., Zhang, C., Chen, C., Guo, Y., Meng, X., and Kan, C. (2018). Allicin Attenuates Lipopolysaccharide-induced A-cute L-ung I-njury in N-eonatal R-ats via the PI3K/Akt P-athway. *Mol. Med. Rep.* 17, 6777–6783. doi:10.3892/mmr.2018.8693

Wen, Z., Hou, W., Wu, W., Zhao, Y., Dong, X., Bai, X., et al. (2018). 6'-O-Galloylpaeoniflorin Attenuates Cerebral Ischemia Reperfusion-Induced Neuroinflammation and Oxidative Stress via PI3K/Akt/Nrf2 Activation. *Oxid. Med. Cell. Longev.* 2018, 8678267. doi:10.1155/2018/8678267

Wu, H., Tremaroli, V., Schmidt, C., Lundqvist, A., Olsson, L. M., Krämer, M., et al. (2020). The Gut Microbiota in Prediabetes and Diabetes: A Population-Based Cross-Sectional Study. *Cell. Metab.* 32, 379–e3. e3. doi:10.1016/j.cmet.2020.06.011

Xu, X., Gao, Z., Yang, F., Yang, Y., Chen, L., Han, L., et al. (2020). Antidiabetic Effects of Gegen Qinlian Decoction via the Gut Microbiota Are Attributable to its Key Ingredient Berberine. *Genomics, proteomics Bioinforma.* 18, 721–736. doi:10.1016/j.gpb.2019.09.007

Yang, C., Liao, A.-M., Cui, Y., Yu, G., Hou, Y., Pan, L., et al. (2021). Wheat Embryo Globulin Protects against Acute Alcohol-Induced Liver Injury in Mice. *Food Chem. Toxicol.* 153, 112240. doi:10.1016/j.fct.2021.112240

Yang, L., Hu, Z., Zhu, J., Liang, Q., Zhou, H., Li, J., et al. (2020). Systematic Elucidation of the Mechanism of Quercetin against Gastric Cancer via Network Pharmacology Approach. *Biomed. Res. Int.* 2020, 3860213. doi:10.1155/2020/3860213

Yin, J., Liang, Y., Wang, D., Yan, Z., Yin, H., Wu, D., et al. (2018). Naringenin Induces Laxative Effects by Upregulating the Expression Levels of C-Kit and SCF, as Well as Those of Aquaporin 3 in Mice with Loperamide-Induced Constipation. *Int. J. Mol. Med.* 41, 649–658. doi:10.3892/ijmm.2017.3301

Yu, S., Guo, Q., Jia, T., Zhang, X., Guo, D., Jia, Y., et al. (2021). Mechanism of Action of Nicotiflorin from Tricyrtis Maculata in the Treatment of Acute Myocardial Infarction: From Network Pharmacology to Experimental Pharmacology. *Dddt* Vol. 15, 2179–2191. doi:10.2147/DDDT.S302617

Zhang, W., Chao, X., Wu, J. Q., Ma, X. B., Yang, Y. L., Wu, Y., et al. (2021a). Exploring the Potential Mechanism of Guchang Zhixie Wan for Treating Ulcerative Colitis by Comprehensive Network Pharmacological Approaches and Molecular Docking Validation as Well as Cell Experiments. *Chem. Biodivers.* 18, e2000810. doi:10.1002/cbdv.202000810

Zhang, Y., Yao, Y., Fu, Y., Yuan, Z., Wu, X., Wang, T., et al. (2021b). Inhibition Effect of Oxyepiberberine Isolated from Coptis Chinensis Franch. On Non-small Cell Lung Cancer Based on a Network Pharmacology Approach and Experimental Validation. *J. Ethnopharmacol.* 278, 114267. doi:10.1016/j.jep.2021.114267

Zheng, H., Liu, Y.-J., Chen, Z.-C., and Fan, G.-Q. (2021). miR-222 Regulates Cell Growth, Apoptosis, and Autophagy of Interstitial Cells of Cajal Isolated from Slow Transit Constipation Rats by Targeting C-Kit. *Indian J. Gastroenterol.* 40, 198–208. doi:10.1007/s12664-020-01143-7

Zhu, F., Xu, S., Zhang, Y., Chen, F., Ji, J., and Xie, G. (2016). Total Glucosides of Paeony Promote Intestinal Motility in Slow Transit Constipation Rats through

Amelioration of Interstitial Cells of Cajal. *PloS one* 11, e0160398. doi:10.1371/journal.pone.0160398

Zhu, X., Shen, W., Wang, Y., Jaiswal, A., Ju, Z., and Sheng, Q. (2017). Nicotinamide Adenine Dinucleotide Replenishment Rescues Colon Degeneration in Aged Mice. *Signal Transduct. Target Ther.* 2, 17017. doi:10.1038/sigtrans.2017.17

Zhuang, Y., Wu, H., Wang, X., He, J., He, S., and Yin, Y. (2019). Resveratrol Attenuates Oxidative Stress-Induced Intestinal Barrier Injury through PI3K/Akt-Mediated Nrf2 Signaling Pathway. *Oxid. Med. Cell. Longev.* 2019, 7591840. doi:10.1155/2019/7591840

Conflict of Interest: The authors declare that the research was conducted in the absence of any commercial or financial relationships that could be construed as a potential conflict of interest.

Publisher's Note: All claims expressed in this article are solely those of the authors and do not necessarily represent those of their affiliated organizations, or those of the publisher, the editors and the reviewers. Any product that may be evaluated in this article, or claim that may be made by its manufacturer, is not guaranteed or endorsed by the publisher.

GLOSSARY

CRC Colorectal cancer
M2-TAMs M2 tumour-associated macrophages
TAMs Tumour-associated macrophages
MDC Monodansylcadaverine
RT-qPCR Real-time polymerase chain reaction
EGF Epidermal growth factor
bFGF Basic fibroblast growth factor
circRNAs Circular RNAs
FBS Foetal bovine serum
DMSO Dimethyl sulfoxide
AVs Autophagic vesicles
POD Peroxidase
DAB Diaminobenzidine
SD Standard deviation
ANOVA Analysis of variance

frontiers | Frontiers in Pharmacology

ORIGINAL RESEARCH
published: 26 May 2022
doi: 10.3389/fphar.2022.889181

Disordered Gut Microbiota in Colorectal Tumor-Bearing Mice Altered Serum Metabolome Related to Fufangchangtai

Mengmeng Cai[1,2,3], *Ya Xiao*[1,2], *Zhibing Lin*[4]*, *Jinmiao Lu*[3,5], *Xiaoyu Wang*[4], *Sajid Ur Rahman*[3,6], *Shilan Zhu*[3,5], *Xiaoyu Chen*[3,5], *Jialin Gu*[1,2], *Yuzhu Ma*[1,2], *Zhaoguo Chen*[3]* and *Jiege Huo*[1,2]*

[1]Affiliated Hospital of Integrated Traditional Chinese and Western Medicine, Nanjing University of Chinese Medicine, Nanjing, China, [2]Jiangsu Province Academy of Traditional Chinese Medicine, Nanjing, China, [3]Key Laboratory of Animal Parasitology of Ministry of Agriculture, Laboratory of Quality and Safety Risk Assessment for Animal Products on Biohazards (Shanghai) of Ministry of Agriculture, Shanghai Veterinary Research Institute, Chinese Academy of Agricultural Sciences, Shanghai, China, [4]School of Agriculture and Biology, Shanghai Jiao Tong University, Shanghai, China, [5]South China Agricultural University, Guangzhou, China, [6]College of Animal Science and Technology, Anhui Agricultural University, Hefei, China

OPEN ACCESS

Edited by:
Hailian Shi,
Shanghai University of Traditional Chinese Medicine, China

Reviewed by:
Zhixing He,
Zhejiang Chinese Medical University, China
Jing Yuan,
Children's Hospital of Capital Institute of Pediatrics, China

***Correspondence:**
Jiege Huo
huojiege@jsatcm.com
Zhaoguo Chen
zhaoguochen@shvri.ac.cn
Zhibing Lin
mdzhibing@163.com

Specialty section:
This article was submitted to Gastrointestinal and Hepatic Pharmacology, a section of the journal Frontiers in Pharmacology

Received: 03 March 2022
Accepted: 18 April 2022
Published: 26 May 2022

Citation:
Cai M, Xiao Y, Lin Z, Lu J, Wang X, Rahman SU, Zhu S, Chen X, Gu J, Ma Y, Chen Z and Huo J (2022) Disordered Gut Microbiota in Colorectal Tumor-Bearing Mice Altered Serum Metabolome Related to Fufangchangtai. Front. Pharmacol. 13:889181. doi: 10.3389/fphar.2022.889181

Purpose: This study aimed to investigate the relationship between gut microbiota (GM) and serum metabolism using antineoplastic Fufangchangtai (FFCT) as the model prescription in the treatment of colorectal cancer (CRC).

Methods: Tumor-bearing mice and normal mice were administered different doses of FFCT. The tumor volume of tumor-bearing mice was observed. The levels of $CD4^+$ and $CD8^+$ T cells in the blood, spleen, and tumor of mice were determined using a flow cytometer. The bacterial microbiota in stool samples from mice and the serum metabolomics of FFCT-treated mice and fecal microbiota transplantation mice were detected using 16s RNA sequencing and liquid chromatography–mass spectrometry (LC/MS), respectively.

Results: The tumor volume of mice showed no significant decrease after FFCT intervention. The levels of $CD4^+$ and $CD8^+$T lymphocytes showed a significant increase under the intervention of FFCT. GM of colorectal tumor-bearing mice and healthy mice were determined, and the diversity and abundance of *Firmicutes*, *Deferribacteres*, *Bacteroidetes*, and *Proteobacteria* were significantly different between the two groups. Furthermore, we found that the levels of matrine, isogingerenone B, and armillaripin were significantly decreased in tumor-bearing mice after FFCT intervention, indicating that the tumor-induced dysbiosis of gut bacteria may affect the absorption and metabolism of FFCT. Under the intervention of FFCT, serum metabolism of mice transplanted with feces from CRC patients showed less metabolites related to FFCT than that from healthy people, indicating that

Abbreviations: ANOVA, analysis of variance; ARSs, aminoacyl-tRNA synthetases; ASVs, amplicon sequence variants; CAC, cancer-associated cachexia; COX, cyclooxygenase; CRC, colorectal cancer; EMP, glycolysis pathway; EPOX, cytochrome P-450 epoxygenase; FFCT, Fufangchangtai; GM, gut microbiota; HMDB, Human Metabolome Database; HPLC, high-performance liquid chromatography; IARS2, isoleucyl-tRNA synthetase 2; KRS, lysyl-tRNA synthetase; LC/MS, Liquid chromatography–mass spectrometry; LOX, lipoxygenase; OTUs, operational taxonomic units; PPP, pentose phosphate pathway; PCoA, principal coordinates analysis; QC, quality control; ROS, reactive oxygen species; SPF, specific pathogen-free; TCA, tricarboxylic acid cycle; TCM, traditional Chinese medicine.

GM could be a single factor affecting the metabolism of FFCT. Furthermore, we found that different doses of FFCT-treated mice had higher abundance of *Roseburia*, *Turicibacter*, and *Flexispira* than that in the non-intervention control group. *Firmicutes* and *Bacteroidetes* in FFCT-treated groups showed a similar trend compared to the healthy group, indicating that FFCT might correct the intestinal microenvironment by modulating gut microbiota in colorectal tumor-bearing mice.

Conclusion: The dysbiosis of GM in tumor-bearing mice reduced the serum metabolites related to FFCT, and FFCT could correct the disordered GM of colorectal tumor-bearing mice to exert efficacy.

Keywords: colorectal cancer, Fufangchangtai, gut microbiota, serum metabolome, traditional Chinese medicine

INTRODUCTION

Colorectal cancer (CRC) is a type of cancer that affects the colon or rectum. Despite the fact that the death rate of CRC patients is steadily decreasing due to population screening and endoscopic surveillance, it is still the third highest in the world in terms of incidence and mortality (Siegel et al., 2020). Gut microbiota (GM), also known as "the new virtual metabolic organ," plays a vital role in stimulating the digestion, producing nutrients, and promoting mucosal barrier immunity (Eckburg et al., 2005; Ramakrishna, 2013; Castellanos et al., 2018; Milosevic et al., 2019). Once GM is out of balance, it contributes to several systemic diseases, including cancer. Many pieces of evidence indicated a strong correlation between the development of CRC and GM dysbiosis (Wu et al., 2009; Zackular et al., 2013; Zhao R. S. et al., 2019). A previous study showed the alterations in the dominant and subdominant families of bacteria in CRC individuals and healthy controls (Sobhani et al., 2011). According to the "driver-passenger theory," GM causes CRC by establishing a tumor microenvironment and inducing epithelial DNA damages and tumorigenesis (Gagniere et al., 2016). Meanwhile, GM also affects the immunity and prognosis of CRC patients by producing immunostimulatory and immunosuppressive cytokines such as IL-17A and IL-9 (Niccolai et al., 2020). Studies also showed that tumor characterized by IL-17-expressing T cells, FOXP3hi Tregs, and immunosuppressive myeloid populations were associated with worse clinical outcome (Fidelle et al., 2020).

There are numerous CRC treatments available, including radical surgery, chemotherapy, radiotherapy, targeted therapy, immunotherapy, and others. However, these treatments have limitations and cause many side effects. Therefore, traditional Chinese medicine (TCM) plays an indispensable role in the prevention of tumor recurrence and metastasis due to its effect on synergy and attenuation. Chinese decoctions such as Xiaoyaosan successfully reduced the tumor volume and tumor weight in mice with CRC xenografts and prolonged the overall survival time through a 21-day intragastric treatment (Zhang Z. et al., 2020). Herbs such as *Matricaria chamomilla* could act as a potent single component against DMH-induced CRC by modulating the Wnt signaling pathway (El Joumaa et al., 2020). Our clinical experience prescription Fufangchangtai (FFCT) has also proved to have an anti-tumor effect. FFCT is a herbal formulation consisting of *Panax ginseng* C. A. Mey (ren shen), *Actinidia chinensis* Planch (teng li gen), *Hedysarum multijugum* Maxim (huang qi), Akebiae Fructus (yu zhi zi), Coicis Semen (yi yi ren), and *Sophora flavescens* Radix (ku shen). The efficacy of FFCT was verified in our previous clinical trials, showing the anti-CRC effect by boosting the body's immune system, improving the patient's quality of life, and reducing side effects (Li, 2019).

As anti-tumor immunity is a part of cancer treatment, the level of immune cells can reflect the therapeutic effect of drugs. The cells involved in anti-tumor immunity mainly include T cells, NK cells, macrophages, dendritic cells (DC), etc. Among them, T-cell response is the most important host response in controlling tumor growth and development. The T-cell subsets involved in anti-tumor immunity are mainly $CD4^+$ and $CD8^+$ T cells. $CD4^+$ T cells can enhance the function of $CD8^+$ T cells by producing lymphokines, activating macrophages or other APCs, and producing tumor necrosis factor. $CD8^+$T cells can secrete lymphokines and recognize the specific antigen on tumor cells so as to directly or indirectly kill tumor cells with the help of $CD4^+$ T cells (Zheng et al., 2021). In our previous clinical study, we found that FFCT could increase the $CD3^+$ T cell levels compared with placebo (Li, 2019).

The majority of TCM are taken orally and absorbed into the bloodstream via the gastrointestinal tract, where it exerts its efficacy. Therefore, TCM can reverse or mitigate varied compositional dysbiosis of GM associated with many diseases besides improving the pathological symptoms (Xu et al., 2017). A study showed that Berberine rescued *Fusobacterium nucleatum*-induced colorectal tumorigenesis by modulating the tumor microenvironment and blocking the activation of tumorigenesis-related pathways (Yu et al., 2015). The classical prescription, "Yi-Yi-Fu-Zi-Bai-Jiang-San" (YYFZBJS) blocked tumor initiation in treating CRC by mediating Tregs and regulating the natural GM of Apc (Min/+) mice including *Bacteroides fragilis*, *Lachnospiraceae*, and so on (Sui et al., 2020). GM also harbors many types of enzymes, allowing plenty of catalytic reactions, which are involved in the biotransformation of TCM components. Even though GM can interact complicatedly with TCM components, whether GM can

influence the therapeutic effect of TCM on CRC remains unknown.

Thus, it is hypothesized that GM dysbiosis affects the serum metabolome of the human body, which is related to TCM in the treatment of CRC. To test the hypothesis, we used FFCT as a model prescription TCM to explore the correlation between GM and the metabolism of TCM in CRC treatment.

MATERIALS AND METHODS

Preparation of Drugs

FFCT was prepared using six kinds of TCM granules, including Panax Ginseng C. A. Mey (ren shen), Actinidia Chinensis Planch (teng li gen), Hedysarum Multijugum Maxim (huang qi), Akebiae Frucyus (yu zhi zi), Coicis Semen (yi yi ren), and Sophorae Flavescentis Radix (ku shen), which were purchased from Jiangsu Hospital of Integrated Traditional Chinese and Western Medicine. The quality of FFCT was monitored using a high performance liquid chromatography (HPLC) analysis as discussed in our previous study (Wang, 2018). The formulated granules were ground into a powder and dissolved in warm distilled water before being administered to mice.

Cells and Animals

CT26-LUC cells were provided by Shanghai Institute of Veterinary Medicine and cultured with RPMI-1640 containing 10% fetal bovine serum, 1% penicillin/streptomycin, and 4 μg/ml puromycin dihydrochloride. Reagents for cell culture were purchased from Thermo Fisher Scientific (Waltham, MA, United States). The incubator's condition was stable at 37°C and 5% CO_2.

All animal experiments were performed in compliance with animal welfare guidelines and approved by the Animal Ethical Committee of Shanghai Veterinary Research Institute, Chinese Academy of Agricultural Sciences (SHVRI-SZ-20200420-01, SHVRI-SZ-20200720-01). Six-week-old female BALB/C mice were purchased from Shanghai Jiesijie Company (Shanghai, China) and housed under SPF condition with 25 ± 2°C and a 12-h light/dark cycle. The mice were given free access to a standard diet and drinking water.

Gut Microbiota Detection Experiment

To explore the difference in GM under different conditions, after 1 week of acclimatization, the mice were randomly divided into five groups: the PBS group (normal mice injected with PBS and administered with ddH_2O, n = 4), the CT26 group (CRC tumor-bearing mice administered with ddH_2O, n = 5), the CT26L group (CRC tumor-bearing mice administered with 0.65 mg/g FFCT, n = 5), the CT26M group (CRC tumor-bearing mice administered with 1.3 mg/g FFCT, n = 5), the CT26H group (CRC tumor-bearing mice administered with 2.6 mg/g FFCT, n = 5). The daily dosage for the CT26M group was obtained based on the daily dosage for patients (10 g/70 kg) clinically, according to the human–mouse transfer formula (mouse dose = human dose × 9.1) (Xu and Chen, 1992).

Before administration, 100 μl of CT26-LUC cells (1×10^6/ml) were inoculated subcutaneously into the flanks of mice (CRC tumor-bearing groups), while 100 μl of PBS was inoculated subcutaneously (PBS group). About 200 μl of ddH_2O was administered to the PBS group and CT26 group, while 200 μl of FFCT suspension was administered to the other groups via gastric gavage, and the drugs were administered for 4 weeks. Tumor growth was measured using a caliper every 3 days and tumor volumes were calculated using the following formula: volume = (length/2) × $(\text{width})^2$. Fluorescence expression in the region of interest (ROI) was used to evaluate the tumor volume based on the Small Animal 3D Multimodality Imaging System (IVIS Spectrum, PerkinElmer, Waltham, MA, United States).

Stool samples of the mice were collected 27 days after administration. Fecal pellets (2–4) were collected from each mouse using a 1.5-ml Eppendorf tube and stored at −80°C until used. Furthermore, blood was collected 24 h after the last oral administration, and serum was separated by centrifuging the blood at 3,000 rpm for 15 min at 4°C and stored at −80°C until analyzed. The stool samples collected from 4–5 mice in each group were detected.

Fufangchangtai Serum Metabolomics Experiment

To explore the FFCT metabolites under tumor-induced gut dysbiosis condition, after 1 week of acclimatization, the mice were randomly divided into four groups: the control group (normal mice injected with PBS and administered with ddH_2O, n = 6), the CT26 group (CRC tumor-bearing mice administered with ddH_2O, n = 6), the CT26H group (CRC tumor-bearing mice administered with 2.6 mg/g FFCT, n = 6) and the CM group (normal mice injected with PBS and administered with 2.6 mg/g FFCT, n = 6). Before administration, 100 μl of CT26-LUC cells (1×10^6/ml) were inoculated subcutaneously into the flanks of the mice (CT26 group and CT26H group), while 100 μl of PBS was inoculated subcutaneously (control group and CM group). About 200 μl of FFCT suspension was given to the CT26H group and CM group via gastric gavage, and the drug administration lasted for 4 weeks. The blood was drawn from the eyeball of the mice and allowed to clot at 4°C for 1 h. After a 15-min centrifugation at 3,000 rpm at 4°C, the supernatant was collected and stored in dry ice for blood mass spectrometry.

Fecal Microbiota Transplantation Experiment

Fresh stool samples from CRC patients without any clinical treatment and healthy people were separately collected. The sampling procedure was approved by the Medical Ethics Committee (2105235-3) of Fudan University Shanghai Cancer Center. CRC patients including one male and three female patients were selected, and their average age was 52.6 ± 16.1. To match the numbers, healthy controls including one male and three female patients were selected with the age of 51.9 ± 4.9. The age and the gender distribution of the two

groups had no significant difference (**Supplementary Table S1**).

Fresh stool samples (15 g per person) were mixed and suspended in 60 ml PBS. The suspension liquid was then filtered using 70-μM meshes, and the filtrate was centrifuged at 2,000 rpm for 10 min. Subsequently, after the removal of the supernatant, the remaining pellet was resuspended in 12-ml PBS (Jian et al., 2020). The mixture was used for fecal microbiota transplantation by gavage (200 μl per mouse).

Before gavage was performed, all mice were treated with a cocktail of broad-spectrum antibiotics including ampicillin (0.2 g/L), vancomycin (0.1 g/L), neomycin (0.2 g/L), and metronidazole (0.2 g/L) in drinking water for 2 weeks (Tsoi et al., 2017). All antibiotics were purchased from Shanghai Macklin Biochemical Co., Ltd. (Shanghai, China). Subsequently, the mice were randomly divided into two groups: the FMT-CA-FFCT group (mice transplanted with feces from CRC patients, $n = 6$) and the FMT-H-FFCT group (mice transplanted with feces from healthy controls, $n = 6$). These two groups were given fecal suspension from CRC patients or healthy people, respectively, for 2 weeks by gavage (twice per week), and a 200-μl high dose of FFCT (2.6 mg/g) was also given by gavage for 2 weeks at the same time. Blood samples were drawn from the eyeballs of the mice 24 h after the last oral administration and left undisturbed to cool at 4°C for 1 h. Serum was separated by centrifuging of blood at 3,000 rpm for 15 min at 4°C and stored at −80°C until analyzed.

Flow Cytometry Analysis

The blood, spleen, and tumor tissues from different groups were separated, and the proportion of $CD3^+CD4^+$ and $CD3^+CD8^+$ T cells was analyzed using flow cytometry. The collected tumor tissues were digested with Collagenase D (1 mg/ml) and DNase I (0.5 mg/ml) and Dispase® II (1.5 U/ml) in RPMI-1640 for 30 min at 37°C. The digested material was passed through a mesh (70 μM) to remove clumps and the filtrate was washed twice and then centrifuged at 400 g for 8 min at room temperature (RT). The collected blood was lysed using lyse solution, after which it was washed with PBS and then centrifuged at 700 g for 5 min. The whole spleen was placed in a cell strainer and crushed, and then passed through a 70-μm mesh to remove clumps and the filtrate was washed twice, and then centrifuged at 400 g for 8 min at RT. A total of 1×10^6 cells were incubated for 30 min at 4°C with the following antibodies: (FITC)-CD3, (PB450)-CD4, (PE)-CD8. All the antibodies were purchased from Becton, Dickinson and Company (BD, NJ, United States). Following two washes with 1 ml of staining buffer, the cells were resuspended in 200-μl staining buffer for analysis on a CytoFLEX flow cytometer (Beckman Coulter Life Sciences, Brea, CA, United States).

Gut Microbiota Analysis

The OMEGA Soil DNA Kit (D5625-01) (Omega Bio-Tek, Norcross, GA, United States) was used to extract the DNA from fecal samples. The quantity and quality of extracted DNAs were measured using a NanoDrop ND-1000 spectrophotometer (Thermo Fisher Scientific, Waltham, MA, United States) and agarose gel electrophoresis, respectively.

Sequencing of the 16S rRNA genes was performed using the Illumina MiSeq platform. Universal 16S primers (338F/806R) with a sample-specific 12 bp barcode were used to amplify the hypervariable V3-V4 region of bacterial 16S rRNA genes. PCR was performed using a thermal cycler Model C1000 (Bio-Rad, Richmond, CA, United States) (Church et al., 2020). The 16s RNA sequencing was performed by Personal Bio (Shanghai, China).

Microbiome bioinformatics were processed and analyzed with the QIIME2 (2019.4) software package (Bolyen et al., 2018). Briefly, Raw sequence data were demultiplexed using the demux plugin following by primers cutting with cutadapt plugin (Martin, 2011). Sequencing reads were quality-filtered, denoised, merged, and chimera removed using the DADA2 plugin (Callahan et al., 2016). Non-singleton amplicon sequence variants (ASVs) were aligned with mafft and used to construct a phylogeny with FastTree-2 (Katoh et al., 2002; Price et al., 2009). Alpha and beta diversity metrics were estimated using the diversity plugin. Taxonomy was assigned to ASVs using the classify-sklearn naïve Bayes taxonomy classifier in feature-classifier plugin against the SILVA Release 132 Database (Kõljalg et al., 2013; Bokulich et al., 2018). QIIME-generated ASV tables were used for downstream statistical analysis.

Serum Metabolomics Analysis

Metabolites are stable in serum and can be quantified, which presents an opportunity in monitoring disease status and exploring biomarkers to predict the efficacy of anticancer therapies (Tian et al., 2018). The serum metabolomics of two groups (CM, CT26H) were detected. The blood was drawn from the eyeball of mice and then stored at 4°C for 1 h. After 15 min of centrifugation at 3,000 rpm at 4°C, the supernatant was collected and stored in dry ice for blood mass spectrometry. Liquid chromatography–mass spectrometry (LC/MS) analysis of the blood was entrusted to Luming Bio company, (Shanghai, China).

A measure of 100 μl of serum from each sample was vortexed with a 10-μl internal standard (0.3 mg/mL L-2-chlorophenylalanine or 0.01 mg/ml Lyso PC 17:0 dissolved in methanol) for 10 s. The mixtures were precipitated by 300-μl mixtures of methanol and acetonitrile (2/1, v/v) and then ultra-sonicated on ice for 10 min, then at −20°C for 30 min. After 10 min of centrifugation (13,000 rpm, 4°C), 300 μl of supernatant from each sample was collected and dried. The dried supernatant was resolved in 400 μl of 20% methanol and then placed at −20°C for 2 h. Then, 150 μl of supernatant per sample was filtered through a 0.22-μM microfilter and transferred into LC sampling vial for LC/MS analysis. Additionally, a quality control (QC) sample was created by mixing an aliquot of equal volume of each sample.

A Dionex UltiMate 3000 RS UHPLC system (Thermo Fisher Scientific, Waltham, MA, United States) coupled with Q-Exactive quadrupole-Orbitrap mass spectrometer (Thermo Fisher Scientific, Waltham, MA, United States) was used to analyze the metabolic profiling in both ESI-positive and ESI-negative ion modes. A quantity of 2 μl of the prepared sample was injected into the ACQUITY UPLC HSS T3 column (1.8 μM, 2.1 × 100 mm). All samples were eluted using a linear gradient from 100% mobile

phase A (0.1% formic acid in water) to 100% mobile phase B (0.1% formic acid in acetonitrile) under the condition that the flow rate was 350 μl/min and the column temperature was 45°C. Linear gradients: 0 min, 5% B; 2 min, 5% B; 4 min, 25% B; 8 min, 50% B; 10 min, 80% B; 14 min, 100% B; 15 min, 100% B; 15.1 min, 5% B; and 16 min, 5% B. The electrospray ionization (ESI) source operating in positive and negative mode (Water, Milford, MA, United States) was used for the mass spectrometry analysis. Parameters of mass spectrometry were as follows: Capillary temperature was set at 320°C, while the aux gas heater temperature was set at 350°C. Sheath gas flow rate was 35 Arb and aux gas flow rate was 8 Arb. The san range was from 100 to 1,000 m/z.

The raw data were processed by the Progenesis QI v2.3 software (Nonlinear Dynamics, Newcastle, United Kingdom) for baseline filtering, peak recognition, peak alignment, and retention time correction. The Human Metabolome Database (HMDB), LIPID MAPS (v2.3), and METLIN database, and a self-built database were used to identify the compounds.

Statistical Analysis

Statistical analysis was performed using Version 22 of SPSS for Windows, and differences were considered significant at a p-value < 0.05. Distributions of variables were examined by Shapiro–Wilk Test according to our sample size, and appropriate tests were applied for further analysis. The tumor volume and percentage of immune cells in different groups were analyzed with analysis of variance (ANOVA). Means from the data, together with estimates of the standard error of the mean and pairwise comparisons (Tukey's or Games-Howell test), were obtained. Clustering of gut microbial communities among different groups was analyzed with Adonis. The alpha diversity analysis was conducted by Dunn's test, while the beta diversity analysis, using the Permanova test. Pairwise comparison in two abnormal distribution groups was analyzed with Mann–Whitney U test. In the analysis of serum mass spectrometry data, the unsupervised principal component analysis (PCA) was used to observe the distribution of samples and the stability of the analysis process, and then the supervised orthogonal partial least squares discrimination analysis (OPLS-DA) was used to describe the differences between the groups. The contribution of each variable to the population was ranked according to the variable importance of projection value (VIP value) obtained from the OPLS-DA model, and the significance of differential metabolites between the groups was verified by a t test and fold change analysis. The Pearson correlation coefficient was used to measure the linear correlation between the two groups. It was considered that the difference was statistically significant when VIP >1.0 and $p < 0.05$.

RESULTS

Fufangchangtai Regulated the Levels of $CD4^+$ and $CD8^+$ T Cells

To analyze the curative effect of FFCT during CRC treatment, we tested the tumor volume and assessed the T cells ($CD4^+CD8^+$) in the blood, spleen, and tumor using a CRC mouse model. As shown in **Figure 1A**, FFTC treatment had no significant influence on the tumor volume in each group ($p > 0.05$). Furthermore, we analyzed the levels of immune cells ($CD3^+CD4^+$ and $CD3^+CD8^+$ T cell) using flow cytometry. Gating strategies are shown in **Supplementary Figure S1**. The results showed that $CD3^+CD4^+$ T cells from the spleen and blood in the FFCT-treated groups were significantly increased compared with the CT26 group, but there was no significant difference in the tumor volume between the two groups (**Figure 1B**). Compared with the CT26 group, the $CD3^+CD8^+$ T cells from the spleen in the CT26H group were increased, but there was no significant difference in the blood and tumor between the two groups (**Figure 1C**). These results suggested that FFCT might enhance the body immunity by increasing the levels of $CD3^+CD8^+$ and $CD3^+CD4^+$ T cells in the blood and spleen.

Fufangchangtai Changed the Gut Microbiota in CRC Tumor-Bearing Mice Model

The gut microbiome of different groups (PBS, CT26, CT26L, CT26M, CT26H) was analyzed using 16s RNA sequencing. The alpha diversity analysis showed that there were no significant differences between the CT26 and PBS group (Dunn's test, $p > 0.05$) (**Figure 2A**). However, beta diversity analysis using both unweighted and weighted UniFrac distances indicated that the PBS group had higher dissimilarities among gut microbial communities than the CT26 group (Permanova, $p < 0.05$; **Figures 2B,C**). The rarefaction curves were close to the saturation platform at the sequencing depth of 10,000, indicating that the data were sufficient to reflect the GM information about all the samples (**Supplementary Figure S2A**). The Venn diagram (**Supplementary Figure S2B**) revealed 1,395 common OTUs across all the five groups. The results showed a significant difference in GM between the tumor-bearing mice and the healthy mice. The principal coordinates analysis (PCoA) revealed the similarity in species abundance composition of two samples in the corresponding dimensions by analyzing the projection distance of the samples on the coordinate axis. Bray and Curtis distance here was used to characterize the community differences between the samples. As for the CT26 group and the PBS group, the PCoA diagram (**Supplementary Figure S3A**) suggested significantly distinct clustering of gut microbial communities between the two groups (Adonis, $p < 0.05$). The rank abundance curve consists of broken lines, and each broken line represents a group. The length of the broken line on the horizontal axis reflects the number of OTU in the specific abundance. The smoother the broken line, the smaller is difference of the OTU diversity in the community. As for the CT26 group and the PBS group, the abundance grade curve (**Supplementary Figure S3B**) demonstrated that the PBS group has higher community similarity than the CT26 group.

The data in **Figure 2D** showed that the composition of the GM in the two groups (CT26 group and PBS group) was

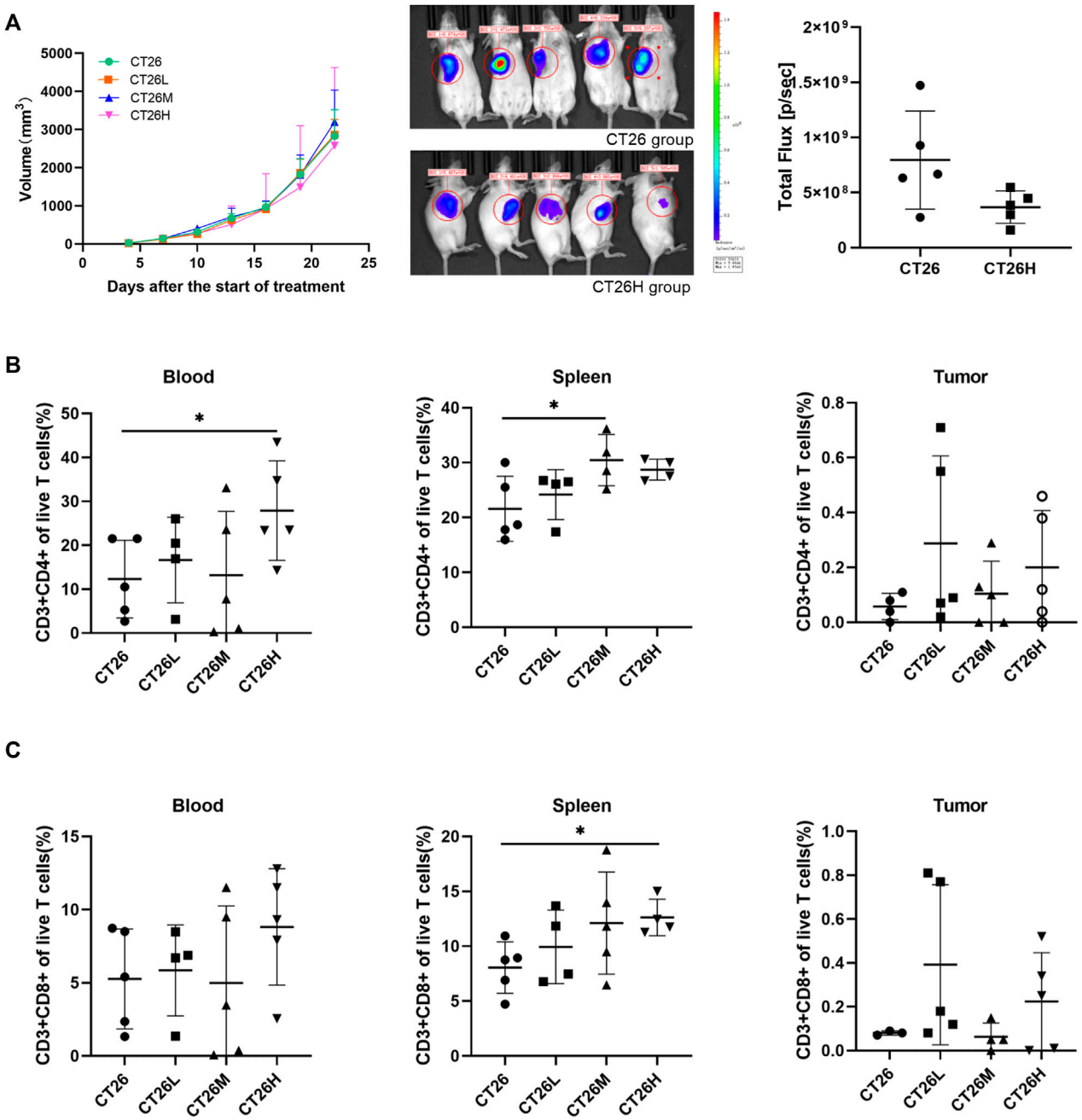

FIGURE 1 | Tumor volume and percentage of lymphocytes among the CT26 group and FFCT-treated groups. **(A)** Tumor volume among the CT26 group and FFCT-treated groups ($p > 0.05$). Percentage of $CD3^+CD4^+$ **(B)** and $CD3^+CD8^+$ T cells **(C)** in the blood, spleen, and tumor tissue of the CT26 tumor-bearing mice treated with FFCT. * represents $p < 0.05$.

mainly characterized by the *Firmicutes*, *Bacteroidetes*, *Proteobacteria*, *TM7*, and *Deferribacteres*. A marked difference between the two groups existed on the distribution of phyla. The abundance of *Firmicutes* and *Deferribacteres* in PBS group was higher than that in the CT26 group ($p < 0.05$), while the abundance of *Bacteroidetes* and *Actinobacteria* was lower ($p < 0.05$). As shown in **Figure 2E**, species composition in the two groups at the genus level was quite different as well. Species with high expression in the CT26 group were *Lactobacillus*, *Alistipes*, *Parabacteroides*, (*Prevotella*), *Adlercreutzia*, *Odoribacter*, *Bacteroides*, *Desulfovibrio*, *Turicibacter*, *Coprococcus*, and *Helicobacter*. The species with low expression in the CT26 group were *Rikenella*, *Oscillospira*, *Roseburia*, *Ruminococcus*,

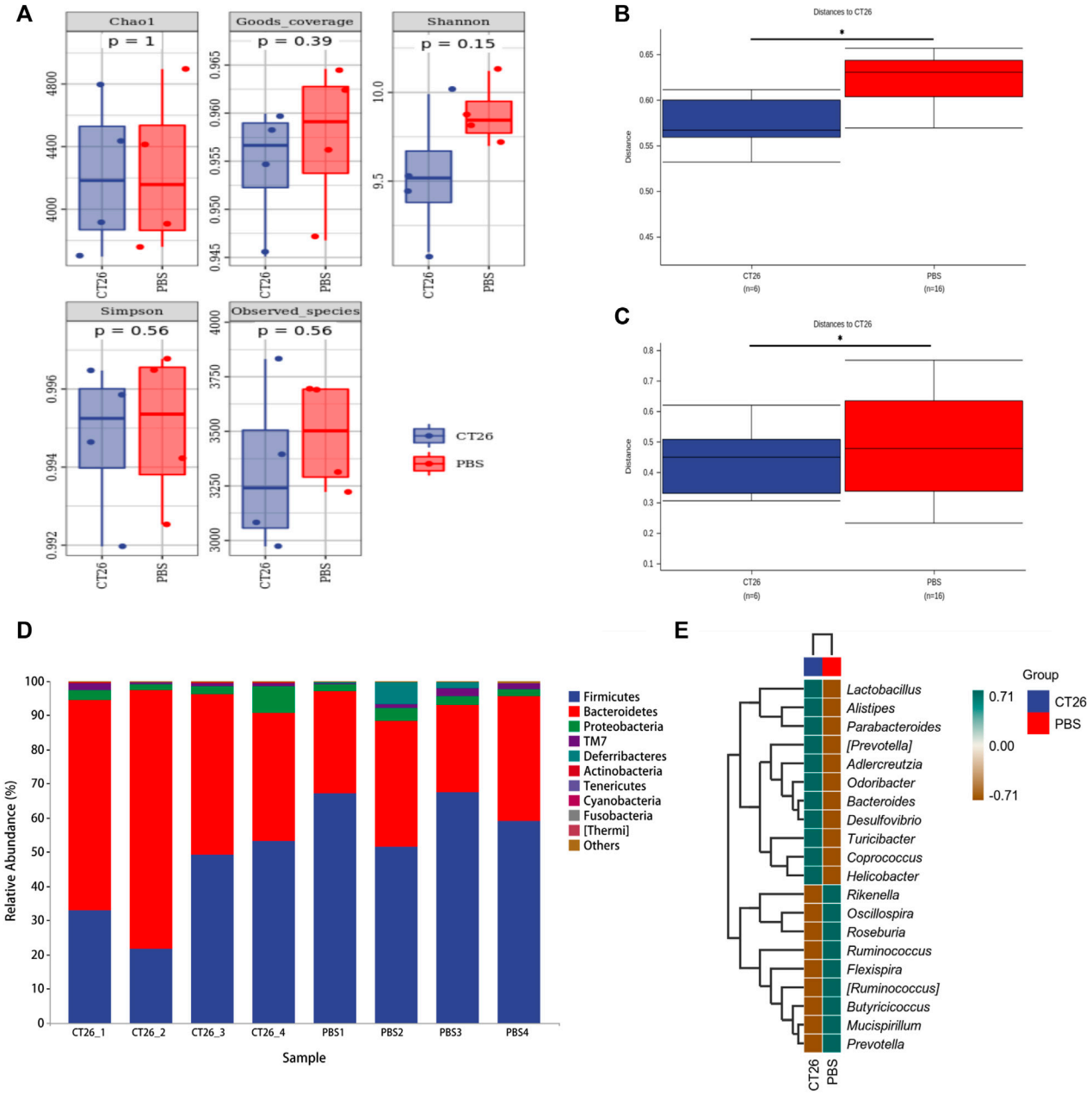

FIGURE 2 | GM differences between the CT26 group and the PBS group. **(A)** Diversity index analysis (Chao1, Good's coverage, Shannon, Simpson, and Observed species) between the CT26 group and the PBS group. **(B)** Differences in unweighted UniFrac distance between the CT26 group and the PBS group. **(C)** Differences in weighted UniFrac distance between the CT26 group and the PBS group. **(D)** Total gut bacterial relative abundance at the taxonomic rank of phylum. **(E)** Heat map of species composition of the gut microbiota in the CT26 group and the PBS group at the genus level. * represents $p < 0.05$.

Flexispira, (*Ruminococcus*), *Butyricicoccus*, *Mucispirillum*, and *Prevotella*.

Tumor-Induced Gut Microbiota Dysbiosis Could Affect Fufangchangtai Metabolites

A high dose of FFCT (2.6 mg/g) was used in tumor-bearing mice (CT26H group) and healthy mice (CM group) for the comparison of serum metabolism between the two groups. In the PCA plot (**Supplementary Figure S4**), the quality control (QC) samples were closely gathered in the center of the scoring chat, showing the good stability of the instrument detection in this experiment. Results of OPLS-DA plot and the top 50 differential metabolites between the CT26 and CM group are shown in **Supplementary Figure S5**, indicating the metabolism of the CT26 group before treatment. In the

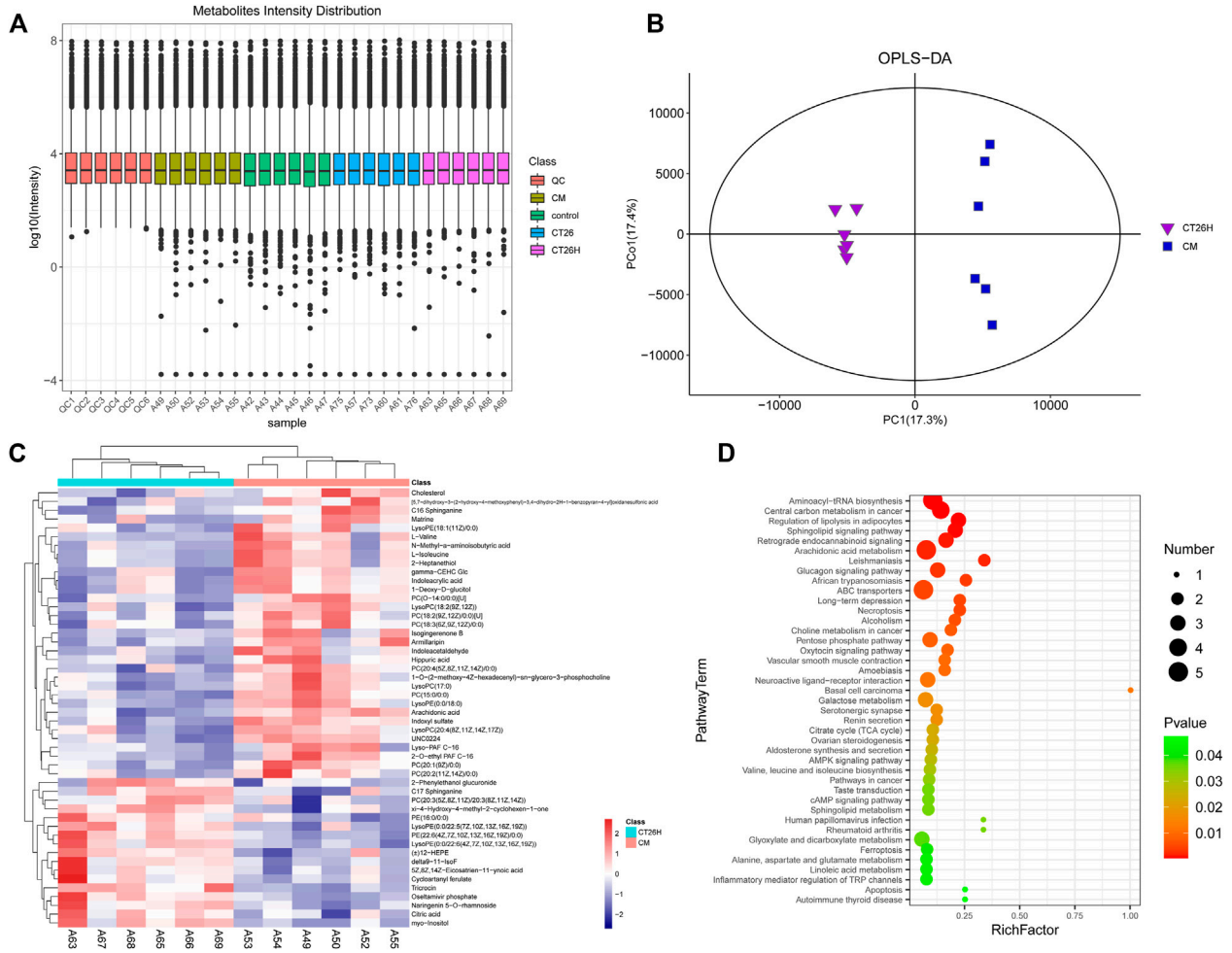

FIGURE 3 | Mass spectrum of serum metabolism in the CT26H and CM groups. **(A)** Metabolites Intensity Distribution box plot of all samples. **(B)** OPLS-DA score plot of the CT26H and CM groups. **(C)** Heat map of the top 50 differential metabolites between the CT26H and CM groups. **(D)** KEGG pathways enriched by significantly different metabolites between the CT26H and CM groups ($p < 0.05$).

Metabolites Intensity Distribution box plot (**Figure 3A**), the median line of each group was on a horizontal line, indicating that the samples were relatively stable. In addition, the dots represented the degree of dispersion, showing a relatively low dispersion in the CM group and CT26 group. The OPLS-DA plot can reflect the variability between the groups and within the groups, as well as the general distribution trend among different samples. OPLS-DA showed a clear separation between the CT26H and CM group, which indicated that the two groups indeed harbored significantly different bacterial microbiota (**Figure 3B**).

Overall, 243 differential metabolites were found between the CT26H group and the CM group. The top 50 differential metabolites and KEGG pathways enriched are shown in **Figures 3C,D**. Serum metabolites including cholesterol, matrine, isogingerenone B, armillaripin, hippuric acid, arachidonic acid, and amino acids (L-valine, N-methyl-a-aminoisobutytric acid, L-isoleucine) were mainly enriched in the CM group. Combined with network retrieval, matrine, isogingerenone B, and armillaripin are mainly related with TCM, indicating that the presence of tumor could affect the metabolism of FFCT (**Figure 3C**). The data in **Figure 3D** show that these differential metabolites were involved in multiple pathways including aminoacyl-tRNA biosynthesis, central carbon metabolism in cancer, regulation of lipolysis in adipocytes, sphingolipid signaling pathway, arachidonic acid metabolism, choline metabolism in cancer and ferroptosis, etc.

Disordered Gut Microbiota of CRC Patients Affected Fufangchangtai Metabolites

The above results showed that disordered GM in colorectal tumor-bearing mice altered the serum metabolome related to FFCT. However, the gut microbiota, or the tumor, that played the key role in the changes in the serum metabolome was unclear. A high dose of FFCT (2.6 mg/g) was used in the FMT-CA group (FMT-CA-FFCT group) and the FMT-H mice

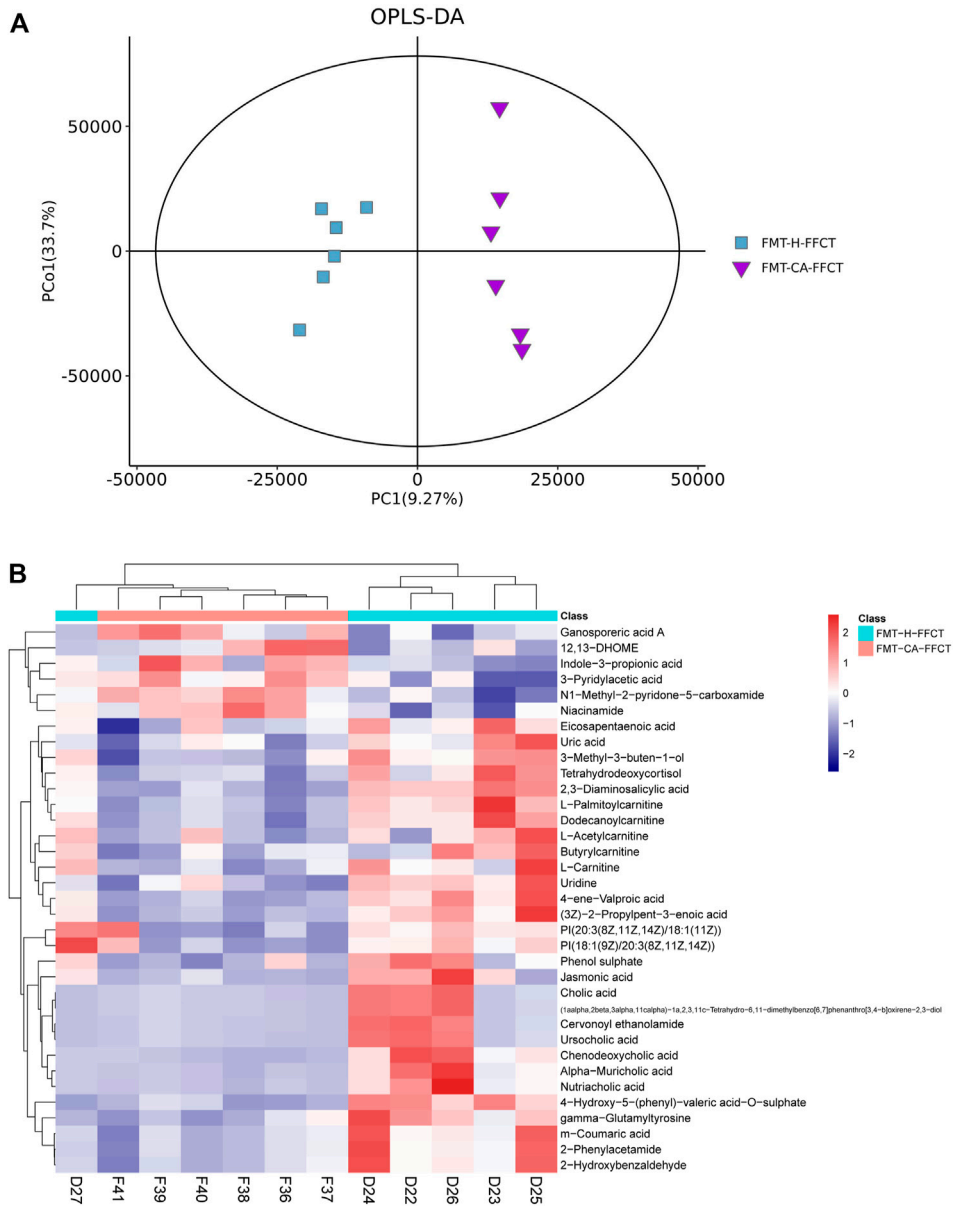

FIGURE 4 | Mass spectrum of serum metabolism in FMT mice. **(A)** OPLS-DA score plot of the FMT-CA-FFCT and FMT-H-FFCT groups. **(B)** Heat map of the top 50 different metabolites between the FMT-CA-FFCT and FMT-H-FFCT groups ($p < 0.05$).

(FMT-H-FFCT group) for the comparison of serum metabolism between the two groups excluding tumor factors. The PCA plot (**Supplementary Figure S6A**) and Metabolites Intensity Distribution box (**Supplementary Figure S6B**) indicate that the samples were relatively stable. As the OPLS-DA plot shows (**Figure 4A**), samples of the two groups (FMT-CA-FFCT and FMT-H-FFCT) were separated clearly, showing that there was certain difference between the two groups. There were 35 different metabolites between the FMT-CA-FFCT group and the FMT-H-FFCT group. The top 50 differential metabolites between the two groups were identified as listed in the hierarchical clustering heat map (*t*-test, $p < 0.05$; **Figure 4B**). Serum metabolites including uric acid, jasmonic acid, m-coumaric acid, cholic acid, ursocholic acid, chenodeoxycholic acid, gamma-glutamyltyrosine, and some kinds of amino acids (butyrylcarnitine, L-palmitoylcarnitine) were higher in the FMT-H-FFCT group than in the FMT-CA-FFCT group. Combined with network retrieval, jasmonic acid and m-coumaric acid are related to TCM, indicating that gut microbiota could affect the metabolism of FFCT as a single factor.

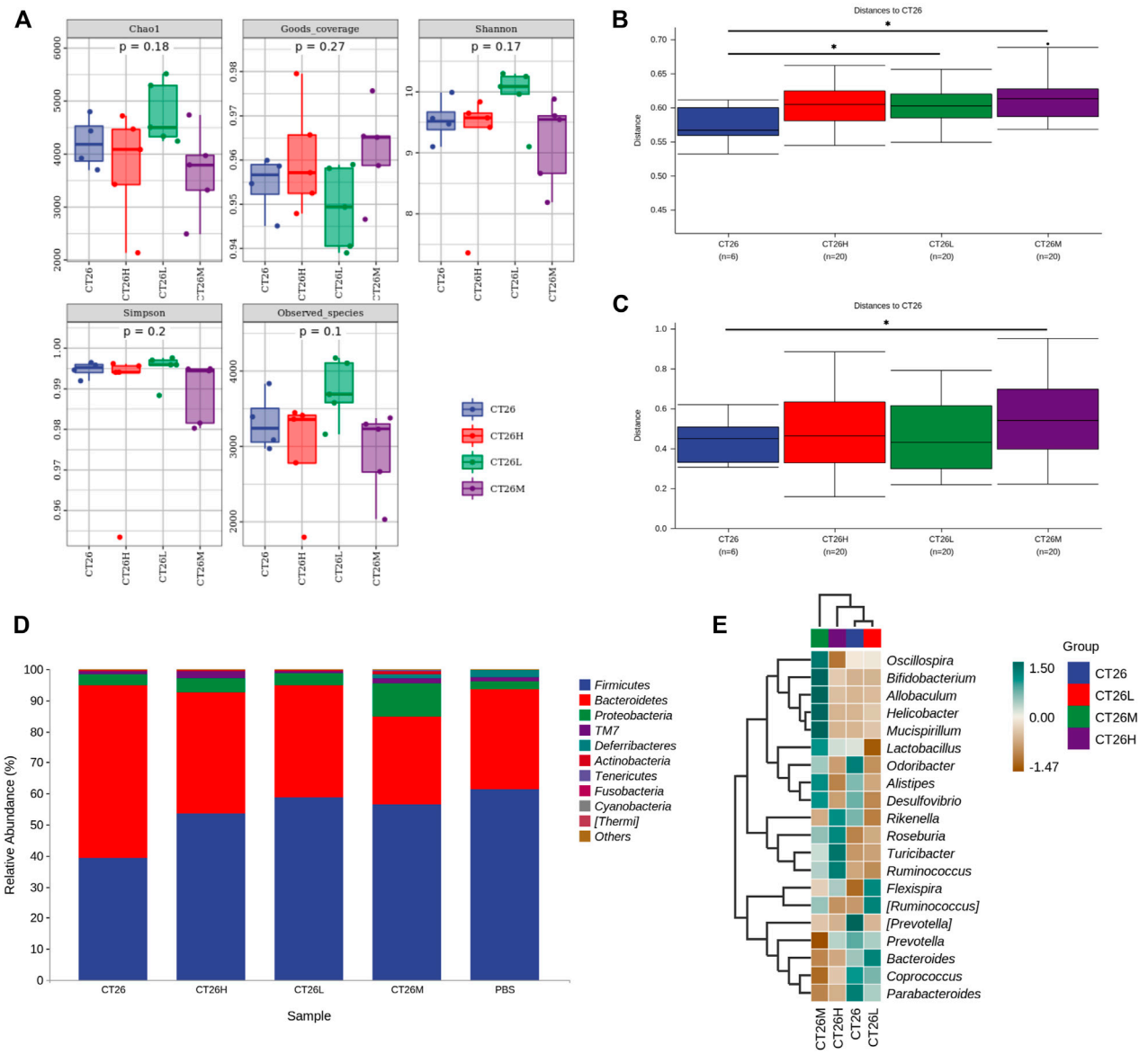

FIGURE 5 | GM differences between the CT26 group and the FFCT-treated groups. **(A)** Diversity index analysis (Chao1, Good's coverage, Shannon, Simpson, and Observed species) between the CT26 group and the FFCT-treated groups. **(B)** Differences in unweighted UniFrac distance between the CT26 group and the FFCT-treated groups. **(C)** Differences in weighted UniFrac distance between the CT26 group and the FFCT-treated groups. **(D)** Total gut bacterial relative abundance at the taxonomic rank of phylum. **(E)** Heat map of species composition of the gut microbiota in the CT26 group and the FFCT-treated groups at the genus level. * represents $p < 0.05$.

Fufangchangtai Ameliorated the Gut Microbiota in Tumor-Bearing Mice

As shown in the aforementioned results, GM and serum metabolism of FFCT between tumor-bearing group and healthy group were quite different. The dysbiosis of GM in tumor-bearing mice was corresponding to less serum metabolites that related to FFCT. Next, 16S rRNA gene sequencing was used to detect the effect of different doses of FFCT on the GM of tumor-bearing mice. As expected, compared with the CRC tumor-bearing group (CT26), FFCT-treated groups (CT26L, CT26M, CT26H) had different a composition of the GM. The PCoA diagram (**Supplementary Figure S7A**) showed that the species abundance composition of the CT26L and CT26M groups was different from the CT26 group (Adonis, $p < 0.05$). The abundance grade curve (**Supplementary Figure S7B**) showed that the FFCT-treated groups had higher community similarity than the CT26 group. The alpha diversity analysis (**Figure 5A**) showed that there were no significant differences in Chao1, Good's coverage, Shannon, Simpson, and Observed species indices between the CT26 group and the FFCT-treated groups (Dunn's test, $p > 0.05$).

However, beta diversity analysis using both unweighted and weighted UniFrac distances indicated that the medium dose FFCT-treated groups had higher dissimilarities among gut microbial communities than the CT26 group (Permanova, $p < 0.05$; **Figures 5B,C**).

The taxonomy in **Figure 5D** shows that the composition of GM in all the five groups was mainly characterized by *Firmicutes*, *Bacteroidetes*, *Proteobacteria*, *TM7*, and *Deferribacteres*. In the distribution of phyla, FFCT-treated groups had higher abundance of *Firmicutes* than the tumor-bearing group, which showed a similar trend with the healthy group. Moreover, with the increase in FFCT concentration, the abundance of *Firmicutes* was decreased. On the contrary, FFCT-treated groups had lower abundance of *Bacteroidetes* than the tumor-bearing group, which also showed a similar trend with the PBS group (Mann–Whitney U, $p > 0.05$). The CT26M group had the least abundance of *Bacteroidetes* and the most abundance of *Proteobacteria* and *Actinobacteria*.

As shown in **Figure 5E**, the following species had a high expression in the CT26 group but a low expression in the FFCT-treated groups: *Odoribacter*, (*Prevotella*), *Prevotella*, *Coprococcus*, and *Parabacteroides*. On the contrary, species like *Roseburia*, *Turicibacter*, and *Flexispira* in the CT26 group were much less expressed than in the FFCT-treated groups. Among these species, *Roseburia* and *Turicibacter* increased with an increase in FFCT concentration.

DISCUSSION

Nowadays, because of its multi-target effect and low toxicity, Chinese medicine has become an essential component in the adjuvant treatment of tumors. However, the mechanism of the therapeutic effect is still not understood. Studies showed that emodin could induce the cancer cell apoptosis via endoplasmic reticulum stress-dependent events, which produced reactive oxygen species (ROS) and regulated the signaling pathways (Zhang Y. et al., 2020). Qinrui Han *et al.* showed that bufarenogin induced intrinsic apoptosis through the cooperation of Bax and adenine nucleotide translocator (Han et al., 2021). Xiao-Qin Zhu *et al.* treated the CRC HCT-116 xenograft mouse model with Qingjie Fuzheng granules and found that this compound suppressed tumor cell proliferation through inhibiting the SHh pathway (Zhu et al., 2020). Yang Li *et al.* performed research on Gegen Qinlian decoction. They tested the immune cells, the cytokines, and the intestinal mucosa tight protein and showed that Gegen Qinlian decoction could enhance immunity and protect the intestinal barrier function by decreasing the relative abundance of *Megamonas* and *Veillonella* and increasing the relative abundance of *Bacteroides*, *Akkermansia*, and *Prevotella* (Li et al., 2020). As Yang's study showed, GM had become a considerable factor in the development and treatment of CRC (Yang and Yu, 2018). Jiyoung Ahn *et al.* tested the community of GM in a study of 47 CRC subjects and 94 control subjects. The authors found that the CRC subjects had a decreased overall microbial community diversity, showing the potentially modifiable nature of the GM and the difference in the GM between CRC patients and healthy people (Ahn et al., 2013). GM is an important part of intestinal mucosal barrier and intestinal immunity. Furthermore, GM can influence physiological and pathological processes of the whole body, including the bioavailability and metabolism of macronutrients and micronutrients as well as metabolites. The vast majority of Chinese medicine are absorbed through intestinal tract to achieve the therapeutic effect, so there is the hypothesis that the GM could affect the absorption and metabolism of Chinese medicine.

In this study, we selected Fufangchangtai (FFCT) as the model prescription drug. The previous multicenter, randomized, double-blind clinical trial found that FFCT improved life quality, improved immune function, and increased the median survival time of CRC patients (Li, 2019). However, the mechanism of its anti-tumor effect is unclear; thus, we chose FFCT as the research object.

Instead of the AOM/DSS induction mice model, the subcutaneous transplantation mice model was used as the CRC tumor-bearing mice model. The AOM/DSS induction mice model is developed by drug administration through the gastrointestinal tract, which not only affects the experimental results of the GM but also has the disadvantages of long modeling cycle, unstable effect, and high mortality. The subcutaneous transplantation mice model is more intuitive and makes the experimental results stable and reliable.

By measuring the tumor volume and fluorescence expression in the ROI, the statistical results showed that FFCT could inhibit the growth of tumor to a certain extent. Perhaps expanding the sample size would help to obtain significant statistical results. At the same time, immune cells including $CD4^+$ and $CD8^+$ T lymphocytes were detected and showed an obvious proliferation under the intervention of FFCT, which was consistent with the results of FFCT clinical research. Studies showed that $CD4^+$ T lymphocytes could take on activities in the immune response against tumor by secreting cytokines and activating $CD8^+$ T lymphocytes (Zheng et al., 2021). It has been shown that high expression of $CD8^+$ T cells linked to a good prognosis in multiple tumors, including colorectal cancer, esophageal cancer, and gastric cancer (Lee et al., 2018; Zhao Y. et al., 2019; Hao et al., 2020). Therefore, our results showed that FFCT exerted anti-tumor effect by enhancing the body's immune responses.

The GM in fecal samples of CRC mice and healthy mice showed that the abundance of *Firmicutes* decreased and *Bacteroidetes* increased in tumor-bearing mice, which were consistent with findings from clinical analysis of CRC patients (Abreu and Peek, 2014). Our study showed that *Coprococcus*, *Helicobacter*, *Desulfovibrio*, etc. had a higher expression in the CT26 group. *Coprococcus*, which is linked to butyrate production and SCFA metabolism (Lin et al., 2021; Liu et al., 2021), was found to be more prevalent in tumor-bearing mice. Sarah Vascellari's study proposed that the high expression of *Coprococcus* was associated with the development of gut inflammatory environment and gastrointestinal dysfunctions (Vascellari et al., 2021) are the pathological factors of CRC. *Helicobacter*, especially *helicobacter hepaticus*, can lead to an

increase in oxidative phosphorylation that may increase DNA-damaging free radicals (Wang et al., 2021). Verena Friedrich colonized a spontaneous fatal colitis transgenic mouse with *helicobacter hepaticus* and discovered that the disease progressed quickly, indicating that this type of bacteria was a disease driver in the colitis model and was not conducive to maintaining intestinal homeostasis (Friedrich et al., 2021). *Desulfovibrio* is considered the virulent bacterium that plays a role in destroying colonic mucosa and inducing intestinal inflammation and bacterial translocation (Yan et al., 2021). Because of the significant difference in the GM between the CRC tumor-bearing mice (CT26 group) and the healthy mice (PBS group), further study was allowed to be carried out in the tumor-bearing model mice.

We detected the serum metabolism of tumor-bearing mice and healthy mice after administration of FFCT to explore whether the dysbiosis of GM under the burden of tumor had an impact on serum metabolism that related to TCM. Metabolites that related to FFCT, such as matrine, isogingerenone B, and armillaripin, were higher in the CM group than in the CT26H group. Matrine is an alkaloid compound isolated from *Radix sophorae flavescentis*, one of the components of FFCT. Many studies showed that matrine has a significant anti-tumor effect (Zhang et al., 2019; Cheng et al., 2020; Gu et al., 2020). Yun Cheng *et al.* treated CRC cells with different concentrations of matrine and found out that matrine could suppress proliferation, migration, and invasion and induce apoptosis of CRC cells via the miR-10b/PTEN pathway (Cheng et al., 2020). Yawei Zhang *et al.* showed that matrine could inhibit SW480 cell survival by activating MIEF1-related mitochondrial division via the LATS2-Hippo pathway (Zhang et al., 2019). Chen Gu *et al.* found that matrine could block circSLC7A6 exosome secretion from cancer-associated fibroblasts. In addition, circSLC7A6 acted both as a promoter for CRC cell proliferation and inhibitor for apoptosis (Gu et al., 2020). Isogingerenone B and armillaripin can be detected, but not quantified in herbs. Studies showed that isogingerenone B was most likely formed from Curcumine (Endo et al., 1990). Curcumine could inhibit human colon cancer cellular growth through cell cycle arrest at the G2/M and G1 phases, as well as stimulated apoptosis by interacting with multiple molecular targets (Pricci et al., 2020). Armillaripin is a kind of proto IRU type sesquiterpenol aromatic ester that is isolated from the mycelium of *Armillaria mellea* (Yang et al., 1990). And sesquiterpenes have a wide range of biological activities, such as anti-tumor, anti-bacterial, anti-inflammatory, antiviral, and so on (Lu Li et al., 2018). The abovementioned three main different metabolites demonstrated that FFCT had a significant effect on cancer treatment. According to the findings, groups with healthy microbiota had more serum metabolites related to FFCT. To confirm that whether GM or tumor itself played the key role in the change of serum metabolome, we detected the serum metabolism of mice transplanted with feces from CRC patients and healthy people, respectively. Metabolites that related to FFCT-like jasmonic acid and m−coumaric acid were much less in the FMT-CA-FFCT group than in the FMT-H-FFCT group, indicating that GM could affect the metabolism of FFCT as a single factor. When combined with the findings of GM experiment, the conclusion could be summarized as follows: a relatively healthy intestinal flora and microenvironment was conducive to drug absorption and metabolism into the blood, resulting in a better therapeutic effect.

Further analysis of metabolic pathways showed that the therapeutic effect of FFCT might be predominantly relevant to the ability of regulating aminoacyl-tRNA biosynthesis, central carbon metabolism in cancer, regulation of lipolysis in adipocytes, and arachidonic acid metabolism. The aminoacyl-tRNA synthetases (ARSs) are an essential and universally distributed family of enzymes that plays a critical role in protein synthesis (Rubio Gomez and Ibba, 2020). Certain ARSs, such as isoleucyl-tRNA synthetase 2 (IARS2) and lysyl-tRNA synthetase (KRS), have been shown to promote colon cancer development. KRS was involved in colon cancer metastasis by inducing M2 macrophage polarization. Soluble factors secreted by M2 macrophages not only induced the activation of intracellular signals in cancer cells, but also activated the adjacent cancer-associated fibroblast, which ultimately remodeled the tumor microenvironment and exacerbated cancer metastasis (Nam et al., 2018). Central carbon metabolism traditionally includes the glycolysis pathway (EMP), pentose phosphate pathway (PPP), and tricarboxylic acid cycle (TCA), and it is the main source of energy required by organisms and provides precursors to other metabolisms in the body. Lipolysis in adipocytes is a key feature of some chronic diseases such as cancer-associated cachexia (CAC) (Yang et al., 2021). Thorhallur Agustsson *et al.*, made a point that although loss of adipose tissue may be less harmful than muscle loss in cancer cachexia, the former seems to precede the latter. Maybe early regulation of lipolysis in adipocytes could slow down or prevent the progressive wasting among cancer patients (Agustsson et al., 2007). The metabolism of arachidonic acid through cyclooxygenase (COX), lipoxygenase (LOX), and cytochrome P-450 epoxygenase (EPOX) pathways leads to the generation of various biologically active eicosanoids, and inhibition of these pathways has generally been shown to inhibit tumor growth/progression (Cathcart et al., 2011). These findings suggested that FFCT could not only regulate pathways related to the occurrence, growth, invasion, and metastasis of tumor, but also involve in substance synthesis and energy supplementation in serum metabolism.

Simultaneously, FFCT was administered to CRC tumor-bearing mice in order to observe GM changes in response to TCM intervention. It was found that the composition of GM in tumor-bearing mice differed significantly before and after FFCT administration. Many pieces of evidence demonstrated that *Firmicutes* was a phylum with documented anti-tumorigenic effects (Bader et al., 2018). *Bacteroidetes*, on the contrary, could drive DNA damages in colon epithelial cells as a potential "driver" of CRC (Tjalsma et al., 2012). As

the abundance of *Firmicutes* was higher and the abundance of *Bacteroidetes* was lower in the FFCT-treated groups, and *Firmicutes*/*Bacteroidetes* was generally regarded as having a significant relevance in the signaling of GM status (Ley et al., 2006). The results indicated that the imbalance of GM in tumor-bearing mice had been regulated by FFCT. The intervention of FFCT increased the abundance of *Turicibacter* and *Roseburia*, and as the FFCT concentration increased, the abundance of these two species increased. *Turicibacter* is involved in fermentation metabolism, and its main metabolite is lactic acid, which has the function of regulating the muscle and anti-fatigue. *Roseburia* can ferment a variety of carbohydrates, increase the content of butyric acid in the intestine, and prevent or treat obesity-related diseases. Studies showed that *Turicibacter* and *Roseburia* had a negative association with intestinal dystrophy (Zhong et al., 2022). Combining the research findings, it is concluded that FFCT altered the structure of GM while maintaining enteral nutrition. However, the specific intestinal protection mechanism needs to be studied further.

This study has limitations. Although there were immunological changes, FFCT showed no direct inhibitory effect on tumor. The combination of FFCT and immunotherapy could be considered to give full play to the anti-tumor effect. Gut microbiota and serum metabolism is a dynamic and complex process. Further studies on the interaction between specific active components of FFCT and targeted gut bacteria may shed more light on these mechanisms.

CONCLUSION

It was pointed out that GM dysbiosis under CRC burden blocked the absorption and metabolism of FFCT, indicating that a healthier intestinal microenvironment was conducive for better efficacy of FFCT. Moreover, FFCT could correct the imbalance in GM of CRC individuals. This study provided a new perspective on the therapeutic effect of FFCT by combining gut microbiota and serum metabolism, as well as a foundation for improving the GM status of CRC patients in clinical treatment, with the goal of achieving a better curative effect.

DATA AVAILABILITY STATEMENT

The datasets presented in this study can be found in online repositories. The names of the repository/repositories and accession number(s) can be found below: https://www.ncbi.nlm.nih.gov/bioproject/PRJNA815928

ETHICS STATEMENT

The studies involving human participants were reviewed and approved by the Medical Ethics Committee of Fudan University Shanghai Cancer Center. The patients/participants provided their written informed consent to participate in this study. The animal study was reviewed and approved by the Laboratory Animal Welfare and Ethics Management Committee of Shanghai Veterinary Research Institute. Written informed consent was obtained from the individual(s) for the publication of any potentially identifiable images or data included in this article.

AUTHOR CONTRIBUTIONS

MC performed the laboratory work and wrote the first draft. ZL developed the concept, managed the sample collection, and supervised the laboratory work and data analysis. YX and SR performed revised and contributed to writing the manuscript. JL, XW, SZ, and XC performed the laboratory work. JG and YM managed the sample collection. JH and ZC supervised, reviewed, and edited the manuscript. All authors read and approved the final manuscript.

FUNDING

This research was funded by the Jiangsu Postgraduate Research and Practice Innovation Program (No. SJCX20_0519), the Leading Talent Project of Jiangsu Province Traditional Chinese Medicine (No. SLJ0211), Jiangsu Digestive Tumor Clinical Medicine Innovation Center of Traditional Chinese Medicine (No. 2021-6), the Project of National Clinical Research Base of Traditional Chinese Medicine in Jiangsu Province (No. JD2019SZXYB02, JD2019SZXYB04), the Science and Technology Project of Jiangsu Administration of Traditional Chinese Medicine (No. JD201712), and the Shanghai Sailing Program (No. 19YF1458600).

ACKNOWLEDGMENTS

We acknowledge and appreciate our colleagues for their valuable efforts and comments on this manuscript.

SUPPLEMENTARY MATERIAL

The Supplementary Material for this article can be found online at: https://www.frontiersin.org/articles/10.3389/fphar.2022.889181/full#supplementary-material

REFERENCE

Abreu, M. T., and Peek, R. M. (2014). Gastrointestinal Malignancy and the Microbiome. *Gastroenterology* 146 (6), 1534–e3.e1533. doi:10.1053/j.gastro.2014.01.001

Agustsson, T., Rydén, M., Hoffstedt, J., van Harmelen, V., Dicker, A., Laurencikiene, J., et al. (2007). Mechanism of Increased Lipolysis in Cancer Cachexia. *Cancer Res.* 67 (11), 5531–5537. doi:10.1158/0008-5472.Can-06-4585

Ahn, J., Sinha, R., Pei, Z., Dominianni, C., Wu, J., Shi, J., et al. (2013). Human Gut Microbiome and Risk for Colorectal Cancer. *J. Natl. Cancer Inst.* 105 (24), 1907–1911. doi:10.1093/jnci/djt300

Bader, J. E., Enos, R. T., Velázquez, K. T., Carson, M. S., Nagarkatti, M., Nagarkatti, P. S., et al. (2018). Macrophage Depletion Using Clodronate Liposomes Decreases Tumorigenesis and Alters Gut Microbiota in the AOM/DSS Mouse Model of colon Cancer. *Am. J. Physiol. Gastrointest. Liver Physiol.* 314 (1), G22–g31. doi:10.1152/ajpgi.00229.2017

Bokulich, N. A., Kaehler, B. D., Rideout, J. R., Dillon, M., Bolyen, E., Knight, R., et al. (2018). Optimizing Taxonomic Classification of Marker-Gene Amplicon Sequences with QIIME 2's Q2-Feature-Classifier Plugin. *Microbiome* 6 (1), 90. doi:10.1186/s40168-018-0470-z

Bolyen, E., Rideout, J. R., Chase, J., Pitman, T. A., Shiffer, A., Mercurio, W., et al. (2018). An Introduction to Applied Bioinformatics: a Free, Open, and Interactive Text. *J. Open Source Educ.* 1 (5), 27. doi:10.21105/jose.00027

Callahan, B. J., McMurdie, P. J., Rosen, M. J., Han, A. W., Johnson, A. J., and Holmes, S. P. (2016). DADA2: High-Resolution Sample Inference from Illumina Amplicon Data. *Nat. Methods* 13 (7), 581–583. doi:10.1038/nmeth.3869

Castellanos, J. G., Woo, V., Viladomiu, M., Putzel, G., Lima, S., Diehl, G. E., et al. (2018). Microbiota-Induced TNF-like Ligand 1A Drives Group 3 Innate Lymphoid Cell-Mediated Barrier Protection and Intestinal T Cell Activation during Colitis. *Immunity* 49 (6), 1077–e5.e1075. doi:10.1016/j.immuni.2018.10.014

Cathcart, M. C., Lysaght, J., and Pidgeon, G. P. (2011). Eicosanoid Signalling Pathways in the Development and Progression of Colorectal Cancer: Novel Approaches for Prevention/intervention. *Cancer Metastasis Rev.* 30 (3-4), 363–385. doi:10.1007/s10555-011-9324-x

Cheng, Y., Yu, C., Li, W., He, Y., and Bao, Y. (2020). Matrine Inhibits Proliferation, Invasion, and Migration and Induces Apoptosis of Colorectal Cancer Cells via miR-10b/PTEN Pathway. *Cancer Biother. Radiopharm.* doi:10.1089/cbr.2020.3800

Church, D. L., Cerutti, L., Gürtler, A., Griener, T., Zelazny, A., and Emler, S. (2020). Performance and Application of 16S rRNA Gene Cycle Sequencing for Routine Identification of Bacteria in the Clinical Microbiology Laboratory. *Clin. Microbiol. Rev.* 33 (4), e00053-19. doi:10.1128/cmr.00053-19

Eckburg, P. B., Bik, E. M., Bernstein, C. N., Purdom, E., Dethlefsen, L., Sargent, M., et al. (2005). Diversity of the Human Intestinal Microbial flora. *Science* 308 (5728), 1635–1638. doi:10.1126/science.1110591

El Joumaa, M. M., Taleb, R. I., Rizk, S., and Borjac, J. M. (2020). Protective Effect of Matricaria Chamomilla Extract against 1,2-Dimethylhydrazine-Induced Colorectal Cancer in Mice. *J. Complement. Integr. Med.* 17 (3). doi:10.1515/jcim-2019-0143

Endo, K., Kanno, E., and Oshima, Y. (1990). Structures of Antifungal Diarylheptenones, Gingerenones A, B, C and Isogingerenone B, Isolated from the Rhizomes of Zingiber Officinale. *Phytochemistry* 29 (3), 797–799. doi:10.1016/0031-9422(90)80021-8

Fidelle, M., Yonekura, S., Picard, M., Cogdill, A., Hollebecque, A., Roberti, M. P., et al. (2020). Resolving the Paradox of Colon Cancer through the Integration of Genetics, Immunology, and the Microbiota. *Front. Immunol.* 11, 600886. doi:10.3389/fimmu.2020.600886

Friedrich, V., Forné, I., Matzek, D., Ring, D., Popper, B., Jochum, L., et al. (2021). Helicobacter Hepaticus Is Required for Immune Targeting of Bacterial Heat Shock Protein 60 and Fatal Colitis in Mice. *Gut Microbes* 13 (1), 1–20. doi:10.1080/19490976.2021.1882928

Gagnière, J., Raisch, J., Veziant, J., Barnich, N., Bonnet, R., Buc, E., et al. (2016). Gut Microbiota Imbalance and Colorectal Cancer. *World J. Gastroenterol.* 22 (2), 501–518. doi:10.3748/wjg.v22.i2.501

Gu, C., Lu, H., and Qian, Z. (2020). Matrine Reduces the Secretion of Exosomal circSLC7A6 from Cancer-Associated Fibroblast to Inhibit Tumorigenesis of Colorectal Cancer by Regulating CXCR5. *Biochem. Biophys. Res. Commun.* 527 (3), 638–645. doi:10.1016/j.bbrc.2020.04.142

Han, Q., Zhang, C., Zhang, Y., Li, Y., Wu, L., and Sun, X. (2021). Bufarenogin Induces Intrinsic Apoptosis via Bax and ANT Cooperation. *Pharmacol. Res. Perspect.* 9 (1), e00694. doi:10.1002/prp2.694

Hao, J., Li, M., Zhang, T., Yu, H., Liu, Y., Xue, Y., et al. (2020). Prognostic Value of Tumor-Infiltrating Lymphocytes Differs Depending on Lymphocyte Subsets in Esophageal Squamous Cell Carcinoma: An Updated Meta-Analysis. *Front. Oncol.* 10, 614. doi:10.3389/fonc.2020.00614

Jian, X., Zhu, Y., Ouyang, J., Wang, Y., Lei, Q., Xia, J., et al. (2020). Alterations of Gut Microbiome Accelerate Multiple Myeloma Progression by Increasing the Relative Abundances of Nitrogen-Recycling Bacteria. *Microbiome* 8 (1), 74. doi:10.1186/s40168-020-00854-5

Katoh, K., Misawa, K., Kuma, K., and Miyata, T. (2002). MAFFT: a Novel Method for Rapid Multiple Sequence Alignment Based on Fast Fourier Transform. *Nucleic Acids Res.* 30 (14), 3059–3066. doi:10.1093/nar/gkf436

Kõljalg, U., Nilsson, R. H., Abarenkov, K., Tedersoo, L., Taylor, A. F., Bahram, M., et al. (2013). Towards a Unified Paradigm for Sequence-Based Identification of Fungi. *Mol. Ecol.* 22 (21), 5271–5277. doi:10.1111/mec.12481

Lee, J. S., Won, H. S., Sun, S., Hong, J. H., and Ko, Y. H. (2018). Prognostic Role of Tumor-Infiltrating Lymphocytes in Gastric Cancer: A Systematic Review and Meta-Analysis. *Medicine (Baltimore)* 97 (32), e11769. doi:10.1097/md.0000000000011769

Ley, R. E., Turnbaugh, P. J., Klein, S., and Gordon, J. I. (2006). Microbial Ecology: Human Gut Microbes Associated with Obesity. *Nature* 444 (7122), 1022–1023. doi:10.1038/4441022a

Li, L. (2019). *Randomized, Double-Blind Controlled Study of Fufangchangtai Granule in the Treatment of colon Cancer*. Doctoral Dissertation. Nanjing: Nanjing University of Chinese Medicine.

Li, Y., Li, Z. X., Xie, C. Y., Fan, J., Lv, J., Xu, X. J., et al. (2020). Gegen Qinlian Decoction Enhances Immunity and Protects Intestinal Barrier Function in Colorectal Cancer Patients via Gut Microbiota. *World J. Gastroenterol.* 26 (48), 7633–7651. doi:10.3748/wjg.v26.i48.7633

Lin, L., Trabi, E. B., Xie, F., and Mao, S. (2021). Comparison of the Fermentation and Bacterial Community in the colon of Hu Sheep Fed a Low-Grain, Non-pelleted, or Pelleted High-Grain Diet. *Appl. Microbiol. Biotechnol.* 105 (5), 2071–2080. doi:10.1007/s00253-021-11158-5

Liu, C., Du, P., Cheng, Y., Guo, Y., Hu, B., Yao, W., et al. (2021). Study on Fecal Fermentation Characteristics of Aloe Polysaccharides *In Vitro* and Their Predictive Modeling. *Carbohydr. Polym.* 256, 117571. doi:10.1016/j.carbpol.2020.117571

Lu Li, S. W., Ma, L. Y., Liu, Q. S., Zhong, B. C., and Zhang, H. F. (2018). The Active Constituents and the Medicinal Value of the Armillariamellea. *J. Jilin Med. Univ.* 39 (04), 307–310.

Martin, M. (2011). Cutadapt Removes Adapter Sequences from High-Throughput Sequencing Reads. *EMBnet j.* 17, 10–12. doi:10.14806/ej.17.1.200

Miller, K. D., Fidler-Benaoudia, M., Keegan, T. H., Hipp, H. S., Jemal, A., and Siegel, R. L. (2020). Cancer Statistics for Adolescents and Young Adults, 2020. *CA Cancer J. Clin.* 70 (1), 443–459. doi:10.3322/caac.2159010.3322/caac.21637

Milosevic, I., Vujovic, A., Barac, A., Djelic, M., Korac, M., Radovanovic Spurnic, A., et al. (2019). Gut-Liver Axis, Gut Microbiota, and its Modulation in the Management of Liver Diseases: A Review of the Literature. *Int. J. Mol. Sci.* 20 (2). doi:10.3390/ijms20020395

Nam, S. H., Kim, D., Lee, D., Lee, H. M., Song, D. G., Jung, J. W., et al. (2018). Lysyl-tRNA Synthetase-Expressing colon Spheroids Induce M2 Macrophage Polarization to Promote Metastasis. *J. Clin. Invest.* 128 (11), 5034–5055. doi:10.1172/JCI99806

Niccolai, E., Russo, E., Baldi, S., Ricci, F., Nannini, G., Pedone, M., et al. (2020). Significant and Conflicting Correlation of IL-9 with Prevotella and Bacteroides in Human Colorectal Cancer. *Front. Immunol.* 11, 573158. doi:10.3389/fimmu.2020.573158

Pricci, M., Girardi, B., Giorgio, F., Losurdo, G., Ierardi, E., and Di Leo, A. (2020). Curcumin and Colorectal Cancer: From Basic to Clinical Evidences. *Int. J. Mol. Sci.* 21 (7), 2364. doi:10.3390/ijms21072364

Price, M. N., Dehal, P. S., and Arkin, A. P. (2009). FastTree: Computing Large Minimum Evolution Trees with Profiles Instead of a Distance Matrix. *Mol. Biol. Evol.* 26 (7), 1641–1650. doi:10.1093/molbev/msp077

Ramakrishna, B. S. (2013). Role of the Gut Microbiota in Human Nutrition and Metabolism. *J. Gastroenterol. Hepatol.* 28 Suppl 4, 9–17. doi:10.1111/jgh.12294

Rubio Gomez, M. A., and Ibba, M. (2020). Aminoacyl-tRNA Synthetases. *Rna* 26 (8), 910–936. doi:10.1261/rna.071720.119

Sobhani, I., Tap, J., Roudot-Thoraval, F., Roperch, J. P., Letulle, S., Langella, P., et al. (2011). Microbial Dysbiosis in Colorectal Cancer (CRC) Patients. *PLoS One* 6 (1), e16393. doi:10.1371/journal.pone.0016393

Sui, H., Zhang, L., Gu, K., Chai, N., Ji, Q., Zhou, L., et al. (2020). YYFZBJS Ameliorates Colorectal Cancer Progression in ApcMin/+ Mice by Remodeling Gut Microbiota and Inhibiting Regulatory T-Cell Generation. *Cell Commun Signal* 18 (1), 113. doi:10.1186/s12964-020-00596-9

Tian, Y., Wang, Z., Liu, X., Duan, J., Feng, G., Yin, Y., et al. (2018). Prediction of Chemotherapeutic Efficacy in Non-small Cell Lung Cancer by Serum Metabolomic Profiling. *Clin. Cancer Res.* 24 (9), 2100–2109. doi:10.1158/1078-0432.Ccr-17-2855

Tjalsma, H., Boleij, A., Marchesi, J. R., and Dutilh, B. E. (2012). A Bacterial Driver-Passenger Model for Colorectal Cancer: beyond the Usual Suspects. *Nat. Rev. Microbiol.* 10 (8), 575–582. doi:10.1038/nrmicro2819

Tsoi, H., Chu, E. S. H., Zhang, X., Sheng, J., Nakatsu, G., Ng, S. C., et al. (2017). Peptostreptococcus Anaerobius Induces Intracellular Cholesterol Biosynthesis in Colon Cells to Induce Proliferation and Causes Dysplasia in Mice. *Gastroenterology* 152 (6), 1419–e5.e1415. doi:10.1053/j.gastro.2017.01.009

Vascellari, S., Melis, M., Palmas, V., Pisanu, S., Serra, A., Perra, D., et al. (2021). Clinical Phenotypes of Parkinson's Disease Associate with Distinct Gut Microbiota and Metabolome Enterotypes. *Biomolecules* 11 (2). doi:10.3390/biom11020144

Wang, J. (2018). *Mechanisms Of FFCT on Inducing Autophagy of colon Cancer Cells and Promoting Polarization of Tumor-Associated Macrophages*. Doctoral Dissertation. Nanjing: Nangjing Medical University.

Wang, Z., Fu, H., Zhou, Y., Yan, M., Chen, D., Yang, M., et al. (2021). Identification of the Gut Microbiota Biomarkers Associated with Heat Cycle and Failure to Enter Oestrus in Gilts. *Microb. Biotechnol.* 14 (4), 1316–1330. doi:10.1111/1751-7915.13695

Wu, S., Rhee, K. J., Albesiano, E., Rabizadeh, S., Wu, X., Yen, H. R., et al. (2009). A Human Colonic Commensal Promotes colon Tumorigenesis via Activation of T Helper Type 17 T Cell Responses. *Nat. Med.* 15 (9), 1016–1022. doi:10.1038/nm.2015

Xu, J., Chen, H. B., and Li, S. L. (2017). Understanding the Molecular Mechanisms of the Interplay between Herbal Medicines and Gut Microbiota. *Med. Res. Rev.* 37 (5), 1140–1185. doi:10.1002/med.21431

Xu, S. Y., and Chen, R. B. X. (1992). *Pharmacology Experimental Methodology (2nd Edition)*. Chin Pharmacol Bull (01), 19.

Yan, S., Tian, S., Meng, Z., Teng, M., Sun, W., Jia, M., et al. (2021). Exposure to Nitenpyram during Pregnancy Causes Colonic Mucosal Damage and Non-alcoholic Steatohepatitis in Mouse Offspring: The Role of Gut Microbiota. *Environ. Pollut.* 271, 116306. doi:10.1016/j.envpol.2020.116306

Yang, J., and Yu, J. (2018). The Association of Diet, Gut Microbiota and Colorectal Cancer: what We Eat May Imply what We Get. *Protein Cell* 9 (5), 474–487. doi:10.1007/s13238-018-0543-6

Yang, Y. H., Hao, Y. M., Liu, X. F., Gao, X., Wang, B. Z., Takahashi, K., et al. (2021). Docosahexaenoic Acid-Enriched Phospholipids and Eicosapentaenoic Acid-Enriched Phospholipids Inhibit Tumor Necrosis Factor-Alpha-Induced Lipolysis in 3T3-L1 Adipocytes by Activating Sirtuin 1 Pathways. *Food Funct.* 12 (11), 4783–4796. doi:10.1039/d1fo00157d

Yang, Y. S., Wang, Y. L., Feng, X. Z., Yu, D. Q., Liang, X. T., He, C. H., et al. (1990). Studies on the Chemical Constituents of Armillaria Mellea Mycelium–VI. Isolation and Structure of Armillaripin. *J. Pharm.* (05), 353–356. doi:10.16438/j.0513-4870.1990.05.008

Yu, Y. N., Yu, T. C., Zhao, H. J., Sun, T. T., Chen, H. M., Chen, H. Y., et al. (2015). Berberine May rescue Fusobacterium Nucleatum-Induced Colorectal Tumorigenesis by Modulating the Tumor Microenvironment. *Oncotarget* 6 (31), 32013–32026. doi:10.18632/oncotarget.5166

Zackular, J. P., Baxter, N. T., Iverson, K. D., Sadler, W. D., Petrosino, J. F., Chen, G. Y., et al. (2013). The Gut Microbiome Modulates Colon Tumorigenesis. *Mbio 4(6)*. doi:10.1128/mBio.00692-13

Zhang, Y., Pu, W., Bousquenaud, M., Cattin, S., Zaric, J., Sun, L. K., et al. (2020a). Emodin Inhibits Inflammation, Carcinogenesis, and Cancer Progression in the AOM/DSS Model of Colitis-Associated Intestinal Tumorigenesis. *Front. Oncol.* 10, 564674. doi:10.3389/fonc.2020.564674

Zhang, Y., Wang, M., Xu, X., Liu, Y., and Xiao, C. (2019). Matrine Promotes Apoptosis in SW480 Colorectal Cancer Cells via Elevating MIEF1-Related Mitochondrial Division in a Manner Dependent on LATS2-Hippo Pathway. *J. Cel Physiol* 234 (12), 22731–22741. doi:10.1002/jcp.28838

Zhang, Z., Shao, S., Zhang, Y., Jia, R., Hu, X., Liu, H., et al. (2020b). Xiaoyaosan Slows Cancer Progression and Ameliorates Gut Dysbiosis in Mice with Chronic Restraint Stress and Colorectal Cancer Xenografts. *Biomed. Pharmacother.* 132, 110916. doi:10.1016/j.biopha.2020.110916

Zhao, R. S., Coker, O. O., Wu, J. L., Zhao, L. Y., Nakatsu, D., Bian, X. Q., et al. (2019a). Gut Microbiota Modulates the Chemopreventive Efficacy of Aspirin on Colon Cancer through Reducing Aspirin Bioavailability. *Gastroenterology* 156 (6), S133. doi:10.1016/s0016-5085(19)37121-5

Zhao, Y., Ge, X., He, J., Cheng, Y., Wang, Z., Wang, J., et al. (2019b). The Prognostic Value of Tumor-Infiltrating Lymphocytes in Colorectal Cancer Differs by Anatomical Subsite: a Systematic Review and Meta-Analysis. *World J. Surg. Oncol.* 17 (1), 85. doi:10.1186/s12957-019-1621-9

Zheng, X., Jin, W., Wang, S., and Ding, H. (2021). Progression on the Roles and Mechanisms of Tumor-Infiltrating T Lymphocytes in Patients with Hepatocellular Carcinoma. *Front. Immunol.* 12, 729705. doi:10.3389/fimmu.2021.729705

Zhong, N., Ma, Y., Meng, X., Sowanou, A., Wu, L., Huang, W., et al. (2022). Effect of Fluoride in Drinking Water on Fecal Microbial Community in Rats. *Biol. Trace Elem. Res.* 200 (1), 238–246. doi:10.1007/s12011-021-02617-1

Zhu, X. Q., Yang, H., Lin, M. H., Shang, H. X., Peng, J., Chen, W. J., et al. (2020). Qingjie Fuzheng Granules Regulates Cancer Cell Proliferation, Apoptosis and Tumor Angiogenesis in Colorectal Cancer Xenograft Mice via Sonic Hedgehog Pathway. *J. Gastrointest. Oncol.* 11 (6), 1123–1134. doi:10.21037/jgo-20-213

Conflict of Interest: The authors declare that the research was conducted in the absence of any commercial or financial relationships that could be construed as a potential conflict of interest.

Publisher's Note: All claims expressed in this article are solely those of the authors and do not necessarily represent those of their affiliated organizations, or those of the publisher, the editors, and the reviewers. Any product that may be evaluated in this article, or claim that may be made by its manufacturer, is not guaranteed or endorsed by the publisher.

frontiers | Frontiers in Pharmacology

ORIGINAL RESEARCH
published: 02 June 2022
doi: 10.3389/fphar.2022.873053

Emodin Ameliorates Acute Pancreatitis-Associated Lung Injury Through Inhibiting the Alveolar Macrophages Pyroptosis

*Xiajia Wu[1†], Jiaqi Yao[1†], Qian Hu[1], Hongxin Kang[1], Yifan Miao[1], Lv Zhu[1], Cong Li[2], Xianlin Zhao[1], Juan Li[1], Meihua Wan[1] and Wenfu Tang[1]**

[1]Department of Integrated Traditional Chinese and Western Medicine, West China Hospital, Sichuan University, Chengdu, China, [2]Research Core Facility, West China Hospital, Sichuan University, Chengdu, China

Objective: To investigate the protective effect of emodin in acute pancreatitis (AP)-associated lung injury and the underlying mechanisms.

Methods: NaT-AP model in rats was constructed using 3.5% sodium taurocholate, and CER+LPS-AP model in mice was constructed using caerulein combined with Lipopolysaccharide. Animals were divided randomly into four groups: sham, AP, Ac-YVAD-CMK (caspase-1 specific inhibitor, AYC), and emodin groups. AP-associated lung injury was assessed with H&E staining, inflammatory cytokine levels, and myeloperoxidase activity. Alveolar macrophages (AMs) pyroptosis was evaluated by flow cytometry. In bronchoalveolar lavage fluid, the levels of lactate dehydrogenase and inflammatory cytokines were measured by enzyme-linked immunosorbent assay. Pyroptosis-related protein expressions were detected by Western Blot.

Results: Emodin, similar to the positive control AYC, significantly alleviated pancreas and lung damage in rats and mice. Additionally, emodin mitigated the pyroptotic process of AMs by decreasing the level of inflammatory cytokines and lactate dehydrogenase. More importantly, the protein expressions of NLRP3, ASC, Caspase1 p10, GSDMD, and GSDMD-NT in AMs were significantly downregulated after emodin intervention.

Conclusion: Emodin has a therapeutic effect on AP-associated lung injury, which may result from the inhibition of NLRP3/Caspase1/GSDMD-mediated AMs pyroptosis signaling pathways.

Keywords: emodin, NLRP3 inflammasome, alveolar macrophage, pyroptosis, acute pancreatitis, acute lung injury

OPEN ACCESS

Edited by:
Mingyu Sun,
Shanghai University of Traditional Chinese Medicine, China

Reviewed by:
Qinghe Meng,
Upstate Medical University, United States
Cheng Zhang,
Anhui Medical University, China

***Correspondence:**
Wenfu Tang
tangwf@scu.edu.cn

†These authors have contributed equally to this work

Specialty section:
This article was submitted to Gastrointestinal and Hepatic Pharmacology, a section of the journal Frontiers in Pharmacology

Received: *10 February 2022*
Accepted: *13 May 2022*
Published: *02 June 2022*

Citation:
Wu X, Yao J, Hu Q, Kang H, Miao Y, Zhu L, Li C, Zhao X, Li J, Wan M and Tang W (2022) Emodin Ameliorates Acute Pancreatitis-Associated Lung Injury Through Inhibiting the Alveolar Macrophages Pyroptosis. Front. Pharmacol. 13:873053. doi: 10.3389/fphar.2022.873053

INTRODUCTION

Acute pancreatitis (AP) is one kind of inflammatory diseases of the pancreas with early local symptoms (e.g., pancreatic edema, abdominal pain, and distension *et al*) and followed by systemic inflammatory response (Xiao et al., 2016). Progression of AP into severe acute pancreatitis (SAP) usually leads to a life-threatening condition with multiple organ dysfunction, particularly acute lung injury (ALI), which is the cause of most deaths during the early phase of AP (Akbarshahi et al., 2012). Accumulating evidence has indicated that the overactivated immune system together with excessive inflammatory response plays a

significant role in the disease progression (Zhang et al., 2016; Kumar, 2020). Therefore, how to effectively constrain local inflammatory response and attenuate AP-related lung injury (SAP-ALI) is key to improving the prognosis of AP and reducing mortality rate among early-stage AP patients.

Emodin is an anthraquinone compound, mainly derived from *rhubarb*, *Polygonum cuspidatum,* and other natural plants (Dong et al., 2016), which has been confirmed to possess anti-inflammatory bioactivity (Xue et al., 2015; Li et al., 2016). In recent years, numerous researches have reported the beneficial effects of emodin against AP progression *in vivo* and *in vitro* (Xu et al., 2016; Xia et al., 2019). Specifically, emodin was proved to ameliorate LPS-induced ALI by inhibiting the release of pulmonary inflammatory cytokines in rats and significantly reduce CIRP-activated inflammatory signaling pathways in rat alveolar macrophages (AMs) (Li et al., 2020; Xu et al., 2021). However, the effect and mechanism of emodin on SAP-ALI remain elusive.

Recently, The NOD-like receptor protein 3 (NLRP3) inflammasome, an intracytoplasmic multiprotein complex, containing NLRP3, apoptosis-associated speck-like protein (ASC) and procaspase-1, has been confirmed to participate in mediating the inflammatory damage process of ALI (Wu et al., 2013; Grailer et al., 2014). Activation of the NLRP3 inflammasome triggers caspase1 maturation and eventually induces caspase1-dependent pyroptosis, a new form of programmed cell death, characterized by pore-formation in the cell membrane, cell rupture, and the leakage of cytoplasmic contents (Shi et al., 2015). Moreover, a caspase-1 inhibitor Ac-YVAD-CMK (AYC) has been reported to alleviate LPS-induced lung injury by inhibiting caspase1-dependent AMs pyroptosis (Wu et al., 2015). AMs account for the major leukocyte population in the airways, through secreting a variety of inflammatory cytokines that can affect the development of ALI drastically under infectious or non-infectious conditions (Gordon et al., 2014; Murray et al., 2014). A growing body of evidence suggests that inflammation and cell death interplay with each other to create a cycle of auto-amplification that leads to further expansion of the inflammatory response. Extensive studies have demonstrated that AMs pyroptosis plays a critical role in acute lung inflammatory injury under various pathogenic conditions (e.g., endotoxin, mechanical ventilation, and *Streptococcus aureus*) (Wu et al., 2015; Yang et al., 2016; Yao and Sun, 2019). Notably, a recent study has demonstrated exosome-mediated activation of NLRP3 inflammasome and the consequent AMs pyroptosis might serve as a potential target for AP treatment (Wu et al., 2020). However, the effect of emodin on NLRP3 inflammasome-dependent AMs pyroptosis during SAP-ALI remains unclear.

To tackle this issue, we established two AP models of pancreatic ductal infusion of sodium taurocholate (NaT-AP) in rats and intraperitoneal injections with caerulein plus LPS (CER+LPS-AP) in mice and investigated the underlying mechanism of emodin on AP-related ALI.

MATERIALS AND METHODS

Animals

Thirty-two male Sprague-Dawley rats (200–250g) and thirty-two C57BL/6J mice (22–25 g) were purchased from the Jiangan Laboratory Animal Center of the Sichuan University (Chengdu, China). All animals were housed in a controlled environment (temperature: 22 ± 2°C, humidity: 65 ± 10%) and received standard chow and water. Rats and mice received adapted feeding for 7 days and fasted for 24 h before AP induction. All the animal experiments were conducted in West China Science and Technology Park of Sichuan University and approved by the Experimental Animal Ethics Committee of the Sichuan University of West China Hospital (protocol number: 2020013A).

Reagents and Antibodies

Sodium taurocholate (909688) was purchased from Bailingwei Technology Co., LTD. (Beijing, China) and emodin was obtained from Beijing Zhongke Quality Inspection (Beijing, China). Caerulein (C9026), LPS (L2880) and Ac-YVAD-CMK (SML0429) were purchased from Sigma-Aldrich (United States). Sodium pentobarbital (B5646) was purchased from Baoxin Biotechnology Co., LTD. (Chengdu, China). Anti-NLRP3 (ab263899), anti-GSDMD (ab219800) and anti-GSDMD-NT (ab215203) were obtained from Abcam (Milton, United Kingdom). Anti-ASC (DF-6304) and anti-Cleaved-Caspase 1 (p10, AF4022) were purchased from Affinity Biosciences (Jiangsu, China). Anti-GAPDH (10494-1-AP) was purchased from Proteintech Company (Chicago, United States).

Establishment of Experimental SAP-ALI Models

Animals were randomly divided into four groups ($n = 8$ for each group): (1) sham group, (2) AP group, (3) AP + AYC group, and (4) AP + emodin group. NaT-AP was induced in rats as described in our previous work (Zhang et al., 2017). In brief, rats were anesthetized by intraperitoneally (i.p.) injecting 2% sodium pentobarbital (40 mg/kg.BW), then 3.5% sodium taurocholate (1 ml/kg) was retrogradely injected into the biliopancreatic duct of rats using a micro-perfusion pump at a rate of 0.1 ml/min. CER+LPS-AP mice were i.p. injected with caerulein 6 times hourly (50 μg/kg) followed by LPS (10 mg/kg) challenge immediately after the last caerulein injection (Ding et al., 2003). Controls were injected with an equal amount of saline. AYC (5 mg/kg), as a positive control, was i.p. injected 1 h before modeling and emodin (10 mg/kg) was intragastrically administered twice at 6 and 12 h post modeling. Our previous work showed that the high dose of emodin (10 mg/kg) was more effective than the low dose of emodin (5 mg/kg) for alleviating SAP-ALI. Therefore, 10 mg/kg of emodin was selected in our experiments (Hu et al., 2021).

Animals were anesthetized with i.p. injection of 2% sodium pentobarbital (40 mg/kg.BW) the next day (24 h after AP induction), blood was collected by cardiac puncture for the

measurement of serum amylase and lipase activity. Lung tissue samples were collected to analyze the myeloperoxidase (MPO) activity and inflammatory cytokines. Pancreas and lung tissue samples were fixed for histological analysis. Bronchoalveolar lavage fluid (BALF) was extracted for AMs separation, and the proinflammatory cytokines and lactic dehydrogenase (LDH) released in the supernatant of BALF were evaluated by ELISA, then the collected AMs were subjected to western blot and flow cytometry.

Detection of Inflammatory Factors in Lung Tissues Tables

After BALF collection, lung homogenates were prepared by the following methods. Briefly, lung tissues were added with 1 ml RIPA lysis buffer (Beyotime, China), then homogenized with a high-flux tissue homogenizer (MX-S, SCILOGEX, United States). After homogenization, the mixer was incubated at 4°C for half an hour and then centrifugated at 13000 ×*g* for 15 min. Finally, the collected supernatants were used to measure inflammatory cytokine levels (including IL-1β, IL-18, and TNF-α) by corresponding ELISA kits (Neobioscience, Shenzhen, China) following the manufacturer's protocol.

Lung MPO Activity

To assess the degree of infiltrated neutrophils, myeloperoxidase (MPO) activity in lung samples was measured by the MPO activity assay kit (Nanjing Jiancheng Bioengineering Institute, China), following the manufacturer's instructions.

Collection of Bronchoalveolar Lavage Fluid (BALF)

Intratracheal injection of 10 ml (1 ml for mice) phosphate-buffered saline (PBS), which also means bronchoalveolar lavage, was performed 4 times on the animals following the anesthesia. Then the collected BALF from the syringe was mixed and centrifugated at 250 × *g* for 5 min. IL-1β and IL-18 in the supernatant were measured using the corresponding ELISA kit (Neobioscience, China), and the level of lactate dehydrogenase (LDH) was measured by an LDH Assay Kit (Beyotime Biotechnology, Haimen city, China). Besides, the pelleted cells were resuspended in conditioned RPMI 1640 medium (fetal bovine serum: 10%; penicillin and streptomycin: 1%). Then they were incubated in 60-mm sterilized dishes (37°C; 5% CO2) for 2 h and then washed twice with a warm medium to remove nonadherent cells. Finally, the whole cells were harvested and subjected to western blotting.

Western Blot

Collected AMs were resuspended on ice with RIPA lysis buffer containing proteinase inhibitors, phosphatase inhibitors, and PMSF for 30 min, then the supernatants were obtained after centrifugation for 15 min (12,000 × *g*, 4°C). Quantification of protein concentrations was determined by a bicinchoninic acid protein assay kit (Beyotime Biotechnology, Haimen city, China). Next, each lysate samples (25 μg/lane) were resolved on 12% SDS-PAGE gels and transferred onto nitrocellulose (NC) or polyvinylidene difluoride (PVDF) membranes. After being blocked in the blocking solution (EpiZyme Biotech, Shanghai, China) for 1 h, membranes were incubated with primary antibodies against NLRP3 (1:1000), Caspase 1 p10 (1:1000), ASC (1:200), GSDMD (1:1000), GSDMD-NT (1:1000), and GAPDH (1:2000) all night at 4°C. The next day, the membranes were washed with TBST 3 times and incubated with horseradish peroxidase (HRP)-labeled secondary antibody at room temperature for 1 h. Finally, blots were visualized through the Bio-Rad imaging system. The relative expression of pyroptosis-related proteins to GAPDH was analyzed and processed by ImageJ software.

Determination of AMs Pyroptosis

The collected AMs from BALF were analyzed by flow cytometry to evaluate the ratio of pyroptotic cell death. Firstly, AMs were stained using FLICA® 660 Caspase-1 Assay regent (Immunochemistry Technologies, United States) at 37°C for 30min in the dark. Pelleted cells were washed two times and then stained with propidium iodide (PI) in the dark at room temperature for 5 min. Flow cytometry (Cytoflex, Beckman) analyzed the rates of double-positive staining (caspase-1 and PI) cells, which were also regarded to be pyroptotic cells.

Histological Examination

The histopathological injury of pancreatic and lung tissues was evaluated after H&E staining. Two independent pathologists scored pancreatic injury by acinar cells edema, infiltrated inflammatory cells, focal hemorrhage, and necrosis (from 0 to 4) as described (Kusske et al., 1996). Assessment of pulmonary injury was scored by interstitial/intra-alveolar edema, alveolar wall thickening, inflammation, and hemorrhage (from 0 to 4) as described (Mikawa et al., 1994).

Statistical Analysis

All Data were presented as mean (standard deviation) and analyzed using GraphPad Prism eight Software. Differences between multiple groups were evaluated by ANOVA and post hoc Tukey's test. $p < 0.05$ was considered significantly different.

RESULTS

Emodin Attenuated AP-Associated Lung Injury in NaT-AP Rats

In this study, two animal models (NaT-AP and CER+LPS-AP) were established. We first tested the effect of emodin on AP-associated lung damage in rats induced by 3.5% sodium taurocholate. As shown in **Figure 1A**, H&E staining results showed obvious acinar cells edema, infiltrated inflammatory cells, focal hemorrhage and necrosis in the pancreas of NaT-AP rats. Conversely, emodin treatment distinctly lowered the pathological injury of the pancreas, with reduced pathological scores. Serum amylase and lipase levels are commonly used biochemical markers in the diagnosis of pancreatitis (Rompianesi et al., 2017). The serum amylase and lipase levels of NaT-AP rats were markedly higher compared with those in the sham group, while they were downregulated by emodin administration.

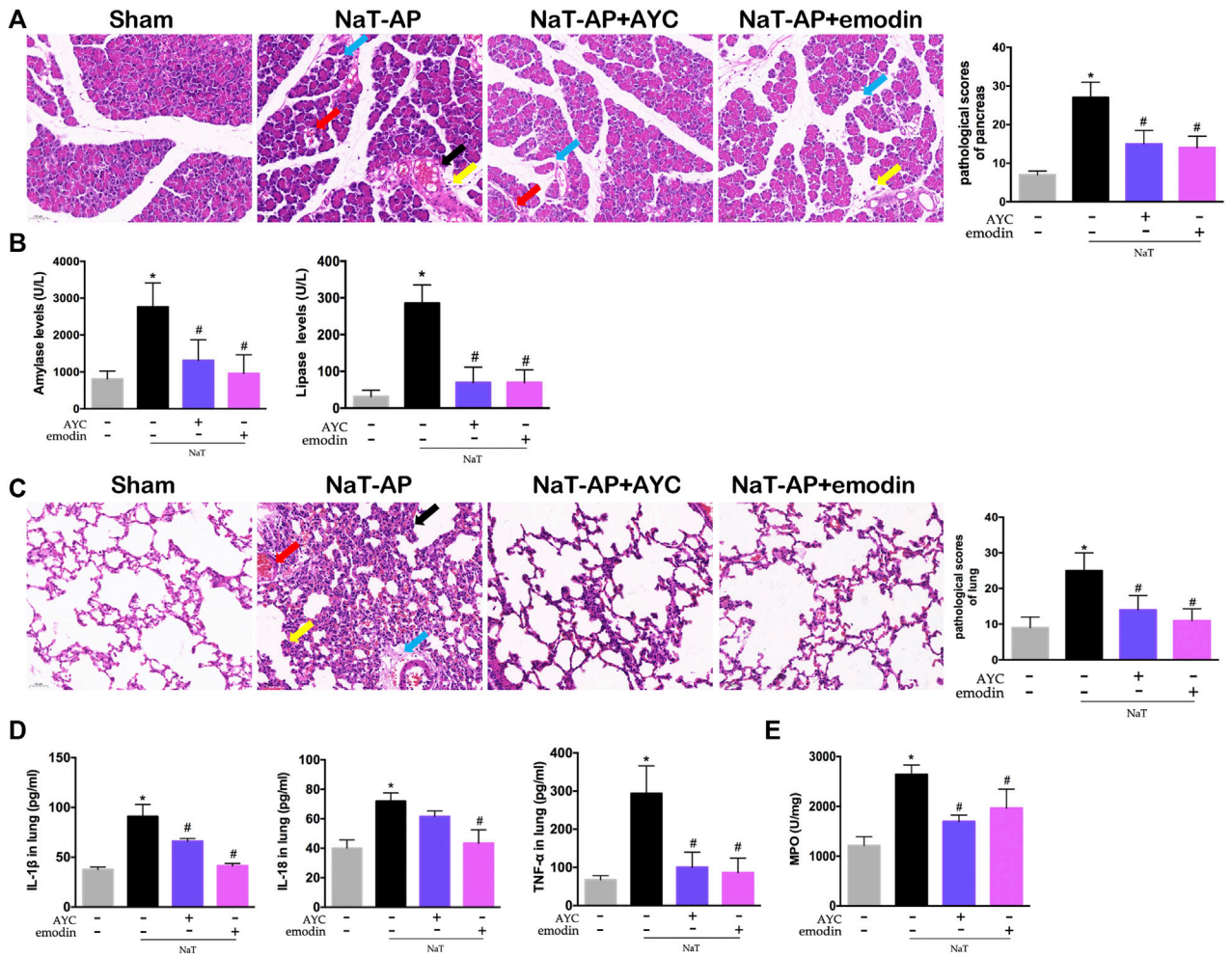

FIGURE 1 | Emodin attenuated AP-associated lung injury in NaT-AP rats. **(A)** H&E staining images (×200) and pathological scores in pancreas from sham rats, NaT-AP rats, NaT-AP + AYC rats, and NaT-AP + emodin rats. Arrows (blue, yellow, red, black) indicated pancreatic edema, inflammation, hemorrhage, and necrosis respectively. **(B)** Serum amylase and lipase levels of each group. **(C)** H&E staining images (×200) and pathological scores in lung tissue of each group. Arrows (blue, yellow, red, black) indicated lung edema, hemorrhage, alveolar septal thickening, and inflammation respectively. **(D)** The levels of IL-1β, IL-18, and TNF-α within lung tissue of each group. **(E)** The expression of MPO activity within lung tissue of each group. $^{*}p < 0.05$ vs. the controls. $^{\#}p < 0.05$ vs. NaT-AP rats.

AYC exerted similar impact on serum amylase and lipase levels compared to emodin in rats (**Figure 1B**).

Then, the effects of emodin on pulmonary damage and inflammatory response were evaluated. NaT-AP rats showed significant pathological changes in the lung tissues, characterized by interstitial/intra-alveolar edema, hemorrhage, alveolar wall thickening and inflammation, accompanied by increased histopathological scores. After emodin and AYC administration, lung injury was effectively mitigated (**Figure 1C**). Moreover, the inflammatory mediators in lung tissue, including IL-1β, IL-18, and TNF-α significantly decreased after emodin and AYC intervention (**Figure 1D**). In addition, lung MPO activity in the AP group was enhanced, indicating extensive immersion of neutrophils, while the intervention of emodin and AYC both imposed inhibitory effect on neutrophil immersion in the lung tissue of AP rats (**Figure 1E**).

Emodin Inhibited AMs Pyroptosis and Secretion of Inflammatory Factors in SAP-ALI Rats

After collecting the BALF, the ratio of pyroptotic AMs was assayed by flow cytometry. NaT-AP group displayed a significantly higher frequency of caspase-1+PI AMs, a hallmark of cell pyroptosis, compared with other groups. Of note, emodin and AYC significantly prevented AMs pyroptosis in NaT-AP rats (**Figure 2A**). Furthermore, we quantified proinflammatory cytokines and analyzed the LDH level in BALF. As a result, IL-1β and IL-18 levels in BALF were much higher in AP rats compared with those in the controls, while these levels decreased after emodin and AYC treatment (**Figure 2B**). Typically, increased level of LDH released in BALF supernatant revealed a higher rate of cell damage or death. As a result, emodin and AYC treatment protected

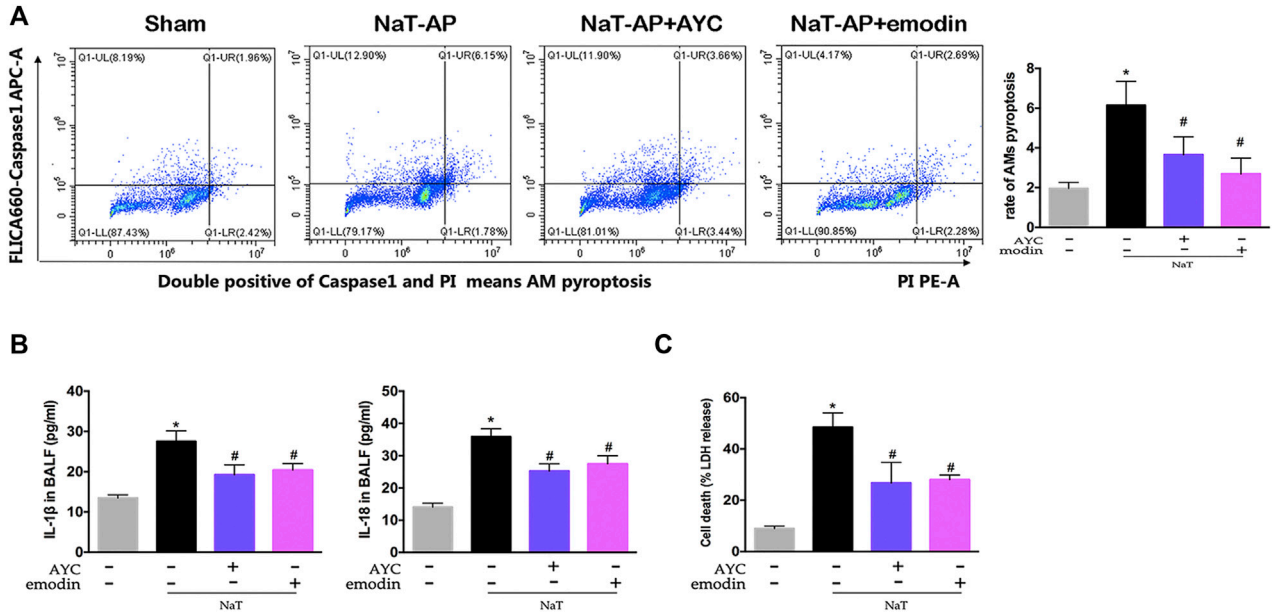

FIGURE 2 | Emodin inhibited AMs pyroptosis and secretion of inflammatory factors in SAP-ALI rats. **(A)** The rate of pyroptotic AMs determined by flow cytometry from sham rats, NaT-AP rats, NaT-AP + AYC rats, and NaT-AP + emodin rats. Double-positive staining cells (caspase-1 and PI) were regarded to be pyroptotic cells. **(B)** the levels of IL-1β and IL-18 of each group in BALF supernatant. **(C)** The LDH level of each group in BALF supernatant. $^{*}p < 0.05$ vs. the controls. $^{\#}p < 0.05$ vs. NaT-AP rats.

alveolar AMs by markedly reducing AP-induced LDH release in BALF in rats (**Figure 2C**).

Emodin Inhibited AMs Pyroptosis by Targeting NLRP3-Caspase1-GSDMD Pathway in SAP-ALI Rats

Besides, we also examined the NLRP3 inflammasome and pyroptosis-related proteins by western blotting. Our results indicated that the protein expression levels of NLRP3, ASC, Caspase1 p10, GSDMD, GSDMD-NT in AMs were apparently elevated in NaT-AP rats, while all these markers mentioned above did not show obvious elevation in their expression levels when caspase1 blockade AYC came into play. Interestingly, emodin showed the same inhibitory effect on NLRP3-Caspase1-GSDMD pathway. The expressions of NLRP3, ASC, Caspase1 p10, GSDMD, GSDMD-NT were significantly decreased after emodin administration. (**Figures 3A–E**).

Emodin Attenuated AP-Associated Lung Injury in CER+LPS-AP Mice

After exploring the therapeutic effect and the underlying mechanism of emodin in NaT-AP rats, we as well investigated its influence on another AP model. H&E staining results showed obvious acinar cells edema, infiltrated inflammatory cells, focal hemorrhage and necrosis in the pancreas of CER+LPS-AP mice. Conversely, emodin treatment effectively alleviated pulmonary injury and lowered the corresponding pathological scores. Meanwhile, the levels of serum amylase and lipase were markedly increased in the CER+LPS-AP group while they were downregulated by either emodin or AYC administration, respectively (**Figure 4B**).

In the next step, pulmonary inflammatory damage was also evaluated in CER+LPS-AP mice. Significant pathological changes together with increased histopathological scores were observed in the lung tissue, consistent with those of NaT-AP rats. After either emodin or AYC administration, the lung injury was effectively ameliorated (**Figure 4C**). Moreover, the secretion of inflammatory cytokines including IL-1β, IL-18, and TNF-α in lung tissue exhibited a downward trend after emodin or AYC intervention (**Figure 4D**). In addition, MPO activity in the AP group was enhanced, while the intervention of emodin or AYC had an inhibitory effect on neutrophil immersion in CER+LPS-AP mice (**Figure 4E**).

Emodin Inhibited AMs Pyroptosis and Secretion of Inflammatory Factors in SAP-ALI Mice

Similarly, AMs from CER+LPS-AP mice displayed a higher ratio of pyroptosis compared with the sham group. Of note, either emodin or AYC could prevent the AMs pyroptosis in CER+LPS-AP mice (**Figure 5A**). Meanwhile, IL-1β and IL-18 levels in BALF were higher in CER+LPS-AP mice compared with those in the sham group, while levels of these cytokines decreased after emodin or AYC treatment (**Figure 5B**). In addition, either emodin or AYC treatment could decrease the AP-induced LDH release (**Figure 5C**). In short, these findings suggested that acute pancreatitis induced AMs pyroptosis in

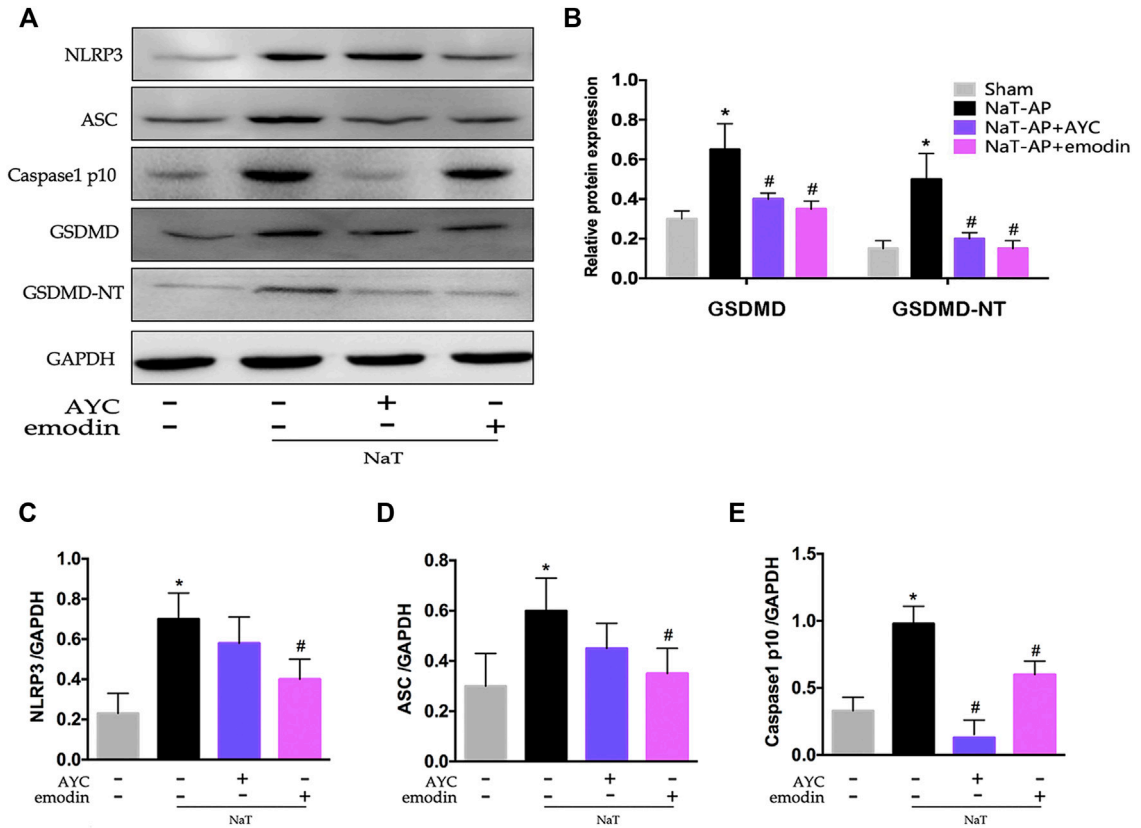

FIGURE 3 | Emodin inhibited AMs pyroptosis by targeting NLRP3-Caspase1-GSDMD pathway in SAP-ALI rats. **(A–E)** Western blots and quantitative analysis of pyroptosis-related proteins (NLRP3, ASC, Caspase1 p10, GSDMD, and GSDMD-NT) relative to GAPDH from sham rats, NaT-AP rats, NaT-AP + AYC rats, and NaT-AP + emodin rats. $^{*}p < 0.05$ vs. the controls. $^{\#}p < 0.05$ vs. NaT-AP rats.

lung tissue. Meanwhile, either emodin or AYC could rescue AMs from their pyroptotic process.

Emodin Inhibited AMs Pyroptosis by Targeting NLRP3-Caspase1-GSDMD Pathway in SAP-ALI Mice

Finally, the pyroptosis-related protein expressions were detected by western blot. The results showed that NLRP3, ASC, Caspase1 p10, GSDMD, and GSDMD-NT expressions in AMs were markedly elevated in CER+LPS-AP mice. Moreover, emodin showed the same effect as AYC, both significantly inhibiting the NLRP3, ASC, Caspase1 p10, GSDMD, GSDMD-NT protein expression in AMs (**Figures 6A–E**).

DISCUSSION

Acute lung injury (ALI) is one kind of primary or secondary disease caused by various intrapulmonary insults and extrapulmonary factors (including but not limited to sepsis, shock, pneumonia, pancreatitis etc) (Cao et al., 2016). Despite a number of methods that have been widely used for the treatment of AP-associated ALI, the mortality and morbidity still remain comparatively high with no approved effective drug or medical therapy so far. Previous research has revealed that emodin could alleviate AP-induced lung inflammatory response syndrome and acute lung injury via Nrf2/HO-1 signaling (Gao et al., 2020; Xu et al., 2021). However, systematic elucidation of the underlying therapeutic mechanism still calls for further investigation. In this study, we established two clinically relevant SAP-ALI models, including primary lung injury caused by caerulein combined with LPS (CER+LPS) and secondary lung injury induced by 3.5% sodium taurocholate (NaT). CER+LPS was an improved method for AP modeling compared with caerulein alone, since only caerulein stimulation did not cause injury of lung, liver, kidney or any other non-pancreatic organs. It has also been reported that the combination of caerulein and LPS could be used to construct severe AP models (Ding et al., 2003; Lerch and Gorelick, 2013). Besides, sodium taurocholate is commonly used to induce SAP model and mainly simulated AP model caused by bile reflux during lower common bile duct obstruction (Aho et al., 1983). As confirmed in our experiment, both sodium taurocholate and CER+LPS could cause damage to the pancreas itself as well as non-pancreatic organs (lung, liver, kidney, etc.). Based on the results, we demonstrated that emodin treatment ameliorated AP-associated lung injury and inflammatory response by inhibition of NLRP3/Caspase1/GSDMD-mediated AMs pyroptosis.

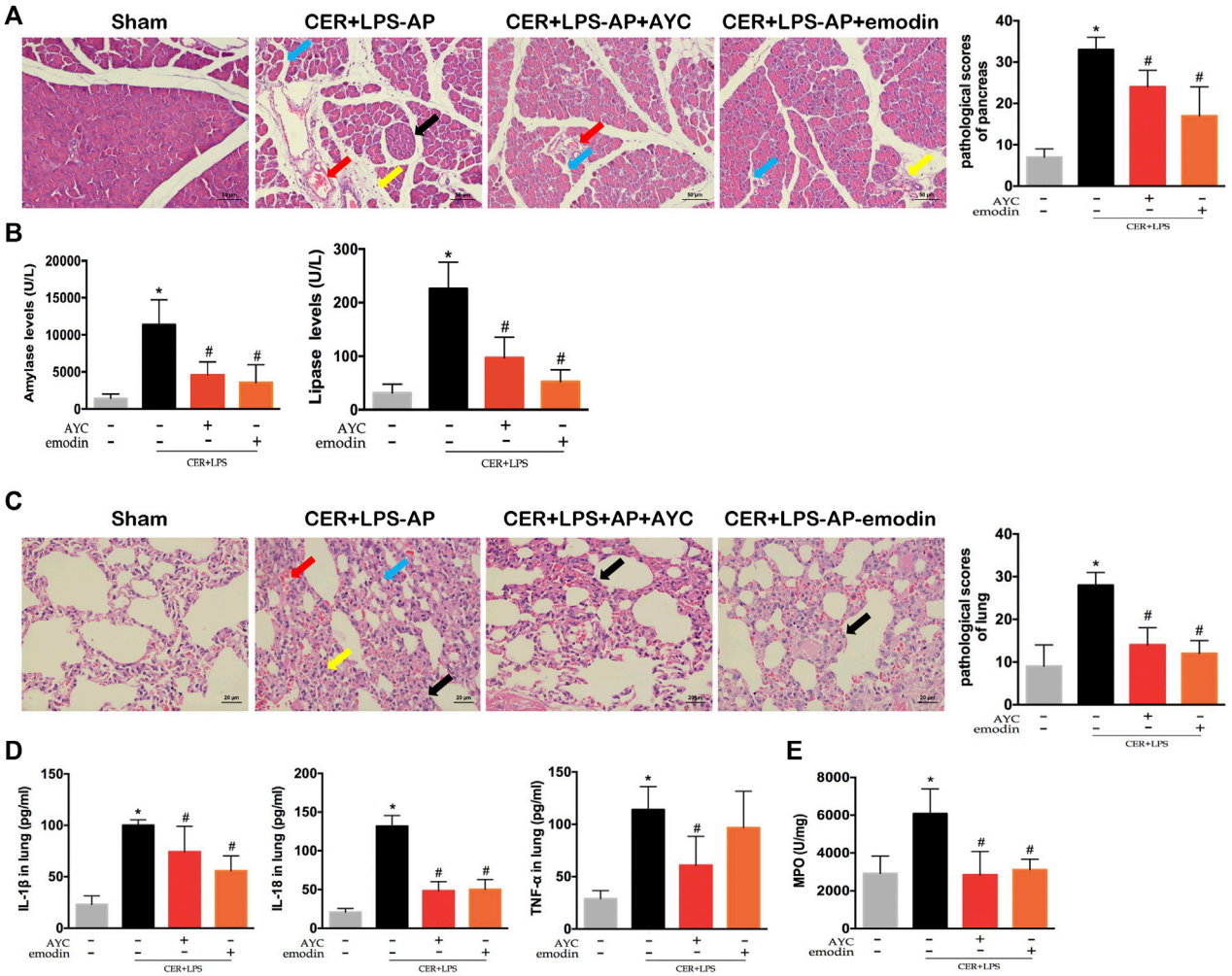

FIGURE 4 | Emodin attenuated AP-associated lung injury in CER+LPS-AP mice. **(A)** H&E staining images (×200) and pathological scores in pancreas from sham mice, CER+LPS-AP mice, CER+LPS-AP + AYC mice, and CER+LPS-AP + emodin mice. Arrows (blue, yellow, red, black) indicated pancreatic edema, inflammation, hemorrhage, and necrosis respectively. **(B)** Serum amylase and lipase levels of each group. **(C)** H&E staining images (×200) and pathological scores in lung tissue of each group. Arrows (blue, yellow, red, black) indicated lung edema, hemorrhage, alveolar septal thickening, and inflammation respectively. **(D)** The levels of IL-1β, IL-18, and TNF-α within the lung tissue of each group. **(E)** The expression of MPO activity of each group. $^{*}p < 0.05$ vs. the controls. $^{\#}p < 0.05$ vs. CER+LPS-AP mice.

Consistent with previous findings (Gao et al., 2020; Jiang et al., 2021), we found that emodin attenuated AP-associated lung injury and mitigated excessive inflammatory response, as assessed by H&E staining, inflammatory cytokine levels and MPO activity. IL-1β and IL-18, as important promoters of inflammation, possess great potential to recruit immune cells like neutrophils and accelerate the release of other inflammatory mediators such as TNF-α and IL-6, triggering inflammation cascades to amplify the inflammatory response significantly during the course of AP (Ma et al., 2012; Bunbupha et al., 2015). MPO is regarded as a reliable marker for neutrophil activation. In this study, we found that emodin to a great extent downregulated the levels of IL-1β, IL-18, TNF-α, and MPO activity in lung tissue in both two types of SAP-ALI models, which is consistent with the protective role of emodin in reducing oxidative stress and inflammasome signals (Xia et al., 2019). In general, the interaction between pulmonary and systemic inflammation enhances the cascade of inflammation within the lungs and therefore exaggerates the progression of SAP-ALI.

Pyroptosis, a kind of caspase1-dependent inflammatory programmed cell death, is a molecular pattern leading to activation of procaspase-1 and secretion of IL-1β and IL-18 that are inherently associated with the inflammasome activation (Zeng et al., 2019). Cell death ways and activation of alveolar macrophages are considered as major factors responsible for the progression of uncontrolled pulmonary inflammation during ALI (Aggarwal et al., 2014; Niesler et al., 2014). Accumulating evidence has suggested that inflammasome-dependent AMs pyroptosis is closely related to ALI induced by a variety of challenges (e.g., lipopolysaccharide,

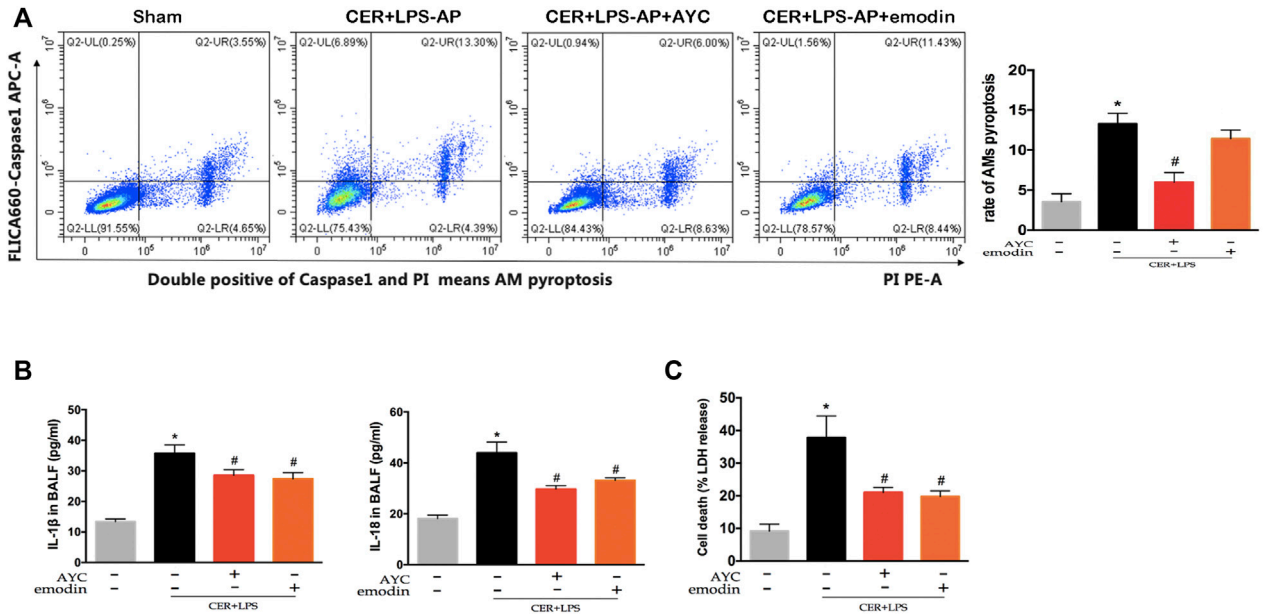

FIGURE 5 | Emodin inhibited AMs pyroptosis and secretion of inflammatory factors in SAP-ALI mice. **(A)** The rate of pyroptotic AMs determined by flow cytometry from sham mice, CER+LPS-AP mice, CER+LPS-AP + AYC mice, and CER+LPS-AP + emodin mice. Double-positive staining cells (caspase-1 and PI) were regarded to be pyroptotic cells. **(B)** the levels of IL-1β and IL-18 of each group in BALF supernatant. **(C)** The level of LDH of each group in BALF supernatant. $^{*}p < 0.05$ vs. the controls. $^{\#}p < 0.05$ vs. CER+LPS-AP mice.

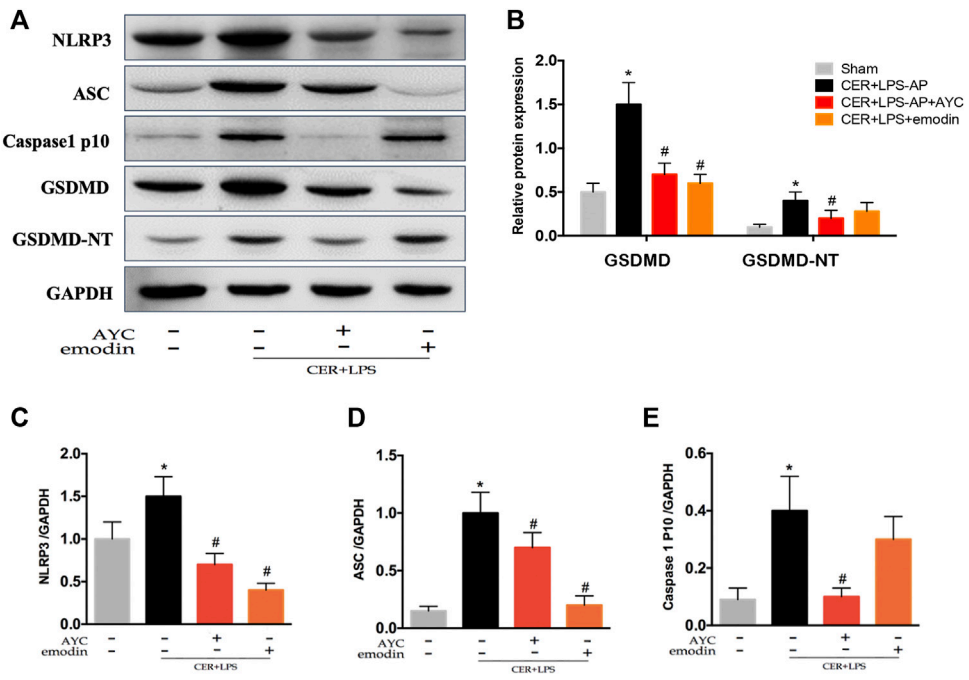

FIGURE 6 | Emodin inhibited AMs pyroptosis by targeting NLRP3-Caspase1-GSDMD pathway in SAP-ALI mice. **(A–E)** Western blots and quantitative analysis of pyroptosis-related proteins (NLRP3, ASC, Caspase1 p10, GSDMD, and GSDMD-NT) relative to GAPDH from sham mice, CER+LPS-AP mice, CER+LPS-AP + AYC mice, and CER+LPS-AP + emodin mice. $^{*}p < 0.05$ vs. the controls. $^{\#}p < 0.05$ vs. CER+LPS-AP mice.

cardiopulmonary bypass, and ischemia-reperfusion *et al*) (Wu et al., 2015; Hou et al., 2018; Fei et al., 2020). It has been reported that AMs are involved in the progression of AP from local pancreatic injury to pulmonary dysfunction, through the release of various substances like inflammatory cytokines, nitric oxide (NO), and arachidonic acid metabolites (Gea-Sorlí and Closa, 2010). Therefore, in this experiment, AMs were accordingly selected as the target cells in the treatment strategy for AP-related lung injury. Moreover, Cheng *et al* reported that a large amount of NO produced by AMs in the lung tissue might be a cause of pulmonary inflammatory damage secondary to sodium taurocholate-induced AP rats (Cheng et al., 2010). However, the specific regulatory role of AMs during SAP-ALI still remains unclarified. To identify this type of pyroptotic cells, active caspase-1 and PI positivity, downstream inflammatory factors and the LDH level were also examined. In this study, the ratio of pyroptotic AMs was increased in the diseased lung tissue, indicating AMs pyroptosis was related to ALI that was induced in NaT-AP rats and CER+LPS-AP mice. Emodin was previously reported to strongly inhibit GSDMD-mediated pyroptosis induced by myocardial ischemia/reperfusion in cardiomyocytes (Ye et al., 2019). Our findings revealed that emodin could as well exert intensive inhibition on AMs pyroptosis in two types of AP models, and its inhibitory effect was similar to that of AYC.

Activation of NLRP3 inflammasome in macrophages played critical roles in the pathogenesis during SAP-ALI (Wu et al., 2020). NLRP3 deficiency or inhibitor attenuated excessive local and systemic inflammation in experimental SAP-ALI model (Fu et al., 2018). In line with other findings, our results showed the NLRP3 inflammasome in AMs was significantly activated both in NaT-AP rats and CER+LPS-AP mice. Emerging evidence showed that emodin had an inhibitory effect on the activation of NLRP3 inflammasome in myocardial injury combined with cardiovascular dysfunction (Ye et al., 2019; Zhang et al., 2020; Dai et al., 2021). In addition, Emodin could attenuate LPS-induced ALI through regulating the NLRP3 inflammasome-dependent pyroptosis signaling pathway (Liu et al., 2021). Importantly, the administration of either emodin or AYC markedly inhibited AP-associated activation of NLRP3 inflammasome in AMs, which was supported by the downregulated expression levels of NLRP3, ASC, and Caspase1 p10. The assembly of this multimeric protein complex triggered the automatic cleavage of pro-caspase-1, which converted into caspase-1. Additionally, N-terminal GSDMD fragment (GSDMD-NT) was generated in the process after gasdermin D (GSDMD) was cleaved by active caspase-1, thus further promoting membrane pore formation and the subsequent inflammatory cascades. Initiated by activation of the inflammasome, pyroptosis did occur in AMs and aggravated ALI during the progression of acute pancreatitis. Consistent with other findings, we similarly observed that the cleavage of GSDMD was promoted under acute pancreatitis. Moreover, both emodin and AYC could downregulate the expression of GSDMD and GSDMD-NT in AMs. To sum up, all evidence favoring the therapeutic effect of emodin on NaT-AP rats and CER+LPS-AP mice was closely related to the inhibitory effect of emodin on AMs pyroptosis by targeting the NLRP3-Caspase1-GSDMD pathway.

CONCLUSION

In summary, the discovery of pyroptosis has greatly broadened our understanding of the pathogenesis of ALI, and in turn targeting this manner of cell death provides new avenues for the effective treatment and management of SAP-ALI. This study used two experimental AP models to explore the roles of AMs pyroptosis during SAP-ALI and pointed out a significant correlation between emodin and AMs pyroptosis signaling pathways. In conclusion, we discovered that emodin could exhibit a therapeutic effect on SAP-ALI via regulating NLRP3-Caspase1-GSDMD signaling pathway. Accordingly, our present study may provide some alternative signaling ways for explaining the pathogenesis of SAP-ALI as well as a novel therapeutic option for treating this disease.

DATA AVAILABILITY STATEMENT

The original contributions presented in the study are included in the article/**Supplementary Material**, further inquiries can be directed to the corresponding author.

ETHICS STATEMENT

The animal study was reviewed and approved by the Animal Ethics Committee of the Sichuan University of West China Hospital.

AUTHOR CONTRIBUTIONS

XW drafted the main part of the manuscript. JY and XW conducted the experiments with the help of QH, YM, LZ and CL. XW, JY, HK, XZ, and JL designed the experiments and analyzed the data. QH and MW edited the manuscript. MW and WT provided funding support and experimental supervision.

FUNDING

This work was supported by National Natural Science Foundation of China (grant numbers: 81873203, 81774160, and 81974552).

ACKNOWLEDGMENTS

Thanks to Li Fu, Jiangrong Deng, Xiangyi Ren, and Yan Wang from the Research Core Facility of West China Hospital for their great assistance in our experiments.

SUPPLEMENTARY MATERIAL

The Supplementary Material for this article can be found online at: https://www.frontiersin.org/articles/10.3389/fphar.2022.873053/full#supplementary-material

REFERENCES

Aggarwal, N. R., King, L. S., and D'Alessio, F. R. (2014). Diverse Macrophage Populations Mediate Acute Lung Inflammation and Resolution. *Am. J. Physiol. Lung Cell Mol. Physiol.* 306 (8), L709–L725. doi:10.1152/ajplung.00341.2013

Aho, H. J., Nevalainen, T. J., and Aho, A. J. (1983). Experimental Pancreatitis in the Rat. Development of Pancreatic Necrosis, Ischemia and Edema after Intraductal Sodium Taurocholate Injection. *Eur. Surg. Res.* 15 (1), 28–36. doi:10.1159/000128330

Akbarshahi, H., Rosendahl, A. H., Westergren-Thorsson, G., and Andersson, R. (2012). Acute Lung Injury in Acute Pancreatitis-Aawaiting the Big Leap. *Respir. Med.* 106 (9), 1199–1210. doi:10.1016/j.rmed.2012.06.003

Bunbupha, S., Prachaney, P., Kukongviriyapan, U., Kukongviriyapan, V., Welbat, J. U., and Pakdeechote, P. (2015). *Clin. Exp. Pharmacol. Physiol.* 42 (11), 1189–1197. doi:10.1111/1440-1681.12472

Cao, Y., Lyu, Y. I., Tang, J., and Li, Y. (2016). MicroRNAs: Novel Regulatory Molecules in Acute Lung Injury/acute Respiratory Distress Syndrome. *Biomed. Rep.* 4 (5), 523–527. doi:10.3892/br.2016.620

Cheng, S., Yan, W., Yang, B., Shi, J., Song, M., and Zhao, Y. (2010). A Crucial Role of Nitric Oxide in Acute Lung Injury Secondary to the Acute Necrotizing Pancreatitis. *Hum. Exp. Toxicol.* 29 (4), 329–337. doi:10.1177/0960327110361760

Dai, S., Ye, B., Chen, L., Hong, G., Zhao, G., and Lu, Z. (2021). Emodin Alleviates LPS-Induced Myocardial Injury through Inhibition of NLRP3 Inflammasome Activation. *Phytother. Res.* 35 (9), 5203–5213. doi:10.1002/ptr.7191

Ding, S. P., Li, J. C., and Jin, C. (2003). A Mouse Model of Severe Acute Pancreatitis Induced with Caerulein and Lipopolysaccharide. *World J. Gastroenterol.* 9 (3), 584–589. doi:10.3748/wjg.v9.i3.584

Dong, X., Fu, J., Yin, X., Cao, S., Li, X., Lin, L., et al. (2016). Emodin: A Review of its Pharmacology, Toxicity and Pharmacokinetics. *Phytother. Res.* 30 (8), 1207–1218. doi:10.1002/ptr.5631

Fei, L., Jingyuan, X., Fangte, L., Huijun, D., Liu, Y., Ren, J., et al. (2020). Preconditioning with rHMGB1 Ameliorates Lung Ischemia-Reperfusion Injury by Inhibiting Alveolar Macrophage Pyroptosis via the Keap1/Nrf2/HO-1 Signaling Pathway. *J. Transl. Med.* 18 (1), 301. doi:10.1186/s12967-020-02467-w

Fu, Q., Zhai, Z., Wang, Y., Xu, L., Jia, P., Xia, P., et al. (2018). NLRP3 Deficiency Alleviates Severe Acute Pancreatitis and Pancreatitis-Associated Lung Injury in a Mouse Model. *Biomed. Res. Int.* 2018, 1294951. doi:10.1155/2018/1294951

Gao, Z., Sui, J., Fan, R., Qu, W., Dong, X., and Sun, D. (2020). Emodin Protects against Acute Pancreatitis-Associated Lung Injury by Inhibiting NLPR3 Inflammasome Activation via Nrf2/HO-1 Signaling. *Drug Des. Devel. Ther.* 14, 1971–1982. doi:10.2147/DDDT.S247103

Gea-Sorlí, S., and Closa, D. (2010). Role of Macrophages in the Progression of Acute Pancreatitis. *World J. Gastrointest. Pharmacol. Ther.* 1 (5), 107–111. doi:10.4292/wjgpt.v1.i5.107

Gordon, S., Plüddemann, A., and Martinez Estrada, F. (2014). Macrophage Heterogeneity in Tissues: Phenotypic Diversity and Functions. *Immunol. Rev.* 262 (1), 36–55. doi:10.1111/imr.12223

Grailer, J. J., Canning, B. A., Kalbitz, M., Haggadone, M. D., Dhond, R. M., Andjelkovic, A. V., et al. (2014). Critical Role for the NLRP3 Inflammasome during Acute Lung Injury. *J. Immunol.* 192 (12), 5974–5983. doi:10.4049/jimmunol.1400368

Hou, L., Yang, Z., Wang, Z., Zhang, X., Zhao, Y., Yang, H., et al. (2018). NLRP3/ASC-mediated Alveolar Macrophage Pyroptosis Enhances HMGB1 Secretion in Acute Lung Injury Induced by Cardiopulmonary Bypass. *Lab. Invest* 98 (8), 1052–1064. doi:10.1038/s41374-018-0073-0

Hu, Q., Yao, J., Wu, X., Li, J., Li, G., Tang, W., et al. (2021). Emodin Attenuates Severe Acute Pancreatitis-Associated Acute Lung Injury by Suppressing Pancreatic Exosome-Mediated Alveolar Macrophage Activation. *Acta Pharm. Sin. B*. In Press. doi:10.1016/j.apsb.2021.10.008

Jiang, N., Li, Z., Luo, Y., Jiang, L., Zhang, G., Yang, Q., et al. (2021). Emodin Ameliorates Acute Pancreatitis-Induced Lung Injury by Suppressing NLRP3 Inflammasome-Mediated Neutrophil Recruitment. *Exp. Ther. Med.* 22 (2), 857. doi:10.3892/etm.2021.10289

Kumar, V. (2020). Pulmonary Innate Immune Response Determines the Outcome of Inflammation during Pneumonia and Sepsis-Associated Acute Lung Injury. *Front. Immunol.* 11, 1722. doi:10.3389/fimmu.2020.01722

Kusske, A. M., Rongione, A. J., Ashley, S. W., McFadden, D. W., and Reber, H. A. (1996). Interleukin-10 Prevents Death in Lethal Necrotizing Pancreatitis in Mice. *Surgery* 120 (2), 284–289. doi:10.1016/s0039-6060(96)80299-6

Lerch, M. M., and Gorelick, F. S. (2013). Models of Acute and Chronic Pancreatitis. *Gastroenterology* 144 (6), 1180–1193. doi:10.1053/j.gastro.2012.12.043

Li, H., Yang, T., Zhou, H., Du, J., Zhu, B., and Sun, Z. (2016). Emodin Combined with Nanosilver Inhibited Sepsis by Anti-inflammatory Protection. *Front. Pharmacol.* 7, 536. doi:10.3389/fphar.2016.00536

Li, X., Shan, C., Wu, Z., Yu, H., Yang, A., and Tan, B. (2020). Emodin Alleviated Pulmonary Inflammation in Rats with LPS-Induced Acute Lung Injury through Inhibiting the mTOR/HIF-1α/VEGF Signaling Pathway. *Inflamm. Res.* 69 (4), 365–373. doi:10.1007/s00011-020-01331-3

Liu, Y., Shang, L., Zhou, J., Pan, G., Zhou, F., and Yang, S. (2021). Emodin Attenuates LPS-Induced Acute Lung Injury by Inhibiting NLRP3 Inflammasome-dependent Pyroptosis Signaling Pathway *In Vitro* and *In Vivo*. *Inflammation* 45 (2), 753–767. doi:10.1007/s10753-021-01581-1

Ma, H. J., Huang, X. L., Liu, Y., and Fan, Y. M. (2012). Sulfur Dioxide Attenuates LPS-Induced Acute Lung Injury via Enhancing Polymorphonuclear Neutrophil Apoptosis. *Acta. Pharmacol. Sin.* 33 (8), 983–990. doi:10.1038/aps.2012.70

Mikawa, K., Maekawa, N., Nishina, K., Takao, Y., Yaku, H., and Obara, H. (1994). Effect of Lidocaine Pretreatment on Endotoxin-Induced Lung Injury in Rabbits. *Anesthesiology* 81 (3), 689–699. doi:10.1097/00000542-199409000-00023

Murray, P. J., Allen, J. E., Biswas, S. K., Fisher, E. A., Gilroy, D. W., Goerdt, S., et al. (2014). Macrophage Activation and Polarization: Nomenclature and Experimental Guidelines. *Immunity* 41 (1), 14–20. doi:10.1016/j.immuni.2014.06.008

Niesler, U., Palmer, A., Fröba, J. S., Braumüller, S. T., Zhou, S., Gebhard, F., et al. (2014). Role of Alveolar Macrophages in the Regulation of Local and Systemic Inflammation after Lung Contusion. *J. Trauma. Acute Care Surg.* 76 (2), 386–393. doi:10.1097/TA.0b013e3182aaa499

Rompianesi, G., Hann, A., Komolafe, O., Pereira, S. P., Davidson, B. R., and Gurusamy, K. S. (2017). Serum Amylase and Lipase and Urinary Trypsinogen and Amylase for Diagnosis of Acute Pancreatitis. *Cochrane Database Syst. Rev.* 4 (4), CD012010. doi:10.1002/14651858.CD012010.pub2

Shi, J., Zhao, Y., Wang, K., Shi, X., Wang, Y., Huang, H., et al. (2015). Cleavage of GSDMD by Inflammatory Caspases Determines Pyroptotic Cell Death. *Nature* 526 (7575), 660–665. doi:10.1038/nature15514

Wu, D. D., Pan, P. H., Liu, B., Su, X. L., Zhang, L. M., Tan, H. Y., et al. (2015). Inhibition of Alveolar Macrophage Pyroptosis Reduces Lipopolysaccharide-Induced Acute Lung Injury in Mice. *Chin. Med. J. Engl.* 128 (19), 2638–2645. doi:10.4103/0366-6999.166039

Wu, J., Yan, Z., Schwartz, D. E., Yu, J., Malik, A. B., and Hu, G. (2013). Activation of NLRP3 Inflammasome in Alveolar Macrophages Contributes to Mechanical Stretch-Induced Lung Inflammation and Injury. *J. Immunol.* 190 (7), 3590–3599. doi:10.4049/jimmunol.1200860

Wu, X. B., Sun, H. Y., Luo, Z. L., Cheng, L., Duan, X. M., and Ren, J. D. (2020). Plasma-derived Exosomes Contribute to Pancreatitis-Associated Lung Injury by Triggering NLRP3-dependent Pyroptosis in Alveolar Macrophages. *Biochim. Biophys. Acta. Mol. Basis. Dis.* 1866 (5), 165685. doi:10.1016/j.bbadis.2020.165685

Xia, S., Ni, Y., Zhou, Q., Liu, H., Xiang, H., Sui, H., et al. (2019). Emodin Attenuates Severe Acute Pancreatitis via Antioxidant and Anti-inflammatory Activity. *Inflammation* 42 (6), 2129–2138. doi:10.1007/s10753-019-01077-z

Xiao, A. Y., Tan, M. L., Wu, L. M., Asrani, V. M., Windsor, J. A., Yadav, D., et al. (2016). Global Incidence and Mortality of Pancreatic Diseases: a Systematic Review, Meta-Analysis, and Meta-Regression of Population-Based Cohort Studies. *Lancet. Gastroenterol. Hepatol.* 1 (11), 45–55. doi:10.1016/S2468-1253(16)30004-8

Xu, J., Huang, B., Wang, Y., Tong, C., Xie, P., Fan, R., et al. (2016). Emodin Ameliorates Acute Lung Injury Induced by Severe Acute Pancreatitis through the Up-Regulated Expressions of AQP1 and AQP5 in Lung. *Clin. Exp. Pharmacol. Physiol.* 43 (11), 1071–1079. doi:10.1111/1440-1681.12627

Xu, Q., Wang, M., Guo, H., Liu, H., Zhang, G., Xu, C., et al. (2021). Emodin Alleviates Severe Acute Pancreatitis-Associated Acute Lung Injury by Inhibiting the Cold-Inducible RNA-Binding Protein (CIRP)-Mediated Activation of the NLRP3/IL-1β/CXCL1 Signaling. *Front. Pharmacol.* 12, 655372. doi:10.3389/fphar.2021.655372

Xue, J., Chen, F., Wang, J., Wu, S., Zheng, M., Zhu, H., et al. (2015). Emodin Protects against Concanavalin A-Induced Hepatitis in Mice through Inhibiting

Activation of the P38 MAPK-NF-Kb Signaling Pathway. *Cell. Physiol. biochem.* 35 (4), 1557–1570. doi:10.1159/000373971

Yang, J., Zhao, Y., Zhang, P., Li, Y., Yang, Y., Yang, Y., et al. (2016). Hemorrhagic Shock Primes for Lung Vascular Endothelial Cell Pyroptosis: Role in Pulmonary Inflammation Following LPS. *Cell Death. Dis.* 7 (9), e2363. doi:10.1038/cddis.2016.274

Yao, L., and Sun, T. (2019). Glycyrrhizin Administration Ameliorates Streptococcus Aureus-Induced Acute Lung Injury. *Int. Immunopharmacol.* 70, 504–511. doi:10.1016/j.intimp.2019.02.046

Ye, B., Chen, X., Dai, S., Han, J., Liang, X., Lin, S., et al. (2019). Emodin Alleviates Myocardial Ischemia/reperfusion Injury by Inhibiting Gasdermin D-Mediated Pyroptosis in Cardiomyocytes. *Drug Des. Devel. Ther.* 13, 975–990. doi:10.2147/DDDT.S195412

Zeng, C., Wang, R., and Tan, H. (2019). Role of Pyroptosis in Cardiovascular Diseases and its Therapeutic Implications. *Int. J. Biol. Sci.* 15 (7), 1345–1357. doi:10.7150/ijbs.33568

Zhang, Y., Li, X., Grailer, J. J., Wang, N., Wang, M., Yao, J., et al. (2016). Melatonin Alleviates Acute Lung Injury through Inhibiting the NLRP3 Inflammasome. *J. Pineal Res.* 60 (4), 405–414. doi:10.1111/jpi.12322

Zhang, Y. M., Ren, H. Y., Zhao, X. L., Li, J., Li, J. Y., Wu, F. S., et al. (2017). Pharmacokinetics and Pharmacodynamics of Da-Cheng-Qi Decoction in the Liver of Rats with Severe Acute Pancreatitis. *World J. Gastroenterol.* 23 (8), 1367–1374. doi:10.3748/wjg.v23.i8.1367

Zhang, Y., Song, Z., Huang, S., Zhu, L., Liu, T., Shu, H., et al. (2020). Aloe Emodin Relieves Ang II-Induced Endothelial Junction Dysfunction via Promoting Ubiquitination Mediated NLRP3 Inflammasome Inactivation. *J. Leukoc. Biol.* 108 (6), 1735–1746. doi:10.1002/JLB.3MA0520-582R

Conflict of Interest: The authors declare that the research was conducted in the absence of any commercial or financial relationships that could be construed as a potential conflict of interest.

Publisher's Note: All claims expressed in this article are solely those of the authors and do not necessarily represent those of their affiliated organizations, or those of the publisher, the editors and the reviewers. Any product that may be evaluated in this article, or claim that may be made by its manufacturer, is not guaranteed or endorsed by the publisher.

frontiers | Frontiers in Pharmacology

ORIGINAL RESEARCH
published: 08 June 2022
doi: 10.3389/fphar.2022.873166

Celastrol Inhibited Human Esophageal Cancer by Activating DR5-Dependent Extrinsic and Noxa/Bim-Dependent Intrinsic Apoptosis

Xihui Chen[1†], *Shiwen Wang*[1,2†], *Li Zhang*[1], *Shuying Yuan*[1], *Tong Xu*[1], *Feng Zhu*[1,2], *Yanmei Zhang*[2] *and Lijun Jia*[1*]

[1]*Cancer Institute, Longhua Hospital, Shanghai University of Traditional Chinese Medicine, Shanghai, China,* [2]*Department of Laboratory Medicine, Huadong Hospital Affiliated to Fudan University, Shanghai, China*

Esophageal squamous cell carcinoma (ESCC) is one of the deadliest digestive system cancers worldwide lacking effective therapeutic strategies. Recently, it has been found that the natural product celastrol plays an anti-cancer role in several human cancers by inducing cell cycle arrest and apoptosis. However, it remains elusive whether and how celastrol suppresses tumor growth of ESCC. In the present study, for the first time, we demonstrated that celastrol triggered both extrinsic and intrinsic apoptosis pathways to diminish the tumor growth of ESCC *in vivo* and *in vitro*. Mechanistic studies revealed that celastrol coordinatively induced DR5-dependent extrinsic apoptosis and Noxa-dependent intrinsic apoptosis through transcriptional activation of ATF4 in ESCC cells. Furthermore, we found that the FoxO3a-Bim pathway was involved in the intrinsic apoptosis of ESCC cells induced by celastrol. Our study elucidated the tumor-suppressive efficacy of celastrol on ESCC and revealed a previously unknown mechanism underlying celastrol-induced apoptosis, highlighting celastrol as a promising apoptosis-inducing therapeutic strategy for ESCC.

Keywords: celastrol, esophageal squamous cell carcinoma (ESCC), tumor growth, extrinsic apoptosis, intrinsic apoptosis

OPEN ACCESS

Edited by:
Hemant Goyal,
The Wright Center, United States

Reviewed by:
Tao Hu,
Evergreen Therapeutics, Inc., United States
Zhen Wang,
Peking Union Medical College Graduate School, China

***Correspondence:**
Lijun Jia
ljjia@shutcm.edu.cn

†These authors have contributed equally to this work

Specialty section:
This article was submitted to Gastrointestinal and Hepatic Pharmacology, a section of the journal Frontiers in Pharmacology

Received: *10 February 2022*
Accepted: *02 May 2022*
Published: *08 June 2022*

Citation:
Chen X, Wang S, Zhang L, Yuan S, Xu T, Zhu F, Zhang Y and Jia L (2022) Celastrol Inhibited Human Esophageal Cancer by Activating DR5-Dependent Extrinsic and Noxa/Bim-Dependent Intrinsic Apoptosis. Front. Pharmacol. 13:873166. doi: 10.3389/fphar.2022.873166

INTRODUCTION

Esophageal cancer is one of the most aggressive digestive system cancers globally (Bray et al., 2018). Esophageal squamous cell carcinoma (ESCC) is the main histologic subtype among all types of esophageal tumors, which is more prevalent in East Asia (Huang and Fu, 2019). At present, surgery combined with neoadjuvant chemotherapy and radiotherapy is the first-line treatment for ESCC (Watanabe et al., 2019). Major limitations of the treatment of ESCC include high toxicity and acquired therapeutic resistance to chemotherapy and radiotherapy, as well as the high recurrence rate of surgery (Leng et al., 2020). In recent years, although some clinical advances have been made in the development of diagnosis and therapeutic techniques, the overall 5-year survival rate for ESCC patients is still very poor (Han et al., 2022). Consequently, it is pressingly needed to facilitate the development of effective strategies for ESCC therapy.

Recently, natural products have been increasingly used in the treatment and prevention of human cancers due to their significant efficacy and few side effects (Deng et al., 2020; Ma et al., 2021; Yang et al., 2021). A variety of natural products were confirmed to exert anti-ESCC activity by inducing apoptosis, regulating autophagy, arresting the cell cycle, and inhibiting metastasis (Ying et al., 2018).

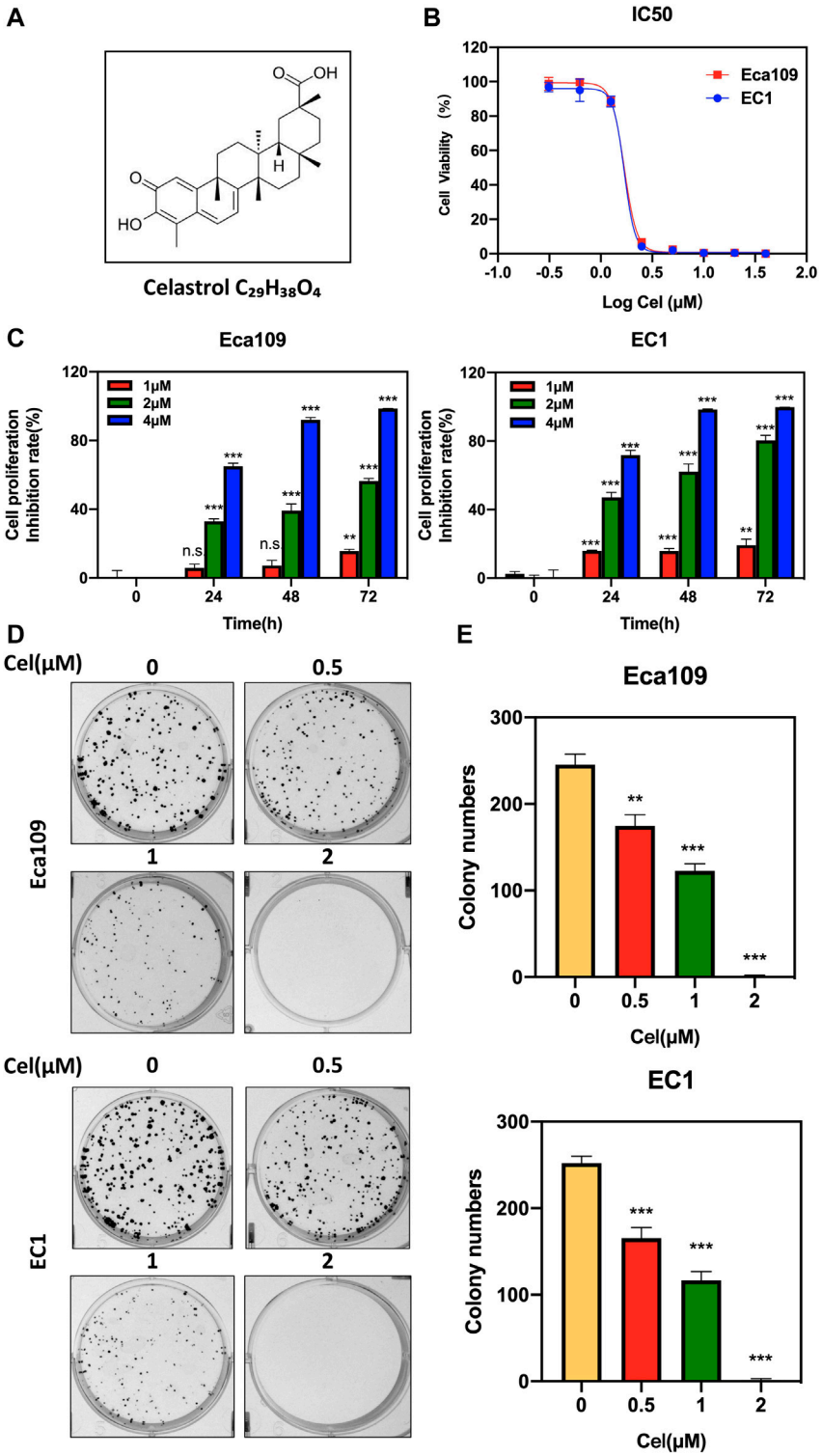

FIGURE 1 | Celastrol inhibited the viability of ESCC cells. **(A)** Chemical structure of celastrol. **(B)** Human ESCC cells Eca109 and EC1 were treated with indicated concentrations of celastrol for 72 h, and cell viability was determined by ATPlite assay. Representative inhibitory curves for each cell line were shown. **(C)** ATPlite assay was used to determine the cell growth of Eca109 and EC1 cells at the indicated concentration of celastrol or DMSO for 0, 24, 48, and 72 h **(D,E)** Representative images of three independent experiments were shown for the inhibition of colony formation by 0.5, 1, and 2 μM celastrol or DMSO for 10 days. Graphs of the relative number of colonies were performed. **denotes $p < 0.01$, ***denotes $p < 0.001$, n.s. denotes not significant.

For example, the natural product berberine was found to inhibit the proliferation of ESCC cells by promoting cell cycle arrest at the G2/M phase (Jiang et al., 2017). Furthermore, echinatin, a compound isolated from the Chinese herb Glycyrrhiza uralensis Fisch, suppressed the growth and invasion of ESCC cells by inducing AKT/mTOR-dependent autophagy and apoptosis (Hong et al., 2020). In addition, the herbal ingredient artesunate inhibited the migration of ESCC cells by interfering with DNA synthesis and destroying the cytoskeleton (Shi et al., 2015). Therefore, natural products exhibited substantial anti-ESCC efficacy, which was expected to provide a new direction for the clinical treatment of ESCC.

The natural product celastrol is a kind of pentacyclic triterpene extracted from the herbaceous plant Tripterygium wilfordii Hook F (TWHF) (**Figure 1A**), which possesses anti-inflammatory, anti-rheumatic, and some other pharmacological activities (Yang et al., 2017; Zhang et al., 2017; Tang et al., 2018; Saito et al., 2019; Wong et al., 2019; Ye et al., 2020). Recent studies have shown that celastrol exerts potential anti-cancer activity in various human cancers, including breast cancer, gastric cancer, lung cancer, and colorectal cancer (Dharambir et al., 2018). It was reported that celastrol inhibited breast cancer cell's metastasis by intervening M2-like polarization by inhibiting STAT6 (Yang et al., 2018). Moreover, celastrol was found to suppress nitric oxide (NOS) synthases and the angiogenesis pathway, thereby inhibiting the growth and migration of colorectal cancer cells (Gao et al., 2019). However, the tumor-suppressive efficacy of celastrol on ESCC and the underlying mechanisms remain largely undefined.

Inducing apoptosis is an effective way to prevent and treat human cancers (Carneiro and El-Deiry, 2020; Shahar and Larisch, 2020). Extrinsic (death receptor-mediated) apoptosis and intrinsic (mitochondrial) apoptosis represent the most important cytotoxic pathways activated by anti-cancer agents (Kale et al., 2017). In extrinsic apoptosis, death receptors, such as Fas and TRAIL, interact with their specific ligands to trigger apoptosis cascades by recruiting and activating the main downstream factor caspase 8 (Daolin et al., 2019). Intrinsic apoptosis is activated by the release of cytochrome c in mitochondria and the cleavage of caspase 9, and is regulated by the balance between pro-survival and pro-apoptotic Bcl-2 protein family members (Diepstraten et al., 2022). So far, the underlying mechanisms of celastrol triggering ESCC apoptosis are still unclarified. Here, for the first time, we validated the anti-tumor activity of celastrol in ESCC both *in vivo* and *in vitro*. Mechanistically, we revealed that celastrol suppressed the tumor growth of ESCC by activating DR5-dependent extrinsic and Noxa/Bim-dependent intrinsic apoptosis. Our findings not only elucidated the tumor-suppressive efficacy of ESCC and its underlying mechanism but also provided preliminary evidence for the clinical treatment of ESCC by celastrol.

MATERIALS AND METHODS

Cell Culture

Human ESCC cell lines Eca109 and EC1 were purchased from the Type Culture Collection of the Chinese Academy of Sciences (Shanghai, China), and cultured in media at 37°C with 5% CO_2. All media consisted of Dulbecco's Modified Eagle's Medium (DMEM, BasalMedia, Shanghai, China), 10% fetal bovine serum (FBS, Biochrom AG, Berlin, Germany), and 1% penicillin-streptomycin solution (BasalMedia, Shanghai, China).

Reagents

Celastrol was acquired from MCE (MedChem Express, Shanghai, China), and the purity of the compounds was ≥99.65%. Celastrol was dissolved in dimethyl sulfoxide (DMSO), and DMSO was used as the vehicle control. For *in vivo* study, celastrol was dissolved first in DMSO and then in 10% 2-hydroxypropyl-β-cyclodextrin (Sangon Biotech, Shanghai, China).

Antibody

Primary antibodies to the following proteins were used: cleaved PARP (c-PARP), cleaved caspase 8 (c-caspase 8), cleaved caspase 9 (c-caspase 9), ATF4, CHOP, Noxa, DR3, Bax, Bad, Bid, Bim, p53, p21, p-histone 3 (p-H3), p-H2AX, p-cdc2 (Cell Signaling Technology, Danvers, MA, United States); DR5 and FoxO3a (Abcam, Cambridge, MA, United States); TNFR1, TNFR2 and β-actin (HuaBio, China).

Cell Viability Assay

For cell viability assay, cells were seeded in black 96-well plates with 2×10^3 cells per well in triplicate and allowed to attach overnight. Cells were treated with DMSO, celastrol, Z-VAD-FMK (MedChem Express, Shanghai, China), or both celastrol and Z-VAD-FMK at the indicated concentrations for the indicated time. According to the manufacturer's protocol, the cell proliferation was measured by ATPlite luminescence assay (PerkinElmer, Norwalk, CT, United States) at the end of the incubation. The IC_{50} values were measured by the Logit method.

Clonogenic Survival Assay

For clonogenic survival assay, cells were seeded in six-well plates with 400 cells per well in triplicate and allowed to attach overnight. Cells were treated with DMSO or celastrol at the indicated concentrations and cultured for 10 days. At the end of incubation, cells were stained with crystal violet. Colonies with more than 50 cells each were counted and photographed with a gel imager (GelDoc XR System, Bio-rad, United States).

Apoptosis Assay

For apoptosis assay, cells were seeded at a density of 2.5×10^5 cells per well in six-well plates and allowed to attach overnight. Cells were exposed to DMSO or celastrol for 24 h and stained with AnnexinV-FITC and PI Apoptosis Kit according to the manufacturer's protocol (Share Biotechnology, Shanghai, China). Data were collected and analyzed using a flow cytometer (Beckman Coulter CytoFLEX, CA, United States).

Cell Cycle Analysis

For cell cycle analysis, cells were seeded at a density of 2.5×10^5 cells per well in six-well plates and allowed to attach overnight. Cells were exposed to DMSO or celastrol for 24 h. And then cells were harvested and fixed in 70% ice-cold ethanol at −20°C overnight. The samples were incubated in propidium iodide

(PI, 36 mg/ml; Sigma, St. Louis, MO, United States) for 15 min at 37°C. The cells were detected by flow cytometer (Beckman Coulter CytoFLEX, State of California, United States). Data of cell cycle were analyzed with FlowJo 8 software.

Western Blot Analysis

Total protein from cultured cells and tumor tissues was collected by using RIPA (Radio Immunoprecipitation Assay) lysis buffer, and protein concentration was quantified using a BCA protein assay kit (Vazyme Biotech, Nanjing, China). 20–40 mg protein was resolved by 7.5–15% SDS-PAGE, followed by electro-transferred to an Immobilon-PVDF Membrane (Merck Millipore Ltd, Tullagreen, Ireland). The membrane was then blocked with 5% skim milk for 1 h at room temperature. After being washed three times with TBST, PVDF membranes were incubated with primary antibodies at 4°C overnight. After washing, corresponding second antibodies were incubated with membranes for 1 h at room temperature, and the membranes were photographed by Tanon 5200 visualizer (Tanon, Shanghai, China).

Real-Time Polymerase Chain Reaction Analysis

According to the manufacturer's instructions, total RNA was isolated by using the Ultrapure RNA kit (ComWin Biotech, Beijing, China). Total RNA was purified and reversed to cDNA by using the PrimerScript reverse transcription reagent kit (Vazyme Biotech, Nanjing, China). The cDNA was quantified with RT-PCR by using the Power SYBR Green PCR MasterMix (Vazyme Biotech, Nanjing, China) on the ABI 7500 thermocycler (Applied Biosystems, Foster City, CA, United States). The mRNA data of each sample were normalized to β-actin. ATF4, CHOP, DR5, Noxa, Bim, and FoxO3a are encoded by *ATF4*, *CHOP* (*DDIT3*), *DR5* (*TNFRSF10B*), *NOXA* (*PMAIP1*), *BIM* (*BCL2L11*), and *FOXO3* genes, respectively. The sequences of the primers were as follows: human *β-actin*: forward 5′-CGTGCGTGACAT TAAGGAGAAG-3′; and reverse 5′-AAGGAAGGCTGGAAG AGTGC-3′; human *ATF4*: forward 5′-ATGACCGAAATG AGCTTCCTG-3′, and reverse 5′-GCTGGAGAACCCATG AGGT-3′; human *CHOP*: forward 5′-AGCCAAAATCAGAGC TGGAA-3′, and reverse 5′-TGGATCAGTCTGGAAAAGCA-3′; human *DR5*: forward 5′-CCAGCAAATGAAGGTGATCC-3′, and reverse 5′-GCACCAAGTCTGCAAAGTCA-3′; human *NOXA*: forward 5′-ACCAAGCCGGATTTGCGATT-3′, and reverse 5′-ACTTGCACTTGTTCCTCGTGG-3′; human *BIM*: forward 5′-TAAGTTCTGAGTGTGACCGAGA-3′, and reverse 5′-GCTCTGTCTGTAGGGAGGTAGG-3′; human *FOXO3*: forward 5′-CAGCCAGTCTATGCAAACCC-3′, and reverse 5′-ATCCAACCCATCAGCATCCA-3′.

siRNA Silencing

The cells were transfected with siRNA oligonucleotides by using Lipofectamine 2000 (Invitrogen, United States). Opti-MEM (Invitrogen, United States) was used to incubate with siRNA and Lipofectamine 2000 according to the manufacturer's instructions. All siRNAs were synthesized by GenePharma (Shanghai, China). The sequences of siRNA were as follows: si*Control*: 5′-UUCUCCGAACGUGUCACGUTT-3′; si*ATF4*-1: 5′-CCCUUCAGAUAAUGAUAGUTT-3′; si*ATF4*-2: 5′-CCT CACTGGCGAGTGTAAA-3′; si*DR5*-1: 5′-AAGACCCUUGUG CUCGUUGUC-3′; si*DR5*-2: 5′-CAGCCGUAGUCUUGAUUG UTT-3′; si*NOXA*-1: 5′-GGUGCACGUUUCAUCAAUUUGTT-3′; si*NOXA*-2: 5′-CCGGCAGAAACUUCUGAAUTT-3′; si*BIM*-1: 5′-UCUUACGACUGUUACGUUAUU-3′; si*BIM*-2: 5′-CAA CCACUAUCUCAGUGCA-3′; si*FOXO3*-1: 5′-GGAACGUGA UGCUUCGCAATT-3′; si*FOXO3*-2: 5′-AGGGAAGUUUGG UCAAUCATT-3′.

In Vivo Xenograft Model

Animal experiments were performed in accordance with the National Guidelines for Experimental Animal Welfare, with approval from the Institutional Animal Care and Use Committee of Longhua Hospital, Shanghai University of Traditional Chinese Medicine. Five-week-old, BALB/c nude female mice were purchased from Lingchang Biological Technology Co., Ltd. (Shanghai, China). Mice were kept and bred at a constant room temperature with a 12:12 h light/dark cycle and fed a standard rodent diet and water. 2×10^7 Eca109 cells were subcutaneously injected into the bilateral flank of each mouse. Then, mice were randomly divided into three experimental groups ($n = 5$): control, 4 mg/kg celastrol treatment group, and 8 mg/kg celastrol treatment group. Mice were treated with either β-cyclodextrin crystalline (vehicle control) or celastrol (4 or 8 mg/kg) via intraperitoneal injection every other day. Tumor volumes were determined by measuring length (l) and width (w) and calculating volume ($V = 0.5 \times l \times w^2$) every other day. Mice were sacrificed, and tumor tissues were weighed and photographed.

Statistical Analysis

The statistical significance of differences between groups was assessed using GraphPad Prism 8 software (San Diego, CA, United States). All data from three independent experiments were expressed as mean ± SEM. The student's t-test was used for the comparison of parameters between groups. p-value of $p < 0.05$ was significant, n.s = not significant. For all tests, three levels of significance ($^*p < 0.05$, $^{**}p < 0.01$, $^{***}p < 0.001$) were used.

RESULTS

Celastrol Inhibited the Viability of Esophageal Squamous Cell Carcinoma Cells

To evaluate the effect of celastrol on the proliferation of ESCC cells, we first examined the IC_{50} values of celastrol on two ESCC cell lines Eca109 and EC1. The IC_{50} values of celastrol on Eca109 and EC1 were 1.688 and 1.684 μM, respectively (**Figure 1B**). Furthermore, we found a time and dose-dependent growth inhibitory efficacy in two ESCC cell lines upon celastrol treatment (**Figure 1C**). In addition, our results showed that celastrol significantly inhibited the colony formation of both

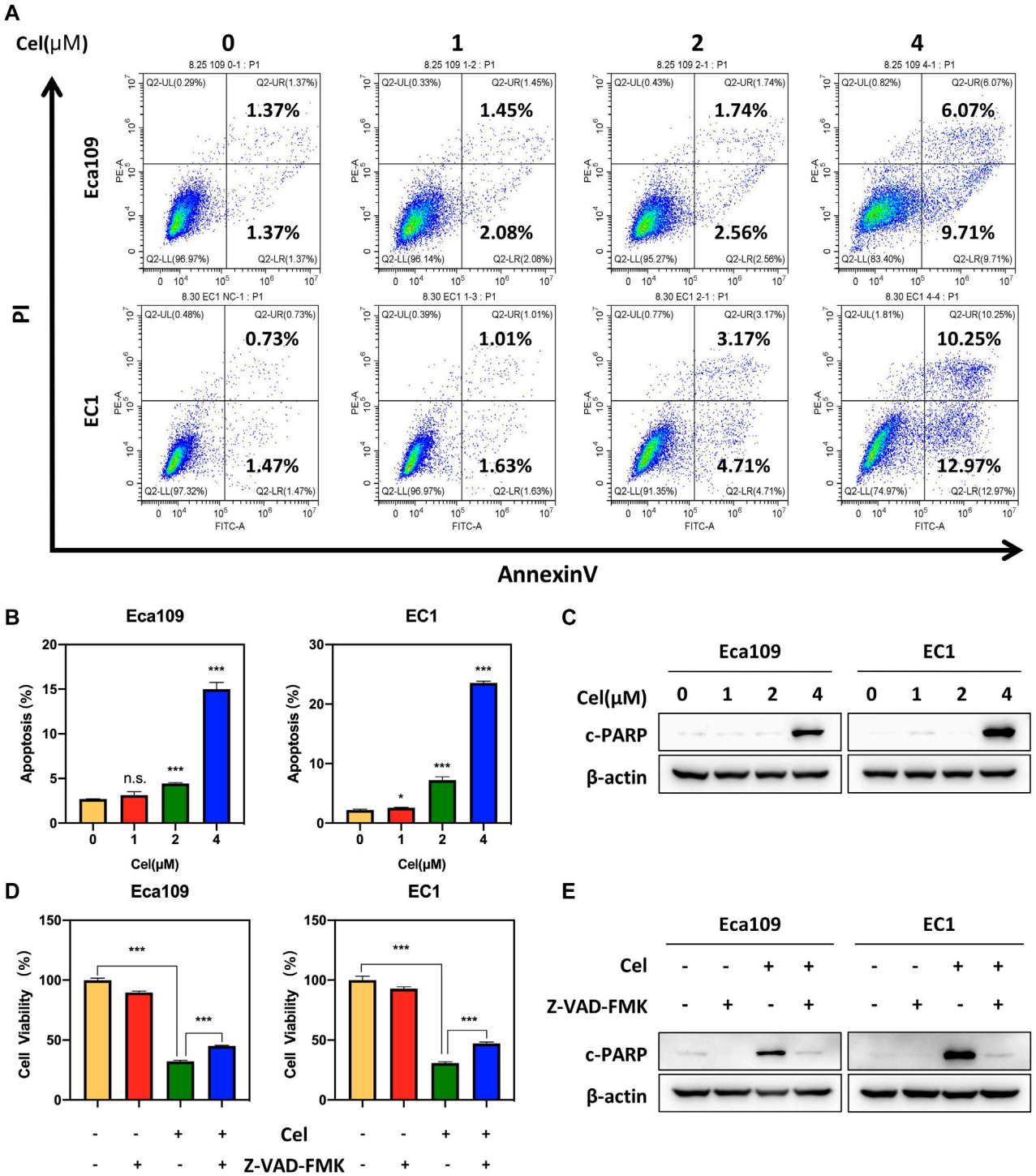

FIGURE 2 | Celastrol induced apoptosis in ESCC cells. **(A,B)** Eca109 and EC1 cells were treated with 1, 2, and 4 μM of celastrol or DMSO for 24 h. And then the cells were stained with Annexin-V-FITC and PI apoptosis kit and tested by the flow cytometric analysis. Data were assessed with GraphPad Prism 8 software. **(C)** Celastrol increased the expression level of c-PARP. Eca109 and EC1 cells were treated with 1, 2, and 4 μM celastrol or DMSO for 24 h, and cell lysates were analyzed by Western blotting with a specific antibody against c-PARP with β-actin as a loading control. **(D)** ATPlite assay was used to determine the cell viability of Eca109 and EC1 cells treated with DMSO, 4 μM celastrol, 20 μM Z-VAD-FMK, or both for 24 h. **(E)** Eca109 and EC1 cells treated with DMSO, 4 μM celastrol, 20 μM Z-VAD-FMK, or both for 24 h, and cell lysates were analyzed by Western blotting using an antibody against c-PARP with β-actin as a loading control. *denotes $p < 0.05$, ***denotes $p < 0.001$, n.s. denotes not significant.

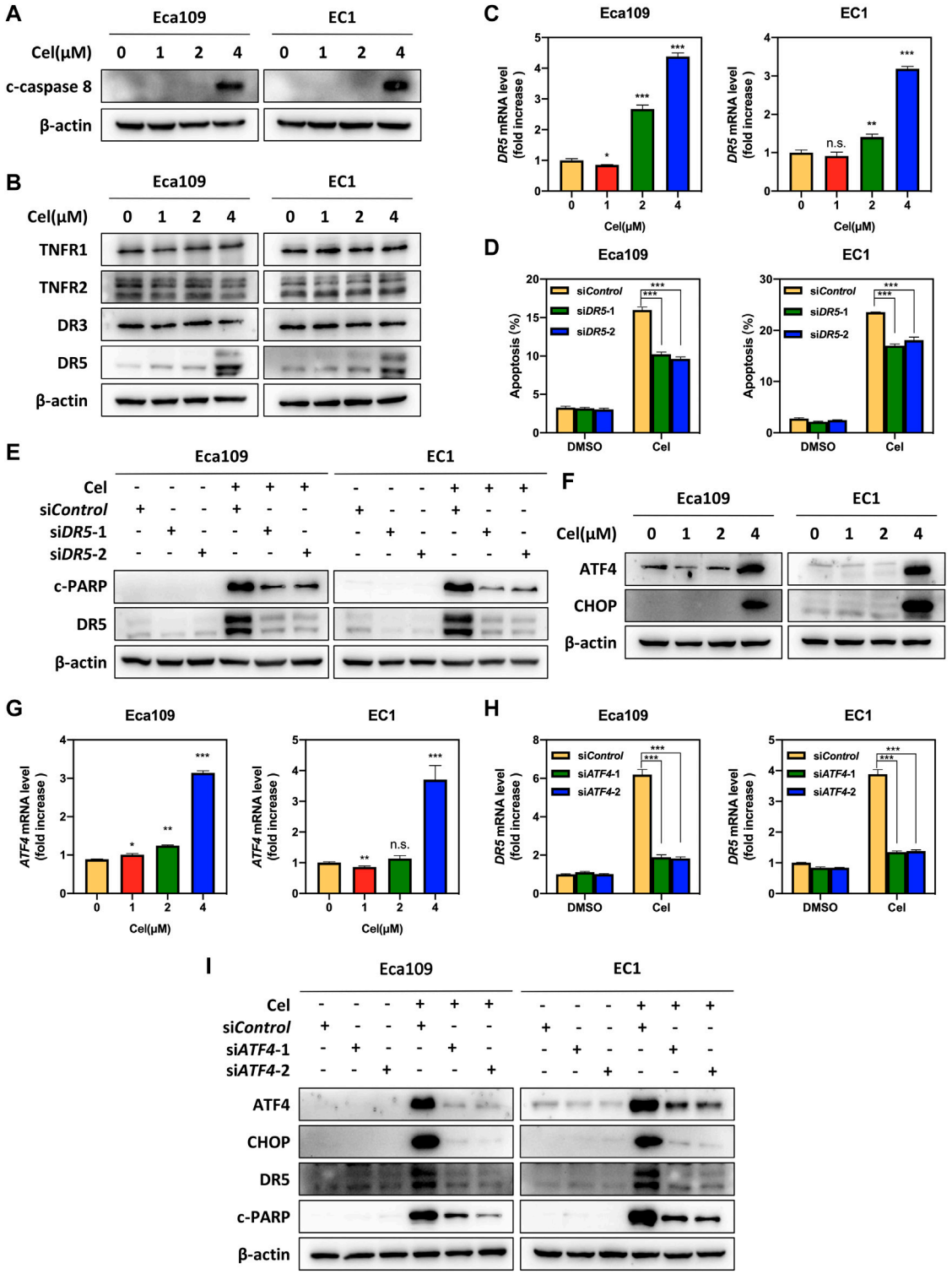

FIGURE 3 | Celastrol activated DR5-dependent extrinsic apoptosis by upregulating ATF4. **(A)** Celastrol induced the activation of caspase 8. Eca109 and EC1 cells were treated with 1, 2, and 4 μM of celastrol or DMSO for 24 h, and cell lysates were analyzed by Western blotting using a specific antibody against c-caspase 8 with β-actin as a loading control. **(B)** Celastrol activated extrinsic apoptosis by upregulated DR5. Eca109 and EC1 cells were treated with 1, 2, and 4 μM of celastrol or DMSO for 24 h, and cell lysates were analyzed by Western blotting using specific antibodies against TNFR1, TNFR2, DR3, and DR5 with β-actin as a loading control. **(C)** Celastrol increased the mRNA level of *DR5*. Eca109 and EC1 cells were treated with 1, 2, and 4 μM of celastrol or DMSO for 24 h, and the mRNA level of *DR5* was determined by the real-time PCR. **(D,E)** Knockdown of DR5 inhibited apoptosis induced by celastrol. Eca109 and EC1 cells were transfected with control or si*DR5* for

(*Continued*)

FIGURE 3 | 72 h, and then treated with 4 μM celastrol or DMSO for 24 h. Apoptosis induction was quantified by Annexin V-FITC/PI double-staining analysis. Cell lysates were analyzed by Western blotting using specific antibodies against c-PARP and DR5 with β-actin as a loading control. **(F)** Celastrol induced the accumulation of ATF4 and CHOP. Eca109 and EC1 cells were treated with 1, 2, and 4 μM of celastrol or DMSO for 24 h. Cell lysates were analyzed by Western blotting using antibodies against ATF4 and CHOP with β-actin as a loading control. **(G)** Celastrol increased the mRNA level of *ATF4*. Eca109 and EC1 cells were treated with1 μM, 2, and 4 μM of celastrol or DMSO for 24 h, and the mRNA level of *ATF4* was determined by the real-time PCR. **(H,I)** Celastrol induced apoptosis of Eca109 and EC1 cells via the ATF4-DR5 axis. Eca109 and EC1 cells were transfected with control or si*ATF4* for 72 h, and then treated with 4 μM celastrol or DMSO for 24 h. The effect of si*ATF4* on *DR5* transcription was analyzed by real-time PCR. Expression levels of ATF4, CHOP, DR5, and c-PARP were assessed by Western blotting with β-actin as a loading control. *denotes $p < 0.05$, **denotes $p < 0.01$, ***denotes $p < 0.001$, n.s. denotes not significant.

two ESCC cell lines in a dose-dependent manner (**Figures 1D,E**). Therefore, these findings demonstrated celastrol obviously inhibited the viability of ESCC cells.

Celastrol Induced Apoptosis in Esophageal Squamous Cell Carcinoma Cells

In order to explore the mechanism of celastrol inhibiting the viability of ESCC cells, we determined the cellular response elicited by celastrol. We observed an obvious feature of apoptosis-shrunk morphology of ESCC cells under the treatment of celastrol (data not shown). Annexin V-FITC/PI double-staining analysis was further used to verify whether celastrol induced apoptosis in ESCC cells. As shown in **Figures 2A,B**, celastrol treatment resulted in a remarkable increase in the apoptotic cell population. Furthermore, we detected the expression of c-PARP, the classical marker of apoptosis. As shown, the expression level of c-PARP was obviously upregulated upon celastrol stimulation (**Figure 2C**). In addition, we found that apoptosis inhibitor Z-VAD-FMK alleviated the inhibition of celastrol on the viability of ESCC cells (**Figures 2D,E**). These results collectively demonstrated that celastrol inhibited the growth of ESCC cells by triggering apoptosis.

Celastrol Induced DR5-Dependent Extrinsic Apoptosis by Transcriptional Activation of ATF4

To further characterize the mechanism underlying celastrol-induced apoptosis, we determined the expression of c-caspase 8, a marker of extrinsic apoptosis. Our data showed that celastrol upregulated the expression of c-caspase 8 in Eca109 and EC1 cells, indicating that celastrol activated extrinsic apoptosis (**Figure 3A**). In order to explore the activation mechanism of extrinsic (death receptor-mediated) apoptosis under celastrol treatment, we evaluated the expression of death receptor family members. Among these death receptors (TNRF1, TNRF2, DR3, and DR5), the protein and mRNA levels of DR5 were significantly increased elicited by celastrol (**Figures 3B,C**). To further define the role of DR5 in celastrol-induced apoptosis, the expression of *DR5* was downregulated using two siRNA sequences. As shown, DR5 knockdown significantly attenuated the percentage of apoptotic cells in ESCC cells (**Figure 3D** and **Supplementary Figure S1A**), and downregulated the expression of c-PARP (**Figure 3E**). These results suggested that celastrol-triggered extrinsic apoptosis was mediated by DR5.

Previous studies reported that anti-cancer agents (e.g., MLN4924) transcriptionally activated ATF4 by inducing ER stress, and subsequently induced CHOP-mediated *DR5* transcription and caspase 8-mediated extrinsic apoptosis (Chen et al., 2016). Therefore, we speculated celastrol activated extrinsic apoptosis through ATF4-DR5 axis. To verify this hypothesis, we first determined the expression of ATF4 and CHOP, and the results showed that celastrol significantly upregulated the expression of ATF4 and CHOP at both protein and mRNA levels (**Figures 3F,G** and **Supplementary Figure S1B**). Next, we determined whether DR5-induced extrinsic apoptosis elicited by celastrol was dependent on ATF4. Our results showed that ATF4 knockdown significantly decreased the mRNA and protein levels of CHOP and DR5, indicating that ATF4 transactivated CHOP and DR5 upon celastrol stimulation (**Figures 3H,I** and **Supplementary Figure S1C**). Meanwhile, the knockdown of ATF4 obviously downregulated the expression of c-PARP (**Figure 3I**). Taken together, these findings demonstrated that celastrol activated extrinsic apoptosis of ESCC cells through the ATF4-DR5 axis.

ATF4 Meditated Celastrol-Induced Noxa Upregulation

To investigate whether celastrol induced intrinsic apoptosis, we determined the expression of c-caspase 9 in ESCC cells exposed to celastrol. As shown, the expression level of c-caspase 9 remarkably upregulated in both two ESCC cell lines (**Figure 4A**). In order to illustrate the mechanism underlying celastrol-induced intrinsic apoptosis, we examined the expression of classical pro-apoptotic proteins, including Bax, Bak, Bid, Noxa, and Bim. As shown, after celastrol treatment, we observed the expression levels of Noxa and Bim, two pro-apoptotic BH3-only members (Kale et al., 2017), strikingly elevated in Eca109 and EC1 cells, while the expression of Bax, Bak, and Bid did not change (**Figures 4B,C**), suggesting that celastrol activated Noxa and Bim. To further define the role of Noxa in celastrol-induced intrinsic apoptosis, the expression of *NOXA* was downregulated by siRNA silencing in celastrol-treated cells. As shown, Noxa knockdown significantly reduced the induction of apoptosis and the cleavage of PARP, highlighting a critical role of Noxa in celastrol-induced intrinsic apoptosis (**Figures 4D,E** and **Supplementary Figure S1D**). Given that Noxa was known to be regulated by ATF4, we, therefore, tested the involvement of ATF4 in celastrol-induced Noxa expression (Sharma et al., 2018). Indeed, downregulation of ATF4 significantly suppressed the induction of Noxa at both mRNA and protein levels (**Figures 4F,G**), supporting the notion that ATF4 meditated celastrol-induced Noxa upregulation.

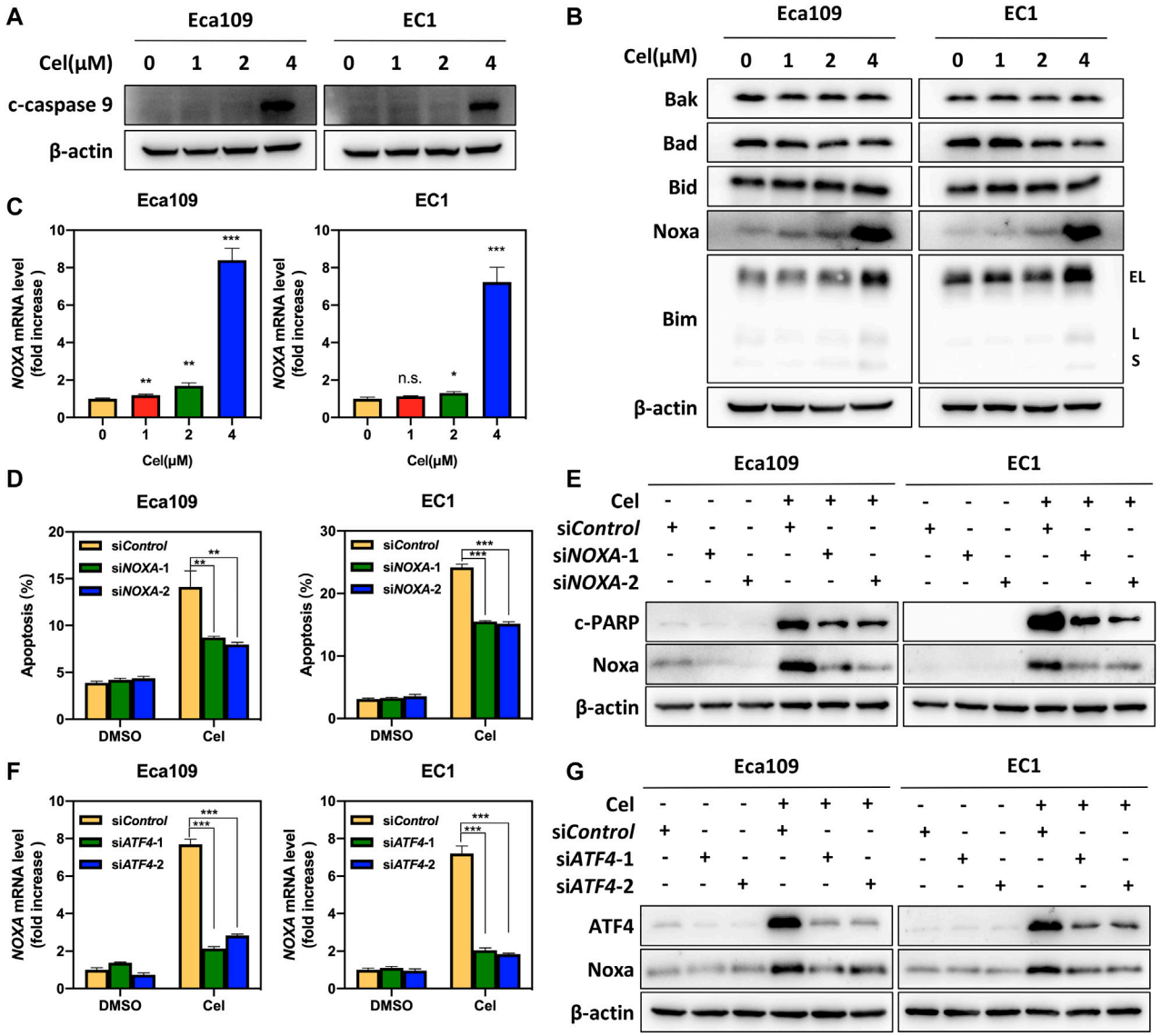

FIGURE 4 | ATF4 meditated celastrol-induced Noxa upregulation. **(A)** Celastrol induced the activation of caspase 9. Eca109 and EC1 cells were treated with 1, 2, and 4 μM of celastrol or DMSO for 24 h, and cell lysates were analyzed by Western blotting using a specific antibody against c-caspase 9 with β-actin as a loading control. **(B)** Celastrol activated extrinsic apoptosis by upregulating Noxa and Bim. Eca109 and EC1 cells were treated with 1, 2, and 4 μM of celastrol or DMSO for 24 h, and then cell lysates were analyzed by Western blotting with specific antibodies against Bak, Bad, Bid, Noxa, and Bim with β-actin as a loading control. Three major Bim isoforms were created by alternative splicing: BimS, BimL, and BimEL. **(C)** Celastrol increased the mRNA level of *NOXA*. Eca109 and EC1 cells were treated with 1, 2, and 4 μM of celastrol or DMSO for 24 h, and the mRNA level of *NOXA* was determined by real-time PCR. **(D)** Knockdown of Noxa inhibited apoptosis induced by celastrol. Eca109 and EC1 cells were transfected with control or si*NOXA* for 72 h, and then treated with 4 μM celastrol or DMSO for 24 h. Apoptosis induction was quantified by Annexin V-FITC/PI double-staining analysis. **(E)** Cell lysates were analyzed by Western blotting using specific antibodies against c-PARP and Noxa with β-actin as a loading control. **(F,G)** ATF4 meditated celastrol-induced Noxa upregulation. Eca109 and EC1 cells were transfected with control or si*ATF4* for 72 h, and then treated with 4 μM celastrol or DMSO for 24 h. The effect of si*ATF4* on *NOXA* transcription was analyzed by real-time PCR. Expression levels of ATF4 and Noxa were assessed by Western blotting analysis with β-actin as a loading control. *denotes $p < 0.05$, **denotes $p < 0.01$, ***denotes $p < 0.001$, n.s. denotes not significant.

FoxO3a Meditated Celastrol-Induced Bim Upregulation

Our aforementioned results indicated that celastrol upregulated the expression of the pro-apoptotic protein Bim (**Figure 4B**). We further found that the mRNA level of *BIM* was significantly elevated upon celastrol treatment (**Figure 5A**). To further determine the potential role of Bim in celastrol-mediated intrinsic apoptosis, the expression of *BIM* was downregulated via siRNA silencing. Our data showed that knockdown of Bim significantly alleviated the percentage of apoptotic cells induced by celastrol (**Figure 5B** and **Supplementary Figure S1E**), along with a reduction of the c-PARP (**Figure 5C**), demonstrating that Bim was involved in celastrol-induced intrinsic apoptosis of

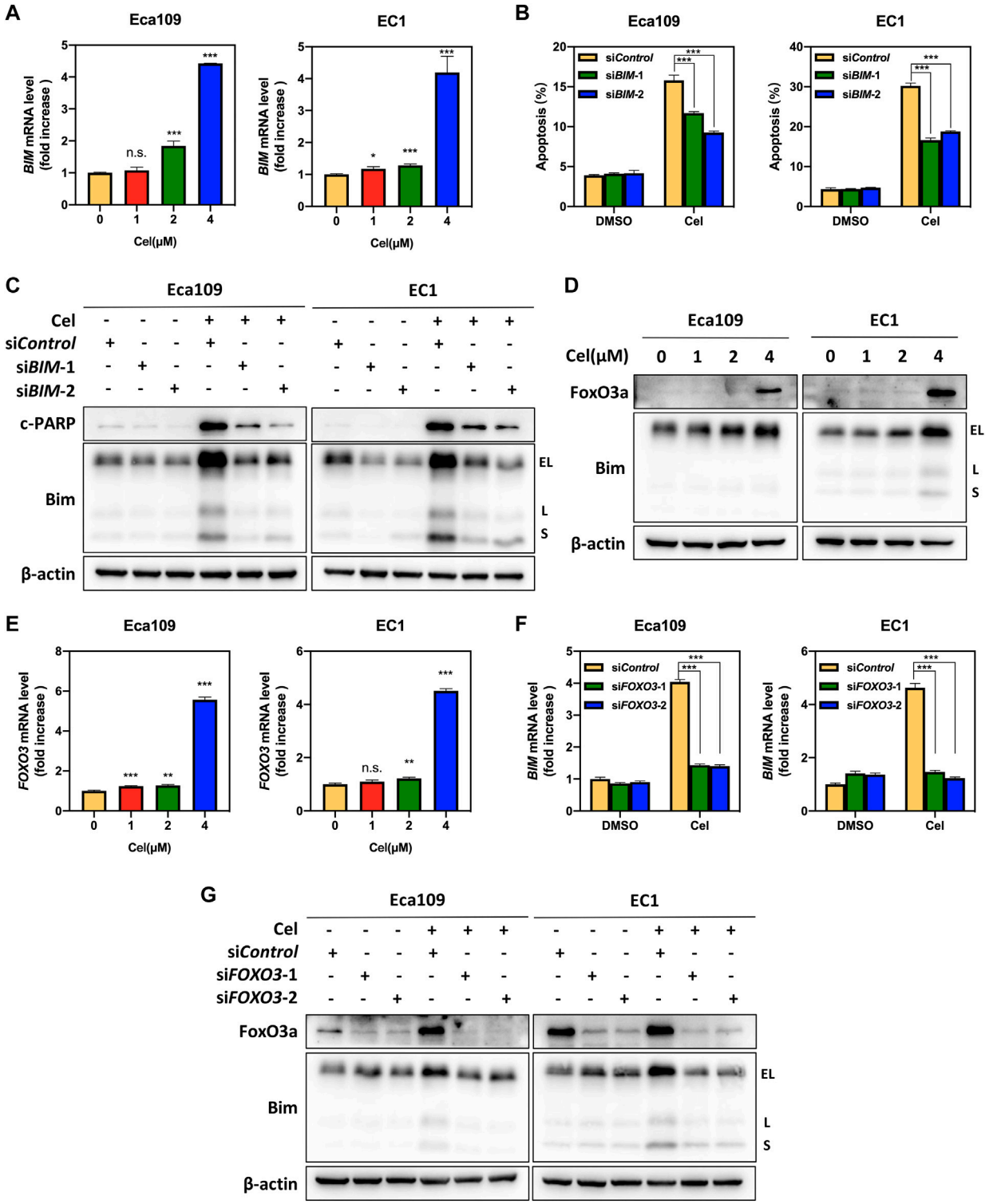

FIGURE 5 | FoxO3a meditated celastrol-induced Bim upregulation. **(A)** Celastrol increased the mRNA level of *BIM*. Eca109 and EC1 cells were treated with 1, 2, and 4 μM of celastrol or DMSO for 24 h. The mRNA level of *BIM* was determined by real-time PCR. **(B,C)** Knockdown of Bim inhibited apoptosis induced by celastrol. Eca109 and EC1 cells were transfected with control or si*BIM* for 72 h, and then treated with 4 μM celastrol or DMSO for 24 h. Apoptosis induction was quantified by Annexin V-FITC/PI double-staining analysis. Cell lysates were analyzed by Western blotting using specific antibodies against c-PARP and Bim with β-actin as a loading control. Three major Bim isoforms were created by alternative splicing: BimS, BimL, and BimEL. **(D,E)** Celastrol induced the upregulation of FoxO3a. Eca109 and EC1 cells were treated with 1, 2, and 4 μM of celastrol or DMSO for 24 h, and cell lysates were analyzed by Western blotting with an antibody against Bim and FoxO3a

(*Continued*)

FIGURE 5 | with β-actin as a loading control. Three major Bim isoforms were created by alternative splicing: BimS, BimL, and BimEL. The mRNA level of *FOXO3* was determined by real-time PCR. **(F,G)** FoxO3a was the response to celastrol-induced Bim upregulation. Eca109 and EC1 cells were transfected (72 h) with control or si*FOXO3*, and treated with 4 μM celastrol for 24 h. The effect of si*FOXO3* on *BIM* transcription was analyzed by real-time PCR. Expression levels of FoxO3a and Bim were assessed by Western blotting analysis with β-actin as a loading control. Three major Bim isoforms were created by alternative splicing: BimS, BimL, and BimEL. *denotes $p < 0.05$, **denotes $p < 0.01$, ***denotes $p < 0.001$, n.s. denotes not significant.

ESCC cells. Considering that *FOXO3*, one of forkhead transcription factor family, is the notable transcription factor regulating *BIM* gene expression in response to apoptosis (Zhenxing et al., 2019). We, therefore, examined the potential role of FoxO3a in celastrol-induced Bim expression. As shown in **Figures 5D,E**, celastrol treatment significantly upregulated the mRNA and protein levels of FoxO3a in ESCC cells. Furthermore, we found that downregulation of FoxO3a significantly inhibited the accumulation of Bim induced by celastrol (**Figures 5F,G**), illustrating that FoxO3a meditated celastrol-induced Bim upregulation. Collectively, our findings demonstrated that celastrol activated intrinsic apoptosis of ESCC cells via the ATF4-Noxa and FoxO3a-Bim axis.

Celastrol Suppressed the Growth of Esophageal Squamous Cell Carcinoma *in vivo*

Finally, we established a subcutaneous transplantation tumor model with Eca109 cells to examine the anti-tumor potential of celastrol *in vivo*. Compared with the control group, celastrol significantly inhibited the tumor growth over time (4 and 8 mg/kg celastrol corresponded to $p < 0.01$ and $p < 0.001$ respectively, **Figure 6A**). Moreover, the tumor weights of the celastrol-treated mice were much lower than those of the control mice ($p < 0.001$, **Figures 6B,C**). During the whole experiment, there was no significant change in animal weights (**Figure 6D**) and no significant morphological difference in liver and kidney (data not shown) between the celastrol-treated group and the control group. In addition, as shown in **Figure 6E**, celastrol triggered extrinsic and intrinsic apoptosis *in vivo*, as evidenced by the accumulation of apoptosis-related proteins in celastrol-treated tumor tissue, including ATF4, DR5, c-caspase 8, Noxa, FoxO3a, Bim, c-caspase 9, as well as c-caspase 3 and c-PARP. Together, our findings indicated that celastrol activated extrinsic and intrinsic apoptosis, thus inhibiting the tumor growth of ESCC both *in vitro* and *in vivo*.

DISCUSSION

ESCC is a highly malignant tumor of the digestive system, and its incidence and mortality rates are rising rapidly (Sung et al., 2021). In recent years, although some progress has been made in the diagnosis and treatment of ESCC, effective therapeutic strategies are still insufficient (Yang et al., 2020). An increasing body of evidence suggested that the natural products exhibited the potential anti-tumor efficacy in ESCC (Ying et al., 2018). In our study, we validated that celastrol was a promising candidate for the treatment of ESCC. We showed that celastrol significantly suppressed the malignant proliferation of ESCC cells, and strikingly inhibited the tumor growth in nude mouse xenograft model. Mechanistically, we demonstrated that celastrol coordinatively triggered DR5-dependent extrinsic apoptosis and Noxa-dependent intrinsic apoptosis through transcriptional activation of ATF4. Furthermore, we revealed that the FoxO3a-Bim pathway contributed to celastrol-induced intrinsic apoptosis of ESCC cells (**Figure 6F**). Our findings demonstrated the substantial inhibitory effect of celastrol on ESCC, which provided an attractive choice for the ESCC treatment.

It was reported that ER stress upregulated the expression of ATF4 and CHOP in response to unfolded protein response (UPR) (Kim et al., 2021). Death receptor DR5, a downstream target of CHOP, was activated after CHOP accumulation, and further triggered apoptosis cascades (Chen et al., 2016). In our study, we found that celastrol activated extrinsic apoptosis through the ATF4-CHOP-DR5 pathway, as evidenced by significantly diminished the expression of CHOP and DR5 after ATF4 knockdown. Except for CHOP and DR5, we found that ATF4 knockdown reduced celastrol-induced Noxa accumulation as well, suggesting that celastrol triggered Noxa-dependent intrinsic apoptosis by transcriptionally activating ATF4. Studies have shown that natural products such as parthenolide and curcumin activate eIF2α through ER stress, which in turn activates ATF4 and triggers apoptosis (Wu et al., 2010; Zhao et al., 2014). Therefore, celastrol might also activate ATF4 through ER stress. The mechanism by which celastrol transcriptionally activated ATF4 needs to be further clarified. Furthermore, our data showed that celastrol up-regulated the expression of p53, which was known to transcriptionally regulate Noxa expression as well (**Supplementary Figure S2B**) (Furukawa et al., 2018). Therefore, apart from ATF4, p53 may also be involved in the upregulation of Noxa induced by celastrol. Interestingly, in addition to Noxa, we found Bim contributed to celastrol-induced intrinsic apoptosis of ESCC cells, and FoxO3a meditated celastrol-induced Bim upregulation. However, FoxO3a knockdown did not completely alleviate celastrol-induced Bim accumulation. Given that other transcription factors (*Smad3*, *E2F1*, *JNK/c-Jun,* and *c-Myc*, etc) that are known to mediate Bim expression, whether these transcription factors are involved in the Bim induction elicited by celastrol remains further exploration (Chen et al., 2014; Muthalagu et al., 2014; Shats et al., 2017; Wildey et al., 2021).

The rapid growth of cancer cells is attributed to the accelerated cell cycle process (Zheng et al., 2019). In view of this, the blockage of the cell cycle process is considered an effective strategy to halt tumor growth (Thu et al., 2018). Previous studies have reported that celastrol prevented tumor cell proliferation by inducing cell cycle arrest (Ni et al., 2019). We found that celastrol treatment increased the cell populations in the G2/M phase of the cell cycle in ESCC cells (**Supplementary Figure S2A**). Furthermore, we showed that

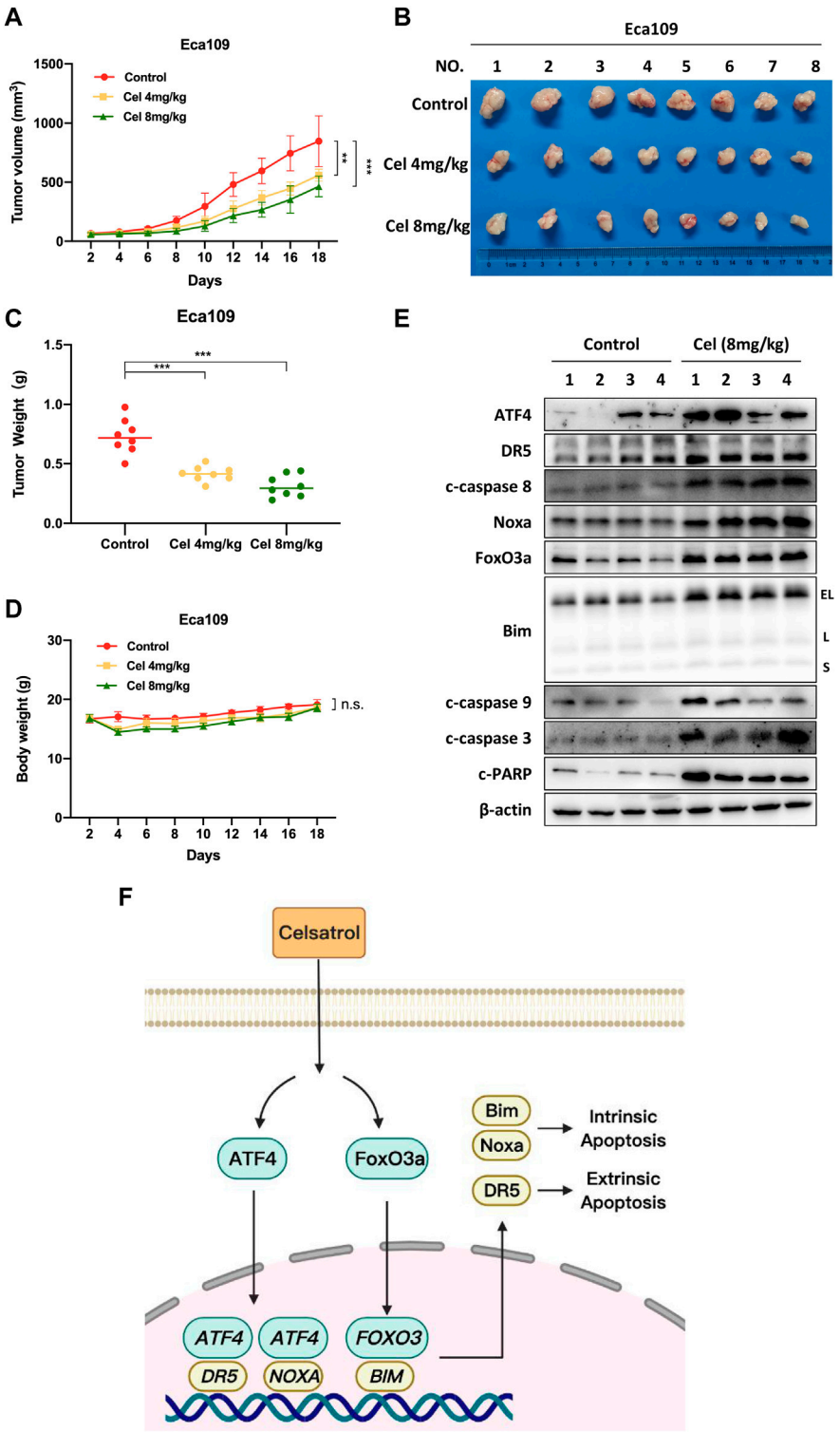

FIGURE 6 | Celastrol suppressed the growth of ESCC *in vivo*. **(A)** Nude mice have subcutaneously transplanted Eca109 cells and are treated with celastrol as described in Materials and Methods. Tumor size was determined with a caliper every other day, and the volume was calculated to construct a growth curve. **(B)** Mice were sacrificed, and tumor tissues were harvested and photographed. **(C)** The tumor weight was measured with an electronic scale on the sacrificed day. **(D)** Body weight of each mouse was recorded every other day during the whole experiment. **(E)** Celastrol induced extrinsic and intrinsic apoptosis *in vivo*. Proteins extracted from tumor tissues were analyzed by Western blotting using specific antibodies against ATF4, DR5, c-caspase 8, Noxa, FoxO3a, Bim, c-caspase 9, c-caspase 3, and c-PARP with β-actin as a loading control. Three major Bim isoforms were created by alternative splicing: BimS, BimL, and BimEL. **(F)** The mechanism of celastrol inhibits

(*Continued*)

FIGURE 6 | the tumor growth of ESCC. Celastrol coordinatively triggered DR5-dependent extrinsic apoptosis and Noxa-dependent intrinsic apoptosis through transcriptional activation of ATF4. FoxO3a-Bim pathway contributed to celastrol-induced intrinsic apoptosis in ESCC cells. **denotes $p < 0.01$, ***denotes $p < 0.001$, n.s. denotes not significant.

celastrol significantly upregulated the expression of the mitotic marker p-histone 3 (p-H3, ser10) and downregulated the expression of G2 phase marker p-cdc2, suggesting that celastrol induced ESCC cells to pass through G2/M checkpoint and then arrest at M phase. In addition, we found that celastrol caused the accumulation of cell cycle inhibitory protein p21 and its upstream protein p53, indicating that celastrol induced M-phase cell cycle arrest through the p53/p21 signaling pathway (**Supplementary Figure S2B**). It is well known that the best-characterized p53 function is the response to acute DNA damage (Boutelle and Attardi, 2021). Our data showed that celastrol significantly upregulated the expression of DNA damage marker p-H2AX, suggesting that celastrol initiated DNA damage and the activation of the p53/p21 signaling pathway, and then promoted cell cycle arrest (**Supplementary Figure S2B**). In fact, the persistence of DNA damage will induce programmed cell death such as apoptosis or cell senescence (Roos et al., 2015; Ou and Schumacher, 2018). Therefore, in our study, it is possible that celastrol caused the persistence of cell DNA damage during cell cycle arrest, which eventually led to apoptosis of ESCC cells. Furthermore, our results showed that caspase inhibitor Z-VAD-FMK only partially rescued the cellular viability after celastrol treatment, indicating that celastrol inhibited the proliferation of ESCC cells by inducing the combinatory effects of both cell cycle arrest and apoptosis.

In summary, our study revealed a previously unknown inhibitory efficacy of celastrol on ESCC by activating DR5-dependent extrinsic and Noxa/Bim-dependent intrinsic apoptosis, suggesting that celastrol was a candidate for apoptosis inducer in recalcitrant human ESCC.

DATA AVAILABILITY STATEMENT

The original contributions presented in the study are included in the article/**Supplementary Material**, further inquiries can be directed to the corresponding author.

ETHICS STATEMENT

The animal study was reviewed and approved by the Animal Experimental Ethics Committee of Longhua Hospital, Shanghai University of Traditional Chinese Medicine.

AUTHOR CONTRIBUTIONS

LJ contributed to the conception and design of the project. XC and SW carried out the experiments and drafted the manuscript, and LJ finalized the manuscript. SY, LZ, and TX performed statistical analyses. FZ and YZ coordinated the study over the entire time. All authors contributed to manuscript revision, read, and approved the submitted version.

FUNDING

This work was supported by the National Natural Science Foundation of China (Grant Nos. 81820108022, 81902380, 82172933), Innovation Program of Shanghai Municipal Education Commission (Grant No. 2019-01-07-00-10-E00056), Shanghai Frontiers Science Center of Disease and Syndrome Biology of Inflammatory Cancer Transformation (Grant No. 2021KJ03-12), National 13th Five-Year Science and Technology Major Special Project for New Drug and Development (Grant No. 2017ZX09304001).

SUPPLEMENTARY MATERIAL

The Supplementary Material for this article can be found online at: https://www.frontiersin.org/articles/10.3389/fphar.2022.873166/full#supplementary-material

REFERENCES

Boutelle, A. M., and Attardi, L. D. (2021). p53 and Tumor Suppression: It Takes a Network. *Trends Cell Biol.* 31 (4), 298–310. doi:10.1016/j.tcb.2020.12.011

Bray, F., Ferlay, J., Soerjomataram, I., Siegel, R. L., Torre, L. A., and Jemal, A. (2018). Global Cancer Statistics 2018: GLOBOCAN Estimates of Incidence and Mortality Worldwide for 36 Cancers in 185 Countries. *CA Cancer J. Clin.* 68 (6), 394–424. doi:10.3322/caac.21492

Carneiro, B. A., and El-Deiry, W. S. (2020). Targeting Apoptosis in Cancer Therapy. *Nat. Rev. Clin. Oncol.* 17 (7), 395–417. doi:10.1038/s41571-020-0341-y

Chen, P., Hu, T., Liang, Y., Li, P., Chen, X., Zhang, J., et al. (2016). Neddylation Inhibition Activates the Extrinsic Apoptosis Pathway through ATF4-CHOP-DR5 Axis in Human Esophageal Cancer Cells. *Clin. Cancer Res.* 22 (16), 4145–4157. doi:10.1158/1078-0432.Ccr-15-2254

Deng, L. J., Qi, M., Li, N., Lei, Y. H., Zhang, D. M., and Chen, J. X. (2020). Natural Products and Their Derivatives: Promising Modulators of Tumor Immunotherapy. *J. Leukoc. Biol.* 108 (2), 493–508. doi:10.1002/jlb.3mr0320-444r

Diepstraten, S. T., Anderson, M. A., Czabotar, P. E., Lessene, G., Strasser, A., and Kelly, G. L. (2022). The Manipulation of Apoptosis for Cancer Therapy Using BH3-Mimetic Drugs. *Nat. Rev. Cancer* 22 (1), 45–64. doi:10.1038/s41568-021-00407-4

Furukawa, H., Makino, T., Yamasaki, M., Tanaka, K., Miyazaki, Y., Takahashi, T., et al. (2018). PRIMA-1 Induces P53-Mediated Apoptosis by Upregulating Noxa in Esophageal Squamous Cell Carcinoma with TP53 Missense Mutation. *Cancer Sci.* 109 (2), 412–421. doi:10.1111/cas.13454

Gao, Y., Zhou, S., Pang, L., Yang, J., Li, H. J., Huo, X., et al. (2019). Celastrol Suppresses Nitric Oxide Synthases and the Angiogenesis Pathway in Colorectal Cancer. *Free Radic. Res.* 1-1153 (3), 324–334. doi:10.1080/10715762.2019.1575512

Han, H., Yang, C., Ma, J., Zhang, S., Zheng, S., Ling, R., et al. (2022). N7-methylguanosine tRNA Modification Promotes Esophageal Squamous Cell

Carcinoma Tumorigenesis via the RPTOR/ULK1/autophagy axis. *Nat. Commun.* 13 (1), 1478. doi:10.1038/s41467-022-29125-7

Hong, P., Liu, Q. W., Xie, Y., Zhang, Q. H., Liao, L., He, Q. Y., et al. (2020). Echinatin Suppresses Esophageal Cancer Tumor Growth and Invasion through Inducing AKT/mTOR-dependent Autophagy and Apoptosis. *Cell Death Dis.* 11 (7), 524. doi:10.1038/s41419-020-2730-7

Huang, T. X., and Fu, L. (2019). The Immune Landscape of Esophageal Cancer. *Cancer Commun. (Lond)* 39 (1), 79. doi:10.1186/s40880-019-0427-z

Jiang, S. X., Qi, B., Yao, W. J., Gu, C. W., Wei, X. F., Zhao, Y., et al. (2017). Berberine Displays Antitumor Activity in Esophageal Cancer Cells *In Vitro*. *World J. Gastroenterol.* 23 (14), 2511–2518. doi:10.3748/wjg.v23.i14.2511

Kale, J., Osterlund, E. J., and Andrews, D. W. (2017). BCL-2 Family Proteins: Changing Partners in the Dance towards Death. *Cell Death Differ.* 25 (1), 65–80. doi:10.1038/cdd.2017.186

Kashyap, D., Sharma, A., Tuli, H. S., Sak, K., Mukherjee, T., and Bishayee, A. (2018). Molecular Targets of Celastrol in Cancer: Recent Trends and Advancements. *Crit. Rev. Oncology/hematology* 128, 70–81. doi:10.1016/j.critrevonc.2018.05.019

Kim, S., Lee, M., Song, Y., Lee, S.-Y., Choi, I., Park, I.-S., et al. (2021). Argininosuccinate Synthase 1 Suppresses Tumor Progression through Activation of PERK/eIF2α/ATF4/CHOP axis in Hepatocellular Carcinoma. *J. Exp. Clin. Cancer Res.* 40 (1), 127. doi:10.1186/s13046-021-01912-y

Leng, X. F., Daiko, H., Han, Y. T., and Mao, Y. S. (2020). Optimal Preoperative Neoadjuvant Therapy for Resectable Locally Advanced Esophageal Squamous Cell Carcinoma. *Ann. N. Y. Acad. Sci.* 1482 (1), 213–224. doi:10.1111/nyas.14508

Liu, Z., Shi, Z., Lin, J., Zhao, S., Hao, M., Xu, J., et al. (2019). Piperlongumine-induced Nuclear Translocation of the FOXO3A Transcription Factor Triggers BIM-Mediated Apoptosis in Cancer Cells. *Biochem. Pharmacol.* 163, 101–110. doi:10.1016/j.bcp.2019.02.012

Ma, L., Zhang, M., Zhao, R., Wang, D., Ma, Y., and Ai, L. (2021). Plant Natural Products: Promising Resources for Cancer Chemoprevention. *Molecules* 26 (4), 933. doi:10.3390/molecules26040933

Muthalagu, N., Junttila, M. R., Wiese, K. E., Wolf, E., Morton, J., Bauer, B., et al. (2014). BIM Is the Primary Mediator of MYC-Induced Apoptosis in Multiple Solid Tissues. *Cell Rep.* 8 (5), 1347–1353. doi:10.1016/j.celrep.2014.07.057

Ni, H., Han, Y., and Jin, X. (2019). Celastrol Inhibits Colon Cancer Cell Proliferation by Downregulating miR-21 and PI3K/AKT/GSK-3β Pathway. *Int. J. Clin. Exp. Pathol.* 12 (3), 808–816. https://pubmed.ncbi.nlm.nih.gov/31933888/

Ou, H. L., and Schumacher, B. (2018). DNA Damage Responses and P53 in the Aging Process. *Blood* 131 (5), 488–495. doi:10.1182/blood-2017-07-746396

Roos, W. P., Thomas, A. D., and Kaina, B. (2015). DNA Damage and the Balance between Survival and Death in Cancer Biology. *Nat. Rev. Cancer* 16 (1), 20–33. doi:10.1038/nrc.2015.2

Saito, K., Davis, K. C., Morgan, D. A., Toth, B. A., Jiang, J., Singh, U., et al. (2019). Celastrol Reduces Obesity in MC4R Deficiency and Stimulates Sympathetic Nerve Activity Affecting Metabolic and Cardiovascular Functions. *Diabetes* 68 (6), 1210–1220. doi:10.2337/db18-1167

Shahar, N., and Larisch, S. (2020). Inhibiting the Inhibitors: Targeting Anti-apoptotic Proteins in Cancer and Therapy Resistance. *Drug Resist Updat* 52, 100712. doi:10.1016/j.drup.2020.100712

Sharma, K., Vu, T. T., Cook, W., Naseri, M., Zhan, K., Nakajima, W., et al. (2018). p53-independent Noxa Induction by Cisplatin Is Regulated by ATF3/ATF4 in Head and Neck Squamous Cell Carcinoma Cells. *Mol. Oncol.* 12 (6), 788–798. doi:10.1002/1878-0261.12172

Shats, I., Deng, M., Davidovich, A., Zhang, C., Kwon, J. S., Manandhar, D., et al. (2017). Expression Level Is a Key Determinant of E2F1-Mediated Cell Fate. *Cell Death Differ.* 24 (4), 626–637. doi:10.1038/cdd.2017.12

Shi, R., Cui, H., Bi, Y., Huang, X., Song, B., Cheng, C., et al. (2015). Artesunate Altered Cellular Mechanical Properties Leading to Deregulation of Cell Proliferation and Migration in Esophageal Squamous Cell Carcinoma. *Oncol. Lett.* 9 (5), 2249–2255. doi:10.3892/ol.2015.2982

Sung, H., Ferlay, J., Siegel, R. L., Laversanne, M., Soerjomataram, I., Jemal, A., et al. (2021). Global Cancer Statistics 2020: GLOBOCAN Estimates of Incidence and Mortality Worldwide for 36 Cancers in 185 Countries. *CA A Cancer J. Clin.* 71 (3), 209–249. doi:10.3322/caac.21660

Tang, D., Kang, R., Berghe, T. V., Vandenabeele, P., and Kroemer, G. (2019). The Molecular Machinery of Regulated Cell Death. *Cell Res.* 29 (5), 347–364. doi:10.1038/s41422-019-0164-5

Tang, M., Cao, X., Zhang, K., Li, Y., Zheng, Q. Y., Li, G. Q., et al. (2018). Celastrol Alleviates Renal Fibrosis by Upregulating Cannabinoid Receptor 2 Expression. *Cell Death Dis.* 9 (6), 601. doi:10.1038/s41419-018-0666-y

Thu, K. L., Soria-Bretones, I., Mak, T. W., and Cescon, D. W. (2018). Targeting the Cell Cycle in Breast Cancer: towards the Next Phase. *Cell Cycle* 17 (15), 1871–1885. doi:10.1080/15384101.2018.1502567

Watanabe, M., Otake, R., Kozuki, R., Toihata, T., Takahashi, K., Okamura, A., et al. (2019). Recent Progress in Multidisciplinary Treatment for Patients with Esophageal Cancer. *Surg. Today* 50 (1), 12–20. doi:10.1007/s00595-019-01878-7

Wildey, G. M., Patil, S., and Howe, P. H. (2021). Smad3 Potentiates Transforming Growth Factor Beta (TGFbeta)-induced Apoptosis and Expression of the BH3-Only Protein Bim in WEHI 231 B Lymphocytes. *J. Biol. Chem.* 278 (20), 18069–18077. doi:10.1074/jbc.M211958200

Wong, V. K. W., Qiu, C., Xu, S. W., Law, B. Y. K., Zeng, W., Wang, H., et al. (2019). Ca2+ Signalling Plays a Role in Celastrol-Mediated Suppression of Synovial Fibroblasts of Rheumatoid Arthritis Patients and Experimental Arthritis in Rats. *Br. J. Pharmacol.* 176 (16), 2922–2944. doi:10.1111/bph.14718

Wu, S. H., Hang, L. W., Yang, J. S., Chen, H. Y., Lin, H. Y., Chiang, J. H., et al. (2010). Curcumin Induces Apoptosis in Human Non-small Cell Lung Cancer NCI-H460 Cells through ER Stress and Caspase Cascade- and Mitochondria-dependent Pathways. *Anticancer Res.* 30 (6), 2125–2133. https://pubmed.ncbi.nlm.nih.gov/20651361/

Yang, H., Liu, C., Jiang, J., Wang, Y., and Zhang, X. (2017). Celastrol Attenuates Multiple Sclerosis and Optic Neuritis in an Experimental Autoimmune Encephalomyelitis Model. *Front. Pharmacol.* 8, 44. doi:10.3389/fphar.2017.00044

Yang, Y., Cheng, S., Liang, G., Honggang, L., and Wu, H. (2018). Celastrol Inhibits Cancer Metastasis by Suppressing M2-like Polarization of Macrophages. *Biochem. Biophys. Res. Commun.* 503 (2), 414–419. doi:10.1016/j.bbrc.2018.03.224

Yang, Y., Li, N., Wang, T.-M., and Di, L. (2021). Natural Products with Activity against Lung Cancer: A Review Focusing on the Tumor Microenvironment. *Ijms* 22 (19), 10827. doi:10.3390/ijms221910827

Yang, Y. M., Hong, P., Xu, W. W., He, Q. Y., and Li, B. (2020). Advances in Targeted Therapy for Esophageal Cancer. *Signal Transduct. Target Ther.* 5 (1), 229. doi:10.1038/s41392-020-00323-3

Ye, S., Luo, W., Khan, Z. A., Wu, G., Xuan, L., Shan, P., et al. (2020). Celastrol Attenuates Angiotensin II-Induced Cardiac Remodeling by Targeting STAT3. *Circ. Res.* 126 (8), 1007–1023. doi:10.1161/circresaha.119.315861

Ye, Z., Chen, Y., Zhang, R., Dai, H., Zeng, C., Zeng, H., et al. (2014). c-Jun N-Terminal Kinase - C-Jun Pathway Transactivates Bim to Promote Osteoarthritis. *Can. J. Physiol. Pharmacol.* 92 (2), 132–139. doi:10.1139/cjpp-2013-0228

Ying, J., Zhang, M., Qiu, X., and Lu, Y. (2018). The Potential of Herb Medicines in the Treatment of Esophageal Cancer. *Biomed. Pharmacother.* 103, 381–390. doi:10.1016/j.biopha.2018.04.088

Zhang, Y., Geng, C., Liu, X., Li, M., Gao, M., Liu, X., et al. (2017). Celastrol Ameliorates Liver Metabolic Damage Caused by a High-Fat Diet through Sirt1. *Mol. Metab.* 6 (1), 138–147. doi:10.1016/j.molmet.2016.11.002

Zhao, X., Liu, X., and Su, L. (2014). Parthenolide Induces Apoptosis via TNFRSF10B and PMAIP1 Pathways in Human Lung Cancer Cells. *J. Exp. Clin. Cancer Res.* 33, 3. doi:10.1186/1756-9966-33-3

Zheng, K., He, Z., Kitazato, K., and Wang, Y. (2019). Selective Autophagy Regulates Cell Cycle in Cancer Therapy. *Theranostics* 9 (1), 104–125. doi:10.7150/thno.30308

Conflict of Interest: The authors declare that the research was conducted in the absence of any commercial or financial relationships that could be construed as a potential conflict of interest.

Publisher's Note: All claims expressed in this article are solely those of the authors and do not necessarily represent those of their affiliated organizations, or those of the publisher, the editors, and the reviewers. Any product that may be evaluated in this article, or claim that may be made by its manufacturer, is not guaranteed or endorsed by the publisher.

frontiers | Frontiers in Pharmacology

REVIEW
published: 11 July 2022
doi: 10.3389/fphar.2022.929161

Natural Products from Actinobacteria as a Potential Source of New Therapies Against Colorectal Cancer: A Review

Yadollah Bahrami[1,2,3]*†, *Sasan Bouk*[1†], *Elham Kakaei*[1] *and Mohammad Taheri*[4,5]*

[1]Department of Medical Biotechnology, School of Medicine, Kermanshah University of Medical Sciences, Kermanshah, Iran, [2]Pharmaceutical Research Center, Kermanshah University of Medical Sciences, Kermanshah, Iran, [3]Department of Medical Biotechnology, School of Medicine, College of Medicine and Public Health, Flinders University, Adelaide, SA, Australia, [4]Institute of Human Genetics, University Hospital Jena, Jena, Germany, [5]Urology and Nephrology Research Center, Shahid Beheshti University of Medical Sciences, Tehran, Iran

OPEN ACCESS

Edited by:
Hailian Shi,
Shanghai University of Traditional Chinese Medicine, China

Reviewed by:
Syed Shams Ul Hassan,
Shanghai Jiao Tong University, China
Zothanpuia,
Mizoram University, India
Gothandam Kodiveri Muthukliannan,
Vellore Institute of Technology, India

***Correspondence:**
Yadollah Bahrami
bahramiyadollah@yahoo.com
Mohammad Taheri
mohammad_823@yahoo.com

†These authors share first authorship

Specialty section:
This article was submitted to Gastrointestinal and Hepatic Pharmacology, a section of the journal Frontiers in Pharmacology

Received: 26 April 2022
Accepted: 07 June 2022
Published: 11 July 2022

Citation:
Bahrami Y, Bouk S, Kakaei E and Taheri M (2022) Natural Products from Actinobacteria as a Potential Source of New Therapies Against Colorectal Cancer: A Review. Front. Pharmacol. 13:929161. doi: 10.3389/fphar.2022.929161

Colorectal cancer (CRC) is a common, and deadly disease. Despite the improved knowledge on CRC heterogeneity and advances in the medical sciences, there is still an urgent need to cope with the challenges and side effects of common treatments for the disease. Natural products (NPs) have always been of interest for the development of new medicines. Actinobacteria are known to be prolific producers of a wide range of bioactive NPs, and scientific evidence highlights their important protective role against CRC. This review is a holistic picture on actinobacter-derived cytotoxic compounds against CRC that provides a good perspective for drug development and design in near future. This review also describes the chemical structure of 232 NPs presenting anti-CRC activity with the being majority of quinones, lactones, alkaloids, peptides, and glycosides. The study reveals that most of these NPs are derived from marine actinobacteria followed by terrestrial and endophytic actinobacteria, respectively. They are predominantly produced by *Streptomyces*, *Micromonospors*, *Saliniospors* and *Actinomadura*, respectively, in which *Streptomyces,* as the predominant contributor generating over 76% of compounds exclusively. Besides it provides a valuable snapshot of the chemical structure-activity relationship of compounds, highlighting the presence or absence of some specific atoms and chemical units in the structure of compounds can greatly influence their biological activities. To the best of our knowledge, this is the first comprehensive review on natural actinobacterial compounds affecting different types of CRC. Our study reveals that the high diversity of actinobacterial strains and their NPs derivatives, described here provides a new perspective and direction for the production of new anti-CRC drugs and paves the way to innovation for drugs discovery in the future. The knowledge obtain from this review can help us to understand the pivotal application of actinobacteria in future drugs development.

Keywords: colorectal cancer, natural products, actinobacteria, secondary metabolites, anti-cancer effects, marine actinobacteria, endophytic actinobacteria, bioactive compounds

1 INTRODUCTION

Colorectal cancer (CRC) is the third most common cancer globally with an annual rate of 10% of new cancer cases. Following lung cancer which is the deadliest cancer worldwide, CRC is the second deadliest cancer in the world, accounting for 9.4% of cancer deaths (Sung et al., 2021). The global burden, prevalence, and deaths from the disease are increasing and expects to reach around 60% by 2030 (Arnold et al., 2017). Environmental factors and genetic factors are involved in the occurrence of this complication. Heredity is a major cause of susceptibility to cancers, and in a case of CRC, it is estimated that 12%–35% of the risk is related to genetic factors. Based on the origin of genetic mutations, CRC is divided into three categories including sporadic (70%), inherited (5%) and familial (25%) (Peters et al., 2015; Mármol et al., 2017). Sporadics are heterogeneous, and different genes undergo point mutations. A specific sequence of mutations triggers with the APC gene following with mutations in the KRAS, TP53, and DCC genes are observed in approximately 70% of CRC cases (Fearon and Vogelstein, 1990). The hereditary group includes two categories namely polyposis and non-polyposis CRC (HNPCC). Two well-known examples for polyposis and HNPCC are familial adenomatous polyposis (FAP) and Lynch syndrome, respectively, in which occurs as a result of mutations in DNA repair genes (Lynch and de la Chapelle, 2003). Familial CRC, caused by hereditary mutations, is the type of cancer that neither its molecular mechanism is precisely known nor cannot be classified as a specific hereditary cancer (Stoffel and Kastrinos, 2014). The most common method of diagnosing, and determining the status of CRC in the clinic is the use of Tumor Node Metastasis (TNM) classification. However, today, due to the heterogeneity of cancer and in order to achieve personalized and targeted therapy, molecular classifications of cancer have been proposed which are indicators of genetic tumor heterogeneity (Turashvili and Brogi, 2017). Microsatellite instability (MSI), chromosomal instability (CIN) and epigenetic instability (CIMP) are the three major causes of genetic instability resulting CRC (Wang W. et al., 2019). Recently, based on such changes and other genetic factors and molecular pathways, another classification called Consensus Molecular Subtypes (CMSs) has been developed, which divides CRCs into four categories namely CMS 1–4 (Guinney et al., 2015). Currently, the most common treatments are surgery and chemotherapy. One of the first chemotherapeutic compounds used to control CRC was 5-fluorouracil (5-FU). This compound, along with leucoverin, due to its modulating effect, became the standard for the management of metastatic CRC (Piawah and Venook, 2019). Oxaliplatin, capsaicin, and topoisomerase inhibitors such as irinotecan are other compounds used in this field (de Gramont et al., 2000). Obvious adverse effects such as gastrointestinal and hematological toxicity as well as neurotoxicity when taking irinotecan and oxaliplatin, respectively, are not unexpected (Bailly, 2019; Guillaumot et al., 2019). Due to the existence of such side effects as well as the challenges associated with cancer metastasis, the use of targeted therapy has been considered. These therapies target the exact molecular pathway involved in causing cancer to inhibit the growth of cancer cells and limit their spread (Baudino, 2015). In this type of treatment, rather using conventional chemical therapies that have less noticeable effects and also have off-targets of healthy cells such as bone marrow and epithelial proliferating cells, compounds such as bevacizumb and cytoximb used to target Vascular endothelial growth factor (VEGF) and EGFR receptors, respectively. However, in such relatively new therapies, in addition to their side effects, even if confirmed in clinical trials, a hypothetical compound can be used and responsive only for a small proportion of patients with this complication due to the heterogeneity of CRC mutations (Piawah and Venook, 2019). Using combination therapy, combining conventional first-line therapies, ie chemotherapy, with natural compounds or targeted therapies such as immunotherapy, can be a good way to improve treatment methods and reduce unwanted adverse effects (Rejhová et al., 2018).

Natural products (NPs) are bioactive substances found in plants as well as fungi, bacteria and marine organisms. These compounds and their derivatives have been increasingly considered in the design of drugs including antibiotics and anti-cancer drugs owing to the variety of structural features and biological activities, as well as low toxicity and side effects. Natural compounds and their derivatives account for about one-third of FDA-approved drugs in the last 20 years (Rejhová et al., 2018; Thomford et al., 2018; Deng et al., 2020). These compounds are chemically included alkaloids, polyphenols, polysaccharides, terpenoids, carotenoids, unsaturated fatty acids and nitrogenous compounds. Natural compounds can affect biological pathways such as cell proliferation and cycle, cancer cell migration and invasion, apoptosis, autophagy and angiogenesis used to treat and alleviate cancer conditions (Rejhová et al., 2018; Huang et al., 2019).

Actinobacteria are prolific producers of a wide range of natural bioactive compounds due to their environmental diversity and consequently, their metabolic potential. They are generally gram-positive bacteria and one of the most diverse groups of microorganisms in nature that are scattered throughout the aquatic and terrestrial environments (Bahrami et al., 2022). In addition to the fact that about two-thirds of the known antibiotics used in clinical medicine are of actinobacterial origin, natural compounds of this origin are also used in the production of a range of anti-cancer, immunosuppressive, anti-parasitic and anti-viral agents (Barka et al., 2016; Van Bergeijk et al., 2020). By knowing that most biosynthetic gene clusters in *Streptomyces*, the largest genus of actinobacteria, are still silent under normal culture conditions, further studies on these microorganisms can be promising to explore more effective biological compounds in which indicates the unknown high potential of these bacteria in the production of secondary metabolites (Onaka, 2017). On the other hand, the presence of actinobacteria such as *bifidobacterium* in the intestinal microbiome has been shown to have a protective effect on CRC, which might be due to producing anticancer metabolites (Toumazi and Constantinou, 2020).

In this article, considering the current situation in the treatment of CRC and the needs to search and discover new

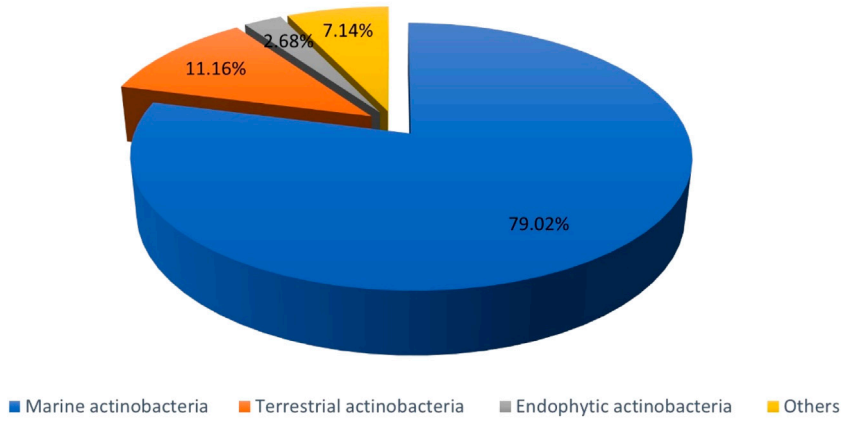

CHART 1 | Distribution of NPs with anti-CRC properties produced by actinobacteria based on Bacterial habitat. The section entitled "Others" includes items such as Mutant actinobacteria, actinobacteria isolated from animals, salt ponds, sea sponge, and synthetics.

effective compounds toward CRC, a comprehensive review of NPs affecting CRC cell lines isolated from actinobacteria has been conducted. The paper also describes the structure of over 230 compounds isolated and identified from actinobacteria in the past decades having anticancer properties based on their ecosystem and biological activity. To the best of our knowledge, this is the first comprehensive review on potential anti-CRC actinobacterial compounds, which can be an excellent guide for designing new drugs toward this disease, and introduce the unique biological potential of this extraordinary resource to the scientific community.

2 THE ECOLOGICAL DIVERSITY OF ACTINOBACTERIA AND THEIR NPS AGAINST COLORECTAL CANCER

Actinobacteria, the vast and diverse branch of microorganisms, in which the genus *Streptomyces* alone, accounts for about 5% of all known bacterial species, are present in diverse ecosystems all over the world. Generally, they are placed in two categories, free and dependent on the host. The free species are widespread in both terrestrial and marine environments. The latter coexist in a wide variety of eukaryotes such as plants, insects, marine organisms, and even mammalian and human tissues such as skin, lungs and intestine (Lewin et al., 2016). Their natural bioactive compounds have various biological activities including antibacterial and anti-cancer, the well-known antitumor compound, doxorubicin, from a soil-derived *Streptomyces peucetius*, or the antitumor and antibacterial compound marinomycin, from a marine actinobacter species *Marinispora* spp. are examples (Arcamone et al., 1969; Kwon et al., 2006).

The proportion of natural bioactive compounds with anti-CRC properties derived from actinobacteria collected off different environments are presented in **Chart 1**. As the figure indicates the majority of compounds are produced by marine actinobacteria accounting for 79.02%. The reason, however, might be owing to the massive diversity of microorganisms in aquatic habitats which attracts more attentions of researchers into the marine ecosystem recently. This high volume of data without doubt highlights the great importance of marine actinobacteria in the production of anti-CRC compounds.

2.1 Natural Products From Marine Actinobacteria With Anti-CRC Activity

The significant diversity of NPs produced by marine actinobacteria is increasing day by day. Apart from the commercial aspect of compounds possessing medicinal properties, marine NPs have also gained special importance in the fields of biocatalysts and biological or microbial pesticides. It seems that the discovery rate of new chemical and bioactive compounds of marine-derived actinobacteria has been higher than its soil types for many years. These actinobacteria, which are often unable to grow *in vitro*, are found in marine habitats such as sea surface microlayer (SML), which contains 1 mm of sea surface, also seabed habitats containing marine sediments and a suitable place for microorganisms to coexist with microphones and macrofauna, fish surface, beach, coastal waters and even on the seabed (Bull et al., 2005; Maldonado et al., 2005; Ward and Bora, 2006). Among the different marine-derived microorganisms, actinomycetes are the largest producers of natural compounds, demonstrating their unparalleled potential. *Streptomyces* and *Micromonosporas* have a high potential for research on antitumor and growth inhibitors compounds (Khalifa et al., 2019). The following section refer to compounds isolated from actinobacteria having anti-CRC properties. The structure of NPs with anti-CRC properties from marine actinobacteria and their mechanism of actions and origins are summarized in **Supplementary Table S1**.

Salinosporamide A **(1)** (Marizomib, NPI-0052), having a fused γ-lactam β-lactone ring, and also its derivatives, salinosporamides

D-J, have shown significant antitumor effects with inhibitory properties on the 20s proteosome (Feling et al., 2003; Jensen et al., 2007; Udwary et al., 2007). The inhibitory effect of these compounds was reported to be through the activation of NF-κB, inhibition of invasion and induction of apoptosis (Ahn et al., 2007). Salinosporamide A **(1)** has been isolated from marine actinobacteria *Salinospora tropica* CNB-392 (Feling et al., 2003; Jensen et al., 2007; Udwary et al., 2007). The anticancer effects of this compound on human colon carcinoma cell lines, namely HCT-116 (IC_{50} = 11 ng/ml) and HCC-2998, as well as a wide range of other tumors such as myeloma, non-hodgkin's lymphoma, CLL and pancreatic carcinoma have been studied (Gulder and Moore, 2010; Sobolevskaia and Kuznetsova, 2010). This compound exhibits a high, stable and tolerable inhibitory effect on proteosome 20 on the xenograft model of colon cancer (Cusack et al., 2006). A combination therapy of compound (**1**) with common chemotherapy agents including 5FU, leucovorin, and oxaliplatin, was also reported to increase their anticancer effects significantly (Cusack et al., 2006). In 2003, few bioactive compounds with antibacterial and antitumor properties, were isolated from the marine derived *actinomadura* sp. M048 (Maskey et al., 2003). The compounds namely questiomycin A **(2)**, N-acetylquestiomycin A **(3)** and chandrananimycin A **(4)**, B **(5)** showed antitumor activity against several cell lines, including human colon carcinoma cell line, HT-29.

Three compounds of 3,6-disubstituted indoles isolated from the marine derived *Streptomyces strain* BL-49-58-005 were studied to evaluate their cytotoxicity effects against cancer cell lines. Indole number two (aldoxime) **(6)** showed activity against various cell lines, including LOVO and LOVO-DOX colon adenocarcinoma cell lines (Sánchez López et al., 2003). Arenamides A **(7)** and B **(8)** are two compounds with moderate anti-cancer activity against the HCT-116 cell line, isolated from the marine derived *Salinispora arenicola* CNT-088 (Asolkar et al., 2009). In addition, study on HEK cells, transfected by NF-κB-Luc/293 exhibited anti-inflammatory and chemoprevention effects of these compounds by blocking TNF induction activation and NF-κB inhibition.

In 2007, three macrolide polyketides compounds were isolated from the marine actinomycetes *Salinispora arenicola strain* CNR-005 (Williams et al., 2007). The compound arenicolide A **(9)** showed moderate cytotoxic activity against HCT-116 cell line with an IC_{50} value of 30 μg/ml. In 2004, a polyketide called aureoverticillactam **(10)** was isolated from the marine derived *S. aureo-verticillatus* NPS001583 (Mitchell et al., 2004). Study on the biological properties of this natural compound showed growth inhibitory properties on HT-29, Jurket Leukemia and B16F10 cell lines. In 2005, several natural chlorinated dihydroquinones compounds, in the form of a terpenoid/polyketide mix, were isolated from the marine derived *actinomycete strain* CNQ-525 collected from ocean sediments near La Jolla, California (Soria-Mercado et al., 2005). Dihydroquinones 1 **(11)**, 2 **(12)** and 4 **(13)**, showed cytotoxic effects against the HCT-116 cell line with the IC_{50} values of 2.4, 0.97, and 1.84 μg/ml, respectively. Cyanosporasides A **(14)** and B, structurally related to sporolides, were isolated from *S. pacifica strain* CNS103. The former one had poor toxicity effects against HCT-116 cell line, with an IC_{50} value of 30 μg/ml (Oh et al., 2006). Polyketides, from the family of manumycin compounds,

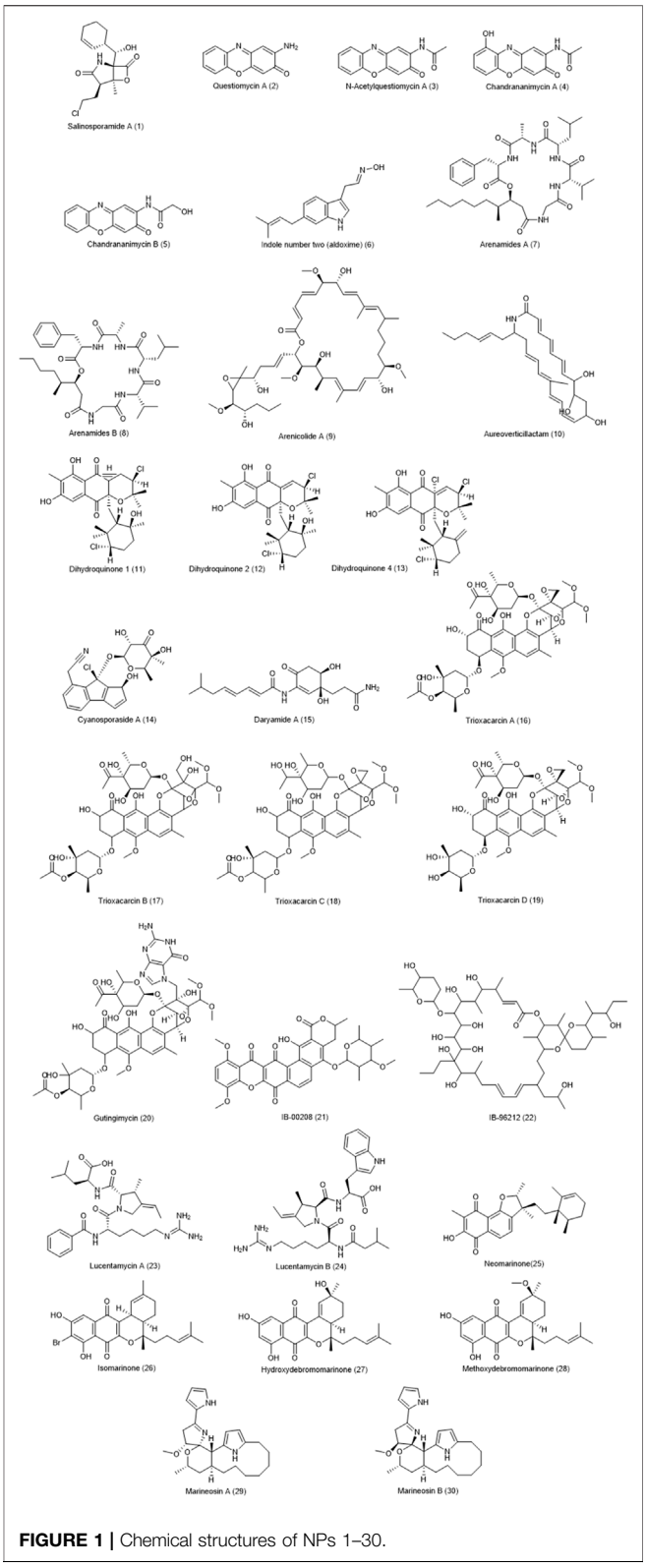

FIGURE 1 | Chemical structures of NPs 1–30.

called daryamides, were reported from *Streptomyces strain* CNQ-085. Their anti-cancer effects against HCT-116 cell line showed good results, especially for type A **(15)** with an IC_{50} value of 3.15 μg/ml (Asolkar et al., 2006).

Compounds isolated from *Streptomyces* sp. isolate B8652 and its derivatives such as trioxacarcins and gutingimycin have been shown to have antitumor effects against a variety of cancer cell lines, including HT-29. Four compounds called trioxacarcin A-D (**16–19**) were reported to have potent antitumor effects against various cell lines, including HT-29. On average, trioxacarcins A **(16)** had the highest effect among the rest, while gutingimycin **(20)** had the lowest toxicity (Maskey et al., 2004a; Maskey et al., 2004b).

The marine derived *Actinomadura* sp. BL-42-PO13-046, collected off the north coast of Spain, produces compound IB-00208 **(21)**, associated with angucyclines and other aromatic polyketides. The compound exhibits cytotoxic effects against human cancer cell lines, HT-29 (colon), SK-MEL-28 (melanoma) and A-549 (lung), as well as P-388 mouse leukemia (Malet-Cascón et al., 2003; Rodríguez et al., 2003). A macrolactone compound called IB-96212 **(22)**, was isolated from the actinobacterium *Micromonospora* sp. L-25-ES25-008 and its anti-cancer effects examined against various cell lines, including HT-29. However, these antitumor effects were reported to be four times more potent in P-388 mouse leukemia (Cañedo et al., 2000; Fernández-Chimeno et al., 2000). The antitumor effects of non-ribosomal peptides, lucentamycins, produced by *Nocardiopsis lucentensis* strain CNR-712, were tested against HCT-116 colon cancer cell line (Cho et al., 2007). Types A **(23)** and B **(24)** showed significant anti-cancer effects against the cell line with IC_{50} values of 0.20 and 11 μM, respectively.

Marinones, including neomarinone **(25)**, isomarinone **(26)**, hydroxydebromomarinone **(27)**, and methoxydebromomarinone **(28)**, are compounds of a polyketide-terpenoid mix nature produced by *actinomycete isolate* CNH-099. These compounds exhibited moderate cytotoxicity against HCT-116 cell line with an IC_{50} value of 8 μg/ml (Hardt et al., 2000; Kalaitzis et al., 2003). *Streptomyces strain* CNQ-617, collected from marine sediments in La Jolla, California, was recognized as the producer of natural marineosins (Boonlarppradab et al., 2008). These compounds showed potential effects on different cancer cell lines, especially on HCT-116, with an IC_{50} value of 0.5 μM for type A **(29)** and 46 μM for type B **(30)**. The chemical structure of compounds 1–30 are presented in **Figure 1**.

Marmycins A **(31)** and B **(32)**, two bioactive natural compounds isolated from the marine actinobacterium *Streptomyces strain* CNH990, have potent anticancer effects on a variety of cancer cell lines (Martin et al., 2007). In the case of the HCT-116 cell line, marmycin A showed far more toxicity (18 folds) than the marmycin B. An average IC_{50} value of 0.022 μM was recorded for marmycin A against 12 human tumor cell lines, including colon cancer. However, the same studies showed weaker effects (mean 3.5 μM) for Marmycin B.

Piericidins were isolated from *Streptomyces* sp. YM14-060 in 2007 (Hayakawa et al., 2007a). Another study in the same year showed their antitumor effects on mouse glial cells transfected with the E1A adenovirus (RG-E1A-7) gene and Neuro-2a mouse neuroblastoma (Hayakawa et al., 2007b). Piericidins C7 and C8 lead to selective cytotoxicity on RG-E1A-7 cells and non-lethal growth inhibition on Neuro-2a cells. The cytotoxicity of various compounds was investigated on etoposide-resistant colon carcinoma cell line HT-29. The results showed that only piericidin A **(33)** among those compounds induces cytotoxicity in the cancer cell line via suppressing the accumulation of GRP78 protein (a drug resistance factor) (Hwang et al., 2008). *Streptomyces* sp. *strain* CNQ 593 was stated to produce non-cyclic and non-ribosomal chlorinated hexadepsipeptide compounds called piperazimycins (Miller et al., 2007). All of these compounds, including piperazimycin A **(34)**, show antitumor activity against colon (HCT-116), melanoma, prostate, and central nervous system cancer cell lines. The toxicity property of piperazimycin A against solid cancer lines was stronger three times those of piperazimycins B **(35)** and C **(36)**.

Staurosporines and their derivatives, are isolated from different species such as komodoquinones-producer *Streptomyces* sp. KS3 and *S. staurosporeus* AM-2282. Staurosporine, produced by *Micromonospora* sp. L-31-CLCO-002 and its natural analogues 4′-N-methyl-5′-hydroxystaurosporine **(37)** and 5′-hydroxystaurosporine **(38)**, were examined in terms of antitumor activity against various cancer cell lines namely lung, melanoma and HT-29 colon carcinoma. The latter two analog compounds had the highest activity against the HT-29 cell line (Omura et al., 1977; Hernández et al., 2000; Itoh et al., 2003). In a 2019 study, a total of 15 compounds of staurosporine derivatives, including 6 new compounds, was isolated from marine derived *Streptomyces* sp. NB-A13 in which 14 of them **(39–52)** had significant effects against SW-620 colon cancer cell lines (Zhou et al., 2019). Staurosporine derivatives No. 7 **(44)** and No. 14 **(51)** were reported to have the strongest cytotoxic function. In 2018, the structure and biological effects of staurosporine derivatives from *Streptomyces coelicolor* M1146 were investigated (Xiao et al., 2018). The compounds were produced by engineering the genes of the spc cluster, and expressing its heterologous. the toxicity of these derivatives was tested against various cancer cell lines. Among those, staurosporine M1 **(53)** showed activities against all of these cell lines, including HCT-116 (IC50 = 1.0M) and staurosporine M2 **(54)**, against HCT-116 cell lines (IC_{50} = 3.9 μM) and Huh 7.5 (IC_{50} = 2.7 μM).

In a 2007 study, the streptokordin **(55)** produced by *Streptomyces* sp. KORDI-3238 showed significant antitumor effects against HCT-15 colon cancer and other cancer cell lines such as MDA-MB-231, leukemia K-562, lung NCI-H23, etc. (Jeong et al., 2006). The antitumor activity of thiocoraline **(56),** produced by *Micromonospora (marina)* sp. L-13-ACM2-092 isolated from soft coral from the coast of Mozambique, Indian Ocean, has documented against HT-29 cell line. The compound, by stopping the cell cycle in G1 phase and slowing the progression of S phase of the cell cycle to G2/M, has antiproliferative effects on the LOVO and SW620 cell lines of the human colon with IC_{50} values of 15 and 500 nM, respectively. The inhibitory effect of compound is due to the inhibition of DNA polymerase α as well as its bilateral entry into the DNA

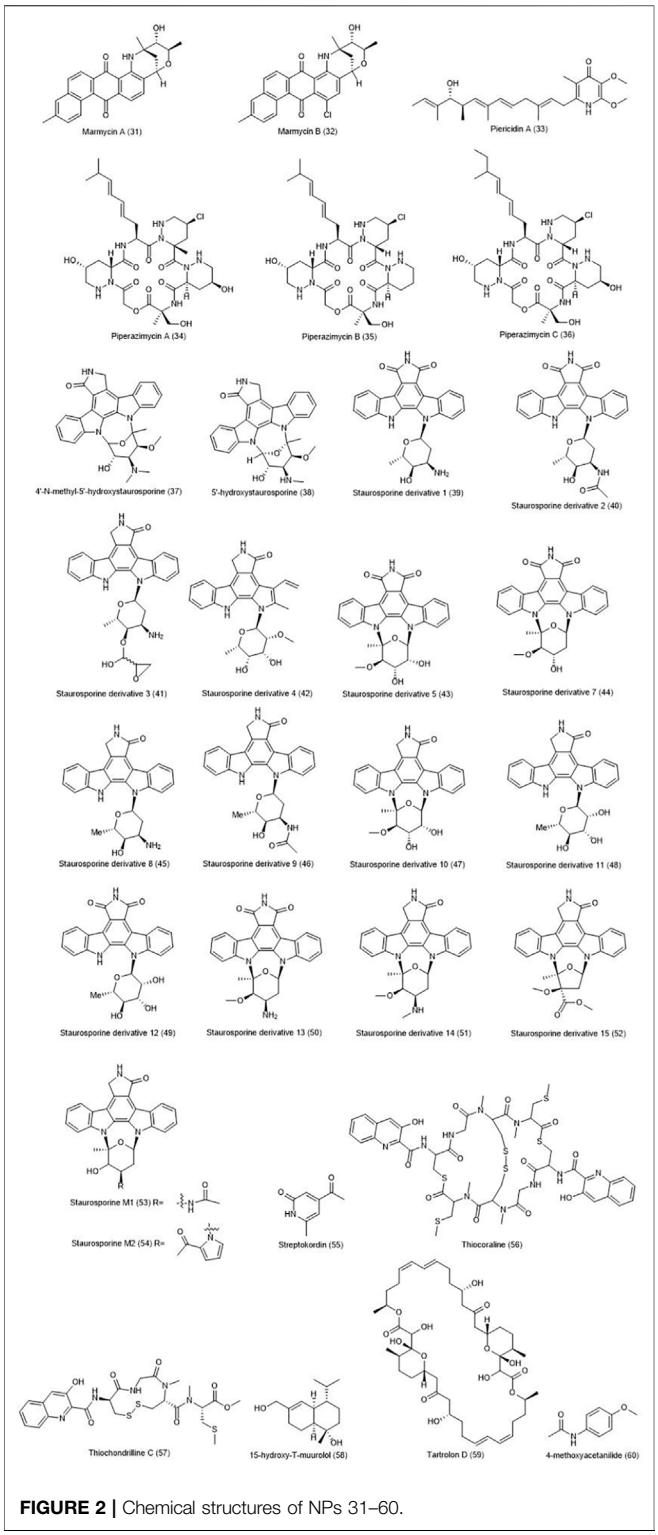

FIGURE 2 | Chemical structures of NPs 31–60.

strand (Romero et al., 1997; Erba et al., 1999). In 2014, *in vivo* studies found that the compound reduced tumorigenesis and proliferation of carcinoid tumor cells by inducing the activation of the notch pathway (Wyche et al., 2014). In 2015, the previously isolated natural compound thiochondrilline C from *Verrucisispora* sp. was synthesized in a special way and the antiproliferative effects of this compound and its derivatives were evaluated on the NCI 60 cancer cell panel (Vippila et al., 2015). Derivative No. 22 of thiochondrilline C **(57)** showed potent antiproliferative effects against CRC cell lines.

The eight t-muurolol compounds were isolated from marine actinobacterium *Streptomyces* strain M491 (Ding et al., 2009). Seven of the eight compounds were evaluated for their cytotoxicity, and MTT assay was performed on 37 human tumor cell lines, including CRC cell lines such as HCT-116 and HT-29. Except for the compound 15-hydroxy-T-muurolol **(58)**, with moderate toxicity effects, the rest of them left no noticeable effects on the t tested cell lines. Macrodiolide tartrolon D **(59)**, isolated from *Streptomyces* sp. MDG-04-17-069 has shown strong cytotoxic effects against human cancer cell lines including colon (HT-29), lung (A549) and breast (MDA-MB-231) (Pérez et al., 2009). 4-methoxyacetanilide **(60)** produced by marine *Streptomyces* sp. SCA29, was stated to inhibit α-glucosidase and α-amylase enzymes, and show antibacterial activity and cytotoxicity against various cancers, including HT-29 cell line (Siddharth and Vittal, 2019). The chemical structure of compounds 31–60 are illustrated in **Figure 2**.

A compound called levantilide C **(61)** has been identified from *Micromonospora* strain FIM07-0019 collected off the shallow coastal waters of Chile (Fei et al., 2013). The compound was reported to have a good antiproliferative activity against human colon cancer cell line SW620 (IC_{50} = 16.4 μM).

Cyanogrisides and their related analogues, produced by *Actinoalloteichus cyanogriseus* and its mutant species, can induce cytotoxic effects on cancer cell lines. Cyanogrisides F **(62)** and G **(63)** have shown cytotoxicity against HCT-116 and leukemia HL-60 cell lines (Fu et al., 2014). In 2014, three secondary metabolites amycofuran, amycolactam and amycocyclopiazonic acid, produced by *Amycolatopsis* sp., a marine sponge associated actinomycete, were examined for cytotoxic effects (Kwon et al., 2014). Amycolactam **(64)** had a significant effect on SNU638 gastric cancer and HCT-116 colon cancer cell line. The other two had little toxic effect.

Compounds called microbacterins A and B, produced by marine actinomycete *Microbacterium sediminis* spp. nov. YLB-01 exhibits significant cytotoxic effects against a panel of cancer cell lines. Microbacterin B **(65)** was stated to have cytotoxicity on all of tested cell lines, including HCT-8 human intestinal adenocarcinoma cell line (Liu et al., 2015). The isolated compounds from marine actinomycete *Pseudonocardia* sp. HS7 and its synthetic derivatives exerted a proliferative inhibitory effect on various cell lines (Ye et al., 2016). The anti-cancer effects of these compounds, called curvularin macrolides (1–5), **(66–70)** and their three synthetic acyl derivatives (5a-5c) **(71–73)** were measured using SRB Assay. They had significant effects on two human CRC lines HCT-15 and SW620.

Two polyhydroxyl macrolide lactone compounds, named PM100117 **(74)** and PM100118 **(75)**, isolated from the marine actinobacterium *Streptomyces caniferus* GUA-06-05-006A, lead to necrosis and significant antitumor effect on CRC HT-29, lung

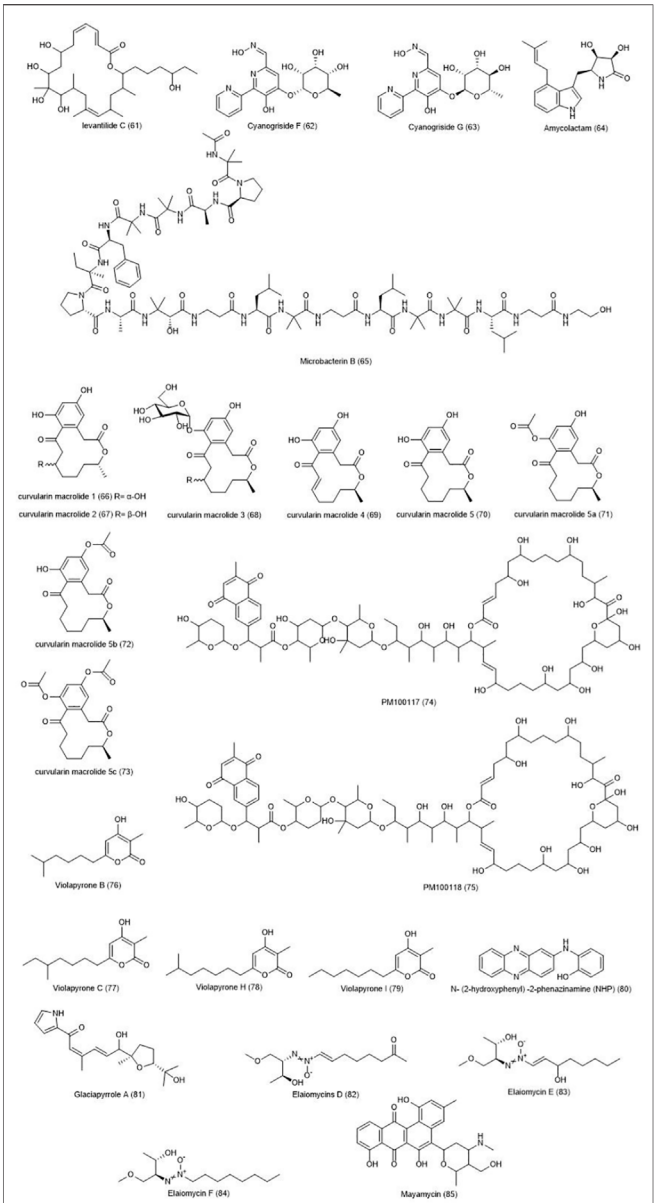

FIGURE 3 | Chemical structures of NPs 61–85.

NSCLCA549 and breast MDA-MB-23 cancer cell lines, by altering the permeability and integrity of cell membranes (Pérez et al., 2016). A-pyrone derivatives, called violapyrones B, C, H and I **(76–79)** isolated from marine actinomycetes associated with starfish, *Streptomyces* sp. 112CH148, from a region in Micronesia, have shown the effects of cytotoxicity against ten human cancer cell lines including HCT-15 and HCT-116 the Colon carcinoma cell lines (Shin et al., 2014). In 2012, the N- (2-hydroxyphenyl) -2-phenazinamine (NHP) **(80)** compound, produced by the marine *actinomycete species* BM-17, belonging to the genus *Nocardia dassonvillei*, was investigated (Gao et al., 2012). In addition to antifungal properties, the compound exhibited cytotoxic properties against HCT-116, cell line. In 2005, the compounds glyciapyrroles A, B, C from the marine derived *Streptomyces* sp. (NPS008187), collected off Alaskan marine sediments, were examined towards cancer cell lines (Macherla et al., 2005). Glaciapyrrole A **(81)**, showed good cytotoxic effects against colon cancer cell line HT-29.

Elaiomycins D-F **(82–84)** with azoxy properties, were isolated from *Streptomyces* sp. strain HKI0708 (Ding et al., 2012). In addition to antibacterial effects, this compound exerted cytotoxic effects against 12 cell lines, including HT-29. Marine *Streptomyces* sp. strain HB202, isolated from the marine sponge *Halichondria panacea*, was examined as a producer of the mayamycin **(85)** compound (Schneemann et al., 2010). The compound has shown a significant toxicity against several bacteria, including antibiotic-resistant bacteria and eight cancer cell lines, including HT-29. **Figure 3** demonstrates the chemical structure of compounds 61–85.

Marinopyrroles produced by the marine *Actinomycetes* CNQ-418, are classified as halometabolites, which contain halogen substituents in their chemical composition and have a variety of biological effects. Several marinopyrroles compounds were isolated from this species that showed antibacterial properties against methicillin-resistant species such as *Staphylococcus aureus* and selective cytotoxic properties against mammalian cancer cell lines namely leukemia such as K562 cells. Marinopyrroles A-F **(86–91)**, were demonstrated toxicity against HCT-116 cell line with IC_{50} values ranging from 1 to 9 μg/ml (Hughes et al., 2008; Doi et al., 2012). Another compound, Lodopyridone **(92)**, produced by *Saccharomonospora* CNQ-490, as a specific alkaloid, left relatively little toxic effect against HCT-116 cell line (IC_{50} = 3.6 μM) (Maloney et al., 2009).

Ammosamide halometabolites isolated from marine actinobacteria have a variety of toxic effects against the HCT-116 cell line. Ammosamides A **(93)** and B **(94)** were isolated from *Streptomyces* CNR-698, which showed a good toxicity with an IC_{50} value of 320 nM (Hughes et al., 2009a). Ammosamide D **(95)** was isolated from another species called *Streptomyces variabilis* SNA-020, which had a weaker cytotoxicity with an IC_{50} value of 3.2–4.9 μM (Pan et al., 2012). These compounds also had selective toxicity against other cancer cell lines. Cellular and molecular studies showed specific targeting of a member of the myosin family, which plays an important role in various mechanisms including the cell cycle (Hughes et al., 2009b).

Five compounds of nitropyrrolins A-E were isolated from the saline culture of the marine bacterium *S. malaysiensis* CNQ-509 (Kwon et al., 2010). They showed relatively poor antibacterial activity against tested organisms, but they showed acceptable cytotoxicity on the HCT-116 cell line. These results report IC_{50} value of 31 μM for type A **(96)** and B **(97)** and IC_{50} value of 5.7 μM for type D **(98)**. In 2013, the cytotoxicity of another halometabolite, chlorizidine **(99),** isolated from the marine *Streptomyces* strain CNH-287 was investigated against HCT-116 cell line, and reported to have a significant cytotoxicity with IC_{50} values of ranging from 3.2 to 4.9 μM (Alvarez-Mico et al., 2013). Terpenoid phenazines containing bromine, called marinocyanins A-F **(100–105)**, have been isolated from marine *actinomycetes MAR4* CNS-284 and CNY-960 (Asolkar et al., 2017). Marinocyanins A and B, in addition to their antifungal

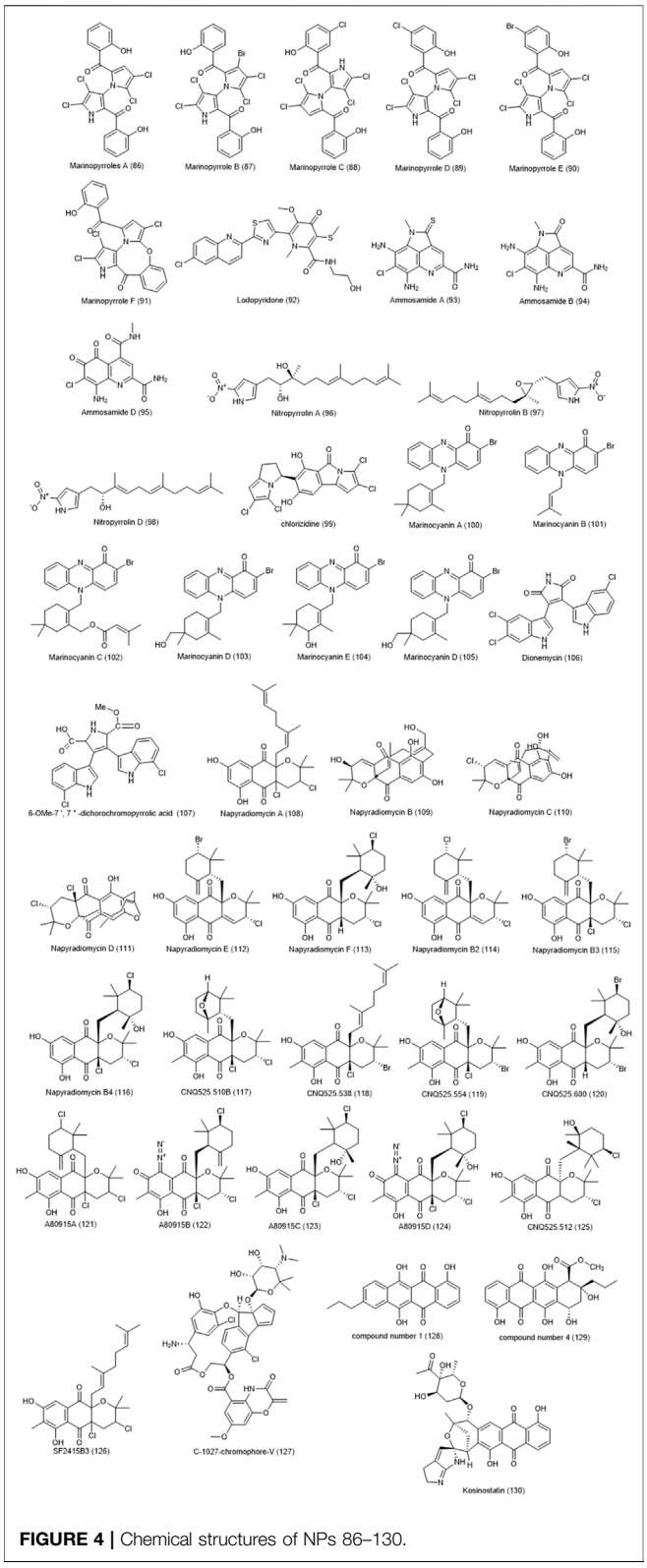

FIGURE 4 | Chemical structures of NPs 86–130.

effects against amphotericin-resistant *Candida albicans*, along with marinocyanins C-F have shown cytotoxic effects towards HCT-116 with IC_{50} values of 0.049 and 0.029 μM, respectively. Two other halo metabolites including dionemycin **(106)** and 6-OMe-7′,7″-dichorochromopyrrolic acid **(107)** were reported by (Song et al., 2020). These two chlorinated bis-indole alkaloids were isolated from the marine *Streptomyces* sp. SCSIO 11791. Both compounds were exhibited significant cytotoxic effects on HCT-116 cell line with IC_{50} values of 4.3 and 13.1 μM, respectively, in addition to their antibacterial activities.

Napyradiomycins A – F **(108–113)** and B2-B4 **(114–116)**, isolated from *Streptomyces* strain CNQ-329 and CNH-070, were stated to have a weak cytotoxic effect against HCT-116 cell line (IC_{50} = 4.19–16 μM/ml) (Cheng et al., 2013; Farnaes et al., 2014). They also showed a mild to moderate inhibitory effect against methicillin-resistant MRSA *S.aureus*. They have a halogenated structure and a combination of terpene and polyctide, with a napthoquinone ring. Strain *Streptomyces* CNQ-525 produces various types of new compound of napyradiomycins called CNQ525.510B, CNQ525.538, CNQ525.554, and CNQ525.600 **(117–120)** as well as other known compounds including B1, B3, B4, A80915A **(121)**, A80915B **(122)**, A80915C **(123)**, A80915D **(124)**, CNQ525.512 **(125)**, and SF2415B3 **(126)**. In the study of the toxicity and inhibitory effect of these compounds against HCT-116 cell line, a range of results with IC_{50} values less than 1 μM to more than 100 μM was obtained.

Actinobacterium *Streptomyces* strain ART 5, collected from the Arctic (eastern Siberia), were identified as a producer of fijiolide compounds A and B as well as C-1027-chromophore-V **(127)**, and C-1027-chromophore-III (Moon et al., 2014). Only two compounds, C-1027-chromophore V and C-1027-chromophore-III, were found to be effective against *Candida albicans*. Also, Chromophore-V was found to have a significant toxicity and antiproliferative activity against breast cancer MDA-MB231 and CRC HCT-116 cell lines with IC_{50} values of 0.9 and 2.7 μM, respectively. In 2012, four new anthracyclinone compounds were isolated from the marine derived *Micromonospora* sp. and their cytotoxicity effects on HCT-8 colon adenocarcinoma cell line were investigated (Sousa Tda et al., 2012). Among them compound number 1 (4,6,11-trihydroxy-9-propyltetracene-5,12-dione) **(128)** and compound number 4 (10β-carbomethoxy-7, 8,9,10-tetrahydro-4,6,7α 9α, 11-pentahydroxy-9-propyltetracene- 5,12-dione) **(129)** showed good cytotoxicity with IC_{50} values of 12.7 and 6.2 μM, respectively. In a 2002 study, kosinostatin **(130)** obtained from marine actinomycete *Micromonospora* sp. TP-A0468 showed a strong antibacterial effect against gram-positive bacteria and moderate effects against gram-negative bacteria and yeasts (Furumai et al., 2002). The cytotoxicity effect of this compound was tested against 39 cancer cell lines and exhibited significant impacts on most of test cell lines including HCT-116, HCT-15, HT-29, KM12, and HCC2998 with IC_{50} values average <1M. The compound inhibits human DNA topoisomerases I and IIα suggesting that the inhibitory effect of this compound occurs through interaction with DNA. The chemical structure of compounds 86 to 130 are shown in **Figure 4**.

In a 2001 study, lomaiviticins A **(131)** and B, isolated from *Micromonospora lomaivitiensis*, were examined against a wide range of human cancer lines including several colon cancer cell lines such as HCT15, CACO2, SW948, COLO205 (He et al., 2001). Lomaiviticin A was reported to have a strong toxicity effect against the tested cell lines with an average IC_{50} values of 0.01–98 ng/ml. lomaiviticins A and B also showed antibacterial effect against gram-positive pathogen species such as *S. aureus*. The compounds were introduced as potentially DNA-damaging compounds.

The actinomycete *Micromonospora aurantiaca* 110B, collected from the mangrove ecosystem in Fujian, China was reported to produce few compounds. Three isoflavonoid glycosides including daidzein-4′-(2-deoxy-α-l-fucopyranoside) **(132)**, daidzein-7-(2-deoxy-α-l-fucopyranoside) **(133)** and daidzein-4′,7-di-(2-deoxy-α-l-fucopyranoside) **(134)**, showed a good toxicity on A549 and HepG2 cancer cell lines, in addition to their appropriate effects on HCT-116 cell line (Wang RJ. et al., 2019). A new meroterpenoid, called actinoranone **(135)**, was isolated from a marine bacterium related to *Streptomyces*, and its cytotoxicity was examined against HCT-116 colon cancer cell line and reported to have a significant effect with LD_{50}: 2.0 μg/ml (Nam et al., 2013). In 2019, three hydroxylated rhamnolipids, called dokdolipids A-C **(136–138)**, were found in marine actinomycete *Actinoalloteichus hymeniacidonis* 179DD-027, isolated from marine sediments on Dokdo Island, Republic of Korea (Choi et al., 2019). Their cytotoxicity was studied against various cancer cell lines, including HCT-15 and reported to have a good activity. It was reported that dokdolipid B had stronger activity than the other two compounds.

In 2019, the antibacterial and anticancer properties of Enediyne Congeners compounds produced by *Micromonospora yangpuensis* DSM 45577 isolated from cup-shaped sponge were examined. yangpumicins A, F, G **(139–141)** was reported to have antibacterial effects against gram-positive and negative pathogenic bacteria as well as a significant cytotoxicity against different human cancer cell lines (Wang Z. et al., 2019). All three compounds showed toxicity at about nM, against A549 lung cancer and Jurket lymphoma cell lines. However, in the case of human CRC cell lines Caco-2 and SKBR-3, the two compounds yangpumicins A and F were found to be 10 times more toxic than yangpumicins G.

Many NPs and metabolites were identified from marine actinomycetes *Saccharomonospora* sp. UR22 and *Dietzia* sp. UR66, isolated from the red sea sponge *Callyspongia siphonella*. (El-Hawary et al., 2018). Among them, the new compound saccharomonosporine A **(142)** and one of the induced metabolites **(143)** showed significant antiproliferative activity against human cancer cell lines HT-29 and HL60 (IC_{50} = 3.6, 3.7 μM respectively). Due to the inhibitory effect of these two compounds on Pim-1 kinase, it has been suggested that the inhibitory effect of these compounds on cancer cells is due to the induction of this function.

The structure and biological effects of 8 cyclizidine alkaloids, together with a known alkaloid, from a marine actinomycete called *Streptomyces* sp. HNA39 were defined. Among them, compound number 2 **(144)**, showed significant toxicity against HCT-116 with IC_{50} values of 8.3 μM and prostate cancer PC3 with IC_{50} values of 0.52 μM. In addition, the compound, along with compounds No. 5, 7 and 8, was stated to inhibit moderately ROCK2 protein kinase (Jiang et al., 2018a). Arenimycin **(145)** is a compound that has been shown to have a strong inhibitory effect on cell division with an IC_{50} value of 1.16 μg/ml against HCT-116 cell line. Arenimycin is an antibiotic consumed against rifampin- and methicillin-resistant *Staphylococcus aureus* produced by marine *actinomycete Salinispora* Arenicola (Asolkar et al., 2010).

New compounds called strepoxepinmycins A-D along with the well-known compound medermycin, have been identified from marine *Streptomyces* sp. XMA39 (Jiang et al., 2018b). They have new medermycin naphthoquinone's chemical structure. It was reported all compounds possess the antibacterial effect on *E. coli* and MRSA species, as well as the antifungal effect on *Candida albicans*. Strepoxepinmycins C and D **(146–147)** were documented to possess good cytotoxic effects on colon cancer HCT-116 (IC_{50} values of 4.4 and 2.9 μM, respectively) cell line. Three new compounds called kendomycins B, C, D **(148–150)** were identified from the marine *Actinomycete Verrucosispora* sp. SCSIO 07399 (Zhang et al., 2019). In addition to their antibacterial activity against six species of gram-positive bacteria, these compounds also showed a suitable cytotoxic effect against several human cancer cell lines. Kendomycins B, C and D were suggested to have a good cytotoxicity against RKO, human colon cancer cell line, with IC_{50} values of 6.1, 3.8 and 36 μM, respectively. Four compounds. cyclo (Pro-Phe) **(151)**, cyclo (Pro-Ala) **(152)**, cyclo (Pro-Val) **(153)**, and cyclo (Pro-Leu) **(154)** with significant effects against HCT-116 cell line have been isolated from *Streptomyces nigra* sp. nov., collected from the rhizosphere soil of the *Avicennia marina* mangrove in China, which is closely related to *S. coerulescens* DSM 40146, *S. bellus* DSM 40185, and *S. coeruleorubidus* DSM 41172 (Chen C. et al., 2018). These compounds have a cytotoxic effect with an IC_{50} values of 32.3, 47.6, 67.2, and 92.6 μg/ml, respectively.

A unique furan-type compound **(155)** has been isolated *Streptomyces* sp. VN1 that was reported to have a good cytotoxic effect (IC_{50} = 123.7 μM) on various cell lines, including HCT-116 (Nguyen et al., 2020). This strain is isolated from the coastal region of Phu Yen Province (central Viet Nam). Petrocidin A **(156)** and 2,3-dihydroxybenzamide **(157)** were identified from *Streptomyces* sp. SBT348, isolated from a Marine Sponge (Cheng et al., 2017). These compounds exert their cytotoxic effect against HT-29 cell line by inhibiting the overexpression of microsomal prostaglandin E2 synthase-1 (IC_{50} = 5.3 and 3.8 μg/ml, respectively). In another study conducted in Turkey (Khan et al., 2019). Two compounds isolated from *Streptomyces cacaoi* 14CM034 have shown significant cytotoxic effects on the Caco-2 cell line through induction of apoptosis and inhibition of autophagy. Polyethers called K41 A **(158)** and compound **(159)** had IC_{50} values of 7.4 and 27.9 μM, respectively.

Two new compounds, neo-actinomycin A **(160)**, neo-actinomycin B **(161)**, along with actinomycin D **(162)**, and actinomycin X2 **(163)**, were isolated from *Streptomyces* sp. IMB094 (Wang et al., 2017). The cytotoxic effects of these compounds on HCT-116 cell line were determined with an

IC_{50} value of 38.7, 339.1, 0.045 and, 0.0075 nM, respectively. Ohmyungsamycin A **(164)**, isolated from marine *Streptomyces* sp. SNJ042, was also reported to have a cytotoxic effect on the same CRC cell line with an IC_{50} value of 7.61 μM (Byun et al., 2020). The compound has been reported to work through caspase-mediated apoptosis, reducing the expression of Skp2 as an oncogenic factor, and increase the expression of p21 and p27, which are CDK inhibitors. The chemical structure of compounds 131 to 164 are presented in **Figure 5**.

2.2 Natural Products From Terrestrial Actinobacteria With Anti-CRC Activity

The soil ecosystem contains an estimated one billion bacterial cells per gram of soil, which includes tens of thousands of different taxa. (Wagg et al., 2014). Actinobacteria play a large role in this diversity. Actinomycetes, with a 90% share, are the most common actinobacteria isolated from this ecosystem (Suela Silva et al., 2013). Therefore, the soil ecosystem can be a valuable reservoir of NPs the structure of some NPs with anti-CRC properties, isolated from terrestrial actinobacteria and their name and mechanism of action and origin are summarized in **Table 1**.

In 2019, the pradimicin-IRD **(165)**, polycyclic compound was isolated from the terrestrial actinobacter *Amycolatopsis* sp. IRD-009 (Bauermeister et al., 2019). In addition to the strong antibacterial effect against *Streptococcus agalactiae*, *Pseudomonas aeruginosa* and *Staphylococcus aureus*, the compound was reported to possess a significant cytotoxic effect on HCT-116 cell line with IC_{50} value of 0.8 μM. Another study simultaneously was also examined the anti-cancer properties of the compound against colon cancer, various human colon cancer cell lines containing common mutations TP53 and KRAS. All of them, unlike the non-cancerous fibroblasts, showed significant sensitivity to the pradimicin-IRD compound. In the study of molecular cellular processes, induction of severe DNA damage, apoptosis and cell cycle arrest were observed. The regulation of p21 expression, independent of TP53, was observed in some cell lines such as HCT 116 TP53−/−, HT-29, SW480 and Caco-2 (Almeida et al., 2019). Karamomycins A-C isolated from soil actinomycete Nonomuraea endophytica strain GW58/450, and their biological effects was studied (Shaaban et al., 2019). Unlike karamomycin B, karamomycin A **(166)** showed non-selective toxicity against 36 human cancer cell lines, including two colon cancer cell lines HT-29 and HCT-116 with an average IC_{50} value of 6.8 μM. Karamomycin C **(167)** with slightly higher toxicity than karamomycin A (IC_{50} = 1.3 μM), showed good results.

Sekgranaticin **(168)**, granaticins A **(169)**, B (**170**) and methyl granaticinate (**171**) were isolated from the soil *Streptomyces* sp. 166, collected from the Tibetan highlands of China (Lv et al., 2019). The cytotoxicity of these compounds against lung, breast, colon carcinoma HCT-116 cell lines as well as human CRC stem cells P6C was evaluated by MTT method. All four compounds had a significant inhibitory effect on all tested cell lines. The strongest cytotoxicity effect on the two cell lines HCT-116 and P6C, was associated with granaticin B with IC_{50} values of 0.01 and 0.28 μM, respectively.

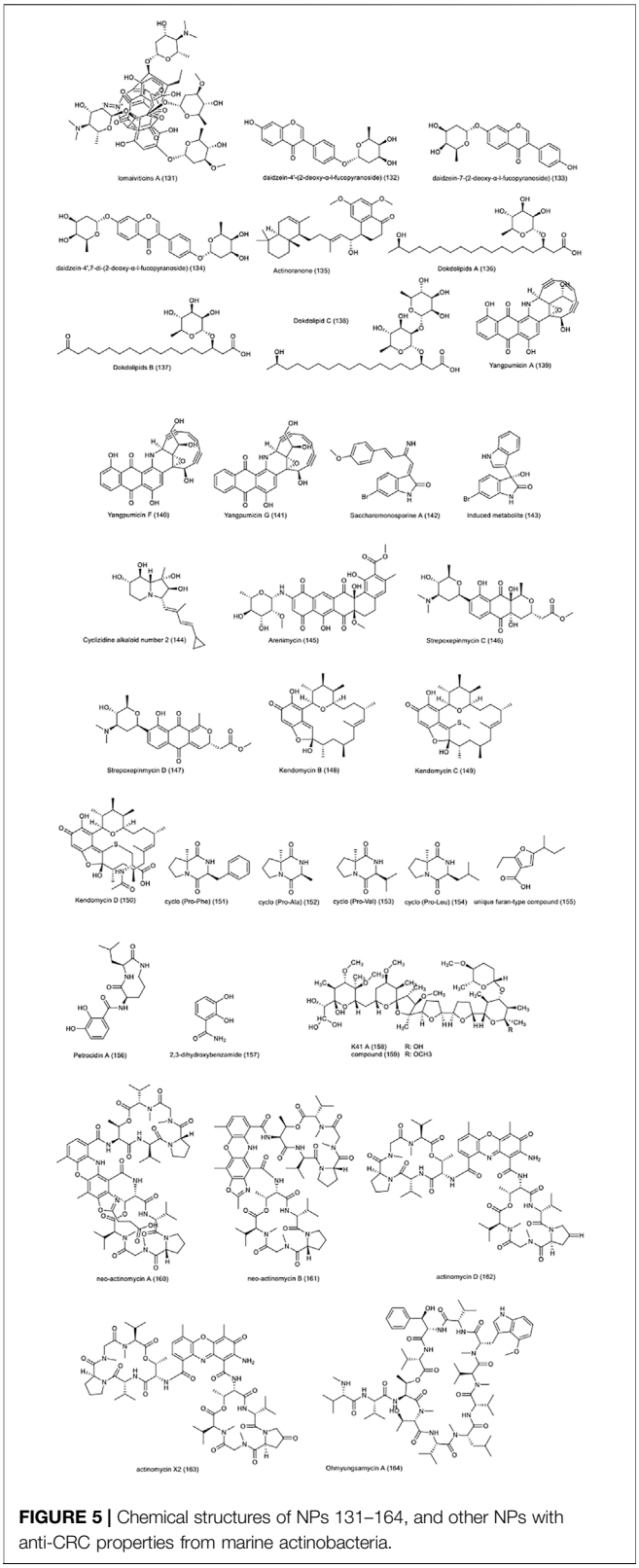

FIGURE 5 | Chemical structures of NPs 131–164, and other NPs with anti-CRC properties from marine actinobacteria.

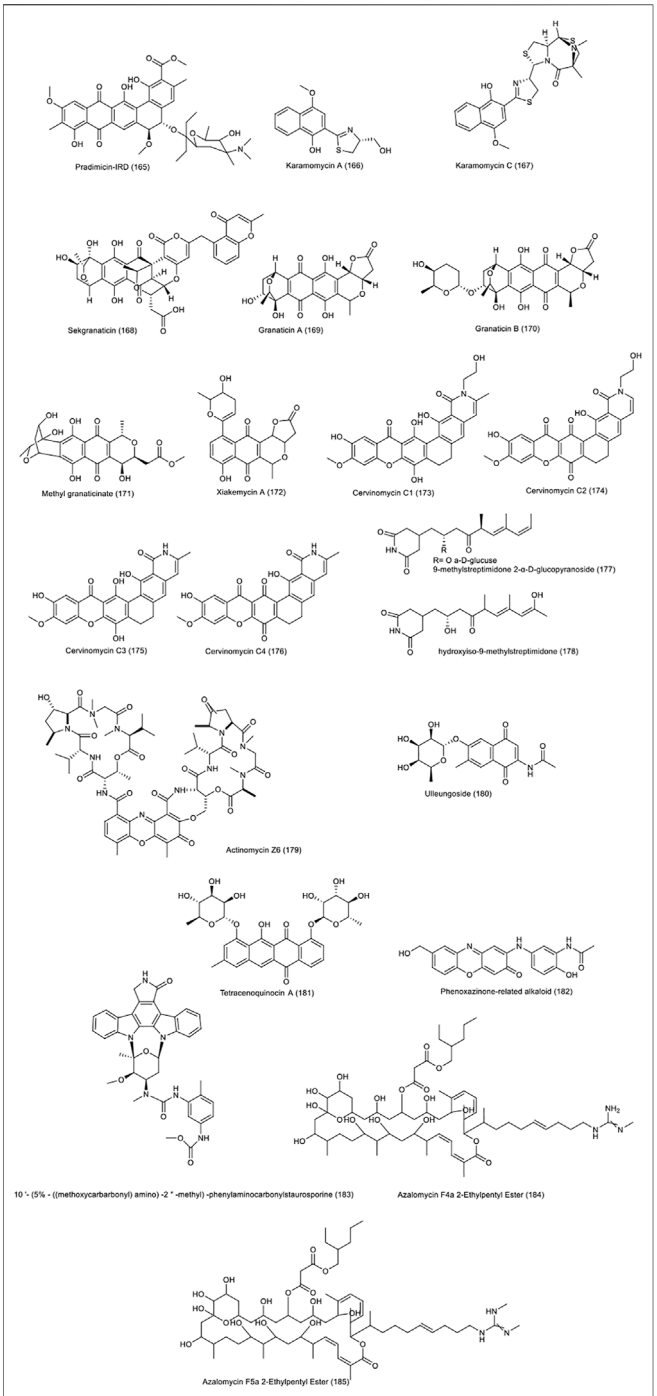

FIGURE 6 | Chemical structure of NPs produced by terrestrial strains of actinobacteria.

Xiakemycin A **(172)**, produced by soil *Streptomyces* sp. CC8-201, in addition to demonstrating a strong antibacterial effect against gram-positive bacteria, has shown a significant toxicity against various human cancer cell lines, including HCT-116 with an IC_{50} value of 0.59 μM (Jiang et al., 2015).

Polycyclic xanthones called cervinomycins C1-4 **(173–176)**, isolated from the soil *Streptomyces* sp. CPCC 204980, showed strong cytotoxicity effects against two cancer cell lines namely pancreatic BxPC-3 and colon HCT-116, with IC_{50} values in the range of 0.9–801.0 nM (Hu et al., 2020). Cervinomycin C3 showed the strongest effect on the HCT-116 cell line with an IC_{50} value of 0.9 nM. These compounds also showed potent antibacterial properties against gram-positive bacteria.

9-methylstreptimidone 2-α-D-glucopyranoside **(177)** and hydroxyiso-9-methylstreptimidone **(178)**, produced by the terrestrial *Streptomyces* sp. HS-NF-780, have shown a moderate cytotoxicity against lung, leukemia and colon cancer cell lines (Zhao et al., 2019). The compounds exhibited toxicity on the HCT-116 cell line with IC_{50} values of 34.83 μg/ml and 36.76 μg/ml, respectively.

A new member of the actinomycin family, called actinomycin Z6 **(179)**, identified from *Streptomyces* sp. KIB-H714. Unlike other Z-type actinomycens, this compound has an additional link between actinoyl chromophore and β-peptidolactone (Dong et al., 2019). The compound exhibited cytotoxicity on different cancer cell lines, including the human colon cancer line SW480 with an IC_{50} value of 1.57 μM. This compound had no antibacterial effects on the two test microorganisms namely *S. aureus* and *C. albicans*.

Three new glycoside compounds, including ulleungoside, 2-methylaminobenzoyl 6-deoxy-α-l-talopyranoside, and naphthomycinoside, were isolated from the terrestrial actinobacter species *Streptomyces* sp. KCB13F030 (Son et al., 2017). Ulleungoside **(180)** showed a significant cytotoxicity effect against several cancer cell lines including SW480 with an IC_{50} value of 9.3 μM. The compound also showed an inhibitory effect on the enzyme indoleamine 2,3-dioxygenase, involved in tryptophan metabolism.

The new compound, tetracenoquinocin A **(181)**, an anthracycline metabolite, was produced by the terrestrial *Streptomyces* sp. NEAU-L3, and its cytotoxicity was studied against three cancer cell lines of lung, liver and human colon in which showed a moderate cytotoxicity with an IC_{50} value of 20.82 μM on HCT-116 colon cancer cell line (Lu et al., 2017). Three new phenoxazinone-related alkaloids and two known compounds exfoliazone and viridobrunnine A, were identified in *Streptomyces* sp. KIB-H1318 (Yang et al., 2018). The second compound of phenoxazinone-related alkaloids **(182)** showed a weak toxicity effect against HeLa and SW480 cancer cell lines, with IC_{50} values of 36.8 and 37.8 μM, respectively.

The cytotoxicity of a staurosporine analog compound called 10′-(5%—((methoxycarbarbonyl)amino)-2″-methyl)-phenylaminocarbonylstaurosporine **(183),** isolated from mangrove soil derived actinomycetes *Streptomyces* sp. (172614) was studied against HCT-116. It was reported the compound showed a significant toxicity with an IC_{50} value of 0.37 μM (Li et al., 2011). The two compounds azalomycin F 2-ethylpentyl ester (4a) **(184)** and Azalomycin F 2-ethylpentyl ester (5a) **(185)** are produced by *Streptomyces* sp. 211726, isolated from mangrove rhizosphere soil (Yuan et al., 2011). Both compounds showed cytotoxic activity with IC_{50} values of 5.64 and 2.58 $\mu g \cdot ml^{-1}$ on the HCT-116 cell line, respectively, in addition to their antifungal activity toward *Candida albicans*. **Figure 6** demonstrates the chemical structure of compounds 165 to 185 .

TABLE 1 | the structure of some NPs with anti-CRC properties from terrestrial actinobacteria and their mechanism of action and origin.

Bacteria	Origin of bacteria	Compound name	Chemical structure	Colorectal Cell line	Special property	country of origin	references
Amycolatopsis sp. IRD-009	Soil sample from Brazilian rainforest	Pradimicin-IRD (165)	Naphthacenequinone, Other hydrocarbones	HCT-116, TP53 −/−, HT-29, SW480 and Caco-2	Severe DNA damage, Apoptosis and cell cycle arrest	Iracemápolis/São Paulo, brazil	Almeida et al. (2019)
Nonomuraea Endophytica Strain GW58/450	Soil of an oak/ beech mixed forest	Karamomycins A and C (166–167)	2-Naphthalen-2-Yl-Thiazole, Azoles	HT-29, HCT-116	—	Stadt Allendorf (Hessen, Germany)	Shaaban et al. (2019)
Streptomyces sp. 166	Clayey cold saline soil	Sekgranaticin, Granaticins A, B and Methyl granaticinate (168–171)	Polyketide-Naphthoquinone, Quinones	HCT-116 and P6C	—	altitude of 4547 m in Nima County (N31°52′, E87°1′), Naqu District, Tibet Autonomous Region, China	Lv et al. (2019)
Streptomyces sp. CC8-201	Soil of a remote karst cave	Xiakemycin A (172)	Naphthoquinone, Quinones	HCT-116	—	suburb of Chongqing city, China	Jiang et al. (2015)
Streptomyces sp. CPCC 204980	Soil sample	Cervinomycins C1-4 (173–176)	Polycyclic Xanthone, Xanthones	HCT-116	—	Mount Emei of Sichuan Province, China	Hu et al. (2020)
Streptomyces sp. HS-NF-780	Soil sample	9-Methylstreptimidone 2-A-D-Glucopyranoside (177) and Hydroxyiso-9-methylstreptimidone (178)	Piperidines	HCT-116	—	Linyi, Shandong province, China	Zhao et al. (2019)
Streptomyces sp. KIB-H714	Soil sample	Actinomycin Z6 (179)	Peptides	SW480	—	Kunming Botany Garden, Kunming, China	Dong et al. (2019)
Streptomyces sp. KCB13F030	Soil sample	Ulleungoside (180)	Glycosides	SW480	Indoleamine 2,3-dioxygenase inhibition	depth of 5–10 cm from Ulleung Island, Korea	Son et al. (2017)
Streptomyces sp. *NEAU-L3*	Soil sample	Tetracenoquinocin A (181)	Aminoglycoside -Naphthacene, Glycosides	HCT-116	—	peak of Dayao Mountain of Guangxi province, China	Lu et al. (2017)
Streptomyces sp. KIB-H1318	Soil sample	A Phenoxazinone-related Alkaloid (182)	Alkaloids	SW480	—	Yuxi, Yunnan province, China	Yang et al. (2018)
Streptomyces sp. (172614)	Soil sample	Staurosporine analog (183)	Alkaloids	HCT-116	—	Jiulongjiangkou Mangrove, Fujian, China	Li et al. (2011)
Streptomyces sp. 211726	Mangrove rhizosphere soil of Heritiera globosa	Azalomycin F (4a) 2-ethylpentyl ester and Azalomycin F (5a) 2-ethylpentyl ester (184–185)	Macrolide, Lactones	HCT-116	—	Wenchang, China	Yuan et al. (2011)
Soil-Derived Actinomadura Strain	Rice field soil	Nonthmicin and Ecteinamycin (201–202)	Polyether/Polyketide, Lactones	mouse colon carcinoma cell line 26-L5	Anti-invasive effect	Thailand	Igarashi et al. (2017)
Micromonospora sp. Strain No. R385-2	Soil sample	Rakicidin A (219)	Lipopeptide, Peptides	HCT-8 and DLD-1	Angiogenesis and hypoxia	Andhra Pradesh, India	McBrien et al. (1995), Yamazaki et al. (2007)
Streptomyces Hygroscopicus	—	Sirolimus (Rapamycin) (224)	Macrocyclic Lactones	HT-29, SW620, and HCT-116	mTOR inhibition	Easter Island (also known as Rapa Nui), Chile	Li et al. (2014), Mussin et al. (2017)

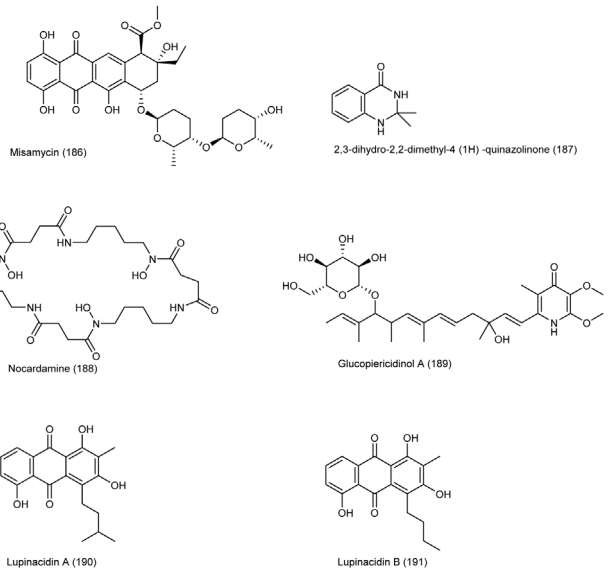

FIGURE 7 | Chemical structure of NPs produced by endophytic strains of actinobacteria.

2.3 Natural Products From Endophytic Actinobacteria With Anti-CRC Activity

Endophytic actinobacteria are group of Gram-positive bacteria that live in symbiotic relationships inside plant tissues (Delbari et al., 2020; Abedinlou et al., 2022). This unique class of actinobacteria has shown high potential to produce a wide range of secondary compounds with diverse biological properties (Bahrami et al., 2022). The research on this category of bacteria has led to the discovery of over 200 new bioactive secondary metabolites having a diverse chemical structure with the being majority alkaloids, polyketides, flavonoids and terpenoids (Dinesh et al., 2017; Bernardi et al., 2019; Delbari et al., 2020). **Table 2** summarizes the structure of some NPs with anti-CRC properties, isolated from terrestrial actinobacteria and their name and mechanism of action and origin.

An anthracycline called misamycin **(186)** is produced by the endophyte *Streptomyces* sp. YIM66403, isolated from the root of *Isodon eriocalyx* which is a traditional medicinal plant collected in China (Li et al., 2015). In addition to its antibiotic properties, the compound has shown a good cytotoxicity on several human cancer cell lines, including the CRC cell line SW4801 with an IC_{50} value of 9.75 μM.

2,3-dihydro-2,2-dimethyl-4 (1H) -quinazolinone **(187)** is a natural compound produced by the endophytic bacterium *Streptomyces sp* RLe8 isolated from the Brazilian plant *Lychnophora ericoides* that has shown significant cytotoxicity on the MDA-MB435, HCT-8, SF-295 and HL-60 cell lines with an IC_{50} value of 1.10 μg/ml on the HCT-8 colon cancer cell line (Conti et al., 2016). Another compound called nocardamine **(188)** produced by another endophytic species isolated from this plant called *Streptomyces cattleya* RLe 4 also showed significant cytotoxicity on these cells.

Two new compounds of glycosylated piericidins and four known compounds were identified from *Streptomyces* sp KIB-H1083, isolated from the traditional medicinal plant *Diaphasiastrum veitchii* (Shang et al., 2018). Among them, glucopiericidinol A **(189)** had a good cytotoxic effect on various cell lines such as HL-60, SMMC-7721, A-549, and MCF-7, although this compound was the weakest one against the SW480 CRC cell line with an IC_{50} value of 32.59 μM.

Lupinacidins A, B **(190–191)** from the endophytic species *Micromonospora lupini* Lupac 08 in non-toxic doses, was able to inhibit the invasive carcinoma cells, murine colon 26-L5, with IC_{50} values of 0.21 and 0.3 μM, respectively (Igarashi et al., 2007). The chemical structure of compounds 186 to 191 are illustrated in **Figure 7**.

2.4 Natural Products From Miscellaneous Actinobacteria With Anti-CRC Activity (From Unconventional Sources or Using Genome Mining)

A new derivative of the spectinabilin **(192)** compound, was identified from *Streptomyces* sp. 1H-GS5, isolated from ant (Liu et al., 2017). The cytotoxicity of this compound, along with another derivative of spectinabilin and the main compound spectinabilin as a positive control, gave good results against lung, liver and colon (HCT-116) cancer cell lines. The new spectinabilin derivative, showed a much stronger effect than the original compound, against the HCT-116 cell line, with an IC_{50} value of 12.8 μg/ml .

A total of 16 natural compounds of bafilomycins and odoriferous sesquiterpenoids were described from *Streptomyces*

TABLE 2 | the structure of some NPs with anti-CRC properties from the endophytic actinobacteria and their mechanism of action and origin.

Bacteria	Origin of bacteria	Compound name	Chemical structure	Colorectal Cell line	Host plant	country of origin	References
Streptomyces sp. YIM66403	Healthy stem of the traditional Chinese medicinal plant Isodon eriocalyx	Misamycin (186)	Anthraquinone, Quinones	SW480	Root of Isodon eriocalyx	Xishuangbanna, Yunnan, China	Li et al. (2015)
Streptomyces sp. RLe8 *and Streptomyces cattleya* RLe 4	Brazilian Medicinal Plant Lychnophora ericoides Mart	2,3-dihydro-2,2-dimethyl-4 (1H) –quinazolinone and Nocardamine also called deferrioxamine (187–188)	Peptides and Quinazolines	HCT-8	Lychnophora ericoides	Brazilian bioma Cerrado, brazil	Conti et al. (2016)
Streptomyces sp KIB-H1083	Traditional Chinese medicinal plant Diaphasiastrum veitchii	Glucopiericidinol A (189)	Aminoglycoside, Glycosides	SW480	Diaphasiastrum veitchii	china	Shang et al. (2018)
Micromonospora lupini Lupac 08	Root nodules of Lupinus angustifolius	Lupinacidin A and B (190–191)	Anthraquinone, Quinones	Murine carcinoma colon 26-L5	Root nodules of Lupinus angustifolius	mid-west Spain	Igarashi et al. (2007)

albolongus, isolated from the feces of the Asian *Elephas maximus* (Ding et al., 2016). Three compounds, 19-methoxybafilomycin C1 amide, bafilomycin C1 and bafilomycin C1 amide **(193–195)**, have significant cytotoxic effects on various cell lines, including BGC-823 human gastric carcinoma, Caco-2 colonic adenocarcinoma, H460 lung carcinoma, and SMMC-7721 hepatocellular carcinoma cell lines, with an IC_{50} range of 0.54–5.02 μM.

Retimycin A **(196)** was produced and identified from *Salinispora* sp. in genome-mining studies (Duncan et al., 2015). This compound showed a significant toxicity (IC_{50} < 0.076 μg/ml) on the HCT-116 cell line. Retimycin A, is a member of the quinomycin-like depsipeptide family. It was identified through the biosynthetic pathway of the rtm gene cluster using HR-MS/MS data, as compared to normal authentic.

Using genome mining, a peptide called curacozole **(197)** was isolated from *Streptomyces curacoi mutant* strain R25 (Kaweewan et al., 2019). The significant inhibitory effect was observed on the cell line of human osteosarcoma HOS (IC_{50} = 10.5 nM) and HCT-116 colon carcinoma (IC_{50} = 8.6 nM).

In 2015, salternamides A-D compounds were isolated from the *halophilic actinomycete* strain (no. HK10) found in salt ponds on Shinui Island in the Republic of Korea. The toxicity of these compounds on 6 human cancer cell lines, including colon, was investigated. The most significant toxicity was related to salternamide A **(198)** compound on HCT-116 colon cancer and SNU638 gastric cancer cell lines (IC_{50} = 0.96 μM) (Kim et al., 2015). The Subsequent studies have shown that this compound can inhibit hypoxia inducible factor (HIF-1α) accumulation in hypoxic conditions and suppress the upstream signaling such as PI3K/Akt/mTOR, p42/p44 MAPK, and STAT3. Stopping the cell cycle at G2/M and induction of apoptosis by this compound in HCT-116 cells were other results of this study (Bach et al., 2015).

In 2018, a mutant species *Streptomyces* sp. SCSIO 1666/17C4 was obtained by inserting cosmid p17C4 into the marine derived *Streptomyces* sp. SCSIO 1666 (Gui et al., 2018). Cosmid was the carrier of the biosynthetic gene l-rhodinose and the gene for glycosyltransferase12 anthracycline antibiotics, including three new derivatives of ε-rhodomycinone and nine new derivatives of β-rhodomycinone, were identified along with three previously known compounds from this species. Almost all compounds had a good cytotoxic effect against different cell lines. The strongest activity against HCT-116 cell line were related to compound number 4 of ε-rhodomycinone derivatives **(199)** and known compound l-rhodinose-l-rhodinose-l-rhodinoserhodomycinone **(200)**, with IC_{50} values of 0.3 and 0.2 μM, respectively. The chemical structure of compounds 192 to 200 are illustrated in **Figure 8**. The chemical composition of NPs with anti-CRC properties from miscellaneous actinobacteria and their mechanism of action and origin are outlined in **Table 3**.

2.5 Actinobacteria as Human Gastrointestinal Tract (Gut) Microbiome

In addition to producing effective bioactive secondary metabolites, actinobacteria have been reported to be one of the four main phyla of the gut microbiota, revealing another aspect of their relationship. It is evident that one of the most associated risk factors for precancerous and cancerous intestine conditions is a change in the gut microbiome and microbiota dysbiosis. The variation in the gut microbiome may generate CRC by destructing host DNA, creating and maintaining a pro-inflammatory condition, and influencing host immune responses (Kværner et al., 2021). Evidence has corroborated that the alteration in the gut microbiome in the early stages of CRC may be employed to diagnose and detect individuals at risk of presenting colorectal adenoma. These changes can also affect the effectiveness of conventional therapies such as radiotherapy and chemotherapy (Zhou et al., 2021). Therefore, several studies, have been conducted to determine specific microbial patterns or significant changes in the intestinal microbial community of patients and healthy individuals, using the molecular study

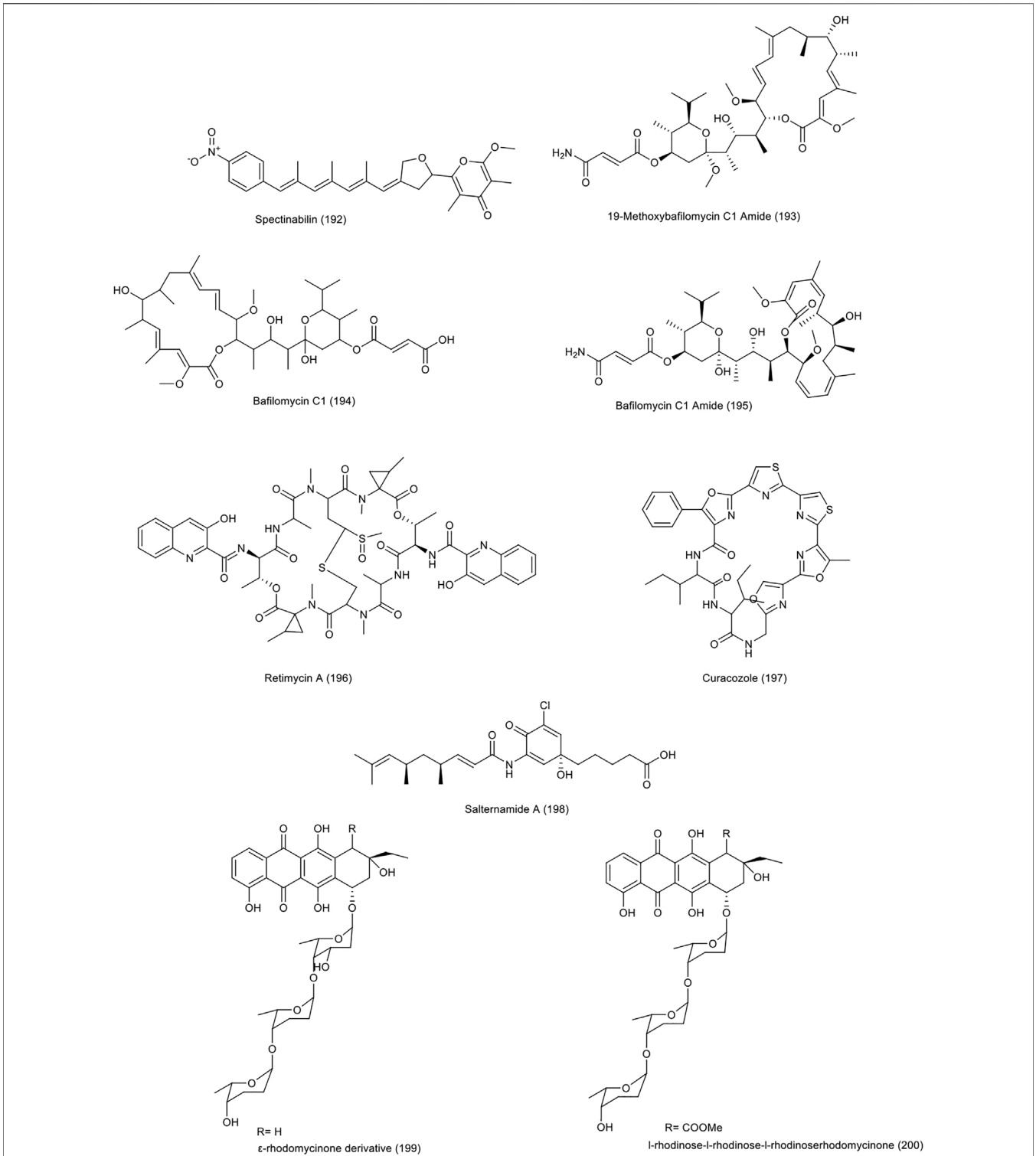

FIGURE 8 | Chemical structure of NPs produced by miscellaneous actinobacteria.

of faecal microbiota, in order to find a suitable biomarker for CRC .

Actinobacteria are reported to play a critical role in the maintenance of gut homeostasis. A study compared healthy individuals (H) and groups with hyperplastic polyps (HP), low-risk adenomas (LRA), high-risk adenomas (HRA), adenocarcinomas (ADK), and the last group included patients with ADK who received chemotherapy or radiotherapy (ADK-T)

TABLE 3 | The structure of some NPs with anti-CRC properties from other actinobacteria and their mechanism of actions and origins.

Bacteria	Origin of Bacteria	Compound	Chemical structure	Colorectal Cell line	Country of Origin	Special property	references
Streptomyces sp. 1h-gs5	Head of ant (Camponotus japonicas Mayr)	A new derivative of the spectinabilin (192)	Pyrone, Pyranes	HCT-116	Northeast Agricultural University, Harbin of Heilongjiang province, China	—	Liu et al. (2017)
Streptomyces albolongus	Fresh fecal samples excreted by healthy adult *Elephas maximus*	19-methoxybafilomycin C1 amide, bafilomycin C1 and bafilomycin C1 amide (193–195)	Macrolide, Lactones	Caco-2	Xishuangbanna National Nature Reserve, Xishuangbanna, Yunnan Province, P. R. China	—	Ding et al. (2016)
Salinispora sp.	—	Retimycin A (196)	Quinomycin-type depsipeptide, Peptides	HCT-116	—	—	Duncan et al. (2015)
Streptomyces curacoi mutant strain r25	—	Curacozole (197)	Oxazole thiazole, Azoles	HCT-116	—	—	Kaweewan et al. (2019)
Halophilic streptomyces strain (no. Hk10)	Saltern	Salternamide A (198)	Polyene, Amides	HCT-116	Shinui Island in the Republic of Korea	Inhibition of HIF-1α accumulation, suppression of upstream signaling, Stopping the cell cycle at G2/M and induction of apoptosis	Bach et al. (2015)
Streptomyces sp. Scsio 1666/17c4	Recombinant	Number 4 of ε-rhodomycinone derivatives and -rhodinose-l-rhodinose-l-rhodinoserhodomycinone (199–200)	Anthraquinone, Quinones	HCT-116	-	-	Gui et al. (2018)
Streptomyces violascens	Fresh fecal samples excreted by healthy adult Ailuropoda melanoleuca (giant panda)	Fusicomycin A, fusicomycin B and isofusicomycin A (203–205)	Fusicoccane diterpene, Terpenes	HCT-116	Yunnan Wild Animal Park, Kunming, Yunnan Province, People's Republic of China	Anti-adhesion, anti-invasion and migration effects	Zheng et al. (2017)
Streptomyces sp. Gku 220	Marine sponge sample	Rakicidin F and C (206–207)	Cyclic depsipeptide, Peptides	murine carcinoma colon 26-L5	Andaman sea, Ranong, Thailand	Anti-invasion	Kitani et al. (2017)
Nanoparticle conjugated -*Streptomyces* sp. Js520	Pristine sediment from the cave	Undecylprodigiosin (211)	Pyrrole, Azoles	HCT-116	mountain Miroc in Serbia	Apoptosis	Nikodinovic-Runic et al. (2014)
Synthesized –Actinomycete z2039-2	Sea Earth	K252c derivative (212)	Indolopyrazolocarbazole, Indoles	HCT-116	coast of Qingdao, China	Apoptosis	Liu et al. (2007), Esvan et al. (2016)

(Mori et al., 2018). Bacterial flora analysis showed that the most common phyla in healthy people are *Firmicutes, Bacteroidetes, Actinobacteria* and *Proteobacteria*. However, patients who are dealing with ADK, *Firmicutes* and *Actinobacteria* are significantly decreased, which can, in addition to the *Lachnospiraceae* family, be considered as good specific biomarkers for H, LRA and HP individuals. Also, in people with preneoplastic/neoplastic lesions, in general, a decrease in the *Firmicutes/Bacteroidetes* ratio can be considered as a marker for intestinal dysbiosis. Comparison between healthy people, people with inflammatory bowel disease (IBD) and those suffering from CRC have shown that the frequencies of the three phyla, *Firmicutes*, *Bacteroidetes*, and *Actinobacteria*, involved in metabolic pathways, are significantly different among them (Ma et al., 2021). Phyla *Firmicutes* and *Actinobacteria* were the main differential bacteria in the healthy group and phyla *Fusobacteria*, *Proteobacteria*, and *Verrucomicrobia* were reported as differential bacteria in the CRC patient group.

In a cohort study between healthy young people (below 30 years old), healthy old group (over 60 years old) and CRC

patients, several bacterial species were reported to be distributed inequality in these groups (Zhang et al., 2021). *Clostridia, Fusobacteria, Actinobacteria*, and *Bifidobacterium* were introduced as potential biomarkers in CRC patients of different ages. *Actinobacteria* at the phylum and class level were more abundant in the older group than in the younger volunteers. Interestingly, the abovementioned frequency was lower in CRC patients than in both healthy groups.

A similar study compared the microbiome of CRC and adjacent normal mucosa tissues by which a significant reduction in the relative abundance of *Firmicutes* and *Actinobacteria* was observed in tumor tissue as compared to adjacent healthy tissues (Gao et al., 2017). In addition, the presence of *Villanelle, Firmicutes*, and *Actinobacteria* (family *Bifidobacteriales*) were reported with the greater frequency in the group without adenoma as compared to the group of patients having adenoma, which is a common precursor for CRC, confirmed the previous results (Hale et al., 2017).

Determining the frequency and specificity of microbiome in CRC patients and the microorganisms involved in the development and progression of this disease can be used as a screening marker to predict and evaluate precancerous evidence based on the present ratio of the protective bacteria to its harmful types. As documented in many studies, phyla such as *Actinobacteria* and *Firmicutes* have been implicated as protective microbiomes against CRC (Hale et al., 2017; Mori et al., 2018; Zhang et al., 2021).

2.5.1 Perspectives on the Relationship Between Gut Microbiome and Cancer

Actinobacteria, these amazing microorganisms that produce a variety of bioactive secondary metabolites, have not withheld their gift from the human body due to their diversity in various habitats. The isolates from intestinal microbiomes in addition to producing the secondary metabolites and their amazing potency of the anticancer effects, these bacteria were introduced as cancer killers. In this view, it is possible that these bacteria, of which actinobacteria constitute a significant part, are enabled not only to prevent CRC locally, but also to inhibit spreading cancer in other organs systemically in the very early stages by producing anti-cancer compounds (Zhou et al., 2017). It has been suggested the difference between the function of these bacteria in preventing cancer and the production of secondary compounds in individuals can be due to the genetic predisposition of individuals and environmental factors such as diet and the amount of antimicrobial use during their lifetime.

A study presented that a significant difference in the abundance of several taxa between adenoma and non-adenoma patients, led to the perspective that the accumulation of sugar, protein and lipids metabolites as well as increased bile acid production can provide environmental conditions in favor of the growth of bile acid-resistant microbes, and these microbes, in turn, provide the conditions for the development of adenomas and CRC, by generating substances such as inflammatory and genotoxic metabolites (Hale et al., 2017).

3 POTENTIAL BIOLOGICAL MECHANISMS AND FUNCTION OF NPS AGAINST COLORECTAL CANCER

3.1 Migration and Invasion

Nonthmicin **(201)** and ecteinamycin **(202)** compounds produced by soil-derived *Actinomadura strain*, in addition to exhibiting strong antibacterial effects against gram-positive bacteria, have shown anti-invasive effect against mouse colon carcinoma cell line 26-L5 (Igarashi et al., 2017). These two compounds, with IC_{50} values of 0.017 and 0.15 μM, respectively, inhibit the invasion of cancer cells into the extracellular matrix; however, they did not show cytotoxicity.

Six new fusicoccane-type diterpenoids were identified from *Streptomyces violascens,* isolated from the feces of the panda *Ailuropoda melanoleuca* (Zheng et al., 2017). Fusicomycin A **(203**, fusicomycin B **(204** and isofusicomycin A **(205)** showed good cytotoxicity against 5 human cancer cell lines including colon carcinoma HCT-116 with IC_{50} values of 6.7, 5.8 and 8.0 μM, respectively. In the study of the effect of these compounds on adhesion, invasion and migration of SMMC7721 hepatocarcinoma cells, fusicomycin B showed a significant anti-adhesion effect and also reduced the number of migrating cells and therefore the anti-invasion and migration effect was recorded in these studies.

Rakicidin F **(206)**, C **(207)**, produced by *Streptomyces* sp. GKU 220 isolated from sea sponge were examined for biological activity (Kitani et al., 2017). Rakicidin F, in addition to its growth inhibitory effect towards *B. subtilis* and *E. coli*, showed higher cytotoxicity than rakicidin C. While treatment of murine carcinoma colon 26-L5 cells with rakicidin C compound at a dose of 1.25 μg, inhibited the invasion of these cells by 30% without causing toxicity.

Androsamide **(208)**, isolated from marine actinomycete *Nocardiopsis,* strain CNT-189 was reported to exhibit antitumor activity against colorectal cell lines in a variety of ways. The effect of this compound on three human cell lines adenocarcinoma (AGS), HCT-116 and Caco-2 showed cytotoxicity with IC_{50} values of 18, 21 and 13 μM, respectively (Lee et al., 2020). Further studies on Caco2 CRC cell line, the androsamide showed the inhibition of migration and invasion of these cancer cells. These results were confirmed in further studies on the expression of related factors such as Snail, Slug, Twist, ZEB1, and ZEB2 and markers such as E-cadherin, N-cadherin, and vimentin at the mRNA and protein levels. Finally, strong suppression of Caco2 cells motility by this compound was reported.

3.2 Apoptosis

It was reported that natural compounds produced by distinct marine actinomycetes namely sharkquinone, resistomycin, undecylprodigiosin, butylcyclopentylprodigiosin, elloxizanones A and B, carboxyexfoliazone and exfoliazone, were able to initiate cell death via internal apoptosis pathway and susceptibility of cancerous to tumor necrosis factor-related apoptosis-inducing ligand (TRAIL). The chemical structure of these compounds is displayed in **Figure 9**. Evident has showed

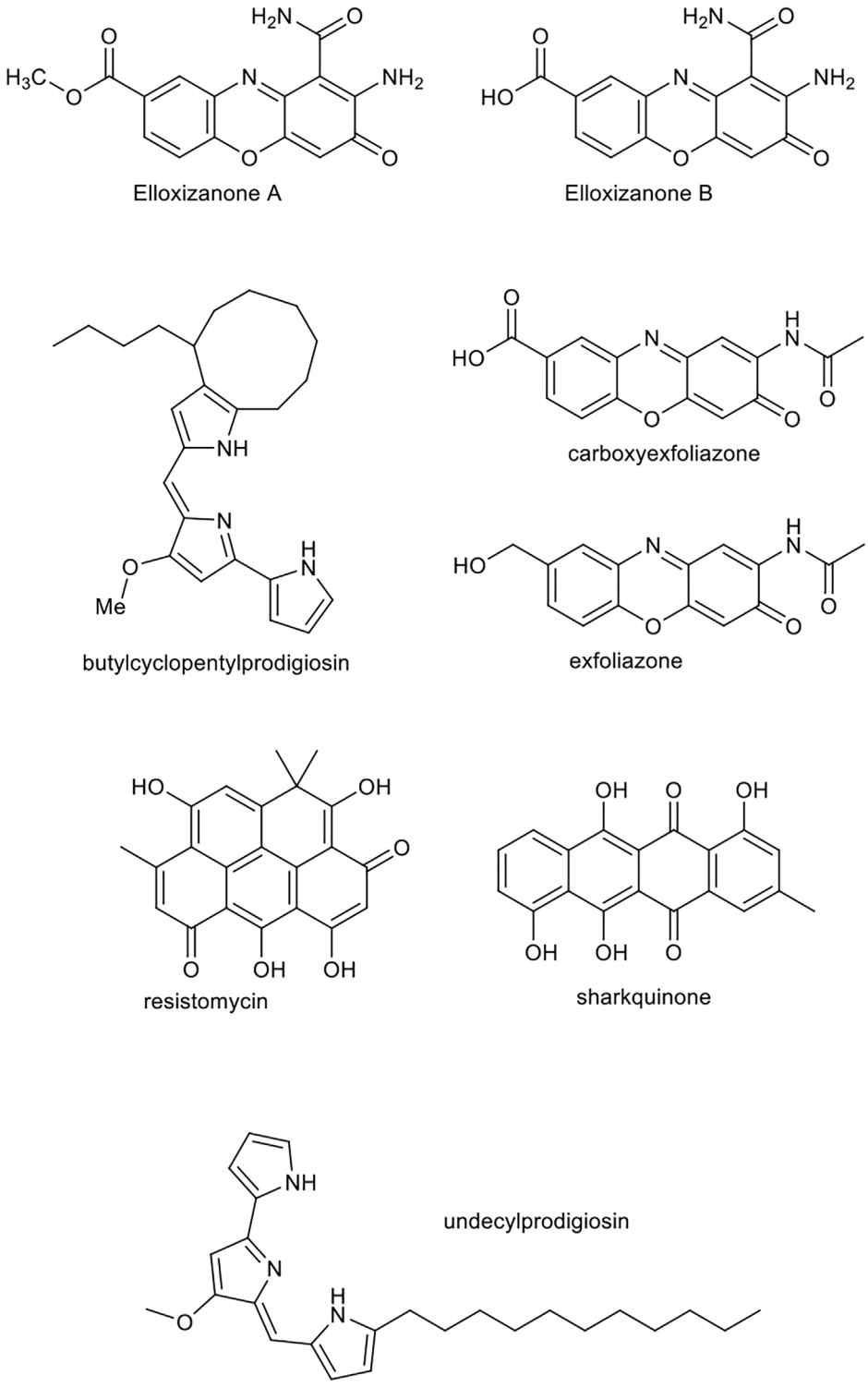

FIGURE 9 | Chemical structure of sharkquinone, resistomycin, undecylprodigiosin, butylcyclopentylprodigiosin, elloxizanones A and B, carboxyexfoliazone and exfoliazone.

that these compounds are able to reduce the expression of X-linked inhibitor of apoptosis protein (XIAP) and survivin factors, which are members of the inhibitor-of-apoptosis protein (IAP) family recognized for their inhibitory effects on caspase (Elmallah et al., 2020). Thereby they can stimulate the apoptosis of human cancer cells. The use of these compounds

could possibly help to fight the resistant cancer cells to TRAIL and its derivatives. A study suggested the above-mentioned pure compounds induce death in breast cancer MDA-MB-231, Jurkat leukemia and HCT-116 colon carcinoma cell lines, and their combination uses with TRAIL, synergistically increase its apoptotic properties. These compounds show hallmarks of apoptosis including activation of pro-caspase -10, -8, -9 and -3 and consequently the increase in lamins A/C and cleavage of PARP in cancer cells.

Two compounds, echinosporin **(209)** and 7-deoxyechinosporin **(210)**, produced by the marine derived *S. albogriseolus A2002*, collected in Jiaozhou Bay, China, were documented to have replication inhibitory effects on different types of cancer (Cui et al., 2007). Echinosporin with relatively strong effects and 7-deoxyechinosporin with weaker effects show cytotoxicity on HCT-15 colon carcinoma cell line. They induce apoptosis and cell cycle arrest generally in the G2/M phase, which are promising.

Metacycloprodigiosin and undecylprodigiosin from the prodigiosin family, were isolated from the marine actinomycete *Saccharopolyspora* sp. nov which showed cytotoxicity against five cancer cell lines namely mouse lymphoma (P388), human leukemia (HL60), human lung carcinoma (A549 and SPCA4) and liver carcinoma (BEL-7402) (Liu et al., 2005). The compound undecylprodigiosin **(211)**, was isolated from the non-marine *Streptomyces* sp. JS520. It was conjugated to gold nanoparticles and showed lethal effects through induction of apoptosis on melanoma A375, lung carcinoma A549, breast cancer MCF-7 and colon HCT-116 (Nikodinovic-Runic et al., 2014).

The compound k252c, produced by strain *actinomycete* Z2039-2, was documented to induce apoptosis in the leukemia cell line K562 (Liu et al., 2007). In 2016, a derivative of this compound (indolopyrazolocarbazole) **(212** was synthesized by replacing the lactam ring with the pyrazole component, which showed moderate lethal effects against leukemia and colon carcinoma K562 and HCT-116 (Esvan et al., 2016).

Manumycin A **(213)**, a compound with the inhibitory activity of Ras farnesyl transfrase, from the marine *Streptomyces* sp. M045 inhibits the growth of Ki-ras-activated mouse fibrosarcoma (Hara et al., 1993; Sattler et al., 1998). A 2000 study demonstrated the inhibition of the signaling pathway of manumycin by inducing apoptosis in the COLO320-DM colon cancer cell line. Finally, they reported that the inhibition of p21 ras processing and signaling was associated with the inhibition of proliferation and induction of apoptosis, and that the presence of the ras mutant gene was not required to exhibit these effects (Di Paolo et al., 2000). However, it was later found that the cytotoxic activity of this compound was independent to the RAS pathway and they reported ROS induction, especially O2−, in cells treated with this compound and were identified as effective compounds on thioredoxin reductase (Tuladhar et al., 2019).

Two tetrocarcin analogues called arisostatins A **(214)** and B were isolated from *Micromonospora* sp. Strain TP-A0316. Arisostatin A showed a good activity against gram-positive bacteria as well as cytotoxicity and antitumor activity against myeloid leukemia cell line U937 and human colon cancer cell line HCC2998 (IC_{50} = 0.22M), breast, lung and brain (Furumai et al., 2000). A 2003 study examined the antitumor effect of this compound on the head and neck cancer cell line; AMC-HN-4.

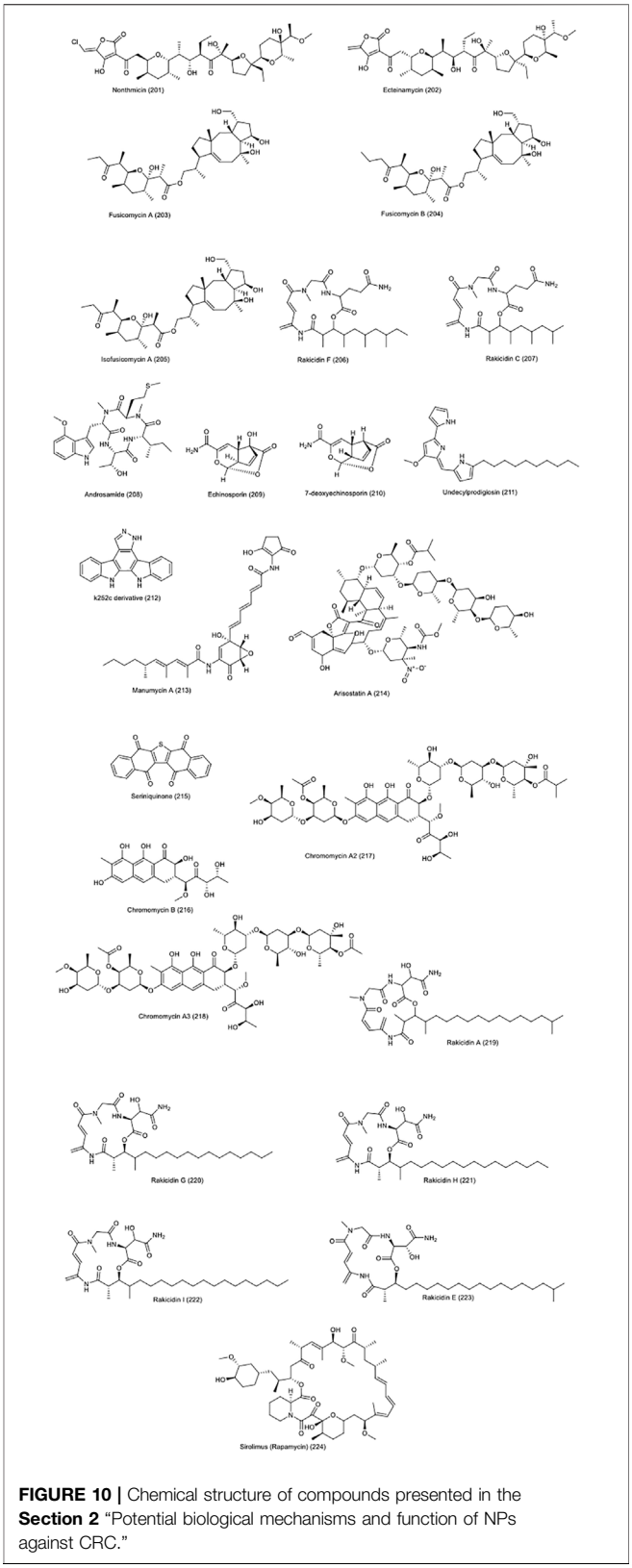

FIGURE 10 | Chemical structure of compounds presented in the **Section 2** "Potential biological mechanisms and function of NPs against CRC."

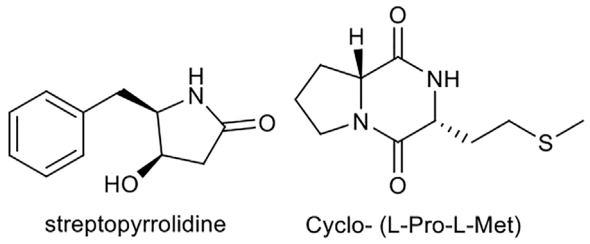

FIGURE 11 | Chemical structure of streptopyrrolidine, and cyclo- (L-Pro-L-Met).

It has been documented that the antitumor effect and the onset of apoptosis in cells treated with this compound is due to the activation of Caspase-3 and the formation of ROS species (Kim et al., 2003). Chemical structure of compounds 201 to 224 are presented in **Figure 10**.

3.3 Autophagy

A study was performed to evaluate the autophagy and apoptosis properties of the compound seriniquinone **(215)**, produced by *Serinicoccus* sp., an actinobacter from the family *Ornithinimicrobiaceae* on various cell lines, including HCT-15 colon cancer cell line (Trzoss et al., 2014). These studies, generally performed on melanoma cell line and HCT-116 colon cancer, suggested that the compound induces autophagocytosis in the examined cells by targeting dermcidin protein; a protein involved in autophagy and apoptosis processes.

Aureolic acid compounds, called chromomycins B, A2, A3 **(216–218)**, from marine actinomycetes *Streptomyces* sp. WBF16 were showed significant antitumor effects against several cancer cell lines, including HCT-116 and HepG2, SGC7901, A549, and COC1. In 2016, a study found that the compound chromomycin A2 exerts its antitumor effects on cancer cells by inducing autophagy through members of the TP53 family (Lu et al., 2012; Ratovitski, 2016).

3.4 Angiogenesis and Hypoxia

Angiogenesis is the process of forming new blood vessels from existing ones that occurs in both physiological and pathological conditions. Various factors are involved in the initiation and development of this process, perhaps the most important of which is VEGF (Nathan and Kannan, 2020). One of the pathological conditions in which angiogenesis is involved is tumor growth and progression. Under hypoxia and oxidative stress, cells begin the process of angiogenesis through factors such as HIF-1α to maintain their survival. The formation of new blood vessels in hypoxic areas of solid tumor cells, such as colon cancer, will lead to better nutrition of the cells and help them to grow and metastasize, and thus tumor progression. It has been shown that the levels of factors involved in angiogenesis and metastasis like VEGF and matrix metalloproteinases (MMPs) increase in the tumor tissue of patients with colon cancer (Auyeung and Ko, 2017).

Many studies are being conducted on the relationship between angiogenesis and cancer in order to identify new factors involved in this process. Factors or compounds that can inhibit angiogenesis or disrupt the process in any way, may be good candidates for the treatment, diagnosis and management of cancer. One of them is TSGA10. It has been shown that the over expression of the compound is associated with decreased HIF-1α transcriptional activity as well as disruption of HIF-1α axis (Mansouri et al., 2016; Amoorahim et al., 2020).

Among the various compounds such as NPs produced by plants and bacteria that affect the process of angiogenesis, NPs of actinomycetic origin, especially marine species, have received increasing attention (Nathan and Kannan, 2020). In a 2008 study, the compound streptopyrrolidine, isolated from the marine derived *Streptomyces* sp. KORDI-3973, after structural and biological examination, has shown an inhibitory effect on the process of angiogenesis (Shin et al., 2008). This compound exhibits a significant effect on HUVECs cells in the presence and absence of VEGF in the study of tube formation assay. The treatment of these cells with streptopyrrolidine, resulted in significant blockade of capillary tube formation, equivalent to the effect of known anti-angiogenesis compound, SU11248. This compound did not show cytotoxicity against the cells used, at of 100 μg/ml concentration. Cyclo- (L-Pro-L-Met) compound, isolated from marine *actinomycete Nocardiopsis* sp. 03N67 was stated to inhibit the angiogenesis, invasion and cell migration of epithelial cells in similar studies using capillary tube formation and migration/invasion assay, at a concentration of 10 μM (Shin et al., 2010). The compound had no cytotoxicity at the reported concentration. **Figure 11** illustrates the chemical structure of these compounds.

In 1995, for the first time, the production of rakicidins A and B, from the soil *Micromonospora* sp. strain No. R385-2, was reported. These compounds showed cytotoxicity against M109 lung cancer cell line (McBrien et al., 1995). In subsequent studies in 2006, rakicidin A **(219)** was reported as a compound with selective toxicity against solid tumors in hypoxic conditions. Hypoxia is a hallmark of solid tumors and has been linked to the angiogenesis and related factors such as HIF-1 and VEGF in tumor progression and spread. the various cell lines, including HCT-8 and DLD-1, related to human colon cancer, were examined and this compound showed 17.5 times more toxicity in hypoxia as compared to normal conditions. In further studies, no change in HIF-1 transcriptional level was observed and the mechanism of action of this compound in hypoxic conditions remained unknown (Yamazaki et al., 2007). In 2018, rakicidins G-I **(220–222)** compounds were isolated from the marine derived *Micromonospora chalcea* FIM 02–523 (Chen L. et al., 2018). These compounds along with known compound rakicidin E **(223)**, were tested against pancreatic PANC-1 and colon HCT-8 cancer cell lines in both normal oxygen and hypoxia conditions in which they were 18.2–20.3 times more toxic in hypoxia conditions.

The distribution of NPs having anti-CRC activities, produced by actinobacteria based on genus is summarized in **Chart 2**. **Chart 2** demonstrates that most of compounds are of *Streptomyces* genera.

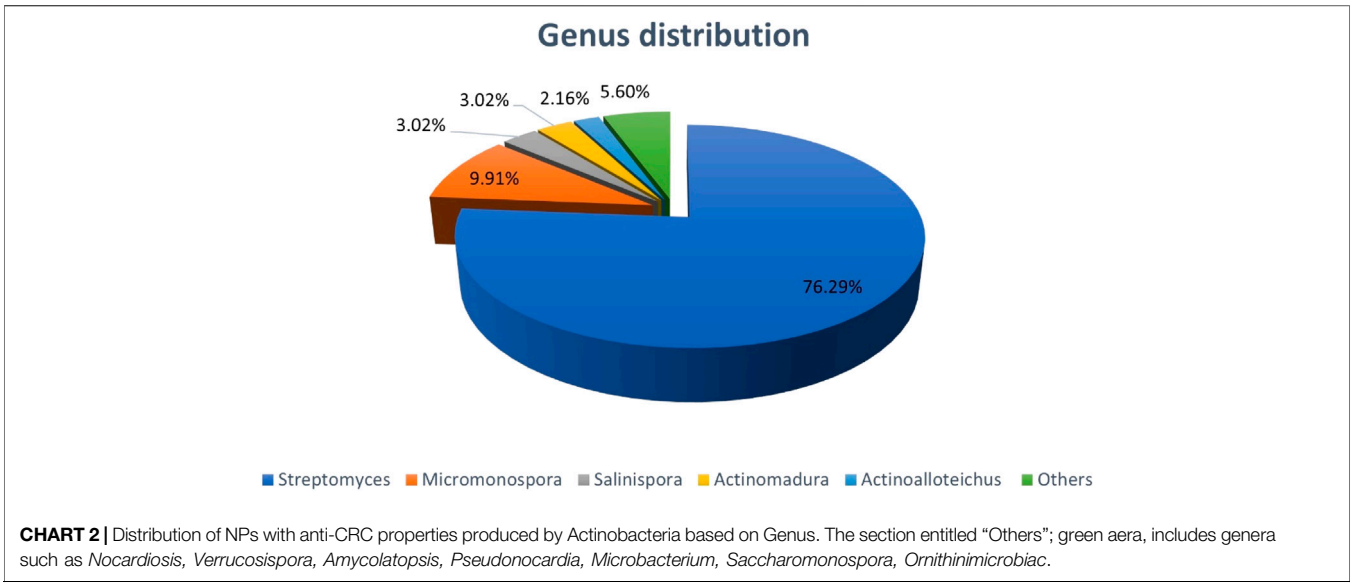

CHART 2 | Distribution of NPs with anti-CRC properties produced by Actinobacteria based on Genus. The section entitled "Others"; green aera, includes genera such as *Nocardiosis, Verrucosispora, Amycolatopsis, Pseudonocardia, Microbacterium, Saccharomonospora, Ornithinimicrobiac*.

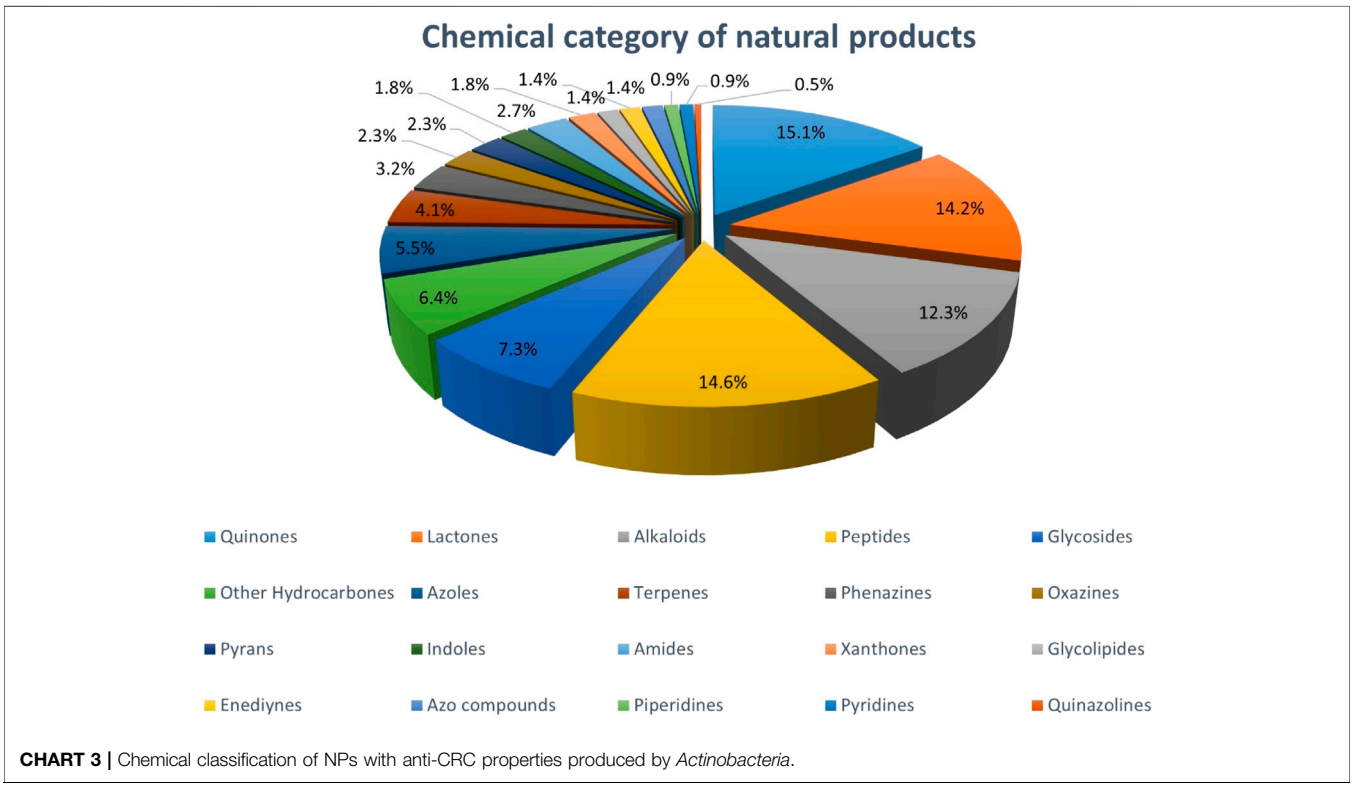

CHART 3 | Chemical classification of NPs with anti-CRC properties produced by *Actinobacteria*.

4 THE STRUCTURE–ACTIVITY RELATIONSHIP OF NATURAL PRODUCTS

The NPs presented in this paper include a wide range of chemical compounds with unique properties. We have tried to put all of them in 20 different chemical categories. As you can see in **Chart 3**, more than 54% of the compounds placed into only four major categories, including quinones, lactones, alkaloids, and peptides. Quinones, which are undoubtedly one of the largest groups of antitumor compounds, account for 16% of the NPs in our study. Although the exact relationship between the quinone moiety in these compounds and the cytotoxic effect is not fully understood, it seems that they often exert their biological effects by targeting DNA (Asche, 2005). The second major category belongs to lactones, accounting for 15% of these NPs. Lactones are able to affect cell growth, signaling and differentiation. So, they can exhibit

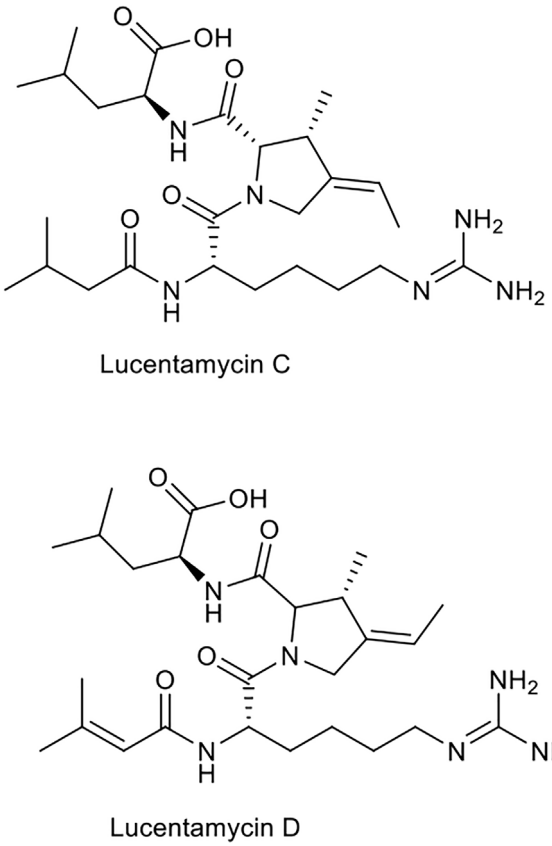

FIGURE 12 | Chemical structure of lucentamycins C and D.

biological effects such as antimicrobial and anticancer properties due to the functional groups attached to them (Konaklieva and Plotkin, 2005).

Here are provided some examples of effective NPs on CRC cell lines with different structural features in order to express the importance of the smallest changes in the chemical structure of compounds in their cytotoxic and anticancer performance.

The obvious difference in the biological function of lucentamycins, suggests the presence of aromatic rings in the structure of compounds is pivotal for their cytotoxic activity (Cho et al., 2007). So that, compounds lucentamycins A and B **(23,24)** having aromatic ring (phenyl and indole rings respectively) showed 75 and 13.6 times more cytotoxicity than lucentamycins C and D (which lack of this moieties) against HCT-116, respectively. **Figure 12** shows the chemical structure of these compounds.

Another example is the differences between central spiroaminal organization and tetrahydropyran conformation in marineosins A and B **(29,30)** have been reported as reasons for the superiority of type A in causing cytotoxicity on the HCT-116 cell line as compared to type B of the compound (Boonlarppradab et al., 2008).

The presence of sugar bridge and bisindolocarbazole is shown to impact on the activity of compounds. For instances, Structure-activity relationship for staurosporine derivatives **(39,52)**, and strong cytotoxic activity for staurosporine derivative No. 7 **(44)** and No. 14 **(51)**, showed the importance of sugar bridge and bisindolocarbazole in those whose exhibited stronger cytotoxicity against cancer cell lines (Zhou et al., 2019).

The presence of halogens into the structures of natural products or synthetic compounds has often reported to improve their biological activity and physicochemical properties. Actinobacteria, in particular, marine *streptomyces* species generate a diverse range of halogenated compounds with a wide spectrum of biological activities. These compounds possess various chemical structures including polyketides, alkaloids (nitrogen-containing compounds) and terpenoids (Wang et al., 2021). It was reported that halogenated substances from marine actinomycetes have crucial biological activities such as antibacterial and anticancer properties. In the case of chlorizidine **(99)**, the presence of the chlorinated 5H-pyrrolo [2,1-a] isoindol-5-one ring, which had not previously been reported in natural compounds, was a possible factor in the effect of cytotoxicity against HCT-116 cell line (Alvarez-Mico et al., 2013).

Another group of natural compounds that have a special chemical structure are halogenated compounds or halometabolites. Halogenation is a common modification of secondary metabolites and can have a critical role in establishing the bioactivity of a compound. The presence of halogen substituents (F, Cl, Br, I) in their structure can usually add and lead to increase the efficacy and properties of a compound including stability and bioactivity. Having various functions, such as the production of toxins and antibodies and other biochemical properties, are due to the presence of halometabolites in their hosts (Kasanah and Triyanto, 2019). The high concentration of chloride and bromine ions in marine environments, it leads to the discovery of more halogenated compounds in secondary metabolites of marine origin than its terrestrial equivalents (Wang et al., 2021).

Compounds such as marinopyrroles A-F **(86–91)**, ammosamides A **(93)** and B **(94)** and marinocyanins A-F **(100–105)** are types of halometabolites, produced by actinobacteria that have been reported to possess significant cytotoxicity against CRC cell lines (Hughes et al., 2008; Hughes et al., 2009a; Doi et al., 2012; Pan et al., 2012; Asolkar et al., 2017).

In a 2012 study, the presence of a conjugated diene unit and a suitable alkyl chain length were shown to be critical for demonstrating specific activity in rakicidin A **(219)** which is cytotoxic against various cell lines (Oku et al., 2014).

5 CELL LINES USED TO STUDY THE ANTI COLORECTAL CANCER PROPERTY OF COMPOUNDS

Our study reveals that a diverse range of cell lines have been employed to assess the anti CRC properties of compounds isolated from actinobacteria which are summarized in **Chart 4**. While each of them can be classified into one of four categories of CMS based on their molecular, genetic and other characteristics

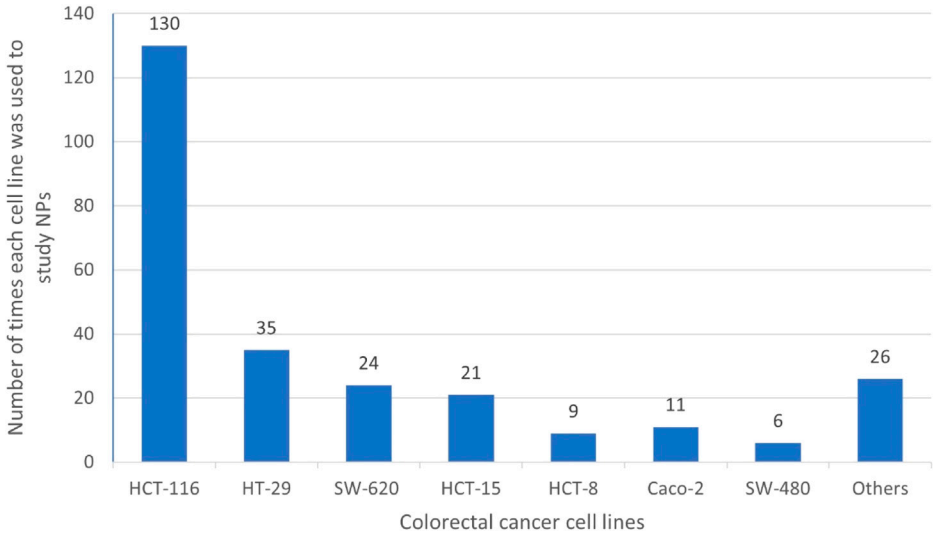

CHART 4 | Frequency of CRC cell lines used to evaluate the effectiveness of various natural compounds from actinobacteria.

and have their own importance. The most common cell lines, been used to study anti CRC of actinobacterial compounds are, HCT-116, followed by the HT-29 with much lower frequency as compared with the former one. These cell lines possess some of the main features of different types of CRC. The selection of proper cancer cell lines can greatly influence the output of a biological experiment. Useful information can be obtained by selecting the appropriate cell line to perform baseline studies on newly identified compounds. For example, HCT-116 cell line based on its characteristics can be classified as CMS4, which is a mesenchymal CRC with the ability of tissue invasion and angiogenesis, whereas the HT-29 cell line is classified as CMS3, a class that includes epithelial cells with metabolic disorders (Berg et al., 2017). HCT-116 cell line has an MSI status and among its important genes, KRAS and PIK3CA are mutated, while HT-29 has an MSS status and BRAF, PIK3CA and TP53 genes are mutated in this cell line (Ahmed et al., 2013). The presence of such molecular differences in cell lines is representative of clinical differences in various types of CRC and also results in differences in response to treatment with different drugs. the utilization of such cell lines in baseline studies has paved the way for future studies in the clinical phase.

6 FDA-APPROVED DRUGS OF ACTINOBACTERIA ORIGIN AFFECTING COLORECTAL CANCER

Mitomycin C is a natural compound isolated from *Streptomyces caespitosus* in 1950. This compound has attracted the attention of scientists by demonstrating selective inhibition of DNA synthesis, mutagenesis, recombination stimulation, chromosome breakdown, DNA crosslinking, etc. as an antibiotic-antitumor. Since then, many studies have been performed to reveal how the cell cycle stop and induces apoptosis by this compound in cancer cells (Tomasz, 1995). Among many studies conducted, it is notable to mention the effect of combination therapy of using mitomycin C and irinotecan in the treatment of CRC, which provides very good results with high tolerance (Ducreux et al., 1998). Mitomycin is currently used as an approved drug in the treatment of various neoplasms, including neoplasms of the breast, bladder, gastrointestinal tract such as colon carcinoma, etc., and even in glaucoma surgery (PubChem, 2004a).

Doxorubicin (DXR), also called adriamycin, is an Anthracyclines compound produced by *Streptomyces peucetius* ATCC 27952, and has reported to have the inhibitory properties on DNA topoisomerase II. This approved drug has anti-cancer effects against various cancers, including thyroid, breast, lung and ovarian cancers, and so on (PubChem, 2004b). Although, in the case of CRC, sometimes the situation is different due to factors such as hereditary resistance to anthracyclines. For example, a study showed that treatment of HT-29 and SW480 cells with aldose reductase (AR) inhibitors such as fidarestat is increased the effect of this drug on cancer cells (Sonowal et al., 2017).

Paclitaxel is a chemotherapy drug that is consumed to treat various solid tumors such as breast, ovary, prostate, lung, etc. In the case of the HT-29-D4 colon cancer cell line, a 2000 study reported that the compound induces apoptosis and activates caspase-8, which is not CD95/CD95-L-dependent (Gonçalves et al., 2000; Trzoss et al., 2014). In 2000, the drug was derived from the endophytic actinomycete *Kitasatospora* sp, isolated from *Taxus baccata* (Caruso et al., 2000; PubChem, 2004c).

Sirolimus (Rapamycin) **(224)** is a compound first isolated from soil *Streptomyces hygroscopicus*. Due to its inhibitory effect on the mTOR pathway, this compound and its derivatives can treat a wide range of diseases such as diabetes, tuberous sclerosis, neurodegenerative and others. Among the therapeutic effects of this compound, anti-CRC properties have also been reported (Li et al., 2014; Mussin et al., 2017).

Everolimus (Afinitor; Novartis) is a derivative of abovementioned compound that has received FDA approval for the treatment of kidney and pancreatic cancers. The use of Everolimus, in combination with compounds such as bevacizumab and mFOLFOX-6 as combination therapy to treat metastatic colorectal cancer, has had significant effects which is in the clinical trial phase (Atkins et al., 2009; Weldon Gilcrease et al., 2019).

7 DISCUSSION

CRC is a common, deadly and heterogeneous disease that kills nearly 900,000 people worldwide each year (Sung et al., 2021). The need for targeted, personalized therapies, as well as those with fewer side effects, has led researchers to constantly look for effective drugs for this disease in various sources, of which natural actinobacterial products have been no exception in recent decades. To the best of our knowledge this is the first study on natural compounds having anti CRC properties from actinobacteria. In reviewing the studies of few past decades on natural actinobacterial products, affecting CRC, our findings revealed the structure of 232 NPs with the properties against CRC cell lines, which are produced by over 119 strains of actinobacteria, the majority of them having a chemical structure of quinones, lactones, alkaloids, and peptides (**Chart 3**). Over 76% of compounds are produced by *streptomyces* strain exclusively. Marine actinobacteria are predominant producers of the anti-colorectal cancer compounds (79.02%), following by terrestrial and endophytic strains counting for 11.16 and 2.68%, respectively. The rest of compounds (7.14%) have been produced by strains living in unconventional environments, synthetic strains (**Chart 1**). Although more attention has been paid to marine actinobacteria in this review, this significant number of compounds, shows the great importance of marine actinobacteria in the field of bioactive products. Even though, the relatively small number of compounds presented here was from the terrestrial ecosystem does not mean to negate the extraordinary importance of soil actinobacteria.

As expected, most of the NPs reported in this review are produced by *Streptomyces* (76.29%), as they constitute the largest genus of actinobacteria. *Micromonospora* and *Salinispora*, both members of the family *Micromonosporaceae*, and *Actinomadura*, with production of 9.91%, 3.02% and 3.02% of anti-CRC compounds, respectively, appear to be other important genera in this field.

The compounds show enormous biological activities, from autophagy, angiogenesis, invasion, migration, apoptosis, to a range of cytotoxicity, some in terms of values comparable to conventional drug compounds to very strong levels of toxicity (with IC_{50} values in ng scale). Even though the mechanism of action of most compounds was not addressed and determined by abundant of published papers, it is notable that these compounds are able to exert their antitumor properties and toxicity through various pathways. Therefore, the biological process and mechanism of actions of compounds involved in the anti-cancer effects is needed to be investigated further. In addition, further studies in this field can reveal the secret of the protective effects of actinobacteria associated with gut and colorectal cancer more clearly. The knowledge of how gut actinobacteria along with lifestyle and microenvironment factors can interfere with the development of CRC at early stage is pivotal to design biomarkers for CRC.

Despite the advances in compound discovery and structure elucidation, our knowledge on structure activities relationship is still limited. Therefore, mining of structure activity relationship is another field, which requires further exploration. In addition, the molecular docking studies might indicate the role of halogen bonding in complexes and uncover the secret of structure activities relationship.

Another point to note is the use of diverse CRC cell lines in previous studies, while in most of them, the reason for selecting each cell line was not specified. It is also clear that the frequency of use of these cell lines is very unequal. Based on the present evidence, the anti-CRC effect of natural actinobacterial compounds, less attention has been paid to the two groups CMS1 and CMS2 and their associated cell lines. In other words, although most of these researches are preliminary studies of the cytotoxic and antitumor effects of natural compounds, it is worth to use cell lines belonging to two or more different CMSs simultaneously, in order to consider the heterogeneity of this cancer and to comprehensively investigate the antitumor effects of a compound.

AUTHOR CONTRIBUTIONS

YB conceived and designed the research. SB and YB wrote the draft of manuscript. SB and EK collected the data and analyzed data. YB and MT supervised the project. YB proofread, revised and approved the manuscript. All authors reviewed the manuscript.

ACKNOWLEDGMENTS

The authors acknowledge funding from the vice-chancellor for the research and technology of KUMS.

SUPPLEMENTARY MATERIAL

The Supplementary Material for this article can be found online at: https://www.frontiersin.org/articles/10.3389/fphar.2022.929161/full#supplementary-material

REFERENCES

Abedinlou, H., Bahrami, Y., Mohammadi, S., and Kakaei, E. (2022). Rare Actinobacteria and Their Potential Biotechnological Applications. *Sci. J. Kurdistan Univ. Med. Sci.* 26 (7), 108–131.

Ahmed, D., Eide, P. W., Eilertsen, I. A., Danielsen, S. A., Eknæs, M., Hektoen, M., et al. (2013). Epigenetic and Genetic Features of 24 Colon Cancer Cell Lines. *Oncogenesis* 2 (9), e71. doi:10.1038/oncsis.2013.35

Ahn, K. S., Sethi, G., Chao, T. H., Neuteboom, S. T., Chaturvedi, M. M., Palladino, M. A., et al. (2007). Salinosporamide A (NPI-0052) Potentiates Apoptosis, Suppresses Osteoclastogenesis, and Inhibits Invasion through Down-Modulation of NF-kappaB Regulated Gene Products. *Blood* 110 (7), 2286–2295. doi:10.1182/blood-2007-04-084996

Almeida, L. C., Bauermeister, A., Rezende-Teixeira, P., Santos, E. A. D., Moraes, L. A. B., Machado-Neto, J. A., et al. (2019). Pradimicin-IRD Exhibits Antineoplastic Effects by Inducing DNA Damage in Colon Cancer Cells. *Biochem. Pharmacol.* 168, 38–47. doi:10.1016/j.bcp.2019.06.016

Alvarez-Mico, X., Jensen, P. R., Fenical, W., and Hughes, C. C. (2013). Chlorizidine, a Cytotoxic 5H-Pyrrolo[2,1-A]isoindol-5-One-Containing Alkaloid from a Marine *Streptomyces* Sp. *Org. Lett.* 15 (5), 988–991. doi:10.1021/ol303374e

Amoorahim, M., Valipour, E., Hoseinkhani, Z., Mahnam, A., Rezazadeh, D., Ansari, M., et al. (2020). TSGA10 Overexpression Inhibits Angiogenesis of HUVECs: A HIF-2α Biased Perspective. *Microvasc. Res.* 128, 103952. doi:10.1016/j.mvr.2019.103952

Arcamone, F., Cassinelli, G., Fantini, G., Grein, A., Orezzi, P., Pol, C., et al. (1969). Adriamycin, 14-hydroxydaunomycin, a New Antitumor Antibiotic from *S. Peucetius Var. Caesius*. *Biotechnol. Bioeng.* 11 (6), 1101–1110. doi:10.1002/bit.260110607

Arnold, M., Sierra, M. S., Laversanne, M., Soerjomataram, I., Jemal, A., and Bray, F. (2017). Global Patterns and Trends in Colorectal Cancer Incidence and Mortality. *Gut* 66 (4), 683–691. doi:10.1136/gutjnl-2015-310912

Asche, C. (2005). Antitumour Quinones. *Mini Rev. Med. Chem.* 5 (5), 449–467. doi:10.2174/1389557053765556

Asolkar, R. N., Freel, K. C., Jensen, P. R., Fenical, W., Kondratyuk, T. P., Park, E. J., et al. (2009). Arenamides A-C, Cytotoxic NFkappaB Inhibitors from the Marine Actinomycete *Salinispora Arenicola*. *J. Nat. Prod.* 72 (3), 396–402. doi:10.1021/np800617a

Asolkar, R. N., Jensen, P. R., Kauffman, C. A., and Fenical, W. (2006). Daryamides A-C, Weakly Cytotoxic Polyketides from a Marine-Derived Actinomycete of the Genus *Streptomyces* Strain CNQ-085. *J. Nat. Prod.* 69 (12), 1756–1759. doi:10.1021/np0603828

Asolkar, R. N., Kirkland, T. N., Jensen, P. R., and Fenical, W. (2010). Arenimycin, an Antibiotic Effective against Rifampin- and Methicillin-Resistant *Staphylococcus aureus* from the Marine Actinomycete *Salinispora Arenicola*. *J. Antibiot. (Tokyo)* 63 (1), 37–39. doi:10.1038/ja.2009.114

Asolkar, R. N., Singh, A., Jensen, P. R., Aalbersberg, W., Carté, B. K., Feussner, K. D., et al. (2017). Marinocyanins, Cytotoxic Bromo-Phenazinone Meroterpenoids from a Marine Bacterium from the *Streptomycete* Clade MAR4. *Tetrahedron* 73 (16), 2234–2241. doi:10.1016/j.tet.2017.03.003

Atkins, M. B., Yasothan, U., and Kirkpatrick, P. (2009). Everolimus. *Nat. Rev. Drug Discov.* 8 (7), 535–536. doi:10.1038/nrd2924

Auyeung, K. K., and Ko, J. K. (2017). Angiogenesis and Oxidative Stress in Metastatic Tumor Progression: Pathogenesis and Novel Therapeutic Approach of Colon Cancer. *Curr. Pharm. Des.* 23 (27), 3952–3961. doi:10.2174/1381612823666170228124105

Bach, D. H., Kim, S. H., Hong, J. Y., Park, H. J., Oh, D. C., and Lee, S. K. (2015). Salternamide A Suppresses Hypoxia-Induced Accumulation of HIF-1α and Induces Apoptosis in Human Colorectal Cancer Cells. *Mar. Drugs* 13 (11), 6962–6976. doi:10.3390/md13116962

Bahrami, Y., Delbari, Y., Buzhani, K. R., Kakaei, E., Mohassel, Y., Bouk, S., et al. (2022). "Endophytic Actinobacteria in Biosynthesis of Bioactive Metabolites and Their Application in Improving Crop Yield and Sustainable Agriculture," in *Natural Products from Actinomycetes: Diversity, Ecology and Drug Discovery*. Editors R.V. Rai, and J.A. Bai (Singapore: Springer Singapore), 119–150. doi:10.1007/978-981-16-6132-7_5

Bailly, C. (2019). Irinotecan: 25 Years of Cancer Treatment. *Pharmacol. Res.* 148, 104398. doi:10.1016/j.phrs.2019.104398

Barka, E. A., Vatsa, P., Sanchez, L., Gaveau-Vaillant, N., Jacquard, C., Meier-Kolthoff, J. P., et al. (2016). Taxonomy, Physiology, and Natural Products of Actinobacteria. *Microbiol. Mol. Biol. Rev.* 80 (1), 1–43. doi:10.1128/mmbr.00019-15

Baudino, T. A. (2015). Targeted Cancer Therapy: The Next Generation of Cancer Treatment. *Curr. Drug Discov. Technol.* 12 (1), 3–20. doi:10.2174/1570163812666150602144310

Bauermeister, A., Calil, F. A., das C L Pinto, F., Medeiros, T. C. T., Almeida, L. C., Silva, L. J., et al. (2019). Pradimicin-IRD from *Amycolatopsis* Sp. IRD-009 and its Antimicrobial and Cytotoxic Activities. *Nat. Prod. Res.* 33 (12), 1713–1720. doi:10.1080/14786419.2018.1434639

Berg, K. C. G., Eide, P. W., Eilertsen, I. A., Johannessen, B., Bruun, J., Danielsen, S. A., et al. (2017). Multi-omics of 34 Colorectal Cancer Cell Lines - a Resource for Biomedical Studies. *Mol. Cancer* 16 (1), 116. doi:10.1186/s12943-017-0691-y

Bernardi, D. I., das Chagas, F. O., Monteiro, A. F., dos Santos, G. F., and de Souza Berlinck, R. G. (2019). "Secondary Metabolites of Endophytic Actinomycetes: Isolation, Synthesis, Biosynthesis, and Biological Activities," in *Progress in the Chemistry of Organic Natural Products 108*. Editors A.D. Kinghorn, H. Falk, S. Gibbons, J.i. Kobayashi, Y. Asakawa, and J.-K. Liu (Cham: Springer International Publishing) . doi:10.1007/978-3-030-01099-7_3

Boonlarppradab, C., Kauffman, C. A., Jensen, P. R., and Fenical, W. (2008). Marineosins A and B, Cytotoxic Spiroaminals from a Marine-Derived Actinomycete. *Org. Lett.* 10 (24), 5505–5508. doi:10.1021/ol8020644

Bull, A. T., Stach, J. E., Ward, A. C., and Goodfellow, M. (2005). Marine Actinobacteria: Perspectives, Challenges, Future Directions. *Ant. Van Leeuwenhoek* 87 (1), 65–79. doi:10.1007/s10482-004-6562-8

Byun, W. S., Kim, S., Shin, Y. H., Kim, W. K., Oh, D. C., and Lee, S. K. (2020). Antitumor Activity of Ohmyungsamycin A through the Regulation of the Skp2-P27 Axis and MCM4 in Human Colorectal Cancer Cells. *J. Nat. Prod.* 83 (1), 118–126. doi:10.1021/acs.jnatprod.9b00918

Cañedo, L. M., Puentes, J. L. F., Baz, J. P., Huang, X.-H., and Rinehart, K. L. (2000). IB-96212, a Novel Cytotoxic Macrolide Produced by a Marine *Micromonospora*. II. Physico-Chemical Properties and Structure Determination. *J. Antibiot.* 53 (5), 479–483. doi:10.7164/antibiotics.53.479

Caruso, M., Colombo, A., Fedeli, L., Pavesi, A., Quaroni, S., Saracchi, M., et al. (2000). Isolation of Endophytic Fungi and Actinomycetes Taxane Producers. *Ann. Microbiol.* 50 (1), 3–14.

Chen, C., Ye, Y., Wang, R., Zhang, Y., Wu, C., Debnath, S. C., et al. (2018a). *Streptomyces Nigra Sp. Nov.* Is a Novel Actinobacterium Isolated from Mangrove Soil and Exerts a Potent Antitumor Activity *In Vitro*. *Front. Microbiol.* 9, 1587. doi:10.3389/fmicb.2018.01587

Chen, L., Zhao, W., Jiang, H.-L., Zhou, J., Chen, X.-M., Lian, Y.-Y., et al. (2018b). Rakicidins G - I, Cyclic Depsipeptides from Marine *Micromonospora Chalcea* FIM 02-523. *Tetrahedron* 74 (30), 4151–4154. doi:10.1016/j.tet.2018.06.039

Cheng, C., Othman, E. M., Stopper, H., Edrada-Ebel, R., Hentschel, U., and Abdelmohsen, U. R. (2017). Isolation of Petrocidin A, a New Cytotoxic Cyclic Dipeptide from the Marine Sponge-Derived Bacterium Streptomyces Sp. SBT348. *Mar. Drugs* 15 (12), 383. doi:10.3390/md15120383

Cheng, Y. B., Jensen, P. R., and Fenical, W. (2013). Cytotoxic and Antimicrobial Napyradiomycins from Two Marine-Derived, MAR 4 *Streptomyces* Strains. *Eur. J. Org. Chem.* 2013 (18), 3751–3757. doi:10.1002/ejoc.201300349

Cho, J. Y., Williams, P. G., Kwon, H. C., Jensen, P. R., and Fenical, W. (2007). Lucentamycins A-D, Cytotoxic Peptides from the Marine-Derived Actinomycete *Nocardiopsis Lucentensis*. *J. Nat. Prod.* 70 (8), 1321–1328. doi:10.1021/np070101b

Choi, B. K., Lee, H. S., Kang, J. S., and Shin, H. J. (2019). Dokdolipids A-C, Hydroxylated Rhamnolipids from the Marine-Derived Actinomycete *Actinoalloteichus Hymeniacidonis*. *Mar. Drugs* 17 (4), 237. doi:10.3390/md17040237

Conti, R., Chagas, F. O., Caraballo-Rodriguez, A. M., Melo, W. G., do Nascimento, A. M., Cavalcanti, B. C., et al. (2016). Endophytic Actinobacteria from the Brazilian Medicinal Plant *Lychnophora Ericoides Mart*. And the Biological Potential of Their Secondary Metabolites. *Chem. Biodivers.* 13 (6), 727–736. doi:10.1002/cbdv.201500225

Cui, C. B., Liu, H. B., Gu, J. Y., Gu, Q. Q., Cai, B., Zhang, D. Y., et al. (2007). Echinosporins as New Cell Cycle Inhibitors and Apoptosis Inducers from

Marine-Derived *Streptomyces Albogriseolus*. *Fitoterapia* 78 (3), 238–240. doi:10.1016/j.fitote.2006.11.017

Cusack, J. C., Jr., Liu, R., Xia, L., Chao, T. H., Pien, C., Niu, W., et al. (2006). NPI-0052 Enhances Tumoricidal Response to Conventional Cancer Therapy in a Colon Cancer Model. *Clin. Cancer Res.* 12 (22), 6758–6764. doi:10.1158/1078-0432.Ccr-06-1151

de Gramont, A., Figer, A., Seymour, M., Homerin, M., Hmissi, A., Cassidy, J., et al. (2000). Leucovorin and Fluorouracil with or without Oxaliplatin as First-Line Treatment in Advanced Colorectal Cancer. *J. Clin. Oncol.* 18 (16), 2938–2947. doi:10.1200/jco.2000.18.16.2938

Delbari, Y., Mohassel, Y., Bahrami, Y., Kakaie, E., and Mostafaie, A. (2020). A Review on Isolation and Identification of Endophytic Actinobacteria, Their Chemical Structure, Bioactive Compounds, and Potential Medical-Pharmaceutical Applications. *J J. Mazandaran Univ. Med. Sci.* 30 (186), 195–217.

Deng, L. J., Qi, M., Li, N., Lei, Y. H., Zhang, D. M., and Chen, J. X. (2020). Natural Products and Their Derivatives: Promising Modulators of Tumor Immunotherapy. *J. Leukoc. Biol.* 108 (2), 493–508. doi:10.1002/JLB.3MR0320-444R

Di Paolo, A., Danesi, R., Nardini, D., Bocci, G., Innocenti, F., Fogli, S., et al. (2000). Manumycin Inhibits Ras Signal Transduction Pathway and Induces Apoptosis in COLO320-DM Human Colon Tumour Cells. *Br. J. Cancer* 82 (4), 905–912. doi:10.1054/bjoc.1999.1018

Dinesh, R., Srinivasan, V., T E, S., Anandaraj, M., and Srambikkal, H. (2017). Endophytic Actinobacteria: Diversity, Secondary Metabolism and Mechanisms to Unsilence Biosynthetic Gene Clusters. *Crit. Rev. Microbiol.* 43 (5), 546–566. doi:10.1080/1040841x.2016.1270895

Ding, L., Ndejouong, Ble. S., Maier, A., Fiebig, H. H., and Hertweck, C. (2012). Elaiomycins D-F, Antimicrobial and Cytotoxic Azoxides from *Streptomyces* Sp. Strain HKI0708. *J. Nat. Prod.* 75 (10), 1729–1734. doi:10.1021/np300329m

Ding, L., Pfoh, R., Rühl, S., Qin, S., and Laatsch, H. (2009). T-muurolol Sesquiterpenes from the Marine *Streptomyces* Sp. M491 and Revision of the Configuration of Previously Reported Amorphanes. *J. Nat. Prod.* 72 (1), 99–101. doi:10.1021/np8006843

Ding, N., Jiang, Y., Han, L., Chen, X., Ma, J., Qu, X., et al. (2016). Bafilomycins and Odoriferous Sesquiterpenoids from *Streptomyces Albolongus* Isolated from elephas Maximus Feces. *J. Nat. Prod.* 79 (4), 799–805. doi:10.1021/acs.jnatprod.5b00827

Doi, K., Li, R., Sung, S. S., Wu, H., Liu, Y., Manieri, W., et al. (2012). Discovery of Marinopyrrole A (Maritoclax) as a Selective Mcl-1 Antagonist that Overcomes ABT-737 Resistance by Binding to and Targeting Mcl-1 for Proteasomal Degradation. *J. Biol. Chem.* 287 (13), 10224–10235. doi:10.1074/jbc.M111.334532

Dong, M., Cao, P., Ma, Y. T., Luo, J., Yan, Y., Li, R. T., et al. (2019). A New Actinomycin Z Analogue with an Additional Oxygen Bridge between Chromophore and β-depsipentapeptide from Streptomyces Sp. KIB-H714. *Nat. Prod. Res.* 33 (2), 219–225. doi:10.1080/14786419.2018.1443097

Ducreux, M., Gil-Delgado, M., André, T., Ychou, M., de Gramond, A., and Khayat, D. (1998). Irinotecan in Combination for Colon Cancer. *Bull. Cancer* Spec No, 43–46.

Duncan, K. R., Crüsemann, M., Lechner, A., Sarkar, A., Li, J., Ziemert, N., et al. (2015). Molecular Networking and Pattern-Based Genome Mining Improves Discovery of Biosynthetic Gene Clusters and Their Products from *Salinispora* Species. *Chem. Biol.* 22 (4), 460–471. doi:10.1016/j.chembiol.2015.03.010

El-Hawary, S. S., Sayed, A. M., Mohammed, R., Khanfar, M. A., Rateb, M. E., Mohammed, T. A., et al. (2018). New Pim-1 Kinase Inhibitor from the Co-culture of Two Sponge-Associated Actinomycetes. *Front. Chem.* 6, 538. doi:10.3389/fchem.2018.00538

Elmallah, M. I. Y., Cogo, S., Constantinescu, A. A., Elifio-Esposito, S., Abdelfattah, M. S., and Micheau, O. (2020). Marine Actinomycetes-Derived Secondary Metabolites Overcome TRAIL-Resistance via the Intrinsic Pathway through Downregulation of Survivin and XIAP. *Cells* 9 (8), 1760. doi:10.3390/cells9081760

Erba, E., Bergamaschi, D., Ronzoni, S., Faretta, M., Taverna, S., Bonfanti, M., et al. (1999). Mode of Action of Thiocoraline, a Natural Marine Compound with Anti-tumour Activity. *Br. J. Cancer* 80 (7), 971–980. doi:10.1038/sj.bjc.6690451

Esvan, Y. J., Giraud, F., Pereira, E., Suchaud, V., Nauton, L., Théry, V., et al. (2016). Synthesis and Biological Activity of Pyrazole Analogues of the Staurosporine Aglycon K252c. *Bioorg Med. Chem.* 24 (14), 3116–3124. doi:10.1016/j.bmc.2016.05.032

Farnaes, L., Coufal, N. G., Kauffman, C. A., Rheingold, A. L., DiPasquale, A. G., Jensen, P. R., et al. (2014). Napyradiomycin Derivatives, Produced by a Marine-Derived Actinomycete, Illustrate Cytotoxicity by Induction of Apoptosis. *J. Nat. Prod.* 77 (1), 15–21. doi:10.1021/np400466j

Fearon, E. R., and Vogelstein, B. (1990). A Genetic Model for Colorectal Tumorigenesis. *Cell.* 61 (5), 759–767. doi:10.1016/0092-8674(90)90186-i

Fei, P., Chuan-Xi, W., Yang, X., Hong-Lei, J., Lu-Jie, C., Uribe, P., et al. (2013). A New 20-membered Macrolide Produced by a Marine-Derived *Micromonospora* Strain. *Nat. Prod. Res.* 27 (15), 1366–1371. doi:10.1080/14786419.2012.740038

Feling, R. H., Buchanan, G. O., Mincer, T. J., Kauffman, C. A., Jensen, P. R., and Fenical, W. (2003). Salinosporamide A: a Highly Cytotoxic Proteasome Inhibitor from a Novel Microbial Source, a Marine Bacterium of the New Genus *Salinospora*. *Angew. Chem. Int. Ed. Engl.* 42 (3), 355–357. doi:10.1002/anie.200390115

Fernández-chimeno, R. I., Cañedo, L., Espliego, F., Grávalos, D., Calle, F. D. L., Fernández-puentes, J. L., et al. (2000). IB-96212, a Novel Cytotoxic Macrolide Produced by a Marine *Micromonospora*. I. Taxonomy, Fermentation, Isolation and Biological Activities. *J. Antibiot.* 53 (5), 474–478. doi:10.7164/antibiotics.53.474

Fu, P., Zhu, Y., Mei, X., Wang, Y., Jia, H., Zhang, C., et al. (2014). Acyclic Congeners from *Actinoalloteichus Cyanogriseus* Provide Insights into Cyclic Bipyridine Glycoside Formation. *Org. Lett.* 16 (16), 4264–4267. doi:10.1021/ol5019757

Furumai, T., Igarashi, Y., Higuchi, H., Saito, N., and Oki, T. (2002). Kosinostatin, a Quinocycline Antibiotic with Antitumor Activity from *Micromonospora* Sp. TP-A0468. *J. Antibiot. (Tokyo)* 55 (2), 128–133. doi:10.7164/antibiotics.55.128

Furumai, T., Takagi, K., Igarashi, Y., Saito, N., and Oki, T. (2000). Arisostatins A and B, New Members of Tetrocarcin Class of Antibiotics from *Micromonospora* Sp. TP-A0316. I. Taxonomy, Fermentation, Isolation and Biological Properties. *J. Antibiot. (Tokyo)* 53 (3), 227–232. doi:10.7164/antibiotics.53.227

Gao, R., Kong, C., Huang, L., Li, H., Qu, X., Liu, Z., et al. (2017). Mucosa-associated Microbiota Signature in Colorectal Cancer. *Eur. J. Clin. Microbiol. Infect. Dis.* 36 (11), 2073–2083. doi:10.1007/s10096-017-3026-4

Gao, X., Lu, Y., Xing, Y., Ma, Y., Lu, J., Bao, W., et al. (2012). A Novel Anticancer and Antifungus Phenazine Derivative from a Marine Actinomycete BM-17. *Microbiol. Res.* 167 (10), 616–622. doi:10.1016/j.micres.2012.02.008

Gonçalves, A., Braguer, D., Carles, G., André, N., Prevôt, C., and Briand, C. (2000). Caspase-8 Activation Independent of CD95/CD95-L Interaction during Paclitaxel-Induced Apoptosis in Human Colon Cancer Cells (HT29-D4). *Biochem. Pharmacol.* 60 (11), 1579–1584. doi:10.1016/s0006-2952(00)00481-0

Gui, C., Yuan, J., Mo, X., Huang, H., Zhang, S., Gu, Y. C., et al. (2018). Cytotoxic Anthracycline Metabolites from a Recombinant *Streptomyces*. *J. Nat. Prod.* 81 (5), 1278–1289. doi:10.1021/acs.jnatprod.8b00212

Guillaumot, M. A., Cerles, O., Bertrand, H. C., Benoit, E., Nicco, C., Chouzenoux, S., et al. (2019). Oxaliplatin-induced Neuropathy: the Preventive Effect of a New Super-oxide Dismutase Modulator. *Oncotarget* 10 (60), 6418–6431. doi:10.18632/oncotarget.27248

Guinney, J., Dienstmann, R., Wang, X., de Reyniès, A., Schlicker, A., Soneson, C., et al. (2015). The Consensus Molecular Subtypes of Colorectal Cancer. *Nat. Med.* 21 (11), 1350–1356. doi:10.1038/nm.3967

Gulder, T. A., and Moore, B. S. (2010). Salinosporamide Natural Products: Potent 20 S Proteasome Inhibitors as Promising Cancer Chemotherapeutics. *Angew. Chem. Int. Ed. Engl.* 49 (49), 9346–9367. doi:10.1002/anie.201000728

Hale, V. L., Chen, J., Johnson, S., Harrington, S. C., Yab, T. C., Smyrk, T. C., et al. (2017). Shifts in the Fecal Microbiota Associated with Adenomatous Polyps. *Cancer Epidemiol. Biomarkers Prev.* 26 (1), 85–94. doi:10.1158/1055-9965.Epi-16-0337

Hara, M., Akasaka, K., Akinaga, S., Okabe, M., Nakano, H., Gomez, R., et al. (1993). Identification of Ras Farnesyltransferase Inhibitors by Microbial Screening. *Proc. Natl. Acad. Sci. U. S. A.* 90 (6), 2281–2285. doi:10.1073/pnas.90.6.2281

Hardt, I. H., Jensen, P. R., and Fenical, W. (2000). Neomarinone, and New Cytotoxic Marinone Derivatives, Produced by a Marine Filamentous Bacterium (Actinomycetales). *Tetrahedron Lett.* 41 (13), 2073–2076. doi:10.1016/s0040-4039(00)00117-9

Hayakawa, Y., Shirasaki, S., Kawasaki, T., Matsuo, Y., Adachi, K., and Shizuri, Y. (2007a). Structures of New Cytotoxic Antibiotics, Piericidins C7 and C8. *J. Antibiot. (Tokyo)* 60 (3), 201–203. doi:10.1038/ja.2007.23

Hayakawa, Y., Shirasaki, S., Shiba, S., Kawasaki, T., Matsuo, Y., Adachi, K., et al. (2007b). Piericidins C7 and C8, New Cytotoxic Antibiotics Produced by a Marine *Streptomyces* Sp. *J. Antibiot. (Tokyo)* 60 (3), 196–200. doi:10.1038/ja.2007.22

He, H., Ding, W. D., Bernan, V. S., Richardson, A. D., Ireland, C. M., Greenstein, M., et al. (2001). Lomaiviticins A and B, Potent Antitumor Antibiotics from *Micromonospora Lomaivitiensis*. *J. Am. Chem. Soc.* 123 (22), 5362–5363. doi:10.1021/ja010129o

Hernández, L. M., Blanco, J. A., Baz, J. P., Puentes, J. L., Millán, F. R., Vázquez, F. E., et al. (2000). 4'-N-methyl-5'-hydroxystaurosporine and 5'-hydroxystaurosporine, New Indolocarbazole Alkaloids from a Marine *Micromonospora* Sp. Strain. *J. Antibiot. (Tokyo)* 53 (9), 895–902. doi:10.7164/antibiotics.53.895

Hu, X., Sun, W., Li, S., Li, L., Yu, L., Liu, H., et al. (2020). Cervinomycins C1-4 with Cytotoxic and Antibacterial Activity from Streptomyces Sp. CPCC 204980. *J. Antibiot. (Tokyo)* 73 (12), 812–817. doi:10.1038/s41429-020-0342-1

Huang, X. M., Yang, Z. J., Xie, Q., Zhang, Z. K., Zhang, H., and Ma, J. Y. (2019). Natural Products for Treating Colorectal Cancer: A Mechanistic Review. *Biomed. Pharmacother.* 117, 109142. doi:10.1016/j.biopha.2019.109142

Hughes, C. C., MacMillan, J. B., Gaudêncio, S. P., Fenical, W., and La Clair, J. J. (2009a). Ammosamides A and B Target Myosin. *Angew. Chem. Int. Ed. Engl.* 48 (4), 728–732. doi:10.1002/anie.200804107

Hughes, C. C., MacMillan, J. B., Gaudêncio, S. P., Jensen, P. R., and Fenical, W. (2009b). The Ammosamides: Structures of Cell Cycle Modulators from a Marine-Derived *Streptomyces* Species. *Angew. Chem. Int. Ed. Engl.* 48 (4), 725–727. doi:10.1002/anie.200804890

Hughes, C. C., Prieto-Davo, A., Jensen, P. R., and Fenical, W. (2008). The Marinopyrroles, Antibiotics of an Unprecedented Structure Class from a Marine *Streptomyces* Sp. *Org. Lett.* 10 (4), 629–631. doi:10.1021/ol702952n

Hwang, J. H., Kim, J. Y., Cha, M. R., Ryoo, I. J., Choo, S. J., Cho, S. M., et al. (2008). Etoposide-resistant HT-29 Human Colon Carcinoma Cells during Glucose Deprivation Are Sensitive to Piericidin A, a GRP78 Down-Regulator. *J. Cell. Physiol.* 215 (1), 243–250. doi:10.1002/jcp.21308

Igarashi, Y., Matsuoka, N., In, Y., In, T., Tashiro, E., Saiki, I., et al. (2017). Nonthmicin, a Polyether Polyketide Bearing a Halogen-Modified Tetronate with Neuroprotective and Antiinvasive Activity from *Actinomadura* Sp. *Org. Lett.* 19 (6), 1406–1409. doi:10.1021/acs.orglett.7b00318

Igarashi, Y., Trujillo, M. E., Martínez-Molina, E., Yanase, S., Miyanaga, S., Obata, T., et al. (2007). Antitumor Anthraquinones from an Endophytic Actinomycete *Micromonospora Lupini* Sp. Nov. *Bioorg Med. Chem. Lett.* 17 (13), 3702–3705. doi:10.1016/j.bmcl.2007.04.039

Itoh, T., Kinoshita, M., Aoki, S., and Kobayashi, M. (2003). Komodoquinone A, a Novel Neuritogenic Anthracycline, from Marine *Streptomyces* Sp. KS3. *J. Nat. Prod.* 66 (10), 1373–1377. doi:10.1021/np030212k

Jensen, P. R., Williams, P. G., Oh, D. C., Zeigler, L., and Fenical, W. (2007). Species-specific Secondary Metabolite Production in Marine Actinomycetes of the Genus *Salinispora*. *Appl. Environ. Microbiol.* 73 (4), 1146–1152. doi:10.1128/aem.01891-06

Jeong, S. Y., Shin, H. J., Kim, T. S., Lee, H. S., Park, S. K., and Kim, H. M. (2006). Streptokordin, a New Cytotoxic Compound of the Methylpyridine Class from a Marine-Derived *Streptomyces* Sp. KORDI-3238. *J. Antibiot. (Tokyo)* 59 (4), 234–240. doi:10.1038/ja.2006.33

Jiang, Y. J., Li, J. Q., Zhang, H. J., Ding, W. J., and Ma, Z. J. (2018a). Cyclizidine-type Alkaloids from *Streptomyces* Sp. HNA39. *J. Nat. Prod.* 81 (2), 394–399. doi:10.1021/acs.jnatprod.7b01055

Jiang, Y. J., Zhang, D. S., Zhang, H. J., Li, J. Q., Ding, W. J., Xu, C. D., et al. (2018b). Medermycin-type Naphthoquinones from the Marine-Derived *Streptomyces* Sp. XMA39. *J. Nat. Prod.* 81 (9), 2120–2124. doi:10.1021/acs.jnatprod.8b00544

Jiang, Z. K., Guo, L., Chen, C., Liu, S. W., Zhang, L., Dai, S. J., et al. (2015). Xiakemycin A, a Novel Pyranonaphthoquinone Antibiotic, Produced by the *Streptomyces* Sp. CC8-201 from the Soil of a Karst Cave. *J. Antibiot. (Tokyo)* 68 (12), 771–774. doi:10.1038/ja.2015.70

Kalaitzis, J. A., Hamano, Y., Nilsen, G., and Moore, B. S. (2003). Biosynthesis and Structural Revision of Neomarinone. *Org. Lett.* 5 (23), 4449–4452. doi:10.1021/ol035748b

Kasanah, N., and Triyanto, T. (2019). Bioactivities of Halometabolites from Marine Actinobacteria. *Biomolecules* 9 (6), 225. doi:10.3390/biom9060225

Kaweewan, I., Komaki, H., Hemmi, H., Hoshino, K., Hosaka, T., Isokawa, G., et al. (2019). Isolation and Structure Determination of a New Cytotoxic Peptide, Curacozole, from *STREPTOMYCES CURACOI* Based on Genome Mining. *J. Antibiot. (Tokyo)* 72 (1), 1–7. doi:10.1038/s41429-018-0105-4

Khalifa, S. A. M., Elias, N., Farag, M. A., Chen, L., Saeed, A., Hegazy, M. F., et al. (2019). Marine Natural Products: A Source of Novel Anticancer Drugs. *Mar. Drugs* 17 (9), 491. doi:10.3390/md17090491

Khan, N., Yılmaz, S., Aksoy, S., Uzel, A., Tosun, Ç., Kirmizibayrak, P. B., et al. (2019). Polyethers Isolated from the Marine Actinobacterium Streptomyces Cacaoi Inhibit Autophagy and Induce Apoptosis in Cancer Cells. *Chem. Biol. Interact.* 307, 167–178. doi:10.1016/j.cbi.2019.04.035

Kim, S. H., Shin, Y., Lee, S. H., Oh, K. B., Lee, S. K., Shin, J., et al. (2015). Salternamides A-D from a Halophilic *Streptomyces* Sp. Actinobacterium. *J. Nat. Prod.* 78 (4), 836–843. doi:10.1021/acs.jnatprod.5b00002

Kim, Y. H., Shin, H. C., Song, D. W., Lee, S. H., Furumai, T., Park, J. W., et al. (2003). Arisostatins A Induces Apoptosis through the Activation of Caspase-3 and Reactive Oxygen Species Generation in AMC-HN-4 Cells. *Biochem. Biophys. Res. Commun.* 309 (2), 449–456. doi:10.1016/j.bbrc.2003.07.009

Kitani, S., Ueguchi, T., Igarashi, Y., Leetanasaksakul, K., Thamchaipenet, A., and Nihira, T. (2017). Rakicidin F, a New Antibacterial Cyclic Depsipeptide from a Marine Sponge-Derived *Streptomyces* Sp. *J. Antibiot.* 71, 139–141. doi:10.1038/ja.2017.92

Konaklieva, M. I., and Plotkin, B. J. (2005). Lactones: Generic Inhibitors of Enzymes? *Mini Rev. Med. Chem.* 5 (1), 73–95. doi:10.2174/1389557053402828

Kværner, A. S., Birkeland, E., Bucher-Johannessen, C., Vinberg, E., Nordby, J. I., Kangas, H., et al. (2021). The CRCbiome Study: a Large Prospective Cohort Study Examining the Role of Lifestyle and the Gut Microbiome in Colorectal Cancer Screening Participants. *BMC Cancer* 21 (1), 930. doi:10.1186/s12885-021-08640-8

Kwon, H. C., Espindola, A. P., Park, J. S., Prieto-Davó, A., Rose, M., Jensen, P. R., et al. (2010). Nitropyrrolins A-E, Cytotoxic Farnesyl-α-Nitropyrroles from a Marine-Derived Bacterium within the Actinomycete Family Streptomycetaceae. *J. Nat. Prod.* 73 (12), 2047–2052. doi:10.1021/np1006229

Kwon, H. C., Kauffman, C. A., Jensen, P. R., and Fenical, W. (2006). Marinomycins A-D, Antitumor-Antibiotics of a New Structure Class from a Marine Actinomycete of the Recently Discovered Genus "marinispora". *J. Am. Chem. Soc.* 128 (5), 1622–1632. doi:10.1021/ja0558948

Kwon, Y., Kim, S. H., Shin, Y., Bae, M., Kim, B. Y., Lee, S. K., et al. (2014). A New Benzofuran Glycoside and Indole Alkaloids from a Sponge-Associated Rare Actinomycete, *Amycolatopsis* Sp. *Mar. Drugs* 12 (4), 2326–2340. doi:10.3390/md12042326

Lee, J., Gamage, C. D. B., Kim, G. J., Hillman, P. F., Lee, C., Lee, E. Y., et al. (2020). Androsamide, a Cyclic Tetrapeptide from a Marine *Nocardiopsis* sp., Suppresses Motility of Colorectal Cancer Cells. *J. Nat. Prod.* 83 (10), 3166–3172. doi:10.1021/acs.jnatprod.0c00815

Lewin, G. R., Carlos, C., Chevrette, M. G., Horn, H. A., McDonald, B. R., Stankey, R. J., et al. (2016). Evolution and Ecology of Actinobacteria and Their Bioenergy Applications. *Annu. Rev. Microbiol.* 70, 235–254. doi:10.1146/annurev-micro-102215-095748

Li, J., Kim, S. G., and Blenis, J. (2014). Rapamycin: One Drug, Many Effects. *Cell. Metab.* 19 (3), 373–379. doi:10.1016/j.cmet.2014.01.001

Li, W., Yang, X., Yang, Y., Zhao, L., Xu, L., and Ding, Z. (2015). A New Anthracycline from Endophytic *Streptomyces* Sp. YIM66403. *J. Antibiot. (Tokyo)* 68 (3), 216–219. doi:10.1038/ja.2014.128

Li, X. B., Tang, J. S., Gao, H., Ding, R., Li, J., Hong, K., et al. (2011). A New Staurosporine Analog from Actinomycetes *Streptomyces* Sp. (172614). *J. Asian Nat. Prod. Res.* 13 (8), 765–769. doi:10.1080/10286020.2011.586342

Liu, C. X., Liu, S. H., Zhao, J. W., Zhang, J., Wang, X. J., Li, J. S., et al. (2017). A New Spectinabilin Derivative with Cytotoxic Activity from Ant-Derived *Streptomyces* Sp. 1H-GS5. *J. Asian Nat. Prod. Res.* 19 (9), 924–929. doi:10.1080/10286020.2016.1254200

Liu, D., Lin, H., Proksch, P., Tang, X., Shao, Z., and Lin, W. (2015). Microbacterins A and B, New Peptaibols from the Deep Sea Actinomycete *Microbacterium Sediminis* Sp. Nov. YLB-01(T). *Org. Lett.* 17 (5), 1220–1223. doi:10.1021/acs.orglett.5b00172

Liu, R., Cui, C. B., Duan, L., Gu, Q. Q., and Zhu, W. M. (2005). Potent *In Vitro* Anticancer Activity of Metacycloprodigiosin and Undecylprodigiosin from a Sponge-Derived Actinomycete *Saccharopolyspora* Sp. Nov. *Arch. Pharm. Res.* 28 (12), 1341–1344. doi:10.1007/bf02977899

Liu, R., Zhu, T., Li, D., Gu, J., Xia, W., Fang, Y., et al. (2007). Two Indolocarbazole Alkaloids with Apoptosis Activity from a Marine-Derived Actinomycete Z(2) 039-2. *Arch. Pharm. Res.* 30 (3), 270–274. doi:10.1007/bf02977605

Lu, C., Zhao, Y., Jia, W. Q., Zhang, H., Qi, H., Xiang, W. S., et al. (2017). A New Anthracycline-type Metabolite from *Streptomyces* Sp. NEAU-L3. *J. Antibiot. (Tokyo)* 70 (10), 1026–1028. doi:10.1038/ja.2017.95

Lu, J., Ma, Y., Liang, J., Xing, Y., Xi, T., and Lu, Y. (2012). Aureolic Acids from a Marine-Derived *Streptomyces* Sp. WBF16. *Microbiol. Res.* 167 (10), 590–595. doi:10.1016/j.micres.2012.06.001

Lv, Q., Fan, Y., Tao, G., Fu, P., Zhai, J., Ye, B., et al. (2019). Sekgranaticin, a SEK34b-Granaticin Hybrid Polyketide from *Streptomyces* Sp. 166. *J. Org. Chem.* 84 (14), 9087–9092. doi:10.1021/acs.joc.9b01022

Lynch, H. T., and de la Chapelle, A. (2003). Hereditary Colorectal Cancer. *N. Engl. J. Med.* 348 (10), 919–932. doi:10.1056/NEJMra012242

Ma, Y., Zhang, Y., Jiang, H., Xiang, S., Zhao, Y., Xiao, M., et al. (2021). Metagenome Analysis of Intestinal Bacteria in Healthy People, Patients with Inflammatory Bowel Disease and Colorectal Cancer. *Front. Cell.. Infect. Microbiol.* 11, 599734. doi:10.3389/fcimb.2021.599734

Macherla, V. R., Liu, J., Bellows, C., Teisan, S., Nicholson, B., Lam, K. S., et al. (2005). Glaciapyrroles A, B, and C, Pyrrolosesquiterpenes from a *Streptomyces* Sp. Isolated from an Alaskan Marine Sediment. *J. Nat. Prod.* 68 (5), 780–783. doi:10.1021/np049597c

Maldonado, L. A., Stach, J. E., Pathom-aree, W., Ward, A. C., Bull, A. T., and Goodfellow, M. (2005). Diversity of Cultivable Actinobacteria in Geographically Widespread Marine Sediments. *Antonie Leeuwenhoek* 87, 11–18. doi:10.1007/s10482-004-6525-0

Malet-cascón, L., Romero, F., Espliego-vázquez, F., Grávalos, D., and Fernández-puentes, J. L. (2003). IB-00208, a New Cytotoxic Polycyclic Xanthone Produced by a Marine-Derived *Actinomadura*. I. Isolation of the Strain, Taxonomy and Biological Activites. *J. Antibiot.* 56 (3), 219–225. doi:10.7164/antibiotics.56.219

Maloney, K. N., Macmillan, J. B., Kauffman, C. A., Jensen, P. R., Dipasquale, A. G., Rheingold, A. L., et al. (2009). Lodopyridone, a Structurally Unprecedented Alkaloid from a Marine Actinomycete. *Org. Lett.* 11 (23), 5422–5424. doi:10.1021/ol901997k

Mansouri, K., Mostafie, A., Rezazadeh, D., Shahlaei, M., and Modarressi, M. H. (2016). New Function of TSGA10 Gene in Angiogenesis and Tumor Metastasis: a Response to a Challengeable Paradox. *Hum. Mol. Genet.* 25 (2), 233–244. doi:10.1093/hmg/ddv461

Mármol, I., Sánchez-de-Diego, C., Pradilla Dieste, A., Cerrada, E., and Rodriguez Yoldi, M. (2017). Colorectal Carcinoma: A General Overview and Future Perspectives in Colorectal Cancer. *Ijms* 18 (1), 197. doi:10.3390/ijms18010197

Martin, G. D., Tan, L. T., Jensen, P. R., Dimayuga, R. E., Fairchild, C. R., Raventos-Suarez, C., et al. (2007). Marmycins A and B, Cytotoxic Pentacyclic C-Glycosides from a Marine Sediment-Derived Actinomycete Related to the Genus *Streptomyces*. *J. Nat. Prod.* 70 (9), 1406–1409. doi:10.1021/np060621r

Maskey, R. P., Helmke, E., Kayser, O., Fiebig, H. H., Maier, A., Busche, A., et al. (2004a). Anti-cancer and Antibacterial Trioxacarcins with High Anti-malaria Activity from a Marine *Streptomycete* and Their Absolute Stereochemistry. *J. Antibiot. (Tokyo)* 57 (12), 771–779. doi:10.7164/antibiotics.57.771

Maskey, R. P., Li, F., Qin, S., Fiebig, H. H., and Laatsch, H. (2003). Chandrananimycins A Approximately C: Production of Novel Anticancer Antibiotics from a Marine *Actinomadura* Sp. Isolate M048 by Variation of Medium Composition and Growth Conditions. *J. Antibiot. (Tokyo)* 56 (7), 622–629. doi:10.7164/antibiotics.56.622

Maskey, R. P., Sevvana, M., Usón, I., Helmke, E., and Laatsch, H. (2004b). Gutingimycin: A Highly Complex Metabolite from a Marine *Streptomycete*. *Angew. Chem. Int. Ed. Engl.* 43 (10), 1281–1283. doi:10.1002/anie.200352312

McBrien, K. D., Berry, R. L., Lowe, S. E., Neddermann, K. M., Bursuker, I., Huang, S., et al. (1995). Rakicidins, New Cytotoxic Lipopeptides from *Micromonospora* Sp. Fermentation, Isolation and Characterization. *J. Antibiot. (Tokyo)* 48 (12), 1446–1452. doi:10.7164/antibiotics.48.1446

Miller, E. D., Kauffman, C. A., Jensen, P. R., and Fenical, W. (2007). Piperazimycins: Cytotoxic Hexadepsipeptides from a Marine-Derived Bacterium of the Genus *Streptomyces*. *J. Org. Chem.* 72 (2), 323–330. doi:10.1021/jo061064g

Mitchell, S. S., Nicholson, B., Teisan, S., Lam, K. S., and Potts, B. C. (2004). Aureoverticillactam, a Novel 22-atom Macrocyclic Lactam from the Marine Actinomycete *Streptomyces Aureoverticillatus*. *J. Nat. Prod.* 67 (8), 1400–1402. doi:10.1021/np049970g

Moon, K., Ahn, C. H., Shin, Y., Won, T. H., Ko, K., Lee, S. K., et al. (2014). New Benzoxazine Secondary Metabolites from an Arctic Actinomycete. *Mar. Drugs* 12 (5), 2526–2538. doi:10.3390/md12052526

Mori, G., Rampelli, S., Orena, B. S., Rengucci, C., De Maio, G., Barbieri, G., et al. (2018). Shifts of Faecal Microbiota during Sporadic Colorectal Carcinogenesis. *Sci. Rep.* 8 (1), 10329. doi:10.1038/s41598-018-28671-9

Mussin, N., Oh, S. C., Lee, K. W., Park, M. Y., Seo, S., Yi, N. J., et al. (2017). Sirolimus and Metformin Synergistically Inhibits Colon Cancer *In Vitro* and *In Vivo*. *J. Korean Med. Sci.* 32 (9), 1385–1395. doi:10.3346/jkms.2017.32.9.1385

Nam, S. J., Kauffman, C. A., Paul, L. A., Jensen, P. R., and Fenical, W. (2013). Actinoranone, a Cytotoxic Meroterpenoid of Unprecedented Structure from a Marine Adapted *Streptomyces* Sp. *Org. Lett.* 15 (21), 5400–5403. doi:10.1021/ol402080s

Nathan, J., and Kannan, R. R. (2020). Antiangiogenic Molecules from Marine Actinomycetes and the Importance of Using Zebrafish Model in Cancer Research. *Heliyon* 6 (12), e05662. doi:10.1016/j.heliyon.2020.e05662

Nguyen, H. T., Pokhrel, A. R., Nguyen, C. T., Pham, V. T. T., Dhakal, D., Lim, H. N., et al. (2020). *Streptomyces Sp.* VN1, a Producer of Diverse Metabolites Including Non-natural Furan-type Anticancer Compound. *Sci. Rep.* 10 (1), 1756. doi:10.1038/s41598-020-58623-1

Nikodinovic-Runic, J., Mojic, M., Kang, Y., Maksimovic-Ivanic, D., Mijatovic, S., Vasiljevic, B., et al. (2014). Undecylprodigiosin Conjugated Monodisperse Gold Nanoparticles Efficiently Cause Apoptosis in Colon Cancer Cells *In Vitro*. *J. Mater Chem. B* 2 (21), 3271–3281. doi:10.1039/c4tb00300d

Oh, D. C., Williams, P. G., Kauffman, C. A., Jensen, P. R., and Fenical, W. (2006). Cyanosporasides A and B, Chloro- and Cyano-Cyclopenta[a]indene Glycosides from the Marine Actinomycete "Salinispora Pacifica". *Org. Lett.* 8 (6), 1021–1024. doi:10.1021/ol052686b

Oku, N., Matoba, S., Yamazaki, Y. M., Shimasaki, R., Miyanaga, S., and Igarashi, Y. (2014). Complete Stereochemistry and Preliminary Structure-Activity Relationship of Rakicidin A, a Hypoxia-Selective Cytotoxin from *Micromonospora* Sp. *J. Nat. Prod.* 77 (11), 2561–2565. doi:10.1021/np500276c

Omura, S., Iwai, Y., Hirano, A., Nakagawa, A., Awaya, J., Tsuchya, H., et al. (1977). A New Alkaloid AM-2282 of *Streptomyces* Origin. Taxonomy, Fermentation, Isolation and Preliminary Characterization. *J. Antibiot. (Tokyo)* 30 (4), 275–282. doi:10.7164/antibiotics.30.275

Onaka, H. (2017). Novel Antibiotic Screening Methods to Awaken Silent or Cryptic Secondary Metabolic Pathways in Actinomycetes. *J. Antibiot. (Tokyo)* 70 (8), 865–870. doi:10.1038/ja.2017.51

Pan, E., Jamison, M., Yousufuddin, M., and MacMillan, J. B. (2012). Ammosamide D, an Oxidatively Ring Opened Ammosamide Analog from a Marine-Derived *Streptomyces Variabilis*. *Org. Lett.* 14 (9), 2390–2393. doi:10.1021/ol300806e

Pérez, M., Crespo, C., Schleissner, C., Rodríguez, P., Zúñiga, P., and Reyes, F. (2009). Tartrolon D, a Cytotoxic Macrodiolide from the Marine-Derived Actinomycete *Streptomyces* Sp. MDG-04-17-069. *J. Nat. Prod.* 72 (12), 2192–2194. doi:10.1021/np9006603

Pérez, M., Schleissner, C., Fernández, R., Rodríguez, P., Reyes, F., Zuñiga, P., et al. (2016). PM100117 and PM100118, New Antitumor Macrolides Produced by a Marine *Streptomyces Caniferus* GUA-06-05-006A. *J. Antibiot.* 69 (5), 388–394. doi:10.1038/ja.2015.121

Peters, U., Bien, S., and Zubair, N. (2015). Genetic Architecture of Colorectal Cancer. *Gut* 64 (10), 1623–1636. doi:10.1136/gutjnl-2013-306705

Piawah, S., and Venook, A. P. (2019). Targeted Therapy for Colorectal Cancer Metastases: A Review of Current Methods of Molecularly Targeted Therapy and the Use of Tumor Biomarkers in the Treatment of Metastatic Colorectal Cancer. *Cancer* 125 (23), 4139–4147. doi:10.1002/cncr.32163

PubChem (2004b). *PubChem Compound Summary for CID 31703, Doxorubicin*. Bethesda (MD): National Library of Medicine US. National Center for Biotechnology Information. [Online]. Available: https://pubchem.ncbi.nlm.nih.gov/compound/Doxorubicin (Accessed June 15, 2021).

PubChem (2004c). *PubChem Compound Summary for CID 36314, Paclitaxel*. Bethesda (MD): National Library of Medicine (US). National Center for

Biotechnology Information. [Online]. Available: https://pubchem.ncbi.nlm.nih.gov/compound/Paclitaxel (Accessed June 16, 2021).

PubChem (2004a). *PubChem Compound Summary for CID 5746, Mitomycin*. Bethesda (MD): National Library of Medicine (US). National Center for Biotechnology Information. [Online]. Available: https://pubchem.ncbi.nlm.nih.gov/compound/Mitomycin (Accessed June 9, 2021).

Ratovitski, E. A. (2016). Tumor Protein (TP)-p53 Members as Regulators of Autophagy in Tumor Cells upon Marine Drug Exposure. *Mar. Drugs* 14 (8), 154. doi:10.3390/md14080154

Rejhová, A., Opattová, A., Čumová, A., Slíva, D., and Vodička, P. (2018). Natural Compounds and Combination Therapy in Colorectal Cancer Treatment. *Eur. J. Med. Chem.* 144, 582–594. doi:10.1016/j.ejmech.2017.12.039

Rodríguez, J. C., Puentes, J. L. F., Baz, J. P., and Cañedo, L. M. (2003). IB-00208, a New Cytotoxic Polycyclic Xanthone Produced by a Marine-Derived *Actinomadura*. II. Isolation, Physico-Chemical Properties and Structure Determination. *J. Antibiot.* 56 (3), 318–321. doi:10.7164/antibiotics.56.318

Romero, F., Espliego, F., Pérez Baz, J., García de Quesada, T., Grávalos, D., de la Calle, F., et al. (1997). Thiocoraline, a New Depsipeptide with Antitumor Activity Produced by a Marine *Micromonospora*. I. Taxonomy, Fermentation, Isolation, and Biological Activities. *J. Antibiot. (Tokyo)* 50 (9), 734–737. doi:10.7164/antibiotics.50.734

Sánchez López, J. M., Martínez Insua, M., Pérez Baz, J., Fernández Puentes, J. L., and Cañedo Hernández, L. M. (2003). New Cytotoxic Indolic Metabolites from a Marine *Streptomyces*. *J. Nat. Prod.* 66 (6), 863–864. doi:10.1021/np0204444

Sattler, I., Thiericke, R., and Zeeck, A. (1998). The Manumycin-Group Metabolites. *Nat. Prod. Rep.* 15 (3), 221–240. doi:10.1039/a815221y

Schneemann, I., Kajahn, I., Ohlendorf, B., Zinecker, H., Erhard, A., Nagel, K., et al. (2010). Mayamycin, a Cytotoxic Polyketide from a Streptomyces Strain Isolated from the Marine Sponge Halichondria Panicea. *J. Nat. Prod.* 73 (7), 1309–1312. doi:10.1021/np100135b

Shaaban, K. A., Shaaban, M., Rahman, H., Grün-Wollny, I., Kämpfer, P., Kelter, G., et al. (2019). Karamomycins A-C: 2-Naphthalen-2-Yl-Thiazoles from *Nonomuraea Endophytica*. *J. Nat. Prod.* 82 (4), 870–877. doi:10.1021/acs.jnatprod.8b00928

Shang, N. N., Zhang, Z., Huang, J. P., Wang, L., Luo, J., Yang, J., et al. (2018). Glycosylated Piericidins from an Endophytic *Streptomyces* with Cytotoxicity and Antimicrobial Activity. *J. Antibiot. (Tokyo)* 71 (7), 672–676. doi:10.1038/s41429-018-0051-1

Shin, H. J., Kim, T. S., Lee, H. S., Park, J. Y., Choi, I. K., and Kwon, H. J. (2008). Streptopyrrolidine, an Angiogenesis Inhibitor from a Marine-Derived *Streptomyces* Sp. KORDI-3973. *Phytochemistry* 69 (12), 2363–2366. doi:10.1016/j.phytochem.2008.05.020

Shin, H. J., Lee, H. S., Lee, J. S., Shin, J., Lee, M. A., Lee, H. S., et al. (2014). Violapyrones H and I, New Cytotoxic Compounds Isolated from *Streptomyces* Sp. Associated with the Marine Starfish *Acanthaster planci*. *Mar. Drugs* 12 (6), 3283–3291. doi:10.3390/md12063283

Shin, H. J., Mondol, M. A. M., Yu, T. K., Lee, H.-S., Lee, Y.-J., Jung, H. J., et al. (2010). An Angiogenesis Inhibitor Isolated from a Marine-Derived Actinomycete, *Nocardiopsis* Sp. 03N67. *Phytochem. Lett.* 3 (4), 194–197. doi:10.1016/j.phytol.2010.07.005

Siddharth, S., and Vittal, R. R. (2019). Isolation, Characterization, and Structural Elucidation of 4-methoxyacetanilide from Marine Actinobacteria *Streptomyces* Sp. SCA29 and Evaluation of its Enzyme Inhibitory, Antibacterial, and Cytotoxic Potential. *Arch. Microbiol.* 201 (6), 737–746. doi:10.1007/s00203-019-01634-y

Sobolevskaia, M. P., and Kuznetsova, T. A. (2010). Biologically Active Metabolites of the Marine Actinobacteria. *Bioorg Khim* 36 (5), 607–621. doi:10.1134/s1068162010050031

Son, S., Ko, S. K., Jang, M., Lee, J. K., Kwon, M. C., Kang, D. H., et al. (2017). Polyketides and Anthranilic Acid Possessing 6-Deoxy-α-L-Talopyranose from a Streptomyces Species. *J. Nat. Prod.* 80 (5), 1378–1386. doi:10.1021/acs.jnatprod.6b01059

Song, Y., Yang, J., Yu, J., Li, J., Yuan, J., Wong, N. K., et al. (2020). Chlorinated Bis-Indole Alkaloids from Deep-Sea Derived *Streptomyces* Sp. SCSIO 11791 with Antibacterial and Cytotoxic Activities. *J. Antibiot. (Tokyo)* 73 (8), 542–547. doi:10.1038/s41429-020-0307-4

Sonowal, H., Pal, P. B., Wen, J. J., Awasthi, S., Ramana, K. V., and Srivastava, S. K. (2017). Aldose Reductase Inhibitor Increases Doxorubicin-Sensitivity of Colon Cancer Cells and Decreases Cardiotoxicity. *Sci. Rep.* 7 (1), 3182. doi:10.1038/s41598-017-03284-w

Soria-Mercado, I. E., Prieto-Davo, A., Jensen, P. R., and Fenical, W. (2005). Antibiotic Terpenoid Chloro-Dihydroquinones from a New Marine Actinomycete. *J. Nat. Prod.* 68 (6), 904–910. doi:10.1021/np058011z

Sousa Tda, S., Jimenez, P. C., Ferreira, E. G., Silveira, E. R., Braz-Filho, R., Pessoa, O. D., et al. (2012). Anthracyclinones from *Micromonospora* Sp. *J. Nat. Prod.* 75 (3), 489–493. doi:10.1021/np200795p

Stoffel, E. M., and Kastrinos, F. (2014). Familial Colorectal Cancer, beyond Lynch Syndrome. *Clin. Gastroenterol. Hepatol.* 12 (7), 1059–1068. doi:10.1016/j.cgh.2013.08.015

Suela Silva, M., Naves Sales, A., Teixeira Magalhães-Guedes, K., Ribeiro Dias, D., and Schwan, R. F. (2013). Brazilian Cerrado Soil Actinobacteria Ecology. *Biomed. Res. Int.* 2013, 503805. doi:10.1155/2013/503805

Sung, H., Ferlay, J., Siegel, R. L., Laversanne, M., Soerjomataram, I., Jemal, A., et al. (2021). Global Cancer Statistics 2020: GLOBOCAN Estimates of Incidence and Mortality Worldwide for 36 Cancers in 185 Countries. *CA A Cancer J. Clin.* 71, 209–249. doi:10.3322/caac.21660

Thomford, N. E., Senthebane, D. A., Rowe, A., Munro, D., Seele, P., Maroyi, A., et al. (2018). Natural Products for Drug Discovery in the 21st Century: Innovations for Novel Drug Discovery. *Int. J. Mol. Sci.* 19 (6), 1578. doi:10.3390/ijms19061578

Tomasz, M. (1995). Mitomycin C: Small, Fast and Deadly (But Very Selective). *Chem. Biol.* 2 (9), 575–579. doi:10.1016/1074-5521(95)90120-5

Toumazi, D., and Constantinou, C. (2020). A Fragile Balance: The Important Role of the Intestinal Microbiota in the Prevention and Management of Colorectal Cancer. *Oncology* 98 (9), 593–602. doi:10.1159/000507959

Trzoss, L., Fukuda, T., Costa-Lotufo, L. V., Jimenez, P., La Clair, J. J., and Fenical, W. (2014). Seriniquinone, a Selective Anticancer Agent, Induces Cell Death by Autophagocytosis, Targeting the Cancer-Protective Protein Dermcidin. *Proc. Natl. Acad. Sci. U. S. A.* 111 (41), 14687–14692. doi:10.1073/pnas.1410932111

Tuladhar, A., Hondal, R. J., Colon, R., Hernandez, E. L., and Rein, K. S. (2019). Effectors of Thioredoxin Reductase: Brevetoxins and Manumycin-A. *Comp. Biochem. Physiol. C Toxicol. Pharmacol.* 217, 76–86. doi:10.1016/j.cbpc.2018.11.015

Turashvili, G., and Brogi, E. (2017). Tumor Heterogeneity in Breast Cancer. *Front. Med. (Lausanne)* 4, 227. doi:10.3389/fmed.2017.00227

Udwary, D. W., Zeigler, L., Asolkar, R. N., Singan, V., Lapidus, A., Fenical, W., et al. (2007). Genome Sequencing Reveals Complex Secondary Metabolome in the Marine Actinomycete *Salinispora Tropica*. *Proc. Natl. Acad. Sci. U. S. A.* 104 (25), 10376–10381. doi:10.1073/pnas.0700962104

Um, S., Choi, T. J., Kim, H., Kim, B. Y., Kim, S. H., Lee, S. K., et al. (2013). Ohmyungsamycins A and B: Cytotoxic and Antimicrobial Cyclic Peptides Produced by Streptomyces Sp. From a Volcanic Island. *J. Org. Chem.* 78 (24), 12321–12329. doi:10.1021/jo401974g

Van Bergeijk, D. A., Terlouw, B. R., Medema, M. H., and Van Wezel, G. P. (2020). Ecology and Genomics of Actinobacteria: New Concepts for Natural Product Discovery. *Nat. Rev. Microbiol.* 18 (10), 546–558. doi:10.1038/s41579-020-0379-y

Vippila, M. R., Ly, P. K., and Cuny, G. D. (2015). Synthesis and Antiproliferative Activity Evaluation of the Disulfide-Containing Cyclic Peptide Thiochondrilline C and Derivatives. *J. Nat. Prod.* 78 (10), 2398–2404. doi:10.1021/acs.jnatprod.5b00428

Wagg, C., Bender, S. F., Widmer, F., and van der Heijden, M. G. (2014). Soil Biodiversity and Soil Community Composition Determine Ecosystem Multifunctionality. *Proc. Natl. Acad. Sci. U. S. A.* 111 (14), 5266–5270. doi:10.1073/pnas.1320054111

Wang, C., Du, W., Lu, H., Lan, J., Liang, K., and Cao, S. (2021). A Review: Halogenated Compounds from Marine Actinomycetes. *Molecules* 26 (9), 2754. doi:10.3390/molecules26092754

Wang, Q., Zhang, Y., Wang, M., Tan, Y., Hu, X., He, H., et al. (2017). Neo-actinomycins A and B, Natural Actinomycins Bearing the 5H-Oxazolo[4,5-B] phenoxazine Chromophore, from the Marine-Derived Streptomyces Sp. IMB094. *Sci. Rep.* 7 (1), 3591. doi:10.1038/s41598-017-03769-8

Wang, R. J., Zhang, S. Y., Ye, Y. H., Yu, Z., Qi, H., Zhang, H., et al. (2019). Three New Isoflavonoid Glycosides from the Mangrove-Derived Actinomycete *Micromonospora Aurantiaca* 110B. *Mar. Drugs* 17 (5), 294. doi:10.3390/md17050294

Wang, W., Kandimalla, R., Huang, H., Zhu, L., Li, Y., Gao, F., et al. (2019). Molecular Subtyping of Colorectal Cancer: Recent Progress, New Challenges and Emerging Opportunities. *Semin. Cancer Biol.* 55, 37–52. doi:10.1016/j.semcancer.2018.05.002

Wang, Z., Wen, Z., Liu, L., Zhu, X., Shen, B., Yan, X., et al. (2019). Yangpumicins F and G, Enediyne Congeners from *Micromonospora Yangpuensis* DSM 45577. *J. Nat. Prod.* 82 (9), 2483–2488. doi:10.1021/acs.jnatprod.9b00229

Ward, A. C., and Bora, N. (2006). Diversity and Biogeography of Marine Actinobacteria. *Curr. Opin. Microbiol.* 9 (3), 279–286. doi:10.1016/j.mib.2006.04.004

Weldon Gilcrease, G., Stenehjem, D. D., Wade, M. L., Weis, J., McGregor, K., Whisenant, J., et al. (2019). Phase I/II Study of Everolimus Combined with mFOLFOX-6 and Bevacizumab for First-Line Treatment of Metastatic Colorectal Cancer. *Invest. New Drugs* 37 (3), 482–489. doi:10.1007/s10637-018-0645-2

Williams, P. G., Miller, E. D., Asolkar, R. N., Jensen, P. R., and Fenical, W. (2007). Arenicolides A-C, 26-membered Ring Macrolides from the Marine Actinomycete *Salinispora Arenicola*. *J. Org. Chem.* 72 (14), 5025–5034. doi:10.1021/jo061878x

Wyche, T. P., Dammalapati, A., Cho, H., Harrison, A. D., Kwon, G. S., Chen, H., et al. (2014). Thiocoraline Activates the Notch Pathway in Carcinoids and Reduces Tumor Progression *In Vivo*. *Cancer Gene Ther.* 21 (12), 518–525. doi:10.1038/cgt.2014.57

Xiao, F., Li, H., Xu, M., Li, T., Wang, J., Sun, C., et al. (2018). Staurosporine Derivatives Generated by Pathway Engineering in a Heterologous Host and Their Cytotoxic Selectivity. *J. Nat. Prod.* 81 (8), 1745–1751. doi:10.1021/acs.jnatprod.8b00103

Yamazaki, Y., Kunimoto, S., and Ikeda, D. (2007). Rakicidin A: A Hypoxia-Selective Cytotoxin. *Biol. Pharm. Bull.* 30 (2), 261–265. doi:10.1248/bpb.30.261

Yang, F. X., Hou, G. X., Luo, J., Yang, J., Yan, Y., and Huang, S. X. (2018). New Phenoxazinone-Related Alkaloids from Strain *Streptomyces* Sp. KIB-H1318. *J. Antibiot. (Tokyo)* 71 (12), 1040–1043. doi:10.1038/s41429-018-0099-y

Ye, X., Anjum, K., Song, T., Wang, W., Yu, S., Huang, H., et al. (2016). A New Curvularin Glycoside and its Cytotoxic and Antibacterial Analogues from Marine Actinomycete Pseudonocardia Sp. HS7. *Nat. Prod. Res.* 30 (10), 1156–1161. doi:10.1080/14786419.2015.1047775

Yuan, G., Lin, H., Wang, C., Hong, K., Liu, Y., and Li, J. (2011). 1H and 13C Assignments of Two New Macrocyclic Lactones Isolated from *Streptomyces* Sp. 211726 and Revised Assignments of Azalomycins F3a, F4a and F5a. *Magn. Reson Chem.* 49 (1), 30–37. doi:10.1002/mrc.2697

Zhang, S., Xie, Q., Sun, C., Tian, X. P., Gui, C., Qin, X., et al. (2019). Cytotoxic Kendomycins Containing the Carbacylic Ansa Scaffold from the Marine-Derived *Verrucosispora* Sp. SCSIO 07399. *J. Nat. Prod.* 82 (12), 3366–3371. doi:10.1021/acs.jnatprod.9b00654

Zhang, Y. K., Zhang, Q., Wang, Y. L., Zhang, W. Y., Hu, H. Q., Wu, H. Y., et al. (2021). A Comparison Study of Age and Colorectal Cancer-Related Gut Bacteria. *Front. Cell. Infect. Microbiol.* 11, 606490. doi:10.3389/fcimb.2021.606490

Zhao, X. L., Wang, H., Xue, Z. L., Li, J. S., Qi, H., Zhang, H., et al. (2019). Two New Glutarimide Antibiotics from *Streptomyces* Sp. HS-NF-780. *J. Antibiot. (Tokyo)* 72 (4), 241–245. doi:10.1038/s41429-019-0143-6

Zheng, D., Han, L., Qu, X., Chen, X., Zhong, J., Bi, X., et al. (2017). Cytotoxic Fusicoccane-type Diterpenoids from *Streptomyces Violascens* Isolated from *Ailuropoda Melanoleuca* Feces. *J. Nat. Prod.* 80 (4), 837–844. doi:10.1021/acs.jnatprod.6b00676

Zhou, B., Hu, Z. J., Zhang, H. J., Li, J. Q., Ding, W. J., and Ma, Z. J. (2019). Bioactive Staurosporine Derivatives from the *Streptomyces* Sp. NB-A13. *Bioorg Chem.* 82, 33–40. doi:10.1016/j.bioorg.2018.09.016

Zhou, H., Yuan, Y., Wang, H., Xiang, W., Li, S., Zheng, H., et al. (2021). Gut Microbiota: A Potential Target for Cancer Interventions. *Cancer Manag. Res.* 13, 8281–8296. doi:10.2147/CMAR.S328249

Zhou, Y. J., Zhao, D. D., Liu, H., Chen, H. T., Li, J. J., Mu, X. Q., et al. (2017). Cancer Killers in the Human Gut Microbiota: Diverse Phylogeny and Broad Spectra. *Oncotarget* 8 (30), 49574–49591. doi:10.18632/oncotarget.17319

Conflict of Interest: The authors declare that the research was conducted in the absence of any commercial or financial relationships that could be construed as a potential conflict of interest.

Publisher's Note: All claims expressed in this article are solely those of the authors and do not necessarily represent those of their affiliated organizations, or those of the publisher, the editors and the reviewers. Any product that may be evaluated in this article, or claim that may be made by its manufacturer, is not guaranteed or endorsed by the publisher.

GLOSSARY

5-FU 5-fluorouracil
Akt or PKB Protein kinase B
CIMP CpG island methylator phenotype
CIN Chromosomal instability
CLL Chronic lymphocytic leukemia
CMSs Consensus molecular subtypes
CRC Colorectal cancer
EGFR Epidermal growth factor receptor
EMT Epithelial-to-mesenchymal transition
FDA Food and drug administration
HIF-1α Hypoxia-inducible factor 1-alpha
HR-MS High resolution mass spectrometry
IBD Inflammatory bowel disease
KRAS gene Kirsten rat sarcoma virus gene
MAPK Mitogen-activated protein kinase
MMPs Matrix metalloproteinases
MRSA Methicillin-resistant *Staphylococcus aureus*
MSI Microsatellite instability
mTOR Mammalian target of rapamycin
NF-κB nuclear factor 'kappa-light-chain-enhancer' of activated B-cells
NPs Natural products
PARP Poly (ADP-ribose) polymerase
PI3K Phosphoinositide 3-kinase
RAS Rat sarcoma virus
ROS Reactive oxygen species
SML Sea surface microlayer
SRB assay Sulforhodamine B assay
STAT3 Signal transducer and activator of transcription 3
TNF Tumor necrosis factor
TNM Tumor node metastasis
TRAIL Tumor necrosis factor-related apoptosis-inducing ligand
TSGA10 Testis-specific Gene Antigen 10
VEGF Vascular endothelial growth factor
XIAP X-linked inhibitor of apoptosis
ZEB1 or 2 Zinc finger E-box binding homeobox 1or 2

frontiers | Frontiers in Pharmacology

TYPE Review
PUBLISHED 15 August 2022
DOI 10.3389/fphar.2022.964793

OPEN ACCESS

EDITED BY
Hemant Goyal,
The Wright Center, United States

REVIEWED BY
Marta Castro,
University of Zaragoza, Spain
Huo Jiege,
Nanjing University of Chinese Medicine, China

*CORRESPONDENCE
Guang Ji,
jiliver@vip.sina.com,
jg@shutcm.edu.cn
Hanchen Xu,
hanson0702@126.com,
hcxu@shutcm.edu.cn

†These authors have contributed equally to this work

SPECIALTY SECTION
This article was submitted to Gastrointestinal and Hepatic Pharmacology, a section of the journal Frontiers in Pharmacology

RECEIVED 09 June 2022
ACCEPTED 18 July 2022
PUBLISHED 15 August 2022

CITATION
Lu L, Dong J, Liu Y, Qian Y, Zhang G, Zhou W, Zhao A, Ji G and Xu H (2022), New insights into natural products that target the gut microbiota: Effects on the prevention and treatment of colorectal cancer.
Front. Pharmacol. 13:964793.
doi: 10.3389/fphar.2022.964793

New insights into natural products that target the gut microbiota: Effects on the prevention and treatment of colorectal cancer

Lu Lu[1†], Jiahuan Dong[1,2†], Yujing Liu[1], Yufan Qian[1], Guangtao Zhang[1,2], Wenjun Zhou[1], Aiguang Zhao[2], Guang Ji[1*] and Hanchen Xu[1*]

[1]Institute of Digestive Diseases, Longhua Hospital, Shanghai University of Traditional Chinese Medicine, Shanghai, China, [2]Department of Oncology, Longhua Hospital, Shanghai University of Traditional Chinese Medicine, Shanghai, China

Colorectal cancer (CRC) is one of the most common malignant carcinomas. CRC is characterized by asymptomatic onset, and most patients are already in the middle and advanced stages of disease when they are diagnosed. Inflammatory bowel disease (IBD) and the inflammatory-cancer transformation of advanced colorectal adenoma are the main causes of CRC. There is an urgent need for effective prevention and intervention strategies for CRC. In recent years, rapid research progress has increased our understanding of gut microbiota. Meanwhile, with the deepening of research on the pathogenesis of colorectal cancer, gut microbiota has been confirmed to play a direct role in the occurrence and treatment of colorectal cancer. Strategies to regulate the gut microbiota have potential value for application in the prevention and treatment of CRC. Regulation of gut microbiota is one of the important ways for natural products to exert pharmacological effects, especially in the treatment of metabolic diseases and tumours. This review summarizes the role of gut microbiota in colorectal tumorigenesis and the mechanism by which natural products reduce tumorigenesis and improve therapeutic response. We point out that the regulation of gut microbiota by natural products may serve as a potential means of treatment and prevention of CRC.

KEYWORDS

colorectal cancer (CRC), gut microbiota, natural products, tumorigenesis, immunotherapy

Introduction

Colorectal cancer (CRC) is one of the most common malignant carcinomas worldwide, and CRC has the third highest incidence and mortality rate according to recent global cancer statistics (Sung et al., 2021). Usually, tumours involving the intestine are diagnosed at advanced metastatic stages of disease. Chronic inflammation is one of the strongest risk factors for CRC (Schmitt and Greten, 2021). Inflammatory bowel disease (IBD), including ulcerative colitis (UC) and Crohn's disease (CD), contributes to CRC (Keller et al., 2019). CRC associated with colitis can progress from inflammation to dysplasia and ultimately to tumour formation (Xu et al., 2020).

Although great efforts have been made in research on CRC treatment, the prognosis of CRC is still poor, and most patients have poor quality of life (Kishore and Bhadra, 2021). There is a strong public health need for effective prevention and intervention strategies for tumorigenesis. The gut flora includes large numbers of diverse species, and rapid research advances in recent years have increased our understanding of these species (Baumann and Jonzier-Perey, 1988). The number of cells in the gut microbiota is approximately twice the number of somatic cells in the human body. Given that each bacterial species is associated with thousands of genes, the gut microbiota genome is many hundred times larger than the human genome, which is typical estimated to contain 20,000 genes (Almeida et al., 2019). With the continued investigation of the pathogenesis of CRC (Song et al., 2015; Xu et al., 2019), the gut microbiota has recently been reported to play a direct role in the development and treatment of CRC (Sougiannis et al., 2019). Colorectal inflammation facilitates the loss of epithelial barrier integrity and promotes the activation of the inflammation-activating transcription factor NF-κB by the intestinal microbiome and its products; activated NF-κB can then accelerate colorectal tumorigenesis by inducing the production of IL-6, TNF-α, and other cytokines (Greten et al., 2004). Some bacterial genera have also been proven to protect against CRC (Appleyard et al., 2011), and this effect may be mediated through the production of metabolites, induction of immunological tolerance, or an ability to outcompete pathogenic bacteria or fungi (Azab et al., 1988). Regulation of dysbiosis reduces CRC development by restoring intestinal epithelial barrier function and modulating inflammatory immune responses (Tilg et al., 2018; Cheng et al., 2020). In addition, the inflammatory cascade mediated by microorganisms profoundly impacts antitumor effects, including those exerted by chemotherapy and immunotherapy (Sougiannis et al., 2019; Shi et al., 2020; Wang et al., 2021a).

Strategies to modulate the gut microbiome have potential for broad application in the prevention of CRC tumorigenesis and the treatment of CRC (Janney et al., 2020). Natural products have shown promise in the treatment of metabolic diseases and tumours by regulating intestinal flora to regulate host physiology and proinflammatory immune responses, which in turn alleviate disease pathology. Theabrownin is effective in the treatment of metabolic disorders *via* its regulation of the gut microbiome (Huang et al., 2019). Omega-3 polyunsaturated fatty acids (PUFAs) have anti-CRC activity, and the increased abundance of several short-chain fatty acid-producing bacteria might be one of the important mechanisms underlying their efficacy (Watson et al., 2018). In addition, intense research has revealed positive effects of the gut microbiome combined with chemotherapy and immunotherapy. Natural products can reduce the side effects of tumour chemotherapy or increase antitumor effects of treatment (Wang et al., 2021b; Yue et al., 2021). They can not only augment the therapeutic efficacy of immunotherapy but also reverse the resistance of CRC to immune checkpoint inhibitors (ICIs) through combined application (Andrews et al., 2021; Zhang et al., 2021). In this review, we outline the mechanism of action by which the gut microbiota participates in tumorigenesis, providing an overview of how natural products decrease tumorigenesis by regulating the intestinal microbiota. We also summarize potential applications of natural products in combination with chemotherapy or immunotherapy. There is no doubt that this review will serve as a foundation for the development of strategies to inhibit inflammatory-cancer transformation and provide new insights into the clinical treatment of CRC.

The role of the gut microbiota in colorectal tumorigenesis

A decade of microbiome studies have revealed that the gut microbiome plays an important role in colorectal diseases and colorectal neoplasms (Lynch and Pedersen, 2016). Through the analysis of the faecal microbiota of a longitudinal cohort of 2045 faecal samples from IBD patients and control subjects in four countries (Spain, Belgium, the United Kingdom and Germany), it was clear that patients with IBD have distinct gut microbiota profiles compared to healthy controls (Pascal et al., 2017). The levels of *Bacteroides*, Firmicutes, Clostridia, Ruminococcaceae, *Bifidobacterium*, *Lactobacillus*, and *Faecalibacterium prausnitzii* were decreased in patients with IBD, while those of Gammaproteobacteria, *Fusobacterium* and *Escherichia coli*, especially adherent-invasive *E. coli* (AIEC), were increased in patients with IBD (Man et al., 2011; Knights et al., 2013). Similar to the study conducted in Western countries, an analysis of the prevalence of species in IBD patients in Asia showed similar results. The China cohort study (Ma et al., 2018) and Korea research (Eun et al., 2016) showed patterns of gut dysbiosis in IBD patients. Analysis of the gut microbiota of CRC patients also showed that some bacteria, such as *Streptococcus gallolyticus*, *F. nucleatum*, *Escherichia coli*, *B. fragilis* and *E.* faecalis, have a high prevalence in CRC patients compared to the normal population, whereas the levels of genera such as

Roseburia, *Clostridium*, *Faecalibacterium* and *Bifidobacterium* are decrease in CRC patients (Feng et al., 2015; Gao et al., 2015; Gagnière et al., 2016; Yu et al., 2017a; Shang and Liu, 2018; Zhang et al., 2019a). Clinical data from different countries show typical intestinal ecological imbalances, which exacerbate the progression of colorectal inflammation and promote colorectal tumorigenesis (Shalapour and Karin, 2020), despite their different genetic characteristics and environmental factors.

A study of AOM-DSS-treated germ-free (GF) mice that were transplanted with faecal microbiota from CRC patients and healthy individuals revealed that the abundance of Gram-negative bacteria, including *Bacteroides*, *Parabacteroides*, *Alistipes*, and *Akkermansia*, was strongly positively correlated with increased tumour burden, while the abundance of members of the Gram-positive Clostridiales, including multiple members of *Clostridium* Group XIVa, was strongly negatively correlated with the formation of tumours (Baxter et al., 2014). Mice treated with azoxymethane show higher intestinal dysplasia after exposure to *P. anaerobius* (Tsoi et al., 2017). However, the role of microbes in the context of intestinal carcinogenesis is complex and diverse. We discovered that GF mice developed significantly more and larger tumours than specific pathogen-free (SPF) mice after AOM and DSS treatment. Recolonization of GF mice with commensal bacteria or administration of lipopolysaccharide (LPS) reduced tumorigenesis (Zhan et al., 2013). Thus, although the intestinal microbiome is capable of driving chronic inflammation and tumorigenesis, commensal bacteria also play important roles in limiting chemically induced injury and tumour development.

Inflammation-related signalling pathways, such as the NF-κB pathway (Wu et al., 2018), Toll-like receptor (TLR) pathway (Li et al., 2014), and Wnt/β-catenin pathway (Schatoff et al., 2017), are closely related to the occurrence and development of tumours. Microbes and their products can activate the major inflammation-activated transcription factor NF-κB; then, by inducing the production of IL-6, TNF, and other cytokines, NF-κB can accelerate the development of colon (Greten et al., 2004; De Santis et al., 2015) and pancreatic (Zhang et al., 2013) cancers. The tumour-promoting effects of bacteria can be enhanced by LPS, which is a component of the outer cell wall of Gram-negative bacteria that protects bacteria against antibiotics or immune cells. The binding of LPS and lipopolysaccharide-binding protein (LBP) can increase its affinity for CD14 receptors. Then, the LPS/LBP/CD14 complex binds to myeloid differentiation factor 2 (MD-2), which is recognized by TLR4 (Potrykus et al., 2021). Activation of this receptor leads to the release of mediators, including MyD88, which stimulates NF-κB to produce proinflammatory cytokines, including TNF-α and IL-1β (Gnauck et al., 2016). Another study also showed that LPS promotes CRC progression by activating TLR4-MyD88-NF-κB signalling in response to *Fusobacterium nucleatum* (Fn) (Zhu et al., 2016), which has been reported to be positively associated with CRC carcinogenesis (Gethings-Behncke et al., 2020; Villar-Ortega et al., 2022); this signalling pathway can activate the Wnt/β-catenin pathway through upregulation of cyclin-dependent kinase 5 (Cdk5), thus promoting the proliferation and migration of cells. The *in vitro* results showed that a cocktail of *Lactobacillus spp*. may exert an antitumorigenic effect by downregulating the expression of the genes encoding β-catenin and CTNNB1 and increasing the expression of genes that control the degradation of the β-catenin complex (Ghanavati et al., 2020). In addition, butyrate inhibits inflammation and carcinogenesis by reducing NF-κB and Wnt signalling (Inan et al., 2000; Uchiyama et al., 2016). The inflammatory response mediated by the microbiota can contribute to the inflammatory response through different signalling pathways, thereby regulating inflammation-related cancer progression (Shalapour and Karin, 2020). LPS is one of the important links in the inflammatory response to microorganisms. On the other hand, microbiota and microbial metabolites can reduce tumorigenesis by regulating inflammatory signalling pathways.

The crucial parameters of enteric infections are colonization resistance, microbiome community structure and niche occupation, and these parameters can be modulated by mucus (Sorbara and Pamer, 2019). To colonize the intestinal epithelium, pathogens have to pass through the mucus that is secreted by goblet cells in the proximal colon and distal colon; thus, mucus provides a physical, chemical and biological line of defence for the host (Sauvaitre et al., 2021). Impaired mucosal barrier function is accompanied by decreased acidic mucin expression, decreased mucus layer thickness, and decreased antimicrobial peptide levels, which are associated with gut dysbiosis (Liang et al., 2020). *Bacteroides* and *Akkermansia* are the two genera whose presence is most strongly correlated with higher rates of tumorigenesis. Both are known to degrade mucin, and the expression of several genes associated with mucin degradation is positively correlated with intestinal inflammation (Bloom et al., 2011; Ganesh et al., 2013; Ng et al., 2013) and tumour incidence (Baxter et al., 2014). *Clostridium perfringens* can exhibit proteolytic and mucinase activity and lead to a thinner mucus layer, which plays a positive role in the pathogenesis of colon inflammatory disease (Machiels et al., 2017). Cathelin-related antimicrobial peptide (CRAMP) (Kurosaka et al., 2005), which cannot be detected after 21 days in infants, is expressed in small intestinal epithelial cells during the neonatal period and significantly protects neonates from the enteric pathogen *Listeria* (Ménard et al., 2008). Additionally, tight junctions (TJs) are critical for transepithelial permeability, and they restrict passage of pathogens, microbes or toxins into the host (Groschwitz and Hogan, 2009). Complex crosstalk between the gut barrier and intestinal microbiota regulates not only host homeostasis but also disease development.

Moreover, tumour and microenvironment cells respond to signals from the microbiota. The intestinal microbiome can regulate heterogeneous cell populations, such as endothelial,

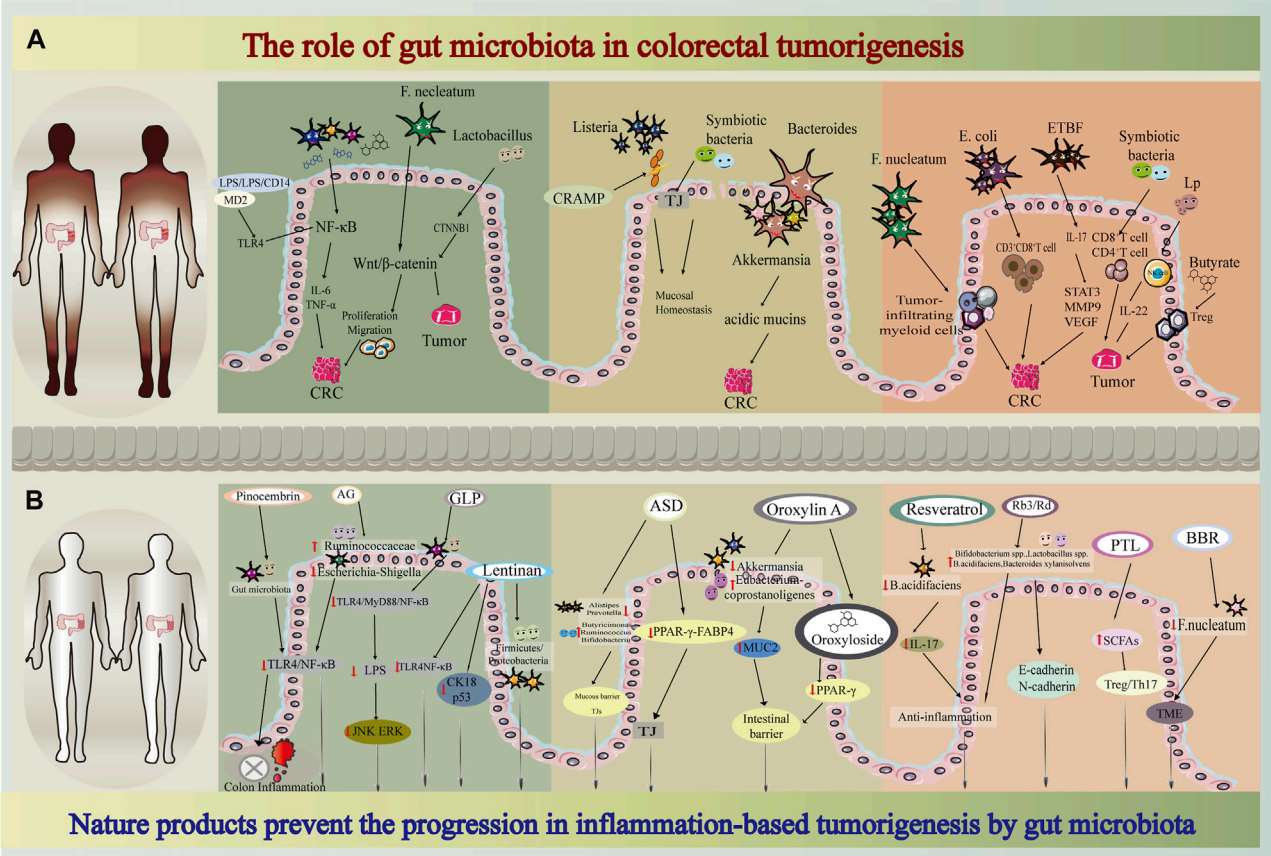

FIGURE 1
Flow diagram of mechanistic study through nature products, gut microbiota, colorectal tumorigenesis **(A)** The role of gut microbiota in colorectal tumorigenesis **(B)** Nature products prevent the progression in inflammation-based tumorigenesis by gut microbiota.

stromal, and immune cells, leading to the secretion of soluble signals (cytokines, chemokines, or growth factors) and generating a favourable microenvironment to support tumour growth and progression (Lu et al., 2021). An experiment in a APC Min/+ mouse model showed that *F. nucleatum* exacerbates tumorigenesis by recruiting tumour-infiltrating myeloid cells (granulocytes, macrophages, dendritic cells (DCs), and MDSCs), and these mice share a proinflammatory signature with *Fusobacterium*-associated human CRC (Kostic et al., 2013; Hanus et al., 2021). *F. nucleatum* can promote tumorigenesis by decreasing $CD3^+$ T cell numbers (Mima et al., 2015). APCMin/+ mice exposed to colibactin-producing *E. coli* exhibit more polyps and decreased $CD3^+$ $CD8^+$ T cell number than noninfected animals or animals infected with *E. coli* strains that lack pks (Lopès et al., 2020). Enterotoxic *Bacteroides fragilis* (ETBF) indirectly induces the ectopic production of chemokines and growth factors by colonic epithelial cells (CECs) through interaction with IL-17 receptors. ETBF also induces submucosal IL-17 expression. IL-17 and transformed CECs jointly promote tumour development by suppressing immune effector cells and activating the STAT3 signalling pathway, together with MMP-9 and VEGF (Thiele Orberg et al., 2017). Dysbiosis stimulates macrophages to increase the phosphorylation of c-Jun in CRC cells and accelerate CRC cell proliferation (Li et al., 2012). These data suggest that bacteria promote a tumour microenvironment (TME) that favours neoplasia progression. Although the mechanism by which the gut microbiota contributes to the TME has not been elucidated, many reports that suggest that the gut microbiota and its metabolites affect antitumor immune responses. A healthy gut microbiome can stabilize T cells that recognize a wide variety of antigens and are activated to differentiate into cytotoxic $CD8^+$ T cells, ultimately infiltrating the tumour and attacking tumour cells (Iida et al., 2013). It has been reported that 11 strains present in the intestinal microbiota can increase $CD8^+$ T cell numbers, enhance the antitumour immune response mediated by $CD8^+$ T cells and inhibit tumour progression. The effect is the same as, or even better than, ICIs (Tanoue et al., 2019). Stimulation of NK cells with *Lactobacillus plantarum* (Lp) enhances IL-22 production, which decreases damage to the intestinal

epithelial barrier (Suzuki, 2013) and delays tumour formation (Niu et al., 2021). Butyrate enhances Treg function in a murine model (Arpaia et al., 2013; Smith et al., 2013).

These studies have shown that the gut microbiota plays an important role in maintaining intestinal homeostasis as well as in the occurrence and development of colorectal inflammatory diseases and tumorigenesis (Figure 1A). Therefore, effective interventions that modulate gut microbes are a powerful strategy to inhibit CRC transformation. Specifically, increasing the commensal flora, reducing the growth of pathogenic bacteria, restoring ecological disturbance, maintaining the intestinal epithelial barrier, and regulating the state of the immune microenvironment decrease colorectal inflammation and tumorigenesis. Natural compounds are strong candidates for achieving these goals.

Natural products prevent the transformation of colorectal inflammation into colorectal cancer by the gut microbiota.

Natural products play an important role in the regulation of immunity and the treatment of disease. A study has shown that treatment with 300 mg/kg resveratrol alleviates gut dysbiosis by increasing the *Firmicutes/Bacteroidetes* ratio, inhibiting the growth of *Enterococcus faecalis*, and increasing the prevalence of the probiotics *Lactobacillus* and *Bifidobacterium* in the gut (Etxeberria et al., 2015). Resveratrol (0.025%) effectively decreases the abundance of the genera *Akkermansia*, *Dorea*, *Sutterella* and *Bilophila* in mice, increases the proportion of *Bifidobacterium* and increases alpha diversity. Resveratrol administration protects colonic tissue from structural deterioration and dysplasia and reduces the expression of several proinflammatory cytokines. Furthermore, treatment with 1.56 μg/ml (6.8 μm) resveratrol markedly inhibits the biofilm formation of Fn under anaerobic conditions (He et al., 2016). Feeding mice 0.5% curcumin for 14 weeks can significantly increase bacterial richness, prevent age-related decreases in alpha diversity, increase the relative abundance of *Lactobacillales*, and decrease the relative abundance of members of the Coriobacterales order (McFadden et al., 2015), which can exert strong anti-inflammatory, antioxidative and antiproliferative effects. Quercetin supplementation decreases the relative abundance of the potentially pathogenic microbe *E. coli* (Zhang et al., 2017a). Both chlorogenic acid (Zhang et al., 2017a) and salvianolic acid A (Wang et al., 2018a) significantly isolate the microbiota and suppress the progression of colitis and CRC. These natural product-mediated alterations in the gut microbiome provide evidence for a protective role of natural products in inflammatory-cancer transformation. Natural products may regulate the *Firmicutes/Bacteroidetes* ratio, increase faecal counts of potentially beneficial microbes and decrease the relative abundance of potentially pathogenic microbes. There is a dose-dependent trend in the regulation of intestinal flora by natural products, but more dose-ranging studies are needed to determine the optimal dose of natural products.

As we described above, the gut microbiota may regulate the transformation of inflammation into cancer through different inflammatory pathways. Pinocembrin, a plant-derived flavonoid, alleviates UC in mice by regulating the gut microbiota and suppressing the TLR4/MD2/NF-κB pathway (Yue et al., 2020). *Ganoderma lucidum* (GLP) was proven to be an effective natural product that protects against AOM/DSS-induced inflammation. GLP alleviates endotoxaemia by inhibiting TLR4/MyD88/NF-κB signalling, ultimately suppressing inflammatory marker expression and MAPK (JNK and ERK) activation (Guo et al., 2021). A mouse model showed that treatment with astragalin (AG) ameliorates metabolic endotoxaemia, improves intestinal mucosal barrier function, and increases the abundance of potentially beneficial bacteria (such as Ruminococcaceae) and decreases the abundance of potentially harmful bacteria (such as *Escherichia* and *Shigella*). Further experiments showed that AG inhibits the relative mRNA expression levels of TLR4 and inhibits NF-κB pathway activation (Peng et al., 2020a). Treatment with α-ketoglutarate, an important intermediary in the NF-κB-mediated inflammatory pathway, tends to minimize the proportion of opportunistic pathogens (*Escherichia* and *Enterococcus*) while increasing the proportion of *Akkermansia*, *Butyricicoccus*, *Clostridium*, and *Ruminococcus* and protecting against inflammation-related CRC (Li et al., 2019). Another study showed the therapeutic potential of lentinan in mouse models of IBD and CAC; lentinan exerts its beneficial effect in mice with IBD and CAC possibly by inhibiting TLR4/NF-κB signalling and the expression of colon cancer markers. 16S rRNA gene sequencing confirmed that lentinan treatment restores the Firmicutes/Proteobacteria ratio to nearly normal levels (Liu et al., 2019). Upregulated expression of TLR4 is a common feature in tissues from IBD and CRC patients (Burgueño et al., 2021). In human tissue microarrays, TLR4 expression increases specifically in CECs as tissues progress from normal to neoplastic stages (Santaolalla et al., 2013; Sussman et al., 2014), and epithelial TLR4 deficiency protects mice from CAC development (Fukata et al., 2009). NF-κB is a key regulator of inflammation, innate immunity, and tissue integrity (Banoth et al., 2015). Natural products can regulate inflammatory pathways and reduce the serum levels of LPS and proinflammatory cytokines (COX-2, MCP-1, TNF-α, IL-6, IL-1β, and IFN-γ), which contribute to suppressing tumorigenesis. On the other hand, natural products can also induce antitumor immunity by regulating the transformation of inflammation, which will be discussed later.

Increasing numbers of studies reveal that traditional herbal extracts have a positive relationship with decreased mortality due to a variety of chronic diseases, such as cardiovascular disease,

cancer and diabetes (Wang et al., 2020a; Bu et al., 2020). However, the physiological effects are in marked contrast to their poor bioavailability (Zhao et al., 2020; Zhi et al., 2020). Products with poor bioavailability may serve as potential substrates for the gut microbiota. These products exert therapeutic effects by modulating the composition of the gut microbiome and affecting the gut barrier (Feng et al., 2019). Akebia saponin D (ASD) significantly modifies the gut microbiome; it reduces the proportions of *Alistipes* and *Prevotella* and enhances the proportions of *Butyricimonas*, *Ruminococcus*, and *Bifidobacterium*. RNA sequencing (RNA-seq) revealed that ASD reduces lipid-induced TJ damage in intestinal epithelial cells *via* downregulation of the PPAR-γ-FABP4 pathway *in vitro* and that the PPAR-γ inhibitor (T0070907) partially blocks the effects of ASD (Yang et al., 2021). Experiments in which colitis was induced by DSS administration demonstrated that oroxylin A, a natural flavonoid, reduces susceptibility to colitis and prevents carcinogenesis in colon (Jung et al., 2012). Oroxylin A upregulates the mRNA level of Muc2 *in vivo*. Analysis of the gut microbial composition showed that treatment with oroxylin A decreases the abundance of *Akkermansia*, which has been confirmed to contribute to the breakdown of the mucus layer (Zhai et al., 2019; Wang et al., 2021c). Additionally, the abundance of *Eubacterium coprostanoligenes* is increased by oroxylin A, contributing to the protection of the colon against colitis and carcinogenesis (Bai et al., 2021). Antibiotic treatment and microbiota transplantation experiments further demonstrated that remodelling of the gut microbiota is required for the bioactivity of oroxylin A. Oroxyloside (Oroxylin A 7-O-glucuronide) is one of the main metabolites of oroxylin A (Chen et al., 2000; Kim et al., 2012; Yao et al., 2014). *In vivo* experiments demonstrate the efficacy of oroxyloside in specifically attenuating pathological damage in colon (Wang et al., 2016). Oroxyloside decreases the secretion of IL-1β, IL-6, and TNF-α, whereas this reduction is reversed by the presence of GW9662, a specific inhibitor of PPARγ. PPARγ acts as an influential pleiotropic regulator of anti-inflammatory, antioxidant, and phagocyte-mediated clearance processes (Su et al., 1999; Desreumaux et al., 2001; Cevallos et al., 2021), and it plays an important role in the physiological function of the gastrointestinal tract (Sarangdhar et al., 2021). These studies showed that natural products can reduce the abundance of bacteria that disrupt the mucus layer and increase the level of TJs, reversing the disruption of the gut mucosal barrier in the early stages of CRC tumorigenesis. The PPARγ signalling pathway plays an important role in the effects of these natural products that depend on the gut microbiota to regulate the intestinal epithelial barrier.

It is of great significance to regulate the intestinal flora and improve the TME in order to prevent and treat tumour occurrence and development. Resveratrol, which is a ligand for the aryl hydrocarbon receptor (AhR),can shift the differentiation of T cells to promote Treg differentiation instead of Th17 differentiation through receptor-ligand interactions (Singh et al., 2007). The polarization of Th17 cells toward an inflammatory state triggers tumorigenesis in CRC (Gálvez, 2014). Interestingly, recent research has shown that Th17 cells are greatly influenced by the microbiome (IvanovAtarashi et al., 2009; Atarashi et al., 2011). Moreover, experiments on mice with IBD proved that resveratrol can decrease the abundance of *B. acidifaciens*, triggering a strong inflammatory cascade response, which as expected, includes the activation of IL-17-dependent pathways (Chung et al., 2018; Alrafas et al., 2019), and attenuating colorectal inflammation. However, another experiment presented different results. Ginsenosides Rb3 and Rd promote the growth of beneficial bacteria, such as *Bifidobacterium spp*, *Lactobacillus spp*, *Bacteroides acidifaciens*, and *Bacteroides xylanisolvens*, while decreasing the abundance of cancer cachexia-associated bacteria, such as *Dysgonomonas* spp. and *Helicobacter spp*. All these changes were correlated with the regulation of proinflammatory cytokine production (Huang et al., 2017). A study on the role of Gegen Qinlian decoction in enhancing the effect of PD-1 blockade in CRC also confirmed the protective effect of *Bacteroides acidifaciens* (Lv et al., 2019). Parthenolide (PTL), a sesquiterpene lactone originally extracted from the shoots of the plant Feverfew (*Tanacetum balsamita*), has been shown to exert potent anticancer and anti-inflammatory effects (Ren et al., 2019; Freund et al., 2020). PTL-treated mice exhibit increased SCFA production, and PTL administration selectively increases the frequency of colonic regulatory T (Treg) cells and decreases the proportion of colonic T helper type 17 (Th17) cells. Notably, PTL's protective effect on colon inflammation disappeared when the gut microbiota is depleted using antibiotic cocktails (Liu et al., 2020a). Moreover, FMT confirmed this gut microbiota-dependent mechanism of action of PTL. As mentioned above, *F. nucleatum* potentiates intestinal tumorigenesis by modulating the tumour-immune microenvironment in mouse models (Kostic et al., 2013). Previous studies have reported that berberine (BBR) (Wu et al., 2012) exerts a preventative effect on colonic tumorigenesis. It has been proven BBR can reverse the *F. nucleatum*-induced imbalance of luminal microbiota and colon tumorigenesis in mice (Yu et al., 2015). These results suggest that natural products are potential therapeutic strategies for ameliorating the inflammatory-cancer transformation of CRC by modulating the gut microbiota, increasing the SCFA content, and regulating the Treg/Th17 balance. Targeting the role of microbes in the TME could improve our ability to prevent the development of cancer and activate the immune system to eliminate existing malignancies.

A number of studies have shown that natural products can inhibit CRC tumorigenesis through an integrated mechanism that involves multiple processes (Figure 1B). Natural products

regulate the composition of the gut microbiota, improve immunity by increasing beneficial bacteria and reducing harmful bacteria, modulate immune cell function and reduce inflammatory responses. Natural products can reduce the abundance of known promoters of multiple processes, such as *Escherichia coli*, Fn, and *Bacteroides fragilis*, and mediate CRC transformation by targeting both the intestinal epithelial barrier and the TME. Interestingly, the classification of healthy and unhealthy flora requires caution. More research is needed to elucidate the molecular mechanisms by which "dual-identity" bacteria elicit different responses. The complex balance between the gut microbiota and host immunity not only affects tumorigenesis but also modulates antitumor effects of personalized cancer treatments.

The effect of natural products on chemotherapeutic effects mediated by the gut microbiota

Currently, the main treatments for CRC are surgery, chemotherapy, radiotherapy, and targeted therapy. Among these options, chemotherapy is the main treatment for advanced or metastatic CRC, and chemotherapy is based on 5-fluorouracil (5-Fu) and platinum (Dekker et al., 2019). However, patients who benefit from 5-Fu-based therapy are prone to develop chemoresistance and are affected by haematopoietic and gastrointestinal toxicities (Blondy et al., 2020; Vodenkova et al., 2020). Hence, we need a new strategy to increase the efficacy of 5-Fu, overcome resistance and reduce nonspecific toxicity.

Evidence shows that the gut microbiota can regulate the effects of chemotherapeutic drugs in *in vivo* and *in vitro* models of CRC (Alexander et al., 2017; Roberti et al., 2020). Fn, which is an anaerobic parasitic bacterium, is increasingly related to CRC, and it has been demonstrated that Fn can promote chemoresistance to 5-Fu (Yu et al., 2017b; Zhang et al., 2019b). Moreover, metabolites of the gut microbiota also have the same effect. A study found that butyrate could promote the effect of oxaliplatin by modulating $CD8^+$ T cell function in the TME by activating the IL-12 signalling pathway (He et al., 2021). On the other hand, many chemotherapeutic drugs, such as 5-Fu, can lead to intestinal damage and alter the diversity of the gut microbiota (Sougiannis et al., 2019; Zhang et al., 2020). Based on these conditions, natural products can enhance the beneficial effects of chemotherapy and reduce the adverse events caused by chemotherapy by modulating the gut microbiota.

Many studies have investigated whether natural products enhance chemosensitivity and modulate the gut microbiota to reduce the adverse events caused by chemotherapeutic drugs in tumour-bearing models. Albuca bracteate polysaccharides (ABPs), which have been reported to exert anti-inflammatory, antioxidant and antitumor effects, synergistically exerted antitumor effects with 5-Fu in CT-26 tumour-bearing mice. The combination treatment resulted in dramatically higher relative abundances of *Ruminococcus*, *Anaerostipes*, and *Oscillospira* (Yuan et al., 2021). In addition, the levels of butyric acid, which is a beneficial SCFA, were higher than those in the 5-Fu treatment group. The combination of another natural product, carboxymethyl pachyman (CMP), with 5-Fu reversed the intestinal shortening and ameliorated the colon injury induced by 5-Fu in CT-26 tumour-bearing mice. Furthermore, CMP can regulate the dysbiosis of the gut microbiota caused by 5-Fu by notably increasing the abundance of *Bacteroidetes*, *Lactobacilli*, and butyric acid- and acetic acid-producing bacteria (Wang et al., 2018b). Similarly, other natural products also exert the same effects (Wang et al., 2018b; Wang et al., 2020b). Thus, the combination of 5-Fu with natural products may maximize the antitumor effect and attenuate the intestinal changes caused by 5-Fu (Figure 2A).

In addition to tumour-bearing mouse models, studies also showed that natural products could attenuate adverse events in 5-Fu-treated models. BBR, which has been used to prevent colorectal adenoma (Chen et al., 2020a), exerts a protective effect in the intestine to ameliorate 5-Fu-induced intestinal mucositis by modifying the gut microbiota in tumour-free rats (Chen et al., 2020b). This study showed that BBR could significantly increase the levels of butyrate and glutamine in faeces. In addition, compared to 5-Fu-treated rats, rats treated with BBR plus 5-Fu show decreased diarrhoea scores, reduced inflammatory responses in the ileum and alleviated intestinal mucosal injury in faecal transplantation experiments, and these changes may be associated with increased butyrate levels among faecal metabolites (Chen et al., 2020b). Similarly, a study evaluated the effects of a volatile oil from *Amomum villosum* (VOA) and its main active compound bornyl acetate (BA) on intestinal mucositis induced by 5-Fu. Both VOA and BA relieve the effects of 5-Fu, enhance the intestinal mucosal barrier and increase the abundance of probiotics, such as *Lactobacillus* (Zhang et al., 2017b). Furthermore, many other natural products exert the same effects observed in the 5-Fu-induced model (Atiq et al., 2019; Wang et al., 2020c; Wu et al., 2020). In addition, not every natural product has the potential to improve chemotherapy-induced diarrhoea. A study showed that neither *Atracylodes macrocephala* essential oil (AMO) nor *Panax ginseng* total saponins (PGS) alone could obviously improve the abnormalities caused by 5-Fu, which include diarrhoea and pathological changes in the ileum and colons. However, the combination of these two natural products suppresses the production of inflammatory cytokines in the intestine, restore the ratios of *Firmicutes*/*Bacteroidetes* (F/B) and reduce the abundance of potential

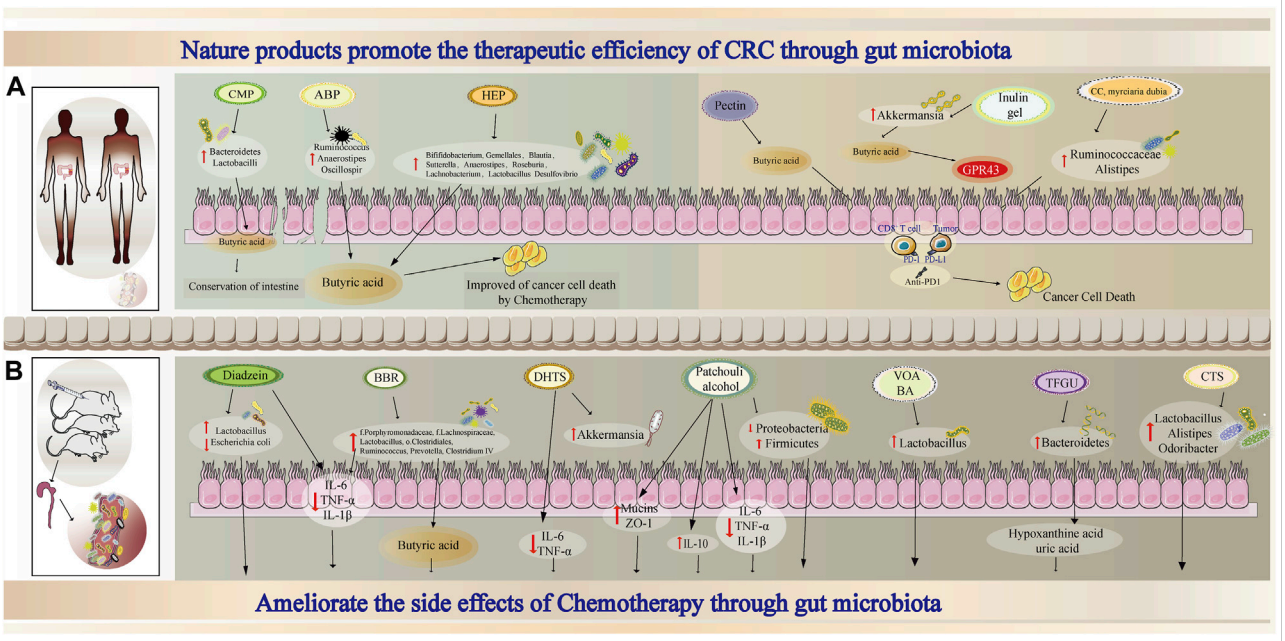

FIGURE 2
Proposed mechanism combined nature products and chemotherapy or immunotherapy through gut microbiota in oncotherapy **(A)** The combination of nature products and chemotherapy or immunotherapy enhances tumor therapeutic effect through gut microbiota **(B)** Nature products ameliorate the side effects of chemotherapy through gut microbiota.

pathogens (Wang et al., 2019). This study indicated that the combination of natural products might be a promising strategy for treating chemotherapy-induced damage.

In addition to 5-Fu, irinotecan (CPT-11) can cause diarrhoea in clinical practice because symbiotic bacterial β-glucuronidases reactivate the drug in the gut (Wallace et al., 2010). However, natural products also improved the diarrhoea caused by CPT-11 in a mouse model. Total flavonoids of *Glycyrrhiza uralensis* (TFGU) exert a protective effect on CPT-11-induced colitis by inhibiting proinflammatory responses and reverse faecal metabolic disorders, including the metabolism of hypoxanthine, uric acid, and purine (Yue et al., 2021). Moreover, crypotanshinone (CTS) relieves 5-Fu/CPT-11-induced colitis in a model of colitis-associated colon cancer (CAC) by regulating the gut microbiota, and this effect is correlated with effects on lipid metabolism (Wang et al., 2021b). Thus, natural products may modulate different chemotherapeutic drug-induced intestinal pathological changes *via* the gut microbiota and its metabolites.

Taken together, these data suggest that natural products can exert synergistic effects with chemotherapy drugs and alleviate adverse effects by modulating the gut microbiota and its metabolites (Figure 2B). Based on these characteristics and advantages, nature products can be a promising part of combined therapies.

The effect of natural products on immunotherapy mediated by the gut microbiota

In addition to the treatments we mentioned, the emergence of immunotherapy has provided a transformative new method for the comprehensive treatment of cancer. Tumour immunotherapies mainly include ICIs, cellular immunotherapy and immune vaccines; in particular, ICIs are widely used in clinical practice. Based on studies, such as KEYNOTE-177 and CheckMate-142, immunotherapy has been recommended by the 2021 NCCN guidelines for the treatment of advanced or metastatic CRC with MSI-H/dMMR (Overman et al., 2017; André et al., 2020; Andre et al., 2021). However, the incidence of dMMR CRC is approximately 5%, and the response rate ranges between 30 and 50% (Gurjao et al., 2019; Sahin et al., 2019; Vasaikar et al., 2019); thus, researchers have focused on the combination of VEGF inhibitors, chemotherapy, and many other specific inhibitors (Guangdong Provincial People's Hospital, 2022; Bristol-Myers, 2022; Tianjin Medical University Cancer Institute and Hospital, 2021). Moreover, natural products have shown promises as immunomodulatory agents. Studies have shown that compared to ICIs alone, the combination of ICIs and natural products can exert synergistic effects on CRC by promoting antigen presentation, enhancing $CD8^+$ T cell cytotoxic activity, increasing T cell infiltration and so

on (Liu et al., 2020b; Liu et al., 2020c; Lee et al., 2021; Xu et al., 2021). This may be a new strategy to transform "cold" tumours into "hot" tumours.

Currently, the gut microbiota has attracted the attention of researchers in terms of its role in antitumor immunotherapy (Cremonesi et al., 2018; Zitvogel et al., 2018; Bouferraa et al., 2021; Matson et al., 2021; Xing et al., 2021). Researchers have adopted multiple mouse models or faecal microbiota transplantation (FMT) models to reveal the relationship between the gut microbiota and ICIs (Sivan et al., 2015; Vétizou et al., 2015; Yi et al., 2018; Elkrief et al., 2019; Zhang et al., 2022). These studies suggest that both the commensal gut microbiota and that of healthy people play an important role in the immune microenvironment. This was also true in a clinical model. V. Gopalakrishnan et al. (Gopalakrishnan et al., 2018) reported that melanoma patients who responded to anti-PD-1 blockade had high abundance of *Faecalibacterium* species, and this population had longer PFS and higher levels of effector $CD4^+$ and $CD8^+$ T cells in systemic circulation. Similarly, the abundance of *B. fragilis* was related to the efficacy of CTLA-4 blockade in melanoma patients and an FMT model (Vétizou et al., 2015). Additionally, other studies described the characteristics of the gut microbiota of different patients who responded to ICIs to predict the outcomes of immunotherapy in patients with NSCLC, hepatocellular carcinoma and gastrointestinal cancer (Jin et al., 2019; Zheng et al., 2019; Peng et al., 2020b). Metabolites of the gut microbiota have also become biomarkers to predict beneficial outcomes of ICI treatment (Mager et al., 2020). Since the gut microbiota affects ICI efficacy and natural products also influence the gut microbiota and immunotherapeutic efficacy as described above, we next asked whether natural products can exert a synergistic effect with immunotherapy by affecting the gut microbiota.

First, natural products can enhance sensitivity to immunotherapy by altering the diversity of the gut microbiota and its metabolites. Inulin combined with anti-PD-1 can significantly increase the relative abundances of *Akkermansia*, *Lactobacillus* and *Roseburia*, which have been reported to be associated with ICI-responsiveness in patients. When the form of the drug administered was changed to an inulin gel, inulin gel plus anti-PD-1 therapy increased the relative abundance of *Akkermansia* and resulted in an increasing trend in the abundance of *Roseburia*. Combined treatment can increase the abundance of the beneficial commensal microbiota and SCFA metabolites to increase $Tcf1^+PD\text{-}1^+CD8^+$ T cell numbers and improve CRC tumour burden (Han et al., 2021). Similarly, dietary consumption of *Lactobacillus*-derived exopolysaccharide increases CCR6+$CD8^+$ T cell numbers in Peyer's patches and enhances ICI therapeutic effects to improve the TME (Kawanabe-Matsuda et al., 2022). Although there are few studies on the effect of the gut microbiota and its metabolites on the efficacy of ICIs in patients with CRC, there are many studies about this topic in other cancers. For example, in patients with melanoma or NSCLC, ginseng polysaccharides (GPs) combined with anti-PD-1 therapy alters the gut microbiota and increases the abundance of SCAFs, especially valeric acid, but not acetic acid. In addition, GPs affect the ratio of kynurenine/tryptophan through gut microbes to increase the response to anti-PD-1, which suppresses Tregs and activates effector T cells (Huang et al., 2021).

Second, in addition to improving sensitivity to immunotherapy, natural products can reverse CRC resistance to ICIs by modulating the balance of the gut microbiota. Polyphenol-rich berry camu-camu (CC, *Myrciaria dubia*), which exerts no antitumour effect when administered orally, exerts a synergistic effect when combined with αPD-1 mAb. In addition, oral administration of castalagin, which is an active compound of CC, can enrich bacterial species associated with efficient immunotherapeutic responses (*Ruminococcaceae* and *Alistipes*) and enhance the $CD8^+/FoxP3^+CD4^+$ ratio in the TME; additionally, it can act as a prebiotic to circumvent anti-PD-1 resistance (Messaoudene et al., 2022). Similarly, pectin reverses the effect of anti-PD-1 in humanized tumour-bearing mice transplanted with the gut microbiota from CRC patients and promotes T cell infiltration and activation (Zhang et al., 2021). Moreover, the results demonstrated that in the individuals administered the combination treatment, unique bacterial modules composed of butyrate-producing bacteria exhibit a better response to immunotherapy. These studies reveal that natural products can reverse CRC resistance to ICIs by modulating the balance of the gut microbiota and provide a new potential approach for overcoming immune resistance.

Finally, ICIs are associated with clinical benefits across cancer types but may be accompanied by adverse events to some extent. A study demonstrated that the abundance of *Bacteroides intestinalis* is correlated with IL-1β production and toxicity caused by the combination of CTLA-4 and PD-1 blockade in patients with melanoma (Andrews et al., 2021). However, more preclinical experiments and clinical practice are still needed to ameliorate the toxicity associated with ICIs; in particular, larger sample sizes are required to explore the alteration of the gut microbiota under these conditions.

Conclusion and perspectives

The development of CRC is a complex pathophysiological process, and the gut microbiota plays an essential role in both inflammation-induced tumour development and tumour treatments. The gut microbiota, which can be used as a biomarker or a prognostic factor, has also become a new target for identifying responses to disease development and treatments. Similarly, natural products, which have the advantages of being easily available, being widely used, and having multiple targets, have also become a promising

method for preventing the development of disease, reducing inflammation, modulating immunity and reversing resistance.

The current research about the prevention of tumorigenesis by natural products and the intestinal flora has highlighted the factors involved in the activation of signalling pathways and improvements in functions that were used to initially elucidate the underlying mechanisms and develop new treatment strategies. Antibiotic depletion and FMT were used to validate causal relationships between natural products and the gut microbiota; the transplantation of the faecal microbiota from donors with diseases who had received treatments protect mice against colitis (Liu et al., 2020a) or colon carcinogenesis (Parker et al., 2021). This indicates the potential role of natural products in preventing tumorigenesis by modifying the intestinal microflora. However, further FMT experiments involving healthy donors and healthy donors treated with natural products (Sui et al., 2020) are needed to explore the complex relationship between natural products and the microbiota. Recent studies have revealed the existence of interactions between the host and intestinal flora (Yang et al., 2018). Currently, representative sets of multiomics studies (Lloyd-Price et al., 2019; Mars et al., 2020) are available for the in-depth analysis of the gut microbiota to understand the molecular mechanisms by which it affects tumorigenesis and tumour progression. These efficient experimental strategies will contribute to the development of effective treatments, which will ultimately prevent tumorigenesis.

The present study provides insights into CRC therapy. There is a delicate balance between epithelial, microbial, and immune cell interactions, and disruption or deviation from this balance can lead to risks of tumour promoting. The use of natural products in treatments allows multiple molecules and processes to be targeted and is a valuable clinical approach for preventing tumorigenesis. These targets include remodelling the normal host/microbial symbiosis system, maintaining the intestinal epithelial mucosal barrier, inhibiting tumour-promoting T regulatory cells, Th17 cells and inflammatory cells, and improving the TME. Natural products can regulate the intestinal flora, improve the efficacy of chemotherapy or immunotherapy, and reduce the adverse effects of some chemotherapy drugs. With the development of additional targeted drugs and immunotherapeutic approaches, researchers are exploring drug combinations to promote optimal antitumor effects. This provides prospects for the potential clinical application of natural products in preventing inflammation from transforming into CRC and in comprehensively treating CRC.

Author contributions

HX and GJ proposed the topic, design the frame and made final revision. LL and JD contributed to original draft preparation and image drawing. YL, YQ, and GZ participated in part of text arrangement and literature collection. WZ and AZ revised the manuscript. All authors have approved the final version of the manuscript.

Funding

This work was supported by the National Nature Science Foundation of China (No. 81874206, 82104466, China), Shanghai Frontiers Science Center of Disease and Syndrome Biology of Inflammatory Cancer Transformation (No.2021KJ03-12, China), Shanghai Rising-Star Program (No. 20QA1409300, China), and the Program for Young Eastern Scholar at Shanghai Institutions of Higher Learning (NoQD2019034).

Conflict of interest

The authors declare that the research was conducted in the absence of any commercial or financial relationships that could be construed as a potential conflict of interest.

Publisher's note

All claims expressed in this article are solely those of the authors and do not necessarily represent those of their affiliated organizations, or those of the publisher, the editors and the reviewers. Any product that may be evaluated in this article, or claim that may be made by its manufacturer, is not guaranteed or endorsed by the publisher.

References

Alexander, J. L., Wilson, I. D., Teare, J., Marchesi, J. R., Nicholson, J. K., and Kinross, J. M. (2017). Gut microbiota modulation of chemotherapy efficacy and toxicity. *Nat. Rev. Gastroenterol. Hepatol.* 14, 356–365. doi:10.1038/nrgastro.2017.20

Almeida, A., Mitchell, A. L., Boland, M., Forster, S. C., Gloor, G. B., Tarkowska, A., et al. (2019). A new genomic blueprint of the human gut microbiota. *Nature* 568, 499–504. doi:10.1038/s41586-019-0965-1

Alrafas, H. R., Busbee, P. B., Nagarkatti, M., and Nagarkatti, P. S. (2019). Resveratrol modulates the gut microbiota to prevent murine colitis development through induction of Tregs and suppression of Th17 cells. *J. Leukoc. Biol.* 106, 467–480. doi:10.1002/JLB.3A1218-476RR

Andre, T., Amonkar, M., Norquist, J. M., Shiu, K. K., Kim, T. W., Jensen, B. V., et al. (2021). Health-related quality of life in patients with microsatellite instability-high or mismatch repair deficient metastatic colorectal cancer treated with first-line

pembrolizumab versus chemotherapy (KEYNOTE-177): An open-label, randomised, phase 3 trial. *Lancet. Oncol.* 22, 665–677. doi:10.1016/S1470-2045(21)00064-4

André, T., Shiu, K. K., Kim, T. W., Jensen, B. V., Jensen, L. H., Punt, C., et al. (2020). Pembrolizumab in microsatellite-instability-high advanced colorectal cancer. *N. Engl. J. Med.* 383, 2207–2218. doi:10.1056/NEJMoa2017699

Andrews, M. C., Duong, C. P. M., Gopalakrishnan, V., Iebba, V., Chen, W. S., Derosa, L., et al. (2021). Gut microbiota signatures are associated with toxicity to combined CTLA-4 and PD-1 blockade. *Nat. Med.* 27, 1432–1441. doi:10.1038/s41591-021-01406-6

Appleyard, C. B., Cruz, M. L., Isidro, A. A., Arthur, J. C., Jobin, C., and De Simone, C. (2011). Pretreatment with the probiotic VSL#3 delays transition from inflammation to dysplasia in a rat model of colitis-associated cancer. *Am. J. Physiol. Gastrointest. Liver Physiol.* 301, G1004–G1013. doi:10.1152/ajpgi.00167.2011

Arpaia, N., Campbell, C., Fan, X., Dikiy, S., van der Veeken, J., deRoos, P., et al. (2013). Metabolites produced by commensal bacteria promote peripheral regulatory T-cell generation. *Nature* 504, 451–455. doi:10.1038/nature12726

Atarashi, K., Tanoue, T., Shima, T., Imaoka, A., Kuwahara, T., Momose, Y., et al. (2011). Induction of colonic regulatory T cells by indigenous Clostridium species. *Science* 331, 337–341. doi:10.1126/science.1198469

Atiq, A., Shal, B., Naveed, M., Khan, A., Ali, J., Zeeshan, S., et al. (2019). Diadzein ameliorates 5-fluorouracil-induced intestinal mucositis by suppressing oxidative stress and inflammatory mediators in rodents. *Eur. J. Pharmacol.* 843, 292–306. doi:10.1016/j.ejphar.2018.12.014

Azab, M. E., Morsy, T. A., Abdel-Aal, T. M., Safar, E. H., Makaram, S. S., el Hady, H. M., et al. (1988). Current prevalence of trichinosis in pigs in Egypt. *J. Egypt. Soc. Parasitol.* 18, 383–389.

Bai, D., Sun, T., Zhao, J., Du, J., Bu, X., Cao, W., et al. (2021). Oroxylin A maintains the colonic mucus barrier to reduce disease susceptibility by reconstituting a dietary fiber-deprived gut microbiota. *Cancer Lett.* 515, 73–85. doi:10.1016/j.canlet.2021.05.018

Banoth, B., Chatterjee, B., Vijayaragavan, B., Prasad, M. V., Roy, P., and Basak, S. (2015). Stimulus-selective crosstalk via the NF-κB signaling system reinforces innate immune response to alleviate gut infection. *Elife* 4. doi:10.7554/eLife.05648

Baumann, P., and Jonzier-Perey, M. (1988). GC and GC-MS procedures for simultaneous phenotyping with dextromethorphan and mephenytoin. *Clin. Chim. Acta.* 171, 211–222. doi:10.1016/0009-8981(88)90146-5

Baxter, N. T., Zackular, J. P., Chen, G. Y., and Schloss, P. D. (2014). Structure of the gut microbiome following colonization with human feces determines colonic tumor burden. *Microbiome* 2, 20. doi:10.1186/2049-2618-2-20

Blondy, S., David, V., Verdier, M., Mathonnet, M., Perraud, A., and Christou, N. (2020). 5-Fluorouracil resistance mechanisms in colorectal cancer: From classical pathways to promising processes. *Cancer Sci.* 111, 3142–3154. doi:10.1111/cas.14532

Bloom, S. M., Bijanki, V. N., Nava, G. M., Sun, L., Malvin, N. P., Donermeyer, D. L., et al. (2011). Commensal Bacteroides species induce colitis in host-genotype-specific fashion in a mouse model of inflammatory bowel disease. *Cell. Host Microbe* 9, 390–403. doi:10.1016/j.chom.2011.04.009

Bouferraa, Y., Chedid, A., Amhaz, G., El Lakkiss, A., Mukherji, D., Temraz, S., et al. (2021). The role of gut microbiota in overcoming resistance to checkpoint inhibitors in cancer patients: Mechanisms and challenges. *Int. J. Mol. Sci.* 22, 8036. doi:10.3390/ijms22158036

Bristol-Myers, S. (2022). An investigational immuno-therapy study of nivolumab, and nivolumab in combination with other anti-cancer drugs, in colon cancer that has come back or has spread (CheckMate142).NCT02060188. Available from: https://clinicaltrials.gov/ct2/show/NCT02060188?cond=NCT02060188&draw=2&rank=1.

Bu, L., Dai, O., Zhou, F., Liu, F., Chen, J. F., Peng, C., et al. (2020). Traditional Chinese medicine formulas, extracts, and compounds promote angiogenesis. *Biomed. Pharmacother.* 132, 110855. doi:10.1016/j.biopha.2020.110855

Burgueño, J. F., Fritsch, J., González, E. E., Landau, K. S., Santander, A. M., Fernández, I., et al. (2021). Epithelial TLR4 signaling activates DUOX2 to induce microbiota-driven tumorigenesis. *Gastroenterology* 160, 797–808.e6. doi:10.1053/j.gastro.2020.10.031

Cevallos, S. A., Lee, J. Y., Velazquez, E. M., Foegeding, N. J., Shelton, C. D., Tiffany, C. R., et al. (2021). 5-Aminosalicylic acid ameliorates colitis and checks dysbiotic *Escherichia coli* expansion by activating PPAR-γ signaling in the intestinal epithelium. *mBio* 12, e03227–20. doi:10.1128/mBio.03227-20

Chen, H., Zhang, F., Li, R., Liu, Y., Wang, X., Zhang, X., et al. (2020). Berberine regulates fecal metabolites to ameliorate 5-fluorouracil induced intestinal mucositis through modulating gut microbiota. *Biomed. Pharmacother.* 124, 109829. doi:10.1016/j.biopha.2020.109829

Chen, Y., Yang, L., and Lee, T. J. (2000). Oroxylin A inhibition of lipopolysaccharide-induced iNOS and COX-2 gene expression via suppression of nuclear factor-kappaB activation. *Biochem. Pharmacol.* 59, 1445–1457. doi:10.1016/s0006-2952(00)00255-0

Chen, Y. X., Gao, Q. Y., Zou, T. H., Wang, B. M., Liu, S. D., Sheng, J. Q., et al. (2020). Berberine versus placebo for the prevention of recurrence of colorectal adenoma: A multicentre, double-blinded, randomised controlled study. *Lancet. Gastroenterol. Hepatol.* 5, 267–275. doi:10.1016/S2468-1253(19)30409-1

Cheng, Y., Ling, Z., and Li, L. (2020). The intestinal microbiota and colorectal cancer. *Front. Immunol.* 11, 615056. doi:10.3389/fimmu.2020.615056

Chung, L., Thiele Orberg, E., Geis, A. L., Chan, J. L., Fu, K., DeStefano Shields, C. E., et al. (2018). Bacteroides fragilis toxin coordinates a pro-carcinogenic inflammatory cascade via targeting of colonic epithelial cells. *Cell. Host Microbe* 23, 203–214.e5. doi:10.1016/j.chom.2018.01.007

Cremonesi, E., Governa, V., Garzon, J. F. G., Mele, V., Amicarella, F., Muraro, M. G., et al. (2018). Gut microbiota modulate T cell trafficking into human colorectal cancer. *Gut* 67, 1984–1994. doi:10.1136/gutjnl-2016-313498

De Santis, S., Cavalcanti, E., Mastronardi, M., Jirillo, E., and Chieppa, M. (2015). Nutritional keys for intestinal barrier modulation. *Front. Immunol.* 6, 612. doi:10.3389/fimmu.2015.00612

Dekker, E., Tanis, P. J., Vleugels, J. L. A., Kasi, P. M., and Wallace, M. B. (2019). Colorectal cancer. *Lancet* 394, 1467–1480. doi:10.1016/S0140-6736(19)32319-0

Desreumaux, P., Dubuquoy, L., Nutten, S., Peuchmaur, M., Englaro, W., Schoonjans, K., et al. (2001). Attenuation of colon inflammation through activators of the retinoid X receptor (RXR)/peroxisome proliferator-activated receptor gamma (PPARgamma) heterodimer. A basis for new therapeutic strategies. *J. Exp. Med.* 193, 827–838. doi:10.1084/jem.193.7.827

Elkrief, A., Derosa, L., Zitvogel, L., Kroemer, G., and Routy, B. (2019). The intimate relationship between gut microbiota and cancer immunotherapy. *Gut Microbes* 10, 424–428. doi:10.1080/19490976.2018.1527167

Etxeberria, U., Arias, N., Boqué, N., Macarulla, M. T., Portillo, M. P., Martínez, J. A., et al. (2015). Reshaping faecal gut microbiota composition by the intake of trans-resveratrol and quercetin in high-fat sucrose diet-fed rats. *J. Nutr. Biochem.* 26, 651–660. doi:10.1016/j.jnutbio.2015.01.002

Eun, C. S., Kwak, M. J., Han, D. S., Lee, A. R., Park, D. I., Yang, S. K., et al. (2016). Does the intestinal microbial community of Korean Crohn's disease patients differ from that of Western patients? *BMC Gastroenterol.* 16, 28. doi:10.1186/s12876-016-0437-0

Feng, Q., Liang, S., Jia, H., Stadlmayr, A., Tang, L., Lan, Z., et al. (2015). Gut microbiome development along the colorectal adenoma-carcinoma sequence. *Nat. Commun.* 6, 6528. doi:10.1038/ncomms7528

Feng, W., Ao, H., Peng, C., and Yan, D. (2019). Gut microbiota, a new frontier to understand traditional Chinese medicines. *Pharmacol. Res.* 142, 176–191. doi:10.1016/j.phrs.2019.02.024

Freund, R. R. A., Gobrecht, P., Fischer, D., and Arndt, H. D. (2020). Advances in chemistry and bioactivity of parthenolide. *Nat. Prod. Rep.* 37, 541–565. doi:10.1039/c9np00049f

Fukata, M., Hernandez, Y., Conduah, D., Cohen, J., Chen, A., Breglio, K., et al. (2009). Innate immune signaling by Toll-like receptor-4 (TLR4) shapes the inflammatory microenvironment in colitis-associated tumors. *Inflamm. Bowel Dis.* 15, 997–1006. doi:10.1002/ibd.20880

Gagnière, J., Raisch, J., Veziant, J., Barnich, N., Bonnet, R., Buc, E., et al. (2016). Gut microbiota imbalance and colorectal cancer. *World J. Gastroenterol.* 22, 501–518. doi:10.3748/wjg.v22.i2.501

Gálvez, J. (2014). Role of Th17 cells in the pathogenesis of human IBD. *ISRN Inflamm.* 2014, 928461. doi:10.1155/2014/928461

Ganesh, B. P., Klopfleisch, R., Loh, G., and Blaut, M. (2013). Commensal Akkermansia muciniphila exacerbates gut inflammation in Salmonella Typhimurium-infected gnotobiotic mice. *PLoS One* 8, e74963. doi:10.1371/journal.pone.0074963

Gao, Z., Guo, B., Gao, R., Zhu, Q., and Qin, H. (2015). Microbiota disbiosis is associated with colorectal cancer. *Front. Microbiol.* 6, 20. doi:10.3389/fmicb.2015.00020

Gethings-Behncke, C., Coleman, H. G., Jordao, H. W. T., Longley, D. B., Crawford, N., Murray, L. J., et al. (2020). Fusobacterium nucleatum in the colorectum and its association with cancer risk and survival: A systematic review and meta-analysis. *Cancer Epidemiol. Biomarkers Prev.* 29, 539–548. doi:10.1158/1055-9965.EPI-18-1295

Ghanavati, R., Akbari, A., Mohammadi, F., Asadollahi, P., Javadi, A., Talebi, M., et al. (2020). Lactobacillus species inhibitory effect on colorectal cancer progression through modulating the Wnt/β-catenin signaling pathway. *Mol. Cell. Biochem.* 470, 1–13. doi:10.1007/s11010-020-03740-8

Gnauck, A., Lentle, R. G., and Kruger, M. C. (2016). The characteristics and function of bacterial lipopolysaccharides and their endotoxic potential in humans. *Int. Rev. Immunol.* 35, 189–218. doi:10.3109/08830185.2015.1087518

Gopalakrishnan, V., Spencer, C. N., Nezi, L., Reuben, A., Andrews, M. C., Karpinets, T. V., et al. (2018). Gut microbiome modulates response to anti-PD-1 immunotherapy in melanoma patients. *Science* 359, 97–103. doi:10.1126/science.aan4236

Greten, F. R., Eckmann, L., Greten, T. F., Park, J. M., Li, Z. W., Egan, L. J., et al. (2004). IKKbeta links inflammation and tumorigenesis in a mouse model of colitis-associated cancer. *Cell.* 118, 285–296. doi:10.1016/j.cell.2004.07.013

Groschwitz, K. R., and Hogan, S. P. (2009). Intestinal barrier function: Molecular regulation and disease pathogenesis. *J. Allergy Clin. Immunol.* 124, 3–20. quiz 1-2. doi:10.1016/j.jaci.2009.05.038

Guangdong Provincial People's Hospital (2022). PD-1 inhibitors combined with VEGF inhibitors for locally advanced dMMR/MSI-H colorectal cancer. NCT04715633. Available from: https://clinicaltrials.gov/ct2/show/NCT04715633?cond=NCT04715633&draw=2&rank=1.

Guo, C., Guo, D., Fang, L., Sang, T., Wu, J., Guo, C., et al. (2021). Ganoderma lucidum polysaccharide modulates gut microbiota and immune cell function to inhibit inflammation and tumorigenesis in colon. *Carbohydr. Polym.* 267, 118231. doi:10.1016/j.carbpol.2021.118231

Gurjao, C., Liu, D., Hofree, M., AlDubayan, S. H., Wakiro, I., Su, M. J., et al. (2019). Intrinsic resistance to immune checkpoint blockade in a mismatch repair-deficient colorectal cancer. *Cancer Immunol. Res.* 7, 1230–1236. doi:10.1158/2326-6066.CIR-18-0683

Han, K., Nam, J., Xu, J., Sun, X., Huang, X., Animasahun, O., et al. (2021). Generation of systemic antitumour immunity via the *in situ* modulation of the gut microbiome by an orally administered inulin gel. *Nat. Biomed. Eng.* 5, 1377–1388. doi:10.1038/s41551-021-00749-2

Hanus, M., Parada-Venegas, D., Landskron, G., Wielandt, A. M., Hurtado, C., Alvarez, K., et al. (2021). Immune system, microbiota, and microbial metabolites: The unresolved triad in colorectal cancer microenvironment. *Front. Immunol.* 12, 612826. doi:10.3389/fimmu.2021.612826

He, Y., Fu, L., Li, Y., Wang, W., Gong, M., Zhang, J., et al. (2021). Gut microbial metabolites facilitate anticancer therapy efficacy by modulating cytotoxic CD8(+) T cell immunity. *Cell. Metab.* 33, 988–1000.e7. doi:10.1016/j.cmet.2021.03.002

He, Z., Huang, Z., Zhou, W., Tang, Z., Ma, R., and Liang, J. (2016). Anti-biofilm activities from resveratrol against Fusobacterium nucleatum. *Front. Microbiol.* 7, 1065. doi:10.3389/fmicb.2016.01065

Huang, F., Zheng, X., Ma, X., Jiang, R., Zhou, W., Zhou, S., et al. (2019). Theabrownin from Pu-erh tea attenuates hypercholesterolemia via modulation of gut microbiota and bile acid metabolism. *Nat. Commun.* 10, 4971. doi:10.1038/s41467-019-12896-x

Huang, G., Khan, I., Li, X., Chen, L., Leong, W., Ho, L. T., et al. (2017). Ginsenosides Rb3 and Rd reduce polyps formation while reinstate the dysbiotic gut microbiota and the intestinal microenvironment in Apc(Min/+) mice. *Sci. Rep.* 7, 12552. doi:10.1038/s41598-017-12644-5

Huang, J., Liu, D., Wang, Y., Liu, L., Li, J., Yuan, J., et al. (2021). Ginseng polysaccharides alter the gut microbiota and kynurenine/tryptophan ratio, potentiating the antitumour effect of antiprogrammed cell death 1/programmed cell death ligand 1 (anti-PD-1/PD-L1) immunotherapy. *Gut* 71, 734–745. doi:10.1136/gutjnl-2020-321031

Iida, N., Dzutsev, A., Stewart, C. A., Smith, L., Bouladoux, N., Weingarten, R. A., et al. (2013). Commensal bacteria control cancer response to therapy by modulating the tumor microenvironment. *Science* 342, 967–970. doi:10.1126/science.1240527

Inan, M. S., Rasoulpour, R. J., Yin, L., Hubbard, A. K., Rosenberg, D. W., and Giardina, C. (2000). The luminal short-chain fatty acid butyrate modulates NF-kappaB activity in a human colonic epithelial cell line. *Gastroenterology* 118, 724–734. doi:10.1016/s0016-5085(00)70142-9

IvanovII, Atarashi, K., Manel, N., Brodie, E. L., Shima, T., Karaoz, U., et al. (2009). Induction of intestinal Th17 cells by segmented filamentous bacteria. *Cell.* 139, 485–498. doi:10.1016/j.cell.2009.09.033

Janney, A., Powrie, F., and Mann, E. H. (2020). Host-microbiota maladaptation in colorectal cancer. *Nature* 585, 509–517. doi:10.1038/s41586-020-2729-3

Jin, Y., Dong, H., Xia, L., Yang, Y., Zhu, Y., Shen, Y., et al. (2019). The diversity of gut microbiome is associated with favorable responses to anti-programmed death 1 immunotherapy in Chinese patients with NSCLC. *J. Thorac. Oncol.* 14, 1378–1389. doi:10.1016/j.jtho.2019.04.007

Jung, M. A., Jang, S. E., Hong, S. W., Hana, M. J., and Kim, D. H. (2012). The role of intestinal microflora in anti-inflammatory effect of baicalin in mice. *Biomol. Ther.* 20, 36–42. doi:10.4062/biomolther.2012.20.1.036

Kawanabe-Matsuda, H., Takeda, K., Nakamura, M., Makino, S., Karasaki, T., Kakimi, K., et al. (2022). *Dietary Lactobacillus-derived exopolysaccharide enhances immune checkpoint blockade therapy*. *Cancer Discov* 12, 1336–1355. doi:10.1158/2159-8290.CD-21-0929

Keller, D. S., Windsor, A., Cohen, R., and Chand, M. (2019). Colorectal cancer in inflammatory bowel disease: Review of the evidence. *Tech. Coloproctol.* 23, 3–13. doi:10.1007/s10151-019-1926-2

Kim, D. H., Yun, C. H., Kim, M. H., Naveen Kumar, C., Yun, B. H., Shin, J. S., et al. (2012). 4'-bromo-5, 6, 7-trimethoxyflavone represses lipopolysaccharide-induced iNOS and COX-2 expressions by suppressing the NF-κB signaling pathway in RAW 264.7 macrophages. *Bioorg. Med. Chem. Lett.* 22, 700–705. doi:10.1016/j.bmcl.2011.10.067

Kishore, C., and Bhadra, P. (2021). Current advancements and future perspectives of immunotherapy in colorectal cancer research. *Eur. J. Pharmacol.* 893, 173819. doi:10.1016/j.ejphar.2020.173819

Knights, D., Lassen, K. G., and Xavier, R. J. (2013). Advances in inflammatory bowel disease pathogenesis: Linking host genetics and the microbiome. *Gut* 62, 1505–1510. doi:10.1136/gutjnl-2012-303954

Kostic, A. D., Chun, E., Robertson, L., Glickman, J. N., Gallini, C. A., Michaud, M., et al. (2013). Fusobacterium nucleatum potentiates intestinal tumorigenesis and modulates the tumor-immune microenvironment. *Cell. Host Microbe* 14, 207–215. doi:10.1016/j.chom.2013.07.007

Kurosaka, K., Chen, Q., Yarovinsky, F., Oppenheim, J. J., and Yang, D. (2005). Mouse cathelin-related antimicrobial peptide chemoattracts leukocytes using formyl peptide receptor-like 1/mouse formyl peptide receptor-like 2 as the receptor and acts as an immune adjuvant. *J. Immunol.* 174, 6257–6265. doi:10.4049/jimmunol.174.10.6257

Lee, E. J., Kim, J. H., Kim, T. I., Kim, Y. J., Pak, M. E., Jeon, C. H., et al. (2021). Sanguisorbae radix suppresses colorectal tumor growth through PD-1/PD-L1 blockade and synergistic effect with pembrolizumab in a humanized PD-L1-expressing colorectal cancer mouse model. *Front. Immunol.* 12, 737076. doi:10.3389/fimmu.2021.737076

Li, S., Fu, C., Zhao, Y., and He, J. (2019). Intervention with α-ketoglutarate ameliorates colitis-related colorectal carcinoma via modulation of the gut microbiome. *Biomed. Res. Int.* 2019, 8020785. doi:10.1155/2019/8020785

Li, T. T., Ogino, S., and Qian, Z. R. (2014). Toll-like receptor signaling in colorectal cancer: Carcinogenesis to cancer therapy. *World J. Gastroenterol.* 20, 17699–17708. doi:10.3748/wjg.v20.i47.17699

Li, Y., Kundu, P., Seow, S. W., de Matos, C. T., Aronsson, L., Chin, K. C., et al. (2012). Gut microbiota accelerate tumor growth via c-jun and STAT3 phosphorylation in APCMin/+ mice. *Carcinogenesis* 33, 1231–1238. doi:10.1093/carcin/bgs137

Liang, W., Peng, X., Li, Q., Wang, P., Lv, P., Song, Q., et al. (2020). FAM3D is essential for colon homeostasis and host defense against inflammation associated carcinogenesis. *Nat. Commun.* 11, 5912. doi:10.1038/s41467-020-19691-z

Liu, F., Ran, F., He, H., and Chen, L. (2020). Astragaloside IV exerts anti-tumor effect on murine colorectal cancer by Re-educating tumor-associated macrophage. *Arch. Immunol. Ther. Exp.* 68, 33. doi:10.1007/s00005-020-00598-y

Liu, W., Fan, T., Li, M., Zhang, G., Guo, W., Yang, X., et al. (2020). Andrographolide potentiates PD-1 blockade immunotherapy by inhibiting COX2-mediated PGE2 release. *Int. Immunopharmacol.* 81, 106206. doi:10.1016/j.intimp.2020.106206

Liu, Y., Zhao, J., Zhao, Y., Zong, S., Tian, Y., Chen, S., et al. (2019). Therapeutic effects of lentinan on inflammatory bowel disease and colitis-associated cancer. *J. Cell. Mol. Med.* 23, 750–760. doi:10.1111/jcmm.13897

Liu, Y. J., Tang, B., Wang, F. C., Tang, L., Lei, Y. Y., Luo, Y., et al. (2020). Parthenolide ameliorates colon inflammation through regulating Treg/Th17 balance in a gut microbiota-dependent manner. *Theranostics* 10, 5225–5241. doi:10.7150/thno.43716

Lloyd-Price, J., Arze, C., Ananthakrishnan, A. N., Schirmer, M., Avila-Pacheco, J., Poon, T. W., et al. (2019). Multi-omics of the gut microbial ecosystem in inflammatory bowel diseases. *Nature* 569, 655–662. doi:10.1038/s41586-019-1237-9

Lopès, A., Billard, E., Casse, A. H., Villéger, R., Veziant, J., Roche, G., et al. (2020). Colibactin-positive *Escherichia coli* induce a procarcinogenic immune environment leading to immunotherapy resistance in colorectal cancer. *Int. J. Cancer* 146, 3147–3159. doi:10.1002/ijc.32920

Lu, L., Liu, Y. J., Cheng, P. Q., Hu, D., Xu, H. C., and Ji, G. (2021). Macrophages play a role in inflammatory transformation of colorectal cancer. *World J. Gastrointest. Oncol.* 13, 2013–2028. doi:10.4251/wjgo.v13.i12.2013

Lv, J., Jia, Y., Li, J., Kuai, W., Li, Y., Guo, F., et al. (2019). Gegen Qinlian decoction enhances the effect of PD-1 blockade in colorectal cancer with microsatellite

stability by remodelling the gut microbiota and the tumour microenvironment. *Cell. Death Dis.* 10, 415. doi:10.1038/s41419-019-1638-6

Lynch, S. V., and Pedersen, O. (2016). The human intestinal microbiome in health and disease. *N. Engl. J. Med.* 375, 2369–2379. doi:10.1056/NEJMra1600266

Ma, H. Q., Yu, T. T., Zhao, X. J., Zhang, Y., and Zhang, H. J. (2018). Fecal microbial dysbiosis in Chinese patients with inflammatory bowel disease. *World J. Gastroenterol.* 24, 1464–1477. doi:10.3748/wjg.v24.i13.1464

Machiels, K., Sabino, J., Vandermosten, L., Joossens, M., Arijs, I., de Bruyn, M., et al. (2017). Specific members of the predominant gut microbiota predict pouchitis following colectomy and IPAA in UC. *Gut* 66, 79–88. doi:10.1136/gutjnl-2015-309398

Mager, L. F., Burkhard, R., Pett, N., Cooke, N. C. A., Brown, K., Ramay, H., et al. (2020). Microbiome-derived inosine modulates response to checkpoint inhibitor immunotherapy. *Science* 369, 1481–1489. doi:10.1126/science.abc3421

Man, S. M., Kaakoush, N. O., and Mitchell, H. M. (2011). The role of bacteria and pattern-recognition receptors in Crohn's disease. *Nat. Rev. Gastroenterol. Hepatol.* 8, 152–168. doi:10.1038/nrgastro.2011.3

Mars, R. A. T., Yang, Y., Ward, T., Houtti, M., Priya, S., Lekatz, H. R., et al. (2020). Longitudinal multi-omics reveals subset-specific mechanisms underlying irritable bowel syndrome. *Cell.* 182, 1137–1140. doi:10.1016/j.cell.2020.10.040

Matson, V., Chervin, C. S., and Gajewski, T. F. (2021). Cancer and the microbiome-influence of the commensal microbiota on cancer, immune responses, and immunotherapy. *Gastroenterology* 160, 600–613. doi:10.1053/j.gastro.2020.11.041

McFadden, R. M., Larmonier, C. B., Shehab, K. W., Midura-Kiela, M., Ramalingam, R., Harrison, C. A., et al. (2015). The role of curcumin in modulating colonic microbiota during colitis and colon cancer prevention. *Inflamm. Bowel Dis.* 21, 2483–2494. doi:10.1097/MIB.0000000000000522

Ménard, S., Förster, V., Lotz, M., Gütle, D., Duerr, C. U., Gallo, R. L., et al. (2008). Developmental switch of intestinal antimicrobial peptide expression. *J. Exp. Med.* 205, 183–193. doi:10.1084/jem.20071022

Messaoudene, M., Pidgeon, R., Richard, C., Ponce, M., Diop, K., Benlaifaoui, M., et al. (2022). A natural Polyphenol exerts antitumor activity and circumvents anti-PD-1 resistance through effects on the gut microbiota. *Cancer Discov.* 12, 1070–1087. doi:10.1158/2159-8290.CD-21-0808

Mima, K., Sukawa, Y., Nishihara, R., Qian, Z. R., Yamauchi, M., Inamura, K., et al. (2015). Fusobacterium nucleatum and T cells in colorectal carcinoma. *JAMA Oncol.* 1, 653–661. doi:10.1001/jamaoncol.2015.1377

Ng, K. M., Ferreyra, J. A., Higginbottom, S. K., Lynch, J. B., Kashyap, P. C., Gopinath, S., et al. (2013). Microbiota-liberated host sugars facilitate post-antibiotic expansion of enteric pathogens. *Nature* 502, 96–99. doi:10.1038/nature12503

Niu, H., Xing, J. H., Zou, B. S., Shi, C. W., Huang, H. B., Jiang, Y. L., et al. (2021). Immune evaluation of recombinant Lactobacillus plantarum with surface display of HA1-DCpep in mice. *Front. Immunol.* 12, 800965. doi:10.3389/fimmu.2021.800965

Overman, M. J., McDermott, R., Leach, J. L., Lonardi, S., Lenz, H. J., Morse, M. A., et al. (2017). Nivolumab in patients with metastatic DNA mismatch repair-deficient or microsatellite instability-high colorectal cancer (CheckMate 142): An open-label, multicentre, phase 2 study. *Lancet. Oncol.* 18, 1182–1191. doi:10.1016/S1470-2045(17)30422-9

Parker, K. D., Maurya, A. K., Ibrahim, H., Rao, S., Hove, P. R., Kumar, D., et al. (2021). Dietary rice bran-modified human gut microbial consortia confers protection against colon carcinogenesis following fecal transfaunation. *Biomedicines* 9, 144. doi:10.3390/biomedicines9020144

Pascal, V., Pozuelo, M., Borruel, N., Casellas, F., Campos, D., Santiago, A., et al. (2017). A microbial signature for Crohn's disease. *Gut* 66, 813–822. doi:10.1136/gutjnl-2016-313235

Peng, L., Gao, X., Nie, L., Xie, J., Dai, T., Shi, C., et al. (2020). Astragalin attenuates dextran sulfate sodium (DSS)-Induced acute experimental colitis by alleviating gut microbiota dysbiosis and inhibiting NF-κB activation in mice. *Front. Immunol.* 11, 2058. doi:10.3389/fimmu.2020.02058

Peng, Z., Cheng, S., Kou, Y., Wang, Z., Jin, R., Hu, H., et al. (2020). The gut microbiome is associated with clinical response to anti-PD-1/PD-L1 immunotherapy in gastrointestinal cancer. *Cancer Immunol. Res.* 8, 1251–1261. doi:10.1158/2326-6066.CIR-19-1014

Potrykus, M., Czaja-Stolc, S., Stankiewicz, M., Kaska, Ł., and Małgorzewicz, S. (2021). Intestinal microbiota as a contributor to chronic inflammation and its potential modifications. *Nutrients* 13, 3839. doi:10.3390/nu13113839

Ren, Y., Li, Y., Lv, J., Guo, X., Zhang, J., Zhou, D., et al. (2019). Parthenolide regulates oxidative stress-induced mitophagy and suppresses apoptosis through p53 signaling pathway in C2C12 myoblasts. *J. Cell. Biochem.* 120, 15695–15708. doi:10.1002/jcb.28839

Roberti, M. P., Yonekura, S., Duong, C. P. M., Picard, M., Ferrere, G., Tidjani Alou, M., et al. (2020). Chemotherapy-induced ileal crypt apoptosis and the ileal microbiome shape immunosurveillance and prognosis of proximal colon cancer. *Nat. Med.* 26, 919–931. doi:10.1038/s41591-020-0882-8

Sahin, I. H., Akce, M., Alese, O., Shaib, W., Lesinski, G. B., El-Rayes, B., et al. (2019). Immune checkpoint inhibitors for the treatment of MSI-H/MMR-D colorectal cancer and a perspective on resistance mechanisms. *Br. J. Cancer* 121, 809–818. doi:10.1038/s41416-019-0599-y

Santaolalla, R., Sussman, D. A., Ruiz, J. R., Davies, J. M., Pastorini, C., España, C. L., et al. (2013). TLR4 activates the β-catenin pathway to cause intestinal neoplasia. *PLoS One* 8, e63298. doi:10.1371/journal.pone.0063298

Sarangdhar, M., Yacyshyn, M. B., Gruenzel, A. R., Engevik, M. A., Harris, N. L., Aronow, B. J., et al. (2021). Therapeutic opportunities for intestinal angioectasia-targeting PPARγ and oxidative stress. *Clin. Transl. Sci.* 14, 518–528. doi:10.1111/cts.12899

Sauvaitre, T., Etienne-Mesmin, L., Sivignon, A., Mosoni, P., Courtin, C. M., Van de Wiele, T., et al. (2021). Tripartite relationship between gut microbiota, intestinal mucus and dietary fibers: Towards preventive strategies against enteric infections. *FEMS Microbiol. Rev.* 45, fuaa052. doi:10.1093/femsre/fuaa052

Schatoff, E. M., Leach, B. I., and Dow, L. E. (2017). Wnt signaling and colorectal cancer. *Curr. Colorectal Cancer Rep.* 13, 101–110. doi:10.1007/s11888-017-0354-9

Schmitt, M., and Greten, F. R. (2021). The inflammatory pathogenesis of colorectal cancer. *Nat. Rev. Immunol.* 21, 653–667. doi:10.1038/s41577-021-00534-x

Shalapour, S., and Karin, M. (2020). Cruel to Be kind: Epithelial, microbial, and immune cell interactions in gastrointestinal cancers. *Annu. Rev. Immunol.* 38, 649–671. doi:10.1146/annurev-immunol-082019-081656

Shang, F. M., and Liu, H. L. (2018). Fusobacterium nucleatum and colorectal cancer: A review. *World J. Gastrointest. Oncol.* 10, 71–81. doi:10.4251/wjgo.v10.i3.71

Shi, Y., Zheng, W., Yang, K., Harris, K. G., Ni, K., Xue, L., et al. (2020). Intratumoral accumulation of gut microbiota facilitates CD47-based immunotherapy via STING signaling. *J. Exp. Med.*, e20192282. doi:10.1084/jem.20192282

Singh, N. P., Hegde, V. L., Hofseth, L. J., Nagarkatti, M., and Nagarkatti, P. (2007). Resveratrol (trans-3, 5, 4′-trihydroxystilbene) ameliorates experimental allergic encephalomyelitis, primarily via induction of apoptosis in T cells involving activation of aryl hydrocarbon receptor and estrogen receptor. *Mol. Pharmacol.* 72, 1508–1521. doi:10.1124/mol.107.038984

Sivan, A., Corrales, L., Hubert, N., Williams, J. B., Aquino-Michaels, K., Earley, Z. M., et al. (2015). Commensal Bifidobacterium promotes antitumor immunity and facilitates anti-PD-L1 efficacy. *Science* 350, 1084–1089. doi:10.1126/science.aac4255

Smith, P. M., Howitt, M. R., Panikov, N., Michaud, M., Gallini, C. A., Bohlooly, Y. M., et al. (2013). The microbial metabolites, short-chain fatty acids, regulate colonic Treg cell homeostasis. *Science* 341, 569–573. doi:10.1126/science.1241165

Song, M., Garrett, W. S., and Chan, A. T. (2015). Nutrients, foods, and colorectal cancer prevention. *Gastroenterology* 148, 1244–1260. e16. doi:10.1053/j.gastro.2014.12.035

Sorbara, M. T., and Pamer, E. G. (2019). Interbacterial mechanisms of colonization resistance and the strategies pathogens use to overcome them. *Mucosal Immunol.* 12, 1–9. doi:10.1038/s41385-018-0053-0

Sougiannis, A. T., VanderVeen, B. N., Enos, R. T., Velazquez, K. T., Bader, J. E., Carson, M., et al. (2019). Impact of 5 fluorouracil chemotherapy on gut inflammation, functional parameters, and gut microbiota. *Brain Behav. Immun.* 80, 44–55. doi:10.1016/j.bbi.2019.02.020

Su, C. G., Wen, X., Bailey, S. T., Jiang, W., Rangwala, S. M., Keilbaugh, S. A., et al. (1999). A novel therapy for colitis utilizing PPAR-gamma ligands to inhibit the epithelial inflammatory response. *J. Clin. Invest.* 104, 383–389. doi:10.1172/JCI7145

Sui, H., Zhang, L., Gu, K., Chai, N., Ji, Q., Zhou, L., et al. (2020). YYFZBJS ameliorates colorectal cancer progression in Apc(Min/+) mice by remodeling gut microbiota and inhibiting regulatory T-cell generation. *Cell. Commun. Signal.* 18, 113. doi:10.1186/s12964-020-00596-9

Sung, H., Ferlay, J., Siegel, R. L., Laversanne, M., Soerjomataram, I., Jemal, A., et al. (2021). Global cancer statistics 2020: GLOBOCAN estimates of incidence and mortality worldwide for 36 cancers in 185 countries. *Ca. Cancer J. Clin.* 71, 209–249. doi:10.3322/caac.21660

Sussman, D. A., Santaolalla, R., Bejarano, P. A., Garcia-Buitrago, M. T., Perez, M. T., Abreu, M. T., et al. (2014). *In silico* and *ex vivo* approaches identify a role for toll-like receptor 4 in colorectal cancer. *J. Exp. Clin. Cancer Res.* 33, 45. doi:10.1186/1756-9966-33-45

Suzuki, T. (2013). Regulation of intestinal epithelial permeability by tight junctions. *Cell. Mol. Life Sci.* 70, 631–659. doi:10.1007/s00018-012-1070-x

Tanoue, T., Morita, S., Plichta, D. R., Skelly, A. N., Suda, W., Sugiura, Y., et al. (2019). A defined commensal consortium elicits CD8 T cells and anti-cancer immunity. *Nature* 565, 600–605. doi:10.1038/s41586-019-0878-z

Thiele Orberg, E., Fan, H., Tam, A. J., Dejea, C. M., Destefano Shields, C. E., Wu, S., et al. (2017). The myeloid immune signature of enterotoxigenic Bacteroides fragilis-induced murine colon tumorigenesis. *Mucosal Immunol.* 10, 421–433. doi:10.1038/mi.2016.53

Tianjin Medical University Cancer Institute and Hospital (2021). PD-1 inhibitor combined with bevacizumab and FOLFIRI regimen in the second-line treatment of advanced colorectal Cancer.NCT05035381. . Available from: https://clinicaltrials.gov/ct2/show/NCT05035381?cond=NCT05035381&draw=2&rank=1.

Tilg, H., Adolph, T. E., Gerner, R. R., and Moschen, A. R. (2018). The intestinal microbiota in colorectal cancer. *Cancer Cell.* 33, 954–964. doi:10.1016/j.ccell.2018.03.004

Tsoi, H., Chu, E. S. H., Zhang, X., Sheng, J., Nakatsu, G., Ng, S. C., et al. (2017). Peptostreptococcus anaerobius induces intracellular cholesterol biosynthesis in colon cells to induce proliferation and causes dysplasia in mice. *Gastroenterology* 152, 1419–1433. doi:10.1053/j.gastro.2017.01.009

Uchiyama, K., Sakiyama, T., Hasebe, T., Musch, M. W., Miyoshi, H., Nakagawa, Y., et al. (2016). Butyrate and bioactive proteolytic form of Wnt-5a regulate colonic epithelial proliferation and spatial development. *Sci. Rep.* 6, 32094. doi:10.1038/srep32094

Vasaikar, S., Huang, C., Wang, X., Petyuk, V. A., Savage, S. R., Wen, B., et al. (2019). Proteogenomic analysis of human colon cancer reveals new therapeutic opportunities. *Cell.* 177, 1035–1049. doi:10.1016/j.cell.2019.03.030

Vétizou, M., Pitt, J. M., Daillère, R., Lepage, P., Waldschmitt, N., Flament, C., et al. (2015). Anticancer immunotherapy by CTLA-4 blockade relies on the gut microbiota. *Science* 350, 1079–1084. doi:10.1126/science.aad1329

Villar-Ortega, P., Expósito-Ruiz, M., Gutiérrez-Soto, M., Ruiz-Cabello Jiménez, M., Navarro-Marí, J. M., and Gutiérrez-Fernández, J. (2022). The association between Fusobacterium nucleatum and cancer colorectal: A systematic review and meta-analysis. *Enferm. Infecc. Microbiol. Clin.* 40, 224–234. doi:10.1016/j.eimce.2022.02.007

Vodenkova, S., Buchler, T., Cervena, K., Veskrnova, V., Vodicka, P., and Vymetalkova, V. (2020). 5-fluorouracil and other fluoropyrimidines in colorectal cancer: Past, present and future. *Pharmacol. Ther.* 206, 107447. doi:10.1016/j.pharmthera.2019.107447

Wallace, B. D., Wang, H., Lane, K. T., Scott, J. E., Orans, J., Koo, J. S., et al. (2010). Alleviating cancer drug toxicity by inhibiting a bacterial enzyme. *Science* 330, 831–835. doi:10.1126/science.1191175

Wang, C., Yang, S., Gao, L., Wang, L., and Cao, L. (2018). Carboxymethyl pachyman (CMP) reduces intestinal mucositis and regulates the intestinal microflora in 5-fluorouracil-treated CT26 tumour-bearing mice. *Food Funct.* 9, 2695–2704. doi:10.1039/c7fo01886j

Wang, D., Zhu, X., Tang, X., Li, H., Yizhen, X., and Chen, D. (2020). Auxiliary antitumor effects of fungal proteins from Hericium erinaceus by target on the gut microbiota. *J. Food Sci.* 85, 1872–1890. doi:10.1111/1750-3841.15134

Wang, J., Feng, W., Zhang, S., Chen, L., Sheng, Y., Tang, F., et al. (2019). Ameliorative effect of Atractylodes macrocephala essential oil combined with Panax ginseng total saponins on 5-fluorouracil induced diarrhea is associated with gut microbial modulation. *J. Ethnopharmacol.* 238, 111887. doi:10.1016/j.jep.2019.111887

Wang, J., Xu, W., Wang, R., Cheng, R., Tang, Z., and Zhang, M. (2021). The outer membrane protein Amuc_1100 of Akkermansia muciniphila promotes intestinal 5-HT biosynthesis and extracellular availability through TLR2 signalling. *Food Funct.* 12, 3597–3610. doi:10.1039/d1fo00115a

Wang, K., Yang, Q., Ma, Q., Wang, B., Wan, Z., Chen, M., et al. (2018). Protective effects of salvianolic acid A against dextran sodium sulfate-induced acute colitis in rats. *Nutrients* 10, E791. doi:10.3390/nu10060791

Wang, L., Wang, R., Wei, G. Y., Wang, S. M., and Du, G. H. (2020). Dihydrotanshinone attenuates chemotherapy-induced intestinal mucositis and alters fecal microbiota in mice. *Biomed. Pharmacother.* 128, 110262. doi:10.1016/j.biopha.2020.110262

Wang, L., Wang, R., Wei, G. Y., Zhang, R. P., Zhu, Y., Wang, Z., et al. (2021). Cryptotanshinone alleviates chemotherapy-induced colitis in mice with colon cancer via regulating fecal-bacteria-related lipid metabolism. *Pharmacol. Res.* 163, 105232. doi:10.1016/j.phrs.2020.105232

Wang, S., Long, S., Deng, Z., and Wu, W. (2020). Positive role of Chinese herbal medicine in cancer immune regulation. *Am. J. Chin. Med.* 48, 1577–1592. doi:10.1142/S0192415X20500780

Wang, X., Sun, Y., Zhao, Y., Ding, Y., Zhang, X., Kong, L., et al. (2016). Oroxyloside prevents dextran sulfate sodium-induced experimental colitis in mice by inhibiting NF-κB pathway through PPARγ activation. *Biochem. Pharmacol.* 106, 70–81. doi:10.1016/j.bcp.2016.02.019

Wang, Z., Hopson, L. M., Singleton, S. S., Yang, X., Jogunoori, W., Mazumder, R., et al. (2021). Mice with dysfunctional TGF-β signaling develop altered intestinal microbiome and colorectal cancer resistant to 5FU. *Biochim. Biophys. Acta. Mol. Basis Dis.* 1867, 166179. doi:10.1016/j.bbadis.2021.166179

Watson, H., Mitra, S., Croden, F. C., Taylor, M., Wood, H. M., Perry, S. L., et al. (2018). A randomised trial of the effect of omega-3 polyunsaturated fatty acid supplements on the human intestinal microbiota. *Gut* 67, 1974–1983. doi:10.1136/gutjnl-2017-314968

Wu, J., Gan, Y., Li, M., Chen, L., Liang, J., Zhuo, J., et al. (2020). Patchouli alcohol attenuates 5-fluorouracil-induced intestinal mucositis via TLR2/MyD88/NF-kB pathway and regulation of microbiota. *Biomed. Pharmacother.* 124, 109883. doi:10.1016/j.biopha.2020.109883

Wu, K., Yang, Q., Mu, Y., Zhou, L., Liu, Y., Zhou, Q., et al. (2012). Berberine inhibits the proliferation of colon cancer cells by inactivating Wnt/β-catenin signaling. *Int. J. Oncol.* 41, 292–298. doi:10.3892/ijo.2012.1423

Wu, T., Wang, G., Chen, W., Zhu, Z., Liu, Y., Huang, Z., et al. (2018). Co-inhibition of BET proteins and NF-κB as a potential therapy for colorectal cancer through synergistic inhibiting MYC and FOXM1 expressions. *Cell. Death Dis.* 9, 315. doi:10.1038/s41419-018-0354-y

Xing, C., Wang, M., Ajibade, A. A., Tan, P., Fu, C., Chen, L., et al. (2021). Microbiota regulate innate immune signaling and protective immunity against cancer. *Cell. Host Microbe* 29, 959–974.e7. e7. doi:10.1016/j.chom.2021.03.016

Xu, H., Liu, Y., Cheng, P., Wang, C., Liu, Y., Zhou, W., et al. (2020). CircRNA_0000392 promotes colorectal cancer progression through the miR-193a-5p/PIK3R3/AKT axis. *J. Exp. Clin. Cancer Res.* 39, 283. doi:10.1186/s13046-020-01799-1

Xu, H., Van der Jeught, K., Zhou, Z., Zhang, L., Yu, T., Sun, Y., et al. (2021). Atractylenolide I enhances responsiveness to immune checkpoint blockade therapy by activating tumor antigen presentation. *J. Clin. Invest.* 146832. doi:10.1172/JCI146832

Xu, H., Wang, C., Song, H., Xu, Y., and Ji, G. (2019). RNA-Seq profiling of circular RNAs in human colorectal Cancer liver metastasis and the potential biomarkers. *Mol. Cancer* 18, 8. doi:10.1186/s12943-018-0932-8

Yang, S., Hu, T., Liu, H., Lv, Y. L., Zhang, W., Li, H., et al. (2021). Akebia saponin D ameliorates metabolic syndrome (MetS) via remodeling gut microbiota and attenuating intestinal barrier injury. *Biomed. Pharmacother.* 138, 111441. doi:10.1016/j.biopha.2021.111441

Yang, X., Yin, F., Yang, Y., Lepp, D., Yu, H., Ruan, Z., et al. (2018). Dietary butyrate glycerides modulate intestinal microbiota composition and serum metabolites in broilers. *Sci. Rep.* 8, 4940. doi:10.1038/s41598-018-22565-6

Yao, J., Hu, R., Sun, J., Lin, B., Zhao, L., Sha, Y., et al. (2014). Oroxylin A prevents inflammation-related tumor through down-regulation of inflammatory gene expression by inhibiting NF-κB signaling. *Mol. Carcinog.* 53, 145–158. doi:10.1002/mc.21958

Yi, M., Yu, S., Qin, S., Liu, Q., Xu, H., Zhao, W., et al. (2018). Gut microbiome modulates efficacy of immune checkpoint inhibitors. *J. Hematol. Oncol.* 11, 47. doi:10.1186/s13045-018-0592-6

Yu, J., Feng, Q., Wong, S. H., Zhang, D., Liang, Q. Y., Qin, Y., et al. (2017). Metagenomic analysis of faecal microbiome as a tool towards targeted non-invasive biomarkers for colorectal cancer. *Gut* 66, 70–78. doi:10.1136/gutjnl-2015-309800

Yu, T., Guo, F., Yu, Y., Sun, T., Ma, D., Han, J., et al. (2017). Fusobacterium nucleatum promotes chemoresistance to colorectal cancer by modulating autophagy. *Cell.* 170, 548–563.e16. doi:10.1016/j.cell.2017.07.008

Yu, Y. N., Yu, T. C., Zhao, H. J., Sun, T. T., Chen, H. M., Chen, H. Y., et al. (2015). Berberine may rescue Fusobacterium nucleatum-induced colorectal tumorigenesis by modulating the tumor microenvironment. *Oncotarget* 6, 32013–32026. doi:10.18632/oncotarget.5166

Yuan, X., Xue, J., Tan, Y., Yang, Q., Qin, Z., Bao, X., et al. (2021). Albuca bracteate polysaccharides synergistically enhance the anti-tumor efficacy of 5-fluorouracil against colorectal cancer by modulating β-catenin signaling and intestinal flora. *Front. Pharmacol.* 12, 736627. doi:10.3389/fphar.2021.736627

Yue, B., Ren, J., Yu, Z., Luo, X., Ren, Y., Zhang, J., et al. (2020). Pinocembrin alleviates ulcerative colitis in mice via regulating gut microbiota, suppressing TLR4/MD2/NF-κB pathway and promoting intestinal barrier. *Biosci. Rep.* 40, BSR20200986. doi:10.1042/BSR20200986

Yue, S. J., Qin, Y. F., Kang, A., Tao, H. J., Zhou, G. S., Chen, Y. Y., et al. (2021). Total flavonoids of Glycyrrhiza uralensis alleviates irinotecan-induced colitis via

modification of gut microbiota and fecal metabolism. *Front. Immunol.* 12, 628358. doi:10.3389/fimmu.2021.628358

Zhai, Q., Feng, S., Arjan, N., and Chen, W. (2019). A next generation probiotic, Akkermansia muciniphila. *Crit. Rev. Food Sci. Nutr.* 59, 3227–3236. doi:10.1080/10408398.2018.1517725

Zhan, Y., Chen, P. J., Sadler, W. D., Wang, F., Poe, S., Núñez, G., et al. (2013). Gut microbiota protects against gastrointestinal tumorigenesis caused by epithelial injury. *Cancer Res.* 73, 7199–7210. doi:10.1158/0008-5472.CAN-13-0827

Zhang, S., Yang, Y., Weng, W., Guo, B., Cai, G., Ma, Y., et al. (2019). Fusobacterium nucleatum promotes chemoresistance to 5-fluorouracil by upregulation of BIRC3 expression in colorectal cancer. *J. Exp. Clin. Cancer Res.* 38, 14. doi:10.1186/s13046-018-0985-y

Zhang, S. L., Han, B., Mao, Y. Q., Zhang, Z. Y., Li, Z. M., Kong, C. Y., et al. (2022). Lacticaseibacillus paracasei sh2020 induced antitumor immunity and synergized with anti-programmed cell death 1 to reduce tumor burden in mice. *Gut Microbes* 14, 2046246. doi:10.1080/19490976.2022.2046246

Zhang, S. L., Mao, Y. Q., Zhang, Z. Y., Li, Z. M., Kong, C. Y., Chen, H. L., et al. (2021). Pectin supplement significantly enhanced the anti-PD-1 efficacy in tumor-bearing mice humanized with gut microbiota from patients with colorectal cancer. *Theranostics* 11, 4155–4170. doi:10.7150/thno.54476

Zhang, T., Lu, S. H., Bi, Q., Liang, L., Wang, Y. F., Yang, X. X., et al. (2017). Volatile oil from amomi fructus attenuates 5-fluorouracil-induced intestinal mucositis. *Front. Pharmacol.* 8, 786. doi:10.3389/fphar.2017.00786

Zhang, X., Liu, Q., Liao, Q., and Zhao, Y. (2020). Pancreatic cancer, gut microbiota, and therapeutic efficacy. *J. Cancer* 11, 2749–2758. doi:10.7150/jca.37445

Zhang, X., Zhu, X., Cao, Y., Fang, J. Y., Hong, J., and Chen, H. (2019). Fecal Fusobacterium nucleatum for the diagnosis of colorectal tumor: A systematic review and meta-analysis. *Cancer Med.* 8, 480–491. doi:10.1002/cam4.1850

Zhang, Y., Yan, W., Collins, M. A., Bednar, F., Rakshit, S., Zetter, B. R., et al. (2013). Interleukin-6 is required for pancreatic cancer progression by promoting MAPK signaling activation and oxidative stress resistance. *Cancer Res.* 73, 6359–6374. doi:10.1158/0008-5472.CAN-13-1558-T

Zhang, Z., Wu, X., Cao, S., Cromie, M., Shen, Y., Feng, Y., et al. (2017). Chlorogenic acid ameliorates experimental colitis by promoting growth of Akkermansia in mice. *Nutrients* 9, E677. doi:10.3390/nu9070677

Zhao, Y., Zhu, Q., Bu, X., Zhou, Y., Bai, D., Guo, Q., et al. (2020). Triggering apoptosis by oroxylin A through caspase-8 activation and p62/SQSTM1 proteolysis. *Redox Biol.* 29, 101392. doi:10.1016/j.redox.2019.101392

Zheng, Y., Wang, T., Tu, X., Huang, Y., Zhang, H., Tan, D., et al. (2019). Gut microbiome affects the response to anti-PD-1 immunotherapy in patients with hepatocellular carcinoma. *J. Immunother. Cancer* 7, 193. doi:10.1186/s40425-019-0650-9

Zhi, H., Jin, X., Zhu, H., Li, H., Zhang, Y., Lu, Y., et al. (2020). Exploring the effective materials of flavonoids-enriched extract from Scutellaria baicalensis roots based on the metabolic activation in influenza A virus induced acute lung injury. *J. Pharm. Biomed. Anal.* 177, 112876. doi:10.1016/j.jpba.2019.112876

Zhu, G., Huang, Q., Huang, Y., Zheng, W., Hua, J., Yang, S., et al. (2016). Lipopolysaccharide increases the release of VEGF-C that enhances cell motility and promotes lymphangiogenesis and lymphatic metastasis through the TLR4- NF-κB/JNK pathways in colorectal cancer. *Oncotarget* 7, 73711–73724. doi:10.18632/oncotarget.12449

Zitvogel, L., Ma, Y., Raoult, D., Kroemer, G., and Gajewski, T. F. (2018). The microbiome in cancer immunotherapy: Diagnostic tools and therapeutic strategies. *Science* 359, 1366–1370. doi:10.1126/science.aar6918

Glossary

CRC Colorectal cancer
IBD Inflammatory bowel disease
UC Ulcerative colitis
CD Crohn's disease
NF-κB Nuclear factor-kappa B
IL-6 Interleukin 6
TNF-α Tumor necrosis factor alpha
PUFAs Polyunsaturated fatty acids
ICIs Immune checkpoint inhibitors
AIEC Adherent-invasive *E. coli*
AOM Azoxymethane
DSS Dextran sulphate sodium
GF Germ-free
LPS Lipopolysaccharide
LBP Lipopolysaccharide-binding protein
MD-2 Myeloid differentiation factor 2
TLR4 Toll-like receptor 4
MyD88 Myeloid differentiation primary response 88
IL-1β Interleukin 1beta
Cdk5 Cyclin-dependent kinase 5
CRAMP Cathelin-related antimicrobial peptide
TJs Tight junctions
APC Adenomatous polyposis coli
DCs Dendritic cells
MDSCs Myeloid-derived suppressor cells
ETBF Enterotoxic *Bacteroides fragilis*
CECs Colonic epithelial cells
IL-17 Interleukin 17
STAT3 Signal transducer and activator of transcription 3
MMP-9 Matrix metalloproteinase 9
VEGF Vascular endothelial growth factor
Lp *Lactobacillus* plantarum
NK cells Nature killer cells
IL-22 Interleukin 22
GLP Ganoderma lucidum
AG astragalin
ASD Akebia saponin D
PTL Parthenolide
BBR berberine
CAC Colitis-associated cancer
COX-2 Cyclooxygenase-2
MCP-1 Monocyte chemoattractant protein-1
IFN-γ Interferon-gamma
PPARγ Peroxisome proliferator-activated receptor gamma
AhR Aryl hydrocarbon receptor
SCFAs Short-chain fatty acids
5-Fu 5-fluorouracil
TME Tumor microenvironment
IL-12 Interleukin 12
CPT-11 Irinotecanl
NCCN National Comprehensive Cancer Network
MSI-H Microsatellite instability High
dMMR Defective DNA mismatch repair
FMT Fecal microbiota transplantation
CTLA-4 Cytotoxic T-lymphocyte associated protein 4
PD-1 Programmed cell death 1
NSCLC
Non-small-cell lung cancers
ABPs Albuca bracteate polysaccharides
CMP Carboxymethyl pachyman
VOA a volatile oil from Amomum villosum
BA Bornyl acetate
AMO Atracylodes macrocephala essential oil
PGS Panax ginseng total saponins`
TFGU Glycyrrhiza uralensis
CTS Crypotanshinone
GPs Ginseng polysaccharides
CC Myrciaria dubia: Polyphenol-rich berry camu-camu.

frontiers | Frontiers in Pharmacology

TYPE Original Research
PUBLISHED 20 September 2022
DOI 10.3389/fphar.2022.946065

OPEN ACCESS

EDITED BY
Hailian Shi,
Shanghai University of Traditional Chinese Medicine, China

REVIEWED BY
Md Abdul Hye Khan,
University of Tennessee Health Science Center (UTHSC), United States
Timur Saliev,
S.D. Asfendiyarov Kazakh National Medical University, Kazakhstan
Yinglei Miao,
The First Affiliated Hospital of Kunming Medical University, China
Tao Yang,
Shanghai University of Traditional Chinese Medicine, China

*CORRESPONDENCE
Jing Yan,
yanjing102@mail.jnmc.edu.cn

SPECIALTY SECTION
This article was submitted to Gastrointestinal and Hepatic Pharmacology, a section of the journal Frontiers in Pharmacology

RECEIVED 17 May 2022
ACCEPTED 29 August 2022
PUBLISHED 20 September 2022

CITATION
Yu W, Li Q, Shao C, Zhang Y, Kang C, Zheng Y, Liu X, Liu X and Yan J (2022), The Cao-Xiang-Wei-Kang formula attenuates the progression of experimental colitis by restoring the homeostasis of the microbiome and suppressing inflammation.
Front. Pharmacol. 13:946065.
doi: 10.3389/fphar.2022.946065

The Cao-Xiang-Wei-Kang formula attenuates the progression of experimental colitis by restoring the homeostasis of the microbiome and suppressing inflammation

Wei Yu, Qi Li, Changlei Shao, Yijia Zhang, Cai Kang, Yang Zheng, Xihao Liu, Xincheng Liu and Jing Yan*

Department of Physiology, Jining Medical University, Jining, Shandong, China

Inflammatory bowel disease (IBD) is pathologically characterized by an immune response accommodative insufficiency and dysbiosis accompanied by persistent epithelial barrier dysfunction. The Cao-Xiang-Wei-Kang (CW) formula has been utilized to treat gastrointestinal disorders in the clinic. The present study was designed to delineate the pharmacological mechanisms of this formula from different aspects of the etiology of ulcerative colitis (UC), a major subtype of IBD. Dextran sodium sulfate (DSS) was given to mice for a week at a concentration of 2%, and the CW solution was administered for 3 weeks. 16S rRNA gene sequencing and untargeted metabolomics were conducted to examine the changes in the microbiome profile, and biochemical experiments were performed to confirm the therapeutic functions predicted by system pharmacology analysis. The CW treatment hampered DSS-induced experimental colitis progression, and the targets were enriched in inflammation, infection, and tumorigenesis, which was corroborated by suppressed caspase 3 (Casp3) and interleukin-1b (IL-1b) and increased cleaved caspase 3 expression and casp-3 activity in the colon samples from colitis mice subjected to the CW therapy. Moreover, the CW therapy rescued the decreased richness and diversity, suppressed the potentially pathogenic phenotype of the gut microorganisms, and reversed the altered linoleic acid metabolism and cytochrome P450 activity in murine colitis models. In our *in vitro* experiments, the CW administration increased the alternative activation of macrophages (Mφs) and inhibited the tumor necrosis factor-α (TNFα)-induced reactive oxygen species (ROS) level and subsequent death in

Abbreviations: IBD, inflammatory bowel disease; CAC, colitis-associated carcinogenesis; CW, Cao-Xiang-Wei-Kang; TCM, traditional Chinese medicine; PPIs, protein–protein interactions; UC, ulcerative colitis; Mφs, macrophages; ISCs, intestinal stem cells; IOs, intestinal organoids; KM, Kaplan–Meier; CC, closeness centrality; BC, betweenness centrality; DC, degree centrality; EC, eigenvector centrality; LAC, local average connectivity; NC, network centrality; GO, Gene Ontology; KEGG, Kyoto Encyclopedia of Genes and Genomes; TNFα, tumor necrosis factor-α; ROS, reactive oxygen species; Casp3, caspase 3; IL-17, interleukin-17; IL-1b, interleukin-1b.

intestinal organoids (IOs). We propose that the CW formula alleviates the progression of murine colitis by suppressing inflammation, promoting mucosal healing, and re-establishing a microbiome profile that favors re-epithelization.

KEYWORDS

ulcerative colitis, inflammatory bowel disease, dysbiosis, mucosal healing, Cao-Wei-Kang formula

Introduction

Inflammatory bowel diseases (IBDs) are systemic diseases and not only impair the gut functions but also influence extraintestinal organs, such as the liver, kidney, and eyes (Rogler et al., 2021). The pathophysiological factors include genetic susceptibility, environmental pollution, pathogen invasion, and dietary habits. Ulcerative colitis (UC) is a major subtype of IBD and predominantly occurs in the colon, accompanied by bloody stool, weight loss, abdominal pain, and a higher risk of developing colitis-associated carcinogenesis (CAC). To successfully intervene with the progression of UC, therapy should take all these pathological symptoms into account. In other words, resolution of inflammation and inflammation-compromised integrity of the colon epithelium, as well as recovery of healthy gut flora and rescued intestinal stem cell viability, are pivotal for UC treatment. Therefore, multi-target drugs exhibit stronger clinical efficacy than exquisitely selective compounds. Derived from the oldest Chinese medical book "Shang Han Lun" and evolving with the modern medical technique, traditional Chinese medicine (TCM) has a long historical application in clinics and is a golden resource for developing multi-target drugs. However, the pharmacological mechanisms of many efficacious drugs need extensive experimental evidence to corroborate the efficacy and guarantee of low toxicity. The emergence of system pharmacology and omics technology helps resolve the difficulty in explaining the synergistic and counteracting effects of multiple herbs included in each TCM formula, providing a chance for the development of TCM.

The Cao-Xiang-Wei-Kang (CW) formula included in Chinese Pharmacopoeia 2020 is composed of *Senna tora* (L.) Roxb (SR), oyster shell (OS), *Gallus gallus domesticus Brisson* (GB), cuttlebone (Cb), *Ferula sinkiangensis* K.M.Shen (FS), and *Dolomiaea berardioidea* (Franch.) C. Shih (DC) (Table 1). This investigation was designed to determine the efficacy of the CW formula from combination logic to experimental evidence by integrating network pharmacology with omics technology and *in vitro* and *in vivo* experiments.

Materials and methods

Network pharmacology

A CW–component–target network was constructed by active components with a cut-off of drug-likeness (0.18) and oral bioavailability (20%). All the plant names have been checked with http://www.theplantlist.org. Based on the database of Laboratory of Systems Pharmacology (Ru et al., 2014), the active components of SR and DC were collected. The active components of OS, Cb, GB, and FS were acquired, according to the published articles (Lee et al., 2010; Pan et al., 2016; Scandiffio et al., 2018; Guo et al., 2020; Kintsu et al., 2020). According to these active components, the targets were obtained from PubChem, and the genes of ulcerative colitis (UC) were collected from GeneCards (Stelzer et al., 2016), Online Mendelian Inheritance in Man (OMIM) (Amberger and Hamosh, 2017), DrugBank (Wishart et al., 2018a), PharmGkb (Barbarino et al., 2018), and Statistics of Therapeutic Target Database (TTD). Based on the commonly shared genes, Gene Ontology (GO) and Kyoto Encyclopedia of Genes and Genomes (KEGG) Pathway Enrichment analyses were conducted (The Gene Ontology Consortium, 2019). The herb–ingredient–target (HIT) interaction network and a protein–protein interaction (PPI)

TABLE 1 The ingredients of the formula.

Scientific Name of the herb	Chinese name	Weight %
Senna tora (L.) Roxb	Jue Ming Zi	35%
oyster shell	Mu Li	20%
Gallus gallus domesticus Brisson	Ji Nei Jin	15%
Cuttlebone	Hai Piao Xiao	15%
Ferula sinkiangensis K.M.Shen	A Wei	10
Dolomiaea berardioidea (Franch.) C.Shih	Mu Xiang	5

network with a confidence score ≥ 0.7 based on the Search Tool for Retrieval of Interacting Genes/Proteins database were computed by CytoNCA (Tang et al., 2015), which calculates the median values of betweenness centrality (BC), closeness centrality (CC), degree centrality (DC), local average connectivity (LAC), eigenvector centrality (EC), and network centrality (NC).

Cao-Xiang-Wei-Kang formula preparation

The CW formula was prepared by mixing the powder of SR, OS, GB, Cb, FS, and DC at a ratio of 7:4:3:3:2:1, respectively. Briefly, the FS powder was diluted in water and mixed with other herbs. The dried drug was smashed and given to mice or subjected to mass spectrometry (MS) detection. To validate the components in the formula, a connected system of LC-30 (Shimadzu)-Hybrid Quadrupole Time-of-Flight MS (TOF MS) with an electrospray ionization source (ESI) was used. The mobile phase system had solution A (acetonitrile) and equate B (0.1% HCOOH-H_2O): 25 min (A:20%: B:80%), 50 min (A:35%: B:65%), 9 min (A:90%: B:10%), and 7 min (A:20%: B:90%). Data were processed in information-dependent acquisition (IDA) with a high-sensitivity mode.

Experimental colitis murine models with the administration of Cao-Xiang-Wei-Kang

Experiments were approved by the guidelines of the Institutional Animal Care and Use Committee of Jining Medical University in China (SYXK-Shandong province-2018-0002).

Mice (Pengyue Animal Center of Shandong province, China) (male, about 22 g, 2 months old) were given 2% dextran sodium sulfate (DSS, MP Biomedicals) for 1 week, and then, the CW formula was administered for 21 days. The dose of the human being was 120 mg/kg per day based on the Chinese Pharmacopoeia 2020 version, and correspondingly, murine was 1.44 g/kg calculated by the Meeh–Rubner formula: Skin surface area = Mass Coefficients × $(\frac{Weight \times \frac{2}{3}}{10000})$. An amount of 36 mg (equal to 1.44 g/kg) (the high dose) or 18 mg (equal to 0.7 g/kg) (the low dose) CW diluted in 200 μl water was administered each day. The positive control of the study was mesalazine (MedChemExpress, China) (Veloso et al., 2021). Every 15 mice were grouped, and five groups were set as follows: 0.9% saline, 2% DSS, the low-CW-DSS group, high-CW-DSS group, and mesalazine group (200 mg/kg). Isoflurane (RWD Life Science, Shenzhen City, China) was used for gas anesthetization. The histopathological score was determined: weight loss (normal: 0; <5%: 1; 5%–10%: 2; 10%–20%: 3; >20%: 4); feces (normal: 0; soft: 1; very soft: 2; liquid: 3); blood test (no blood within 2 min: 0; positive in 10 s: 1; light purple within 10 s: 2; heavy purple within 10 s: 3) (Leagene, China); and histological indices (destruction of the epithelium, immune cell infiltrates, edema, and crypt loss, each for 1).

The colon samples were soaked in paraformaldehyde (PFA) for 72 h, embedded in paraffin and then cut into 3-μm thick slices, and subjected to hematoxylin and eosin (H&E) staining.

Serum isolation

After the high-dose treatment of CW, we collected the serum from colitis mice in 2 hours for the following experiments. To examine the toxicity, NCM460 cells, an epithelial cell line derived from the normal colon of a 68-year-old Hispanic male, were treated with serum and subjected to an MTT assay (3- [4,5-dimethylthiazol-2-yl]-2,5-diphenyl tetrazolium bromide) and cellular immunofluorescence assay with PI staining (Abcam, United States).

Enzyme-linked immunosorbent assay

Enzyme-linked immunosorbent assay (ELISA) kits were bought from Abcam and were utilized to examine the cytokine concentrations in the serum: TNFα (sensitivity: 0.1 pg/ml; range: 47–3,000 pg/ml) and IL-1b ELISA kits (sensitivity: 15.2 pg/ml; range: 28.1–1,800 pg/ml).

16S rRNA gene amplicon sequencing data analysis

The feces and mucus within the colon were collected and mixed and processed by 16S rRNA gene sequencing. The raw data were filtered by Trimmomatic (Bolger et al., 2014), and paired-end reads were produced after chimera removal by UCHIME. Corrected paired-end reads generated circular consensus sequencing (CCS) reads, which were distinguished based on the barcode sequences. After removing chimeras, an OTU (operational taxonomic unit) analysis was performed with a similarity >97%. Species annotation and taxonomic analysis, diversity analysis including alpha and beta diversity, significant difference analysis, and functional prediction were performed. Differential analysis among groups was calculated by the *t*-test. The rarefaction curve and Shannon curve were plotted using Mothur and R packages. The rank abundance curve (Guo et al., 2020) was generated by ranking the features in each sample based on abundance and plotting them in abundance rank (X-axis) and relative abundance (Y-axis) (Salari et al., 2016). Beta diversity analysis was processed by QIIME software to compare species diversity between different samples utilizing binary jaccard, which was an OTU-based algorithm. Principal coordinates analysis (PCoA) was drawn by the R language tool, and PERMANOVA (Adonis) created by the vegan package was used to analyze whether there was a significant difference in beta diversity between samples from different groups (Xie et al., 2020). LEfSe [Linear Discriminant

analysis (LDA) Effect Size] was conducted to identify biomarkers with statistical difference between different groups (Zhou et al., 2020). Metastatsconducted a *t*-test on species richness data between groups at the taxonomic level of the genus (Hu et al., 2018). Krona, as a powerful metagenomic visualization tool, demonstrates species annotation. Each fan means the corresponding annotation's proportion (Ondov et al., 2011). PICRUSt (Phylogenetic Investigation of Communities by Reconstruction of Unobserved States) analysis was conducted to predict the alterations in KEGG pathways. The raw data were available with the accession number in SRA (PRJNA827781).

Untargeted metabolomics

Fecal and mucus samples were treated with methanol and standard internal substances. After the ultrasound and frozen treatment, the samples were centrifuged. The supernatant was subjected to ultra-high-performance liquid chromatography (UHPLC) coupled with TOF-MS (Garcia and Barbas, 2011). Acquisition software (Analyst TF 1.7, AB Sciex) was utilized to assess the full scan survey MS data, which were then converted by ProteoWizard and generated the retention time (RT), mass-to-charge ratio (m/z) values, and peak intensity. According to the in-house MS2 database, substances were identified and determined by orthogonal projections to latent structures-discriminant analysis (OPLS-DA). The cut-off was p value < 0.05, fold change (FC) > 1, and Variable Importance in the Projection (VIP) > 1. The HMDB (Human Metabolome Database) (Wishart et al., 2018b) and KEGG database were utilized to annotate metabolites.

Peritoneal macrophage isolation

Mice were anesthetized, and sterilized PBS was injected into the abdominal cavity. After massage, the liquids were isolated and centrifuged. The pellet was diluted in RPMI-1640 complete medium.

Microparticle phagocytic experiment

Diluted microparticles (Thermo Fisher, United States) [fluorescein isothiocyanate (FITC) wavelength-488 nm] were incubated with peritoneal Mφs collected from anesthetized mice for 2 h at 37°C, were centrifuged and washed, and subjected to flow cytometry analysis.

Wound healing assay

A density of 10^5 NCM460 cells was seeded in the 24-well cell culture plate at a 37°C 5% CO_2 incubator. When reaching 100% confluency, a scratch was made, and a transwell insert (Corning, 0.3 μm diameter, United States) carrying 10^4 peritoneal Mφs was placed. After 24 h, the cells in five random fields were examined.

Western blotting

Total protein (40 μg) was subjected to SDS-PAGE (sodium dodecyl sulfate–polyacrylamide gel electrophoresis) and transferred. After blockage, antibodies [CASP3, vascular endothelial growth factor A (VEGFa), IL-1b, IL-10, and arginase 1 (ARG1)] were incubated with the membrane for 24 h. After washing with PBS, secondary antibodies conjugated with horseradish peroxidase (HRP) were utilized, and an enhanced chemiluminescence (ECL) substrate was added to visualize the protein bands. All chemicals were bought from Invitrogen, United States.

Caspase-3 activity assay

The colon samples were subjected to the Caspase-3 activity assay kit (Abcam, United States), and the absorbance was determined at an optical density at 405 nm (BioTek Instruments, Inc.).

Intestinal organoid culture

The small intestine was cut into small pieces and washed with cold PBS until the solution became clear. After 35 min of digestion by the digestive solution (Yu et al., 2020), the filtered medium was centrifuged and cultured in a growth medium. After 9 days, tumor necrosis factor-α (TNFα) was added with or without the CW serum. After 24 h, IOs were incubated at 37°C with propidium iodide (PI)/Hoechst33342 (480 nm/630 nm) for 20 min. To measure mitochondrial stress, MitoSOX™ Red mitochondrial superoxide indicator (590 nm) was added. After 10 min at 37°C, cells were examined using a fluorescent microscope. Two dyes and culturing reagents were bought from Thermo Fisher and STEMCELL Technologies, respectively.

Statistical analysis

Data are means ± SEM. $^*p < 0.05$, $^{**}p < 0.01$, and $^{***}p < 0.001$. Every experiment was repeated at least five times. Comparisons between two groups were analyzed by unpaired Student's *t*-test. GraphPad 8.0 and R software were utilized.

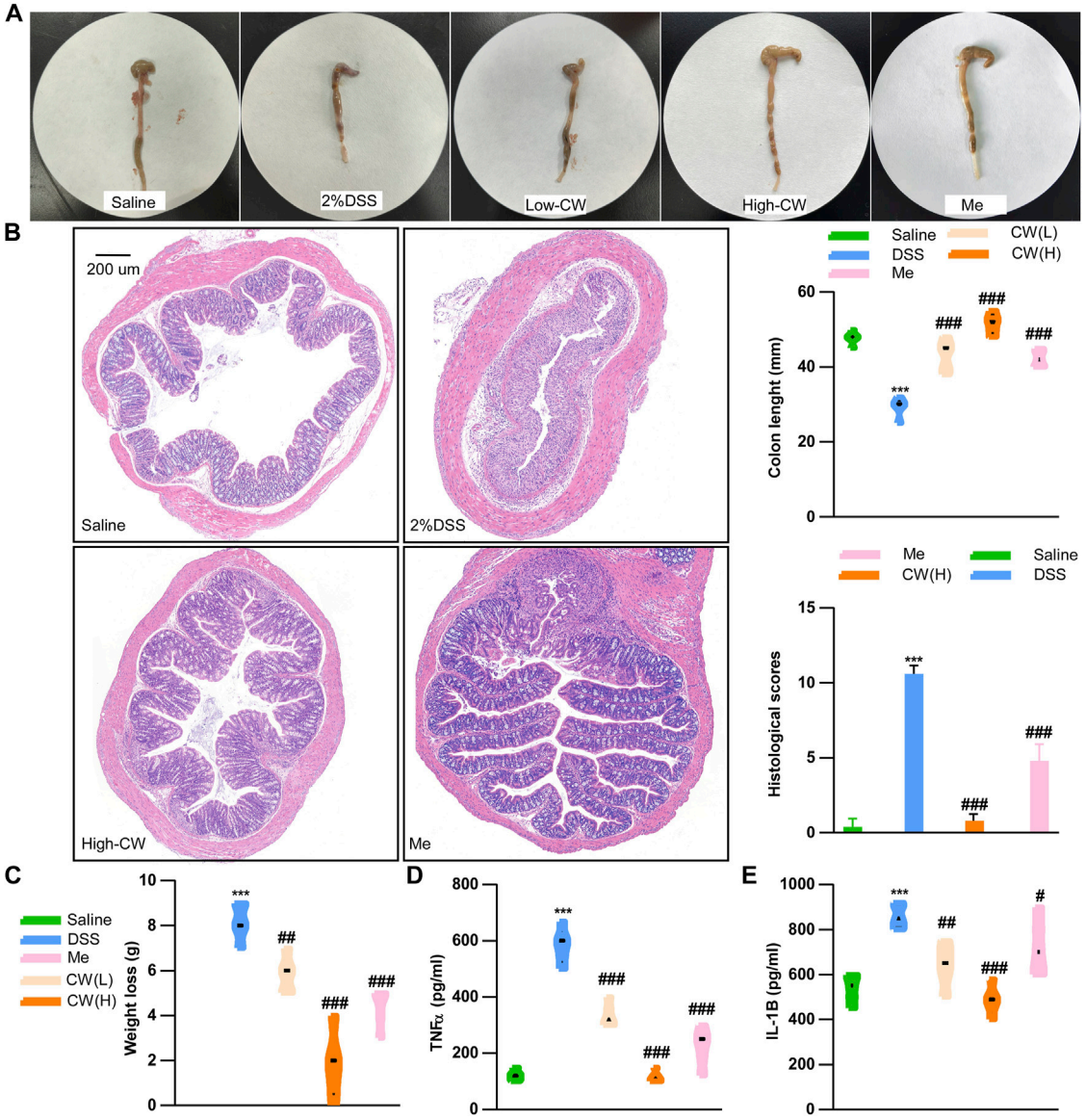

FIGURE 1
CW formula alleviates the progression of experimental colitis. Colon tissue and colon length **(A)**, HE staining and histological scores of the colon **(B)**, weight loss **(C)**, serum TNFα **(D),** and IL-1b **(E)** levels in ulcerative colitis (UC) murine models after the CW treatment (n = 15). *indicates a statistically significant difference from the saline group, and #indicates a statistically significant difference from the DSS group.

Results

Therapeutic role of the Cao-Xiang-Wei-Kang formula against experimental colitis

We determined the chemical profile of the CW formula by UPLC-MS/MS and identified the presence of the ingredients (Supplementary Figure S1, Supplementary Table S1). DSS exacerbated weight loss, caused rectal bleeding, shortened the colon length, and induced edema. These symptoms were markedly alleviated by the CW therapy at a low and high dose (1.44 g/kg). As compared with the mesalazine treatment, the high dose of CW produced a longer colon (Figure 1A). H&E staining showed that the high dose of CW successfully rescued colitis-caused crypt loss and alleviated epithelial breach, as well as immune cell infiltrates, showing its superiority in mucosal healing and resolution of inflammation compared with mesalazine (Figure 1B). Of note, both doses of CW rescued weight loss (Figure 1C) and suppressed the DSS-evoked IL-1b and TNFα levels (Figures 1D,E).

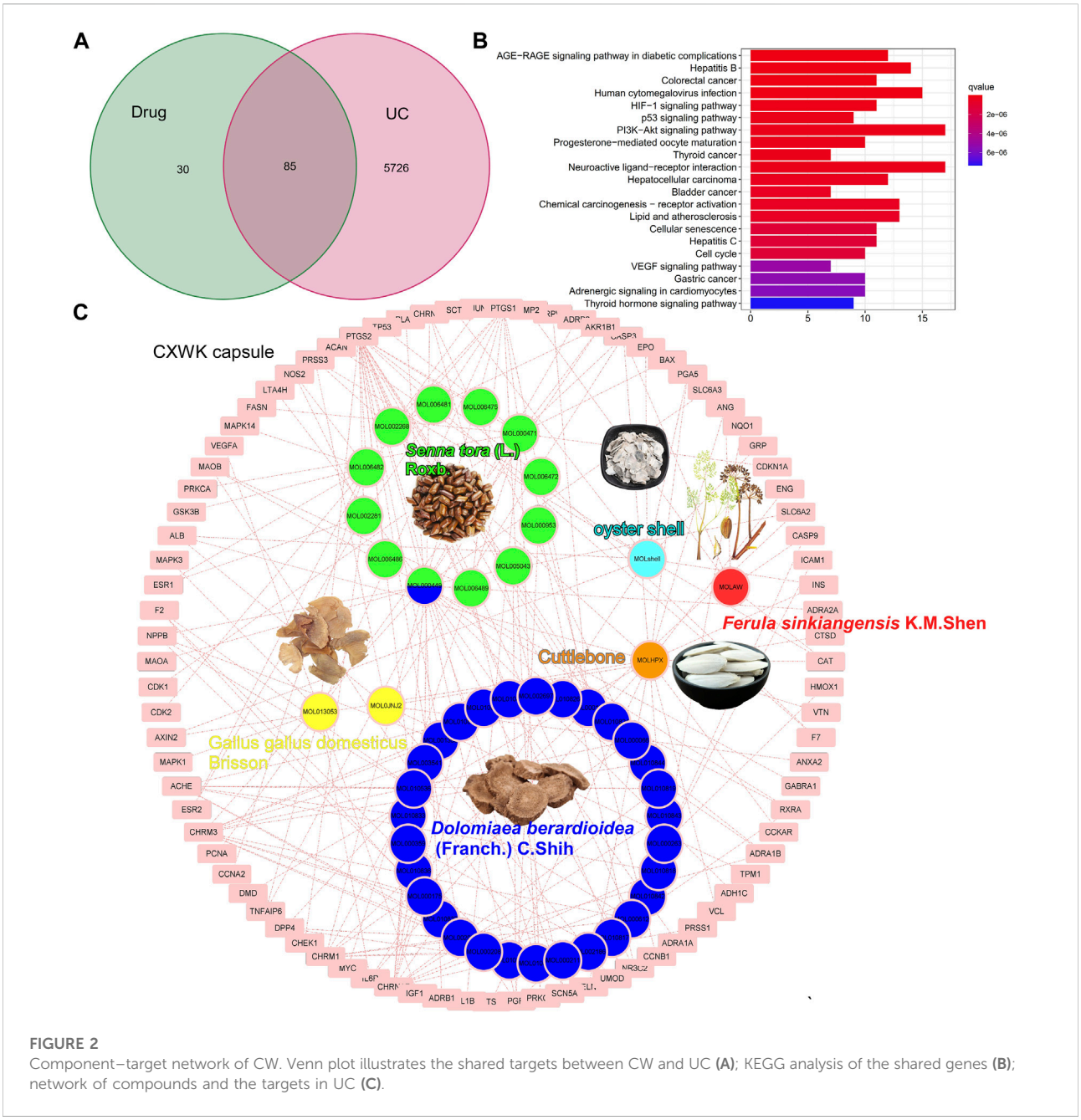

FIGURE 2
Component–target network of CW. Venn plot illustrates the shared targets between CW and UC **(A)**; KEGG analysis of the shared genes **(B)**; network of compounds and the targets in UC **(C)**.

Herb–Ingredient–Target network of Cao-Xiang-Wei-Kang

The CW formula encompassed six herbs (Supplementary Table S2) and shared 85 putative targets with the acquired 5811 colitis-relevant genes (Figure 2A). A HIT network representing the interactions between active components and targeted genes was established: pink rectangle nodes represented colitis-associated genes, and nodes with different colors inside were active components (Figure 2C). Based on the database and published articles, 12 active components of SR, 30 of DC, and 2 of GB were identified, while OS, FS, and Cb had three components. Among the 115 targets of these components, 85 genes were associated with the progression of colitis.

The KEGG analysis demonstrated that these shared genes were enriched in carcinogenesis, infections, neuroactive ligand–receptor interaction, and VEGF and HIF-1 signaling pathways (Figure 2B). As illustrated in the pie charts, and weight or target proportion, SR occupied much of the formula

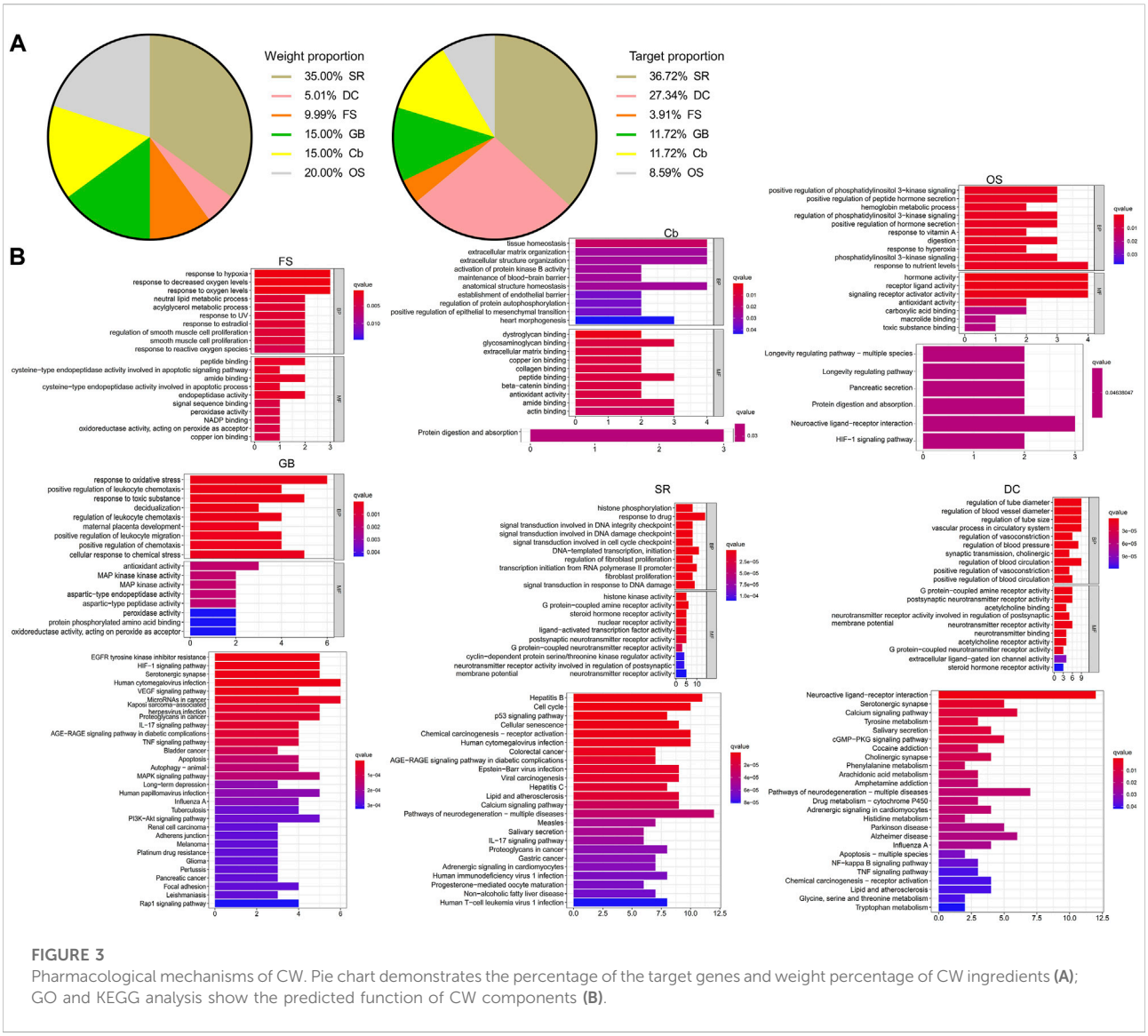

FIGURE 3
Pharmacological mechanisms of CW. Pie chart demonstrates the percentage of the target genes and weight percentage of CW ingredients **(A)**; GO and KEGG analysis show the predicted function of CW components **(B)**.

(Figure 3A). All the ingredients are associated with infection and CRC, as well as inflammatory responses (Figure 3B).

Based on the shared genes between colitis and the CW formula, a PPI network with a PPI enrichment *p*-value (<1.0e-16) was established utilizing the STRING database, and a sub-network composed of 24 genes is shown in Figure 4A with the median values (BC: 16.157288675, CC: 0.151452282, DC: 5, EC: 0.0531741455, LAC: 1.625, and NC: 2.5833333335). To predict the major active components in the formula, the calculated 24 hub genes and corresponding components were utilized to construct a component–hub gene network (Figure 4B). Western blotting confirmed that the high dose of CW treatment significantly suppressed the protein abundance of Casp3 and IL-1b, and increased the Casp3 activity (Figures 4C,D), indicating an alleviated inflammation by the CW formula.

The Cao-Xiang-Wei-Kang formula rescued dysbiosis in murine colitis models

To determine the effect of the CW formula on microbiota composition, 16S rRNA gene sequencing was conducted utilizing the feces and mucus. All sample libraries covered >99%, suggesting a sufficient library size to represent most microbes (Supplementary Table S3). DSS treatment led to a marked decrease in the alpha-diversity of microbiota including Chao and Ace, and Shannon indexes, as well as the Simpson index, all of which were reversed by the CW therapy (1.44 g/kg) (Figure 5A). β-diversity was calculated by the binary Jaccard method. Principal Co-ordinates Analysis (PCoA) combined with PERMANOVA showed that CW treatment significantly altered the β-diversity of commensal microorganisms (Figure 5B). Non-metric multidimensional scaling analysis (NMDS) indicated the CW-DSS group clustered

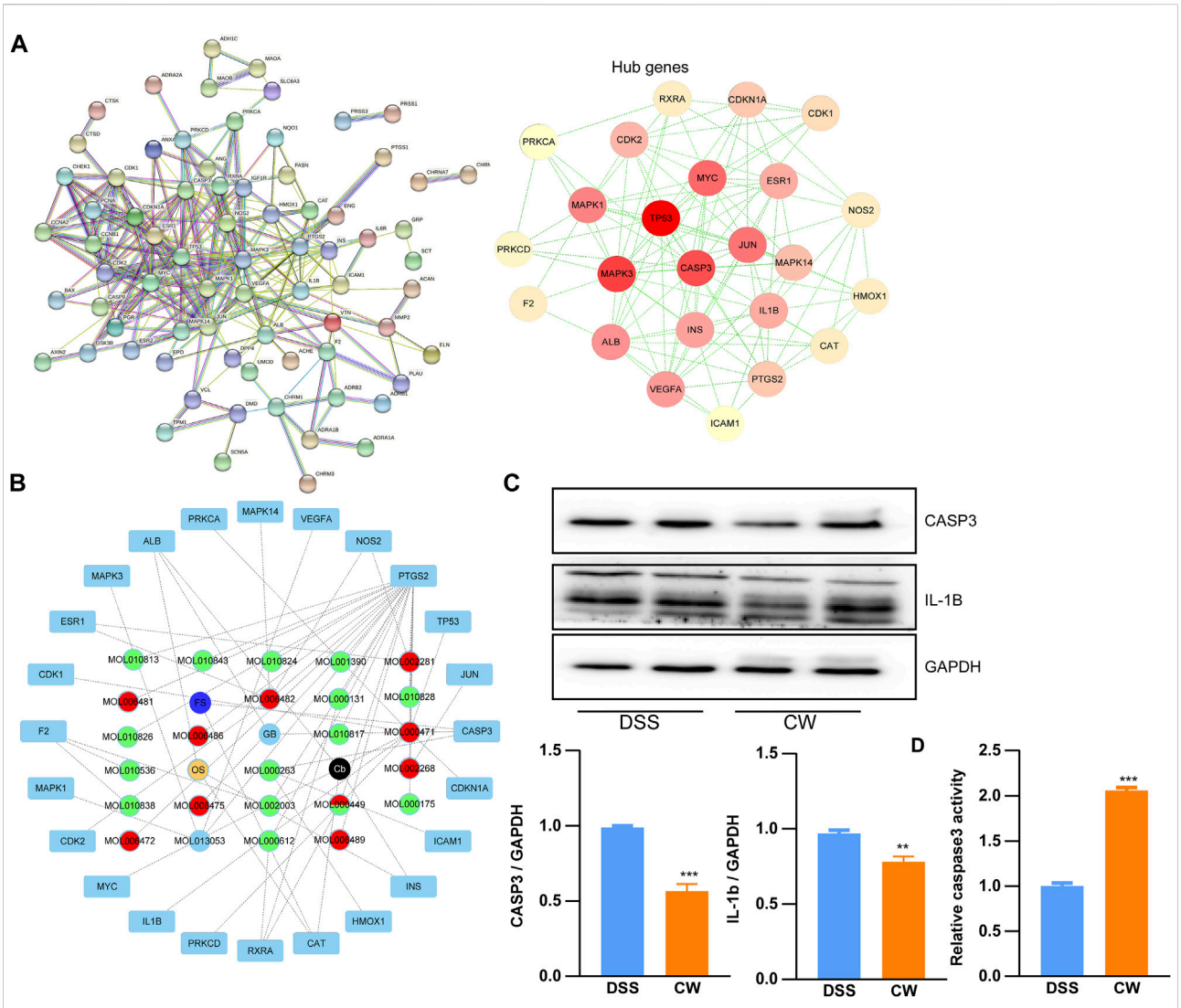

FIGURE 4
Protein–protein interaction network of the CW formula. Interaction network **(A)**; hub gene–component network **(B)**; and the expression of Casp3 and IL-1b, as well as the Casp3 activity in the colon samples from colitis mice with or without CW treatment **(C,D)** (*n* = 5). *indicates a statistically significant difference from the DSS group.

distinctly from the DSS group with a stress value of 0.02 (Figure 5C). At the phylum level, we observed an apparent reduction in Bacteroidota and Firmicutes in the DSS group compared with other groups, with an increase in Proteobacteria (Figure 5D). LEFSe showed that the CW treatment increased the relative abundance of the phyla Bacteroidota and Firmicutes, whereas decreased the prevalence of Proteobacteria at the phylum level. The administration of CW suppressed the abundance of species *Romboutsia ilealis*, *Bacteroides thetaiotaomicron*, *Paeniclostridium sordellii*, and *Escherichia*, and *Shigella*, while increased *Lachnospiraceae NK4A136*, *Phascolarctobacterium faecium*, *Mucispirillum schaedleri*, and *Helicobacter winghamensis* (Figure 5E). BugBase feature prediction calculated by Mann–Whitney–Wilcoxon analysis showed that the CW treatment significantly reversed the DSS-induced abundance of potentially pathogenic phenotype microorganisms (Figure 5F). PICRUSt analysis demonstrated that the administration of XQ inhibited infectious diseases and cancers, and lipid metabolism, controlled the digestive system, and improved the immune system (Figure 5G).

To examine the alterations in the metabolic profile, untargeted metabolomics was performed. OPLS-DAOPLA-DA showed that the metabolites between the saline and the DSS group were clustered distinctly between the two groups with Q2Y (0.894, 0.782) and R2Y (0.953, 0.953) (Supplementary Figure S2A). A Q2 value of more than 0.5 indicates the precise

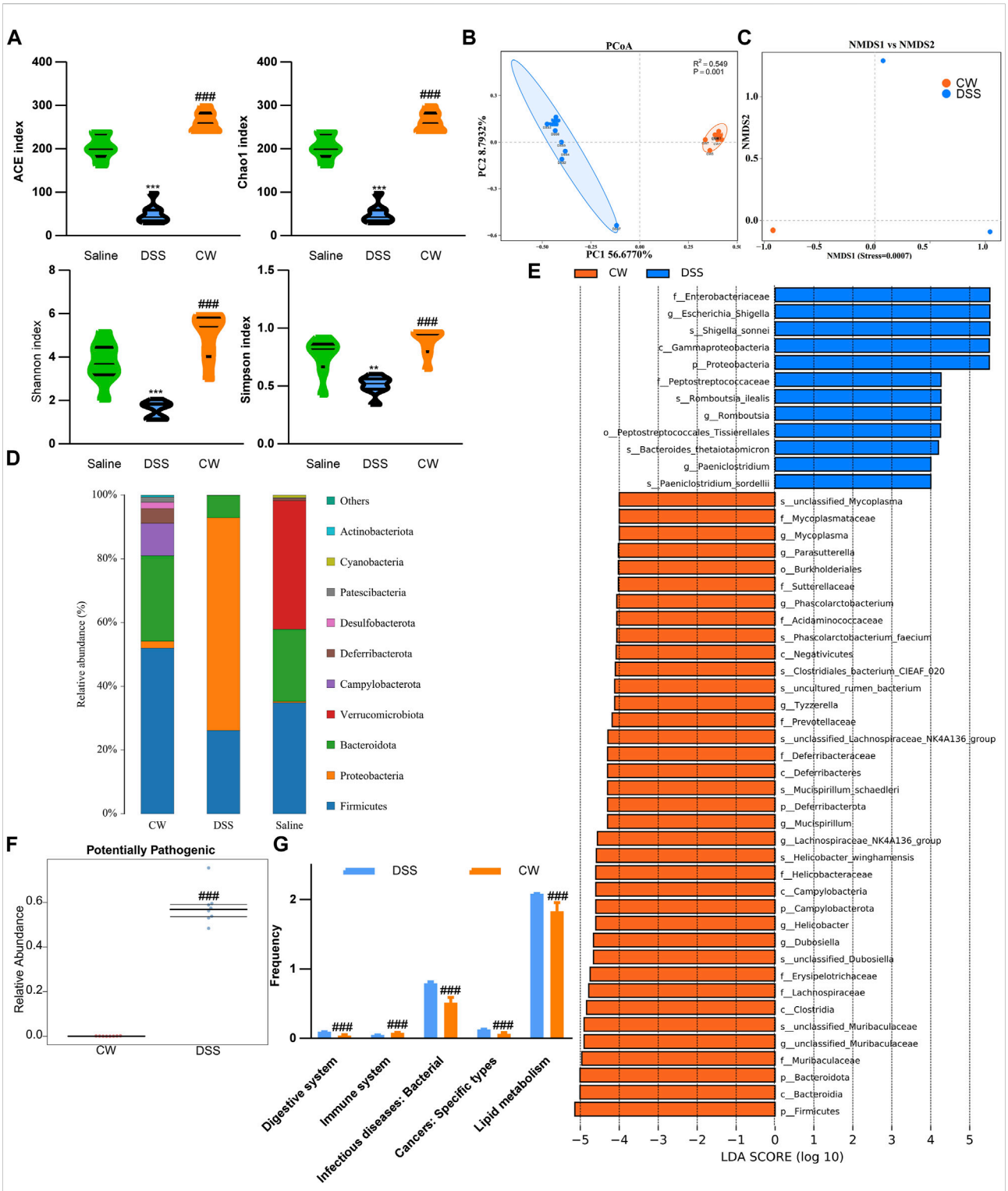

FIGURE 5
Alteration in the microbiota profile in UC murine models after CW treatment. Alpha-diversity of microbial communities in mice undergoing colitis and treated with CW **(A)**. PCoA **(B)** and NMDS **(C)** show the clustering of gut flora; microbiota composition at the phylum **(D)**; LEFSe **(E)** illustrates the abundance of bacterial species in experimental colitis murine models after CW administration; BugBase **(F)** and PICRUSt **(G)** prediction. *indicates a statistical difference from the saline group, and #indicates a difference from the DSS group.

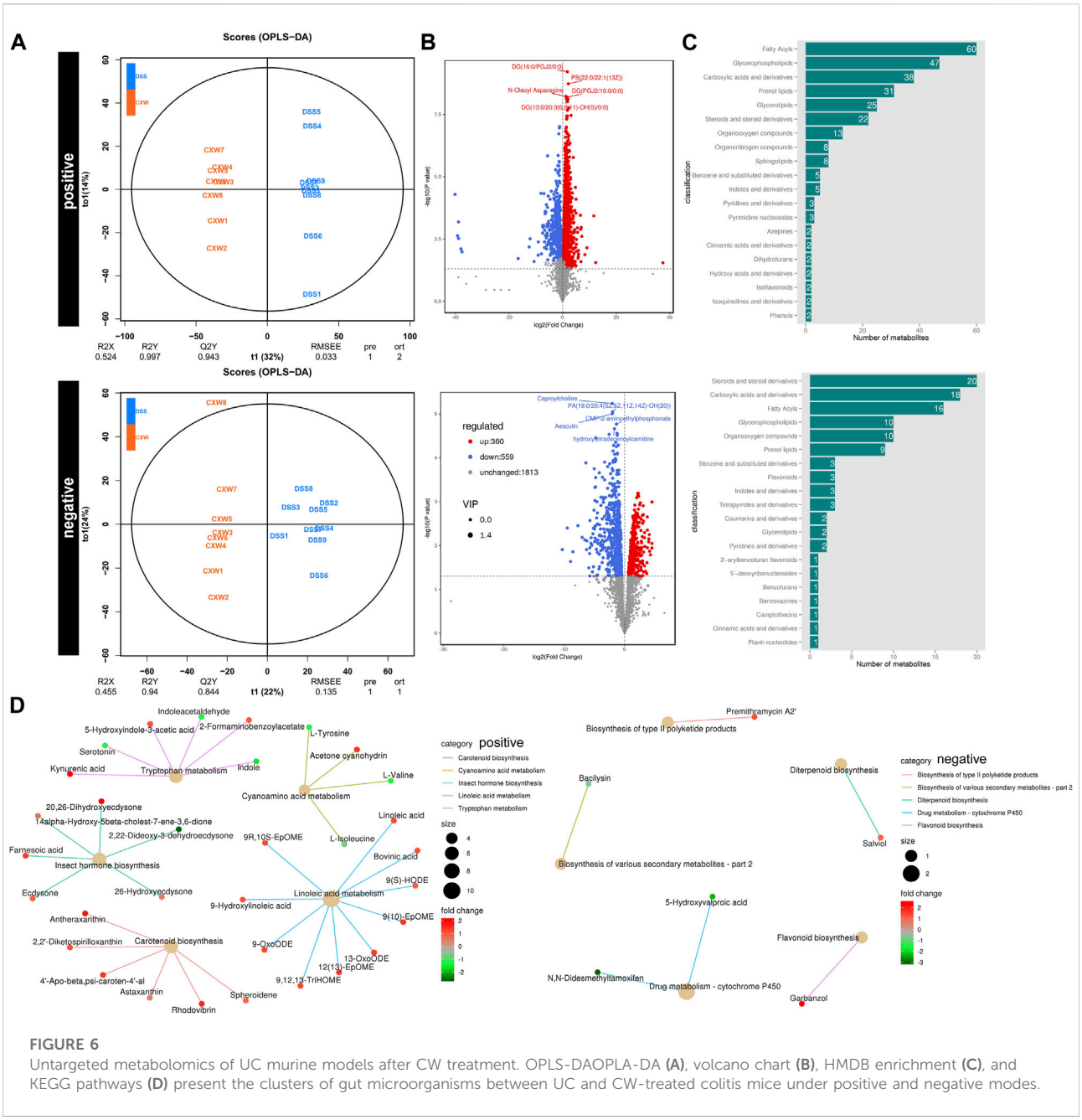

FIGURE 6
Untargeted metabolomics of UC murine models after CW treatment. OPLS-DAOPLA-DA **(A)**, volcano chart **(B)**, HMDB enrichment **(C)**, and KEGG pathways **(D)** present the clusters of gut microorganisms between UC and CW-treated colitis mice under positive and negative modes.

predictivity of the model. A permutation test was performed to validate the model, and R2 and Q2 should be higher than the permutated models with a vertical axis intersection of Q2 that was lower than zero. As illustrated, the intersection of Q2 was (0.0, −1.35) and (0.0,−1.35), which confirmed the validity of the OPLS-DA model (Supplementary Figure S2B). According to VIP, the top five regulated outlier metabolites in the DSS group are shown in (Supplementary Figure S2C, Supplementary Table S4). The KEGG analysis showed that DSS suppressed linoleic acid metabolism, whereas it increased the cytochrome P450 activity (Supplementary Figure S2D).

OPLS-DAOPLA-DA combined with a permutation test also validated the differential metabolites between the DSS and DSS-CW (1.44 g/kg) groups with Q2Y (0.943, 0.844) and R2Y (0.997, 0.94) (Figure 6A). The top five regulated metabolites are listed in Figure 6B (Supplementary Table S5). The differential metabolites between the CW and DSS groups were associated with carboxylic acids and derivatives, glycerophospholipids, fatty acyls, and steroids and derivatives (Figure 6C). The administration of the CW abolished the DSS-induced cytochrome P450 activity and DSS-impaired linoleic acid metabolism, and inhibited serotonin levels in mice subjected to colitis (Figure 6D).

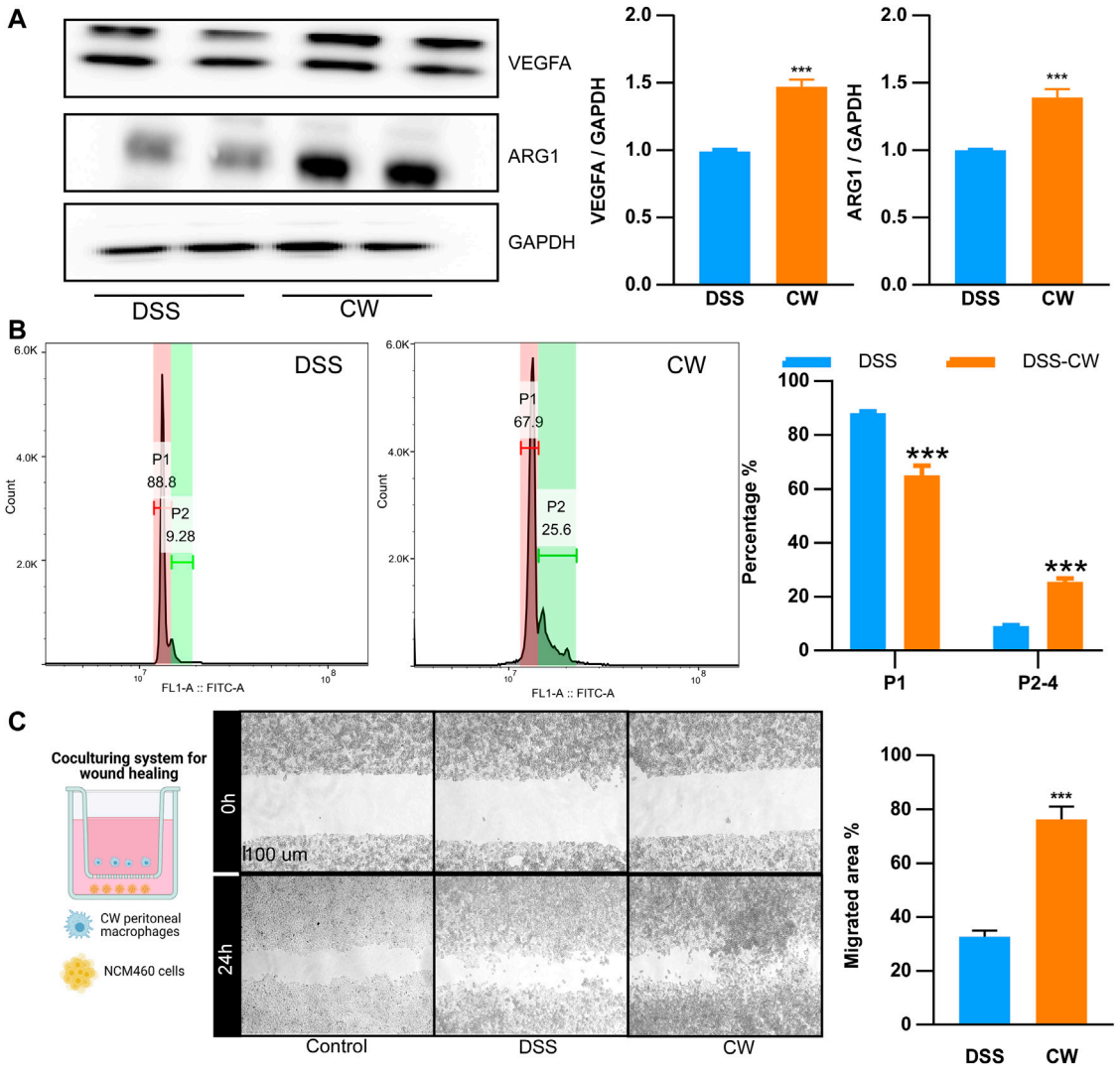

FIGURE 7
CW facilitates the alternative activation of macrophages. The protein abundance of Arg1 and Vegfa **(A)** in peritoneal macrophages from UC murine models after CW treatment (n = 5); phagocytic capacity of peritoneal macrophages from UC murine models after CW treatment **(B)** (n = 5); wound healing assay **(C)** showing the migration of NCM460 cells in the presence of peritoneal macrophages from the CW group (n = 5). *indicates a statistical difference from the DSS group.

Cao-Xiang-Wei-Kang promoted the alternative activation of peritoneal macrophages

Peritoneal Mφs were collected from UC murine models. The CW formula increased the protein abundance of Vegfa and Arg1 (Figure 7A). As shown in microparticle experiments, the CW treatment increased the proportion of P2–P4 from 9.28% to 25.6% (Figure 7B), suggesting an enhanced M2 transition and alleviated inflammatory reactions. Moreover, NCM460 cells were co-cultured with the CW peritoneal Mφs for 24 h. The wound healing experiment showed an increased migration in the CW group, confirming the favored wound healing capacity of M2 Mφs (Figure 7C).

Cao-Xiang-Wei-Kang formula rescued the death of intestinal stem cells

IOs are composed of nearly all the intestinal cell types, including epithelial cells, endocrine cells, and paneth cells, hence being considered an ideal tool to reflect the status of epithelial recovery. We treated IOs with TNFα (20 ng/ml, 24 h) to construct an *ex vivo* UC cellular model. The serum

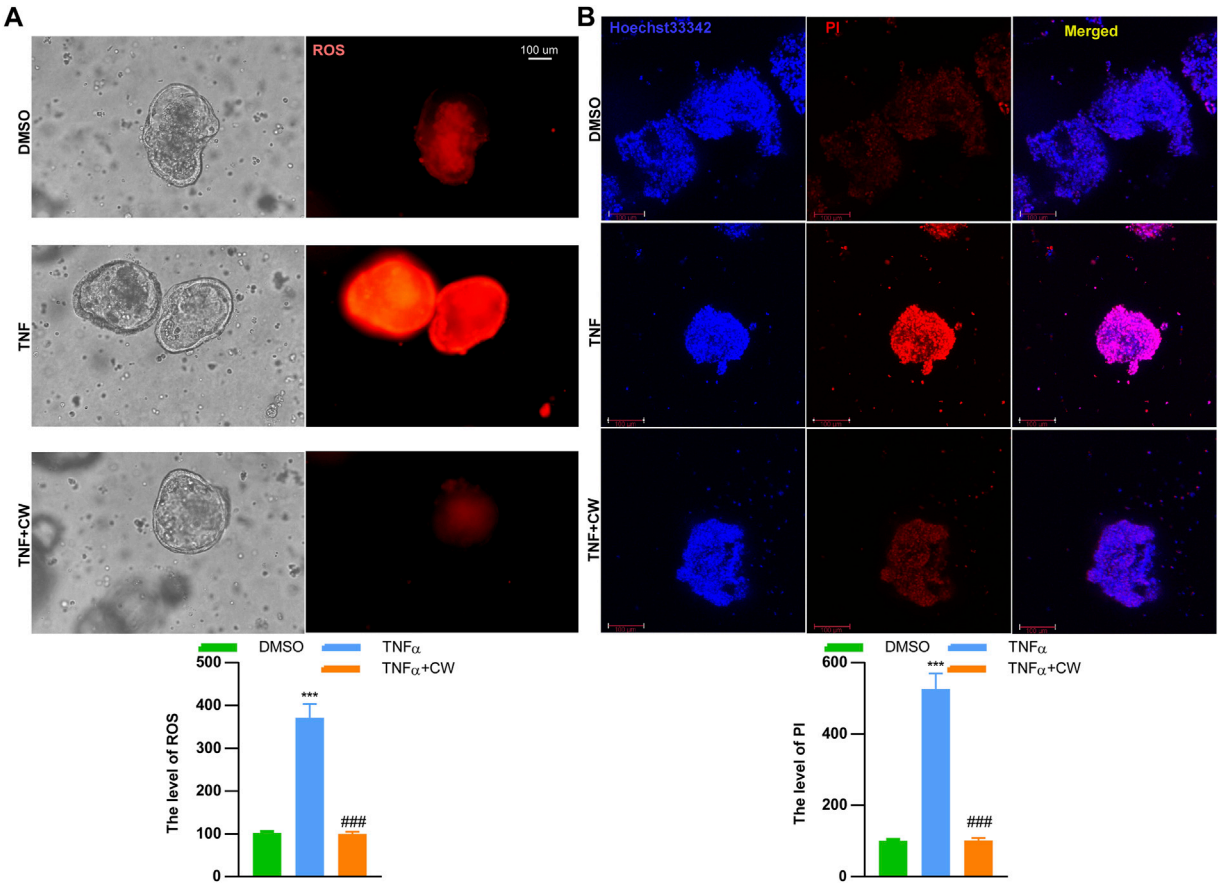

FIGURE 8
CW serum rescues inflammation-induced cell death of intestinal organoids. The mitochondrial stress **(A)** in TNFα-treated intestinal organoids with the CW serum for 24 h; Hoechst 33342/PI staining **(B)** (n = 5). *indicates a statistical difference from the DMSO group; #indicates a difference from the TNFα group.

was isolated from murine colitis models subjected to the CW treatment and healthy blank controls, and both doses of CW serum did not induce apoptosis and impaired the viability of NCM460 cells (Supplementary Figure S3). TNFα treatment increased the ROS level, and this elevation was diminished by the CW serum (Figure 8A). Moreover, TNFα-induced IO death was also rescued after the administration of the CW serum (Figure 8B).

Discussion

UC occurs mainly in the colon due to a broad spectrum of factors including the microbiome, genetic susceptibility, diet, host immune status, and environment. Patients with UC suffer from mental disorders and physical disadvantages, for example, rectal bleeding, abdominal pain, malnutrition, and diarrhea, with a higher risk of developing CAC than non-UC cohorts (Weingarden and Vaughn, 2017).

Given the rule of "Jun-Chen-Zuo-Shi" in TCM formula theories (Wang et al., 2020a) and the analysis of network pharmacology, SR was responsible for 35% of the weight and 36.7% of the targets in the CW formula and was, thus, considered the major ingredient "Jun," the targets of which were enriched in infections, cancers, the IL-17 signaling pathway, and neurotransmitter receptor activity, as well as liver diseases including hepatitis and non-alcoholic fatty liver disease. As a potent anti-inflammatory and anti-oxidant ingredient that can treat DSS-induced colitis (Kim et al., 2011; Hou et al., 2018), SR is also able to restrain the colonization of pathological microbes (Sung et al., 2004) and protects from liver injury (Paudel et al., 2018).

OS, Cb, and GB are natural organs from oyster, sepia, and *Gallus gallus domesticus Brisson*, respectively. Since each occupied about 20% of the weight of the CW formula, they were classified as "Chen." Both OS and Cb are mainly composed of calcium carbonate that exerts an anti-erosive effect against hydrochloric acid from gastric juice (Scandiffio et al., 2018), as well as of chitin (Scandiffio et al., 2018; Kintsu et al., 2020), which promotes the proliferation and

differentiation of stem cells (Ho et al., 2021), thereby facilitating wound healing (Francesko and Tzanov, 2011; Lim et al., 2015; Qiu et al., 2020). Noteworthy is the regulated protein processing by OS and Cb predicted by the KEGG analysis, implying that they work synergistically with GB, in which protein is the predominant component. Additionally, OS also improves the host immunity (Malhotra and Kang, 2013; Shi et al., 2021) by increasing SMAD1/5/8 expression (Ho et al., 2021), while the anti-oxidant Cb (Ramasamy et al., 2014) has been reported to protect against gastric ulcers (Qiu et al., 2020) and functions as a nutritional supplementation due to high-soluble amino acid and mineral levels in Cb (Ramasamy et al., 2014). KEGG analysis demonstrated that OS focused on responses to nutrients and hyperoxia, and gastrointestinal functions, including pancreatic secretion, and Cb contributed to re-epithelization by regulating tissue structure homeostasis, which was conducive to the integrity of the endothelial barrier. Consistent with OS and Cb, GB has a historical application in the treatment of ulcers and inflammatory disorders due to its anti-inflammatory, detoxifying, and anti-oxidant effects (Mahmoudi et al., 2013; Pan et al., 2016; Gao et al., 2020; Xiao et al., 2021), as well as the wound healing–promoting property (Salari et al., 2016; Yoo et al., 2017). The targets of GB had a strong correlation with inflammatory reactions, such as TNF, IL-17, HIF-1 signaling pathways, carcinogenesis, and VEGF-regulated migration, as well as responses to oxidative stress, toxic substance, and chemical stress. Apparently, OS and Cb are preferentially improving gastrointestinal functions and epithelial recovery, and providing nutrients, whereas GB shows a potent anti-inflammatory effect. "Chen" improves and expands the efficacy of the CW formula.

DC and FS were considered "Zuo" since they took only 15% of the whole formula. It is worth noting that DC attenuates the progression of DSS-induced colitis (Xie et al., 2020; Zhou et al., 2020), owing to its potent pharmacological activities, for instance, anti-CAC (Hu et al., 2018), anti-inflammation (Rayan et al., 2011; Butturini et al., 2014), and anti-pathogens (Tang et al., 2010; Hasson et al., 2013). Moreover, gastrointestinal spasms (Guo et al., 2014) and diarrhea (Mu et al., 2017) that occur in patients with IBD and murine colitis models could also be alleviated by DC. The anti-bacterial (Iranshahi et al., 2008) and anti-cancer activities (Zhang et al., 2015; Wang et al., 2020b) of FS added to the capacity for combating dysbiosis and preventing CAC. "Zuo" highlights the therapeutic value of the formula, owing to its potent pharmacological activities, and the low dose would not raise toxicity concerns.

Collectively, we summarized the therapeutic strategy of the CW formula from three aspects. To begin with, SR, GB, and DC have anti-inflammatory and anti-oxidant activities, all of which contribute to the resolution of inflammation and inflammation-compromised epithelial barrier function and pain (Baskol et al., 2008), as evidenced by the markedly decreased IL-1b expression and CASP3-dependent pyroptosis (Naji et al., 2016; Li et al., 2022) in murine colitis models subjected to the CW therapy. Mφs are a paradigm of immune cells with a highly plastic capacity able to change their phenotypes in response to environmental cues. M1 Mφs are responsible for initiating innate immunity, while M2 Mφs favor the resolution of inflammation and wound healing (Remmerie and Scott, 2018; Soto-Heredero et al., 2020). CW administration enhanced the expression of M2 markers, Arg1, and VEGFa, indicating an inhibited inflammatory response and a favored re-epithelization.

Second, bloody stool occurs in patients with UC and exacerbates the pain and mental suffering (Bounds and Kelsey, 2007), which could be rescued by accelerated wound healing accomplished by OS, Cb, and GB. Our *in vitro* experiments corroborated that TNFα exacerbated ROS production and induced necroptosis and pyroptosis, which was ameliorated by the CW serum. Moreover, the CW treatment increased VEGFa expression, which is pivotal for mucosal healing and recovery, and CW-treated Mφs improved NCM460 cell migration. Altogether, the CW formula was able to stop gastrointestinal bleeding and help mucosal recovery.

Third, an efficacious modulation of the gut microbiome was accomplished by SR and DC. The components of SR are against several pathogens including *Clostridium perfringens* (Ali et al., 2021), and the broad spectrum of the anti-bacterial activity of DC indicates the therapeutic value in combating infections (Munyaka et al., 2016). In full accordance with our results, DSS-induced colitis decreases the richness and diversity of the gut microbiota, both of which were reversed by the CW formula, highlighting its contribution to the remodeling of gut microbiota. An imbalanced gut commensal flora often begins with an increased prevalence of Proteobacteria and *Bacteroides thetaiotaomicron,* which have been considered potential diagnostic signatures of dysbiosis, depression, and colitis (Shin et al., 2015; Wang et al., 2022), and the CW therapy considerably suppressed their colonization. Moreover, DSS treatment induced the colonization of the genera *Escherichia* and *Shigella*, which is involved in the development of UC into CAC (Tang et al., 2020), which was also inhibited by CW treatment. Additionally, the increased relative abundance of *Dubosiella* and *Lachonospiraceae NK4A136, Mucispirillum schaedleri*, and *Lachnospiraceae* by CW is negatively correlated with the levels of inflammation-promoting cytokines (Wan et al., 2021) and favors gut barrier integrity (Herp et al., 2019; Ma et al., 2020). Altogether, CW treatment restores the colonization of gut commensal flora and plays a protective role in the gut.

Last but not least, the spasmolytic and anti-diarrheal effect of DC, the immunity-orchestrated OS, the nutrition-supplemented Cb, and the hepatoprotective role of DC (Ge et al., 2020) and SR (Paudel et al., 2018) underlie the success of the CW formula in colitis intervention. Moreover, since most TCM formulas have multiple herbs functioning in a synergistic or counteracting mode to achieve homeostasis, drug resistance and metabolism are the major challenges for drug efficacy and safety. Among the six ingredients, Cb, GB, and OS are atoxic. The dosage of DC in the CW formula for adults was 0.3 g/d, which is far less than the recommended level 3–6 g/d in Chinese Pharmacopoeia 2020 (Huang et al., 2021) and hence resolves the concern regarding toxicity (Bei-Xuan et al., 2016). The potential hepatoxicity of SR

(Yang et al., 2021) and FS might be counteracted by the detoxifying effect of GB (Mahmoudi et al., 2013; Pan et al., 2016; Gao et al., 2020; Xiao et al., 2021). As a result, 16S rRNA gene sequencing results confirmed that the CW therapy inhibited the prevalence of *Shigella sonne*, which contributes to drug resistance (Starling, 2017). As seen in our metabolomic analysis, Cytochromes P450 (CYPs), enzymes with catalytic activities regulating drug metabolism and toxicity (Guengerich et al., 2016), were enhanced during DSS-induced colitis, which was reversed after the CW treatment, suggesting a resolved issue regarding toxicity.

Collectively, the anti-colitis effect of the CW formula is attributed to multiple active components. We constructed a target–component network utilizing hub genes calculated by network pharmacology and their corresponding components and found that all of the six ingredients, which are 29 components, were associated with the hub genes, which might be the key active components of the CW formula to treat colitis and needs further pharmacokinetic investigation.

Conclusion

We posit that the CW formula is an efficient formula to treat colitis by combining low-toxic ingredients with atoxic medicinal animal organs, and it suppresses inflammation and the prevalence of pathogens, with the concomitant improvements in gut immunity and nutrient supply. Nevertheless, the therapeutic effects of each component merit closer investigation, which could pave the way for adding to the understanding of this formula.

Data availability statement

The datasets presented in this study can be found in online repositories. The names of the repository/repositories and accession number(s) can be found at: https://www.ncbi.nlm.nih.gov; PRJNA827781.

Ethics statement

The animal study was reviewed and approved by the Institutional Animal Care and Use Committee of Jining Medical University in China (SYXK-Shandong province-2018-0002).

Author contributions

Study concept and design: JY. Data acquisition: JY, WY, CS, YZ, CK, YZ, XHL, and XCL. Data analysis and interpretation: WY. Drafting of the manuscript: JY. Obtained funding: JY and WY. All data were generated in-house, and no paper mill was used. All authors agree to be accountable for all aspects of work ensuring integrity and accuracy.

Funding

The investigation was funded by the scientific function of Jining Medical University (JYGC2021KJ003).

Conflict of interest

The authors declare that the research was conducted in the absence of any commercial or financial relationships that could be construed as a potential conflict of interest.

Publisher's note

Supplementary material

The Supplementary Material for this article can be found online at: https://www.frontiersin.org/articles/10.3389/fphar.2022.946065/full#supplementary-material

SUPPLEMENTARY TABLE S1
LC-MS/MS identified active components of CW.

SUPPLEMENTARY TABLE S2
Targets of CW.

SUPPLEMENTARY TABLE S3
Alpha diversity indices of the gut microbiota after CW treatment.

SUPPLEMENTARY TABLE S4
Altered metabolites in the fecal samples from colitis mice.

SUPPLEMENTARY TABLE S5
Altered metabolites in the fecal samples from colitis mice after CW treatment.

SUPPLEMENTARY FIGURE S1
LC-MS/MS identified CW components.

SUPPLEMENTARY FIGURE S2
Alteration in the microbiome profile in murine colitis models OPLS-DAOPLA-DA ,**(A)** permutation test **(B)**, and volcano chart **(C)** showing the metabolite clusters between saline and colitis mice under positive and negative modes; KEGG pathways **(D)**.

SUPPLEMENTARY FIGURE S3
MTT assay evaluating the toxicity of the CW serum PI staining **(A)** and MTT assay **(B)** of the NCM460 cells with different concentrations of the CW serum (CW-low: 0.7 g/kg ; high: 1.4 g/kg).

References

Ali, M. Y., Park, S., and Chang, M. (2021). Phytochemistry, ethnopharmacological uses, biological activities, and therapeutic applications of Cassia obtusifolia L. A comprehensive review. *Molecules* 26, 6252. doi:10.3390/molecules26206252

Amberger, J. S., and Hamosh, A. (2017). Searching online mendelian inheritance in man (OMIM): A knowledgebase of human genes and genetic phenotypes. *Curr. Protoc. Bioinforma.* 58, 1. doi:10.1002/cpbi.27

Barbarino, J. M., Whirl-Carrillo, M., Altman, R. B., and Klein, T. E. (2018). PharmGKB: A worldwide resource for pharmacogenomic information. *Wiley Interdiscip. Rev. Syst. Biol. Med.* 10, e1417. doi:10.1002/wsbm.1417

Baskol, M., Baskol, G., Koçer, D., Ozbakir, O., and Yucesoy, M. (2008). Advanced oxidation protein products: A novel marker of oxidative stress in ulcerative colitis. *J. Clin. Gastroenterol.* 42, 687–691. doi:10.1097/MCG.0b013e318074f91f

Bei-Xuan, H. E., Yang, Y. T., Yu-Lin, H. E., Peng, C., and Cao, Z. X. (2016). *Preliminary study on volatile oil of common aucklandia root in embryotoxicity of zebrafish*. Peking city, China: China Journal of Traditional Chinese Medicine and Pharmacy.

Bolger, A. M., Lohse, M., and Usadel, B. (2014). Trimmomatic: A flexible trimmer for illumina sequence data. *Bioinformatics* 30, 2114–2120. doi:10.1093/bioinformatics/btu170

Bounds, B. C., and Kelsey, P. B. (2007). Lower gastrointestinal bleeding. *Gastrointest. Endosc. Clin. N. Am.* 17, 273–288. doi:10.1016/j.giec.2007.03.010

Butturini, E., Di Paola, R., Suzuki, H., Paterniti, I., Ahmad, A., Mariotto, S., et al. (2014). Costunolide and Dehydrocostuslactone, two natural sesquiterpene lactones, ameliorate the inflammatory process associated to experimental pleurisy in mice. *Eur. J. Pharmacol.* 730, 107–115. doi:10.1016/j.ejphar.2014.02.031

Francesko, A., and Tzanov, T. (2011). Chitin, chitosan and derivatives for wound healing and tissue engineering. *Adv. Biochem. Eng. Biotechnol.* 125, 1–27. doi:10.1007/10_2010_93

Gao, Y., Zhang, X., Ren, G., Wu, C., Qin, P., and Yao, Y. (2020). Peptides from extruded lupin (lupinus albus L.) regulate inflammatory activity via the p38 MAPK signal transduction pathway in RAW 264.7 cells. *J. Agric. Food Chem.* 68, 11702–11709. doi:10.1021/acs.jafc.0c02476

Garcia, A., and Barbas, C. (2011). Gas chromatography-mass spectrometry (GC-MS)-based metabolomics. *Methods Mol. Biol.* 708, 191–204. doi:10.1007/978-1-61737-985-7_11

Ge, M. X., Liu, H. T., Zhang, N., Niu, W. X., Lu, Z. N., Bao, Y. Y., et al. (2020). Costunolide represses hepatic fibrosis through WW domain-containing protein 2-mediated Notch3 degradation. *Br. J. Pharmacol.* 177, 372–387. doi:10.1111/bph.14873

Guengerich, F. P., Waterman, M. R., and Egli, M. (2016). Recent structural insights into cytochrome P450 function. *Trends Pharmacol. Sci.* 37, 625–640. doi:10.1016/j.tips.2016.05.006

Guo, H., Zhang, J., Gao, W., Qu, Z., and Liu, C. (2014). Gastrointestinal effect of methanol extract of Radix Aucklandiae and selected active substances on the transit activity of rat isolated intestinal strips. *Pharm. Biol.* 52, 1141–1149. doi:10.3109/13880209.2013.879601

Guo, K., Ge, J., Zhang, C., Lv, M. W., Zhang, Q., Talukder, M., et al. (2020). `Cadmium induced cardiac inflammation in chicken (Gallus gallus) via modulating cytochrome P450 systems and Nrf2 mediated antioxidant defense. *Chemosphere* 249, 125858. doi:10.1016/j.chemosphere.2020.125858

Hasson, S. S., Al-Balushi, M. S., Alharthy, K., Al-Busaidi, J. Z., Aldaihani, M. S., Othman, M. S., et al. (2013). Evaluation of anti-resistant activity of Auklandia (Saussurea lappa) root against some human pathogens. *Asian pac. J. Trop. Biomed.* 3, 557–562. doi:10.1016/S2221-1691(13)60113-6

Herp, S., Brugiroux, S., Garzetti, D., Ring, D., Jochum, L. M., Beutler, M., et al. (2019). Mucispirillum schaedleri antagonizes Salmonella virulence to protect mice against colitis. *Cell Host Microbe* 25, 681–694. e8. doi:10.1016/j.chom.2019.03.004

Ho, W. F., Lee, M. H., Thomas, J. L., Li, J. A., Wu, S. C., Hsu, H. C., et al. (2021). Porous biphasic calcium phosphate granules from oyster shell promote the differentiation of induced pluripotent stem cells. *Int. J. Mol. Sci.* 22, 9444. doi:10.3390/ijms22179444

Hou, J., Gu, Y., Zhao, S., Huo, M., Wang, S., Zhang, Y., et al. (2018). Anti-inflammatory effects of aurantio-obtusin from seed of Cassia obtusifolia L. Through modulation of the NF-κB pathway. *Molecules* 23, E3093. doi:10.3390/molecules23123093

Hu, M., Liu, L., and Yao, W. (2018). Activation of p53 by costunolide blocks glutaminolysis and inhibits proliferation in human colorectal cancer cells. *Gene* 678, 261–269. doi:10.1016/j.gene.2018.08.048

Huang, Z., Wei, C., Yang, K., Yu, Z., Wang, Z., and Hu, H. (2021). Aucklandiae radix and vladimiriae radix: A systematic review in ethnopharmacology, phytochemistry and pharmacology. *J. Ethnopharmacol.* 280, 114372. doi:10.1016/j.jep.2021.114372

Iranshahi, M., Hosseini, S. T., Shahverdi, A. R., Molazade, K., Khan, S. S., and Ahmad, V. U. (2008). Diversolides A-G, guaianolides from the roots of Ferula diversivittata. *Phytochemistry* 69, 2753–2757. doi:10.1016/j.phytochem.2008.08.009

Kim, S. J., Kim, K. W., Kim, D. S., Kim, M. C., Jeon, Y. D., Kim, S. G., et al. (2011). The protective effect of Cassia obtusifolia on DSS-induced colitis. *Am. J. Chin. Med.* 39, 565–577. doi:10.1142/S0192415X11009032

Kintsu, H., Nishimura, R., Negishi, L., Kuriyama, I., Tsuchihashi, Y., Zhu, L., et al. (2020). Identification of methionine -rich insoluble proteins in the shell of the pearl oyster, Pinctada fucata. *Sci. Rep.* 10, 18335. doi:10.1038/s41598-020-75444-4

Lee, J. H., Choi, S., Lee, Y., Lee, H. J., Kim, K. H., Ahn, K. S., et al. (2010). Herbal compound farnesiferol C exerts antiangiogenic and antitumor activity and targets multiple aspects of VEGFR1 (Flt1) or VEGFR2 (Flk1) signaling cascades. *Mol. Cancer Ther.* 9, 389–399. doi:10.1158/1535-7163.MCT-09-0775

Li, N., Chen, J., Geng, C., Wang, X., Wang, Y., Sun, N., et al. (2022). Myoglobin promotes macrophage polarization to M1 type and pyroptosis via the RIG-I/Caspase1/GSDMD signaling pathway in CS-AKI. *Cell Death Discov.* 8, 90. doi:10.1038/s41420-022-00894-w

Lim, S. C., Lee, K. M., and Kang, T. J. (2015). Chitin from cuttlebone activates inflammatory cells to enhance the cell migration. *Biomol. Ther.* 23, 333–338. doi:10.4062/biomolther.2015.062

Ma, L., Ni, Y., Wang, Z., Tu, W., Ni, L., Zhuge, F., et al. (2020). Spermidine improves gut barrier integrity and gut microbiota function in diet-induced obese mice. *Gut Microbes* 12, 1–19. doi:10.1080/19490976.2020.1832857

Mahmoudi, M., Ebrahimzadeh, M. A., Pourmorad, F., Rezaie, N., and Mahmoudi, M. A. (2013). Anti-inflammatory and analgesic effects of egg yolk: A comparison between organic and machine made. *Eur. Rev. Med. Pharmacol. Sci.* 17, 472–476.

Malhotra, N., and Kang, J. (2013). SMAD regulatory networks construct a balanced immune system. *Immunology* 139, 1–10. doi:10.1111/imm.12076

Mu, J., Dan, L., Zhu, S., Wang, C., Qu, X., Fan, B., et al. (2017). *The experimental research of costustoot relieves delayed-coset diarrhea caused by irinotecan*. Guangdong: Guangdong Chemical Industry.

Munyaka, P. M., Rabbi, M. F., Khafipour, E., and Ghia, J. E. (2016). Acute dextran sulfate sodium (DSS)-induced colitis promotes gut microbial dysbiosis in mice. *J. Basic Microbiol.* 56, 986–998. doi:10.1002/jobm.201500726

Naji, A., Muzembo, B. A., Yagyu, K., Baba, N., Deschaseaux, F., Sensebe, L., et al. (2016). Endocytosis of indium-tin-oxide nanoparticles by macrophages provokes pyroptosis requiring NLRP3-ASC-Caspase1 axis that can be prevented by mesenchymal stem cells. *Sci. Rep.* 6, 26162. doi:10.1038/srep26162

Ondov, B. D., Bergman, N. H., and Phillippy, A. M. (2011). Interactive metagenomic visualization in a Web browser. *BMC Bioinforma.* 12, 385. doi:10.1186/1471-2105-12-385

Pan, H., Song, S., Ma, Q., Wei, H., Ren, D., and Lu, J. (2016). Preparation, identification and antioxidant properties of black-bone silky fowl (Gallus gallus domesticus Brisson) iron(II)-Oligopeptide chelate. *Food Technol. Biotechnol.* 54, 164–171. doi:10.17113/ftb.54.02.16.4166

Paudel, P., Jung, H. A., and Choi, J. S. (2018). Anthraquinone and naphthopyrone glycosides from Cassia obtusifolia seeds mediate hepatoprotection via Nrf2-mediated HO-1 activation and MAPK modulation. *Arch. Pharm. Res.* 41, 677–689. doi:10.1007/s12272-018-1040-4

Qiu, L., Yao, L., Fang, Y., Wang, L., Xue, M., Lin, Z., et al. (2020). Effect of cuttlebone on healing of indomethacin-induced acute gastric mucosal lesions in rats. *Evid. Based. Complement. Altern. Med.* 2020, 9592608. doi:10.1155/2020/9592608

Ramasamy, P., Subhapradha, N., Shanmugam, V., and Shanmugam, A. (2014). Extraction, characterization and antioxidant property of chitosan from cuttlebone Sepia kobiensis (Hoyle 1885). *Int. J. Biol. Macromol.* 64, 202–212. doi:10.1016/j.ijbiomac.2013.12.008

Rayan, N. A., Baby, N., Pitchai, D., Indraswari, F., Ling, E. A., Lu, J., et al. (2011). Costunolide inhibits proinflammatory cytokines and iNOS in activated murine BV2 microglia. *Front. Biosci.* 3, 1079–1091. doi:10.2741/e312

Remmerie, A., and Scott, C. L. (2018). Macrophages and lipid metabolism. *Cell. Immunol.* 330, 27–42. doi:10.1016/j.cellimm.2018.01.020

Rogler, G., Singh, A., Kavanaugh, A., and Rubin, D. T. (2021). Extraintestinal manifestations of inflammatory bowel disease: Current concepts, treatment, and implications for disease management. *Gastroenterology* 161, 1118–1132.

Ru, J., Li, P., Wang, J., Zhou, W., Li, B., Huang, C., et al. (2014). Tcmsp: A database of systems pharmacology for drug discovery from herbal medicines. *J. Cheminform* 6, 13.

Salari, M., Salari, R., Dadgarmoghadam, M., Khadem-Rezaiyan, M., and Hosseini, M. (2016). Efficacy of egg yolk and nitroglycerin ointment as treatments for acute anal fissures: A randomized clinical trial study. *Electron. Physician* 8, 3035–3041. doi:10.19082/3035

Scandiffio, P., Mantilla, T., Amaral, F., França, F., Basting, R., and Turssi, C. (2018). Anti-erosive effect of calcium carbonate suspensions. *J. Clin. Exp. Dent.* 10, e776–e780. doi:10.4317/jced.54994

Shi, Y., Pan, X., Xu, M., Liu, H., Xu, H., and He, M. (2021). The role of Smad1/5 in mantle immunity of the pearl oyster Pinctada fucata martensii. *Fish. Shellfish Immunol.* 113, 208–215. doi:10.1016/j.fsi.2021.04.001

Shin, N. R., Whon, T. W., and Bae, J. W. (2015). Proteobacteria: Microbial signature of dysbiosis in gut microbiota. *Trends Biotechnol.* 33, 496–503. doi:10.1016/j.tibtech.2015.06.011

Soto-Heredero, G., Gomez de Las Heras, M. M., Gabande-Rodriguez, E., Oller, J., and Mittelbrunn, M. (2020). Glycolysis - a key player in the inflammatory response. *FEBS J.* 287, 3350–3369. doi:10.1111/febs.15327

Starling, S. (2017). Bacterial secretion: Shigella sonnei has the edge. *Nat. Rev. Microbiol.* 15, 450–451. doi:10.1038/nrmicro.2017.74

Stelzer, G., Rosen, N., Plaschkes, I., Zimmerman, S., Twik, M., Fishilevich, S., et al. (2016). The GeneCards suite: From gene data mining to disease genome sequence analyses. *Curr. Protoc. Bioinforma.* 54, 1. doi:10.1002/cpbi.5

Sung, B. K., Kim, M. K., Lee, W. H., Lee, D. H., and Lee, H. S. (2004). Growth responses of Cassia obtusifolia toward human intestinal bacteria. *Fitoterapia* 75, 505–509. doi:10.1016/j.fitote.2004.03.012

Tang, Q., Cang, S., Jiao, J., Rong, W., Xu, H., Bi, K., et al. (2020). Integrated study of metabolomics and gut metabolic activity from ulcerative colitis to colorectal cancer: The combined action of disordered gut microbiota and linoleic acid metabolic pathway might fuel cancer. *J. Chromatogr. A* 1629, 461503. doi:10.1016/j.chroma.2020.461503

Tang, Y., Li, M., Wang, J., Pan, Y., and Wu, F. X. (2015). CytoNCA: A cytoscape plugin for centrality analysis and evaluation of protein interaction networks. *Biosystems.* 127, 67–72. doi:10.1016/j.biosystems.2014.11.005

Tang, Y. P., Hou, P. F., Duan, J. A., Liu, P., and Su, S. L. (2010). *Inhibitory effects of sesquiterpenes from Common Aucklandia Root on proliferation of five kinds cultured cancer cells* in vitro. Peking city, China: China Journal of Traditional Chinese Medicine and Pharmacy.

The Gene Ontology Consortium (2019). The gene Ontology resource: 20 years and still GOing strong. *Nucleic Acids Res.* 47, D330–d338. doi:10.1093/nar/gky1055

Veloso, P. M., Machado, R., and Nobre, C. (2021). Mesalazine and inflammatory bowel disease - from well-established therapies to progress beyond the state of the art. *Eur. J. Pharm. Biopharm.* 167, 89–103. doi:10.1016/j.ejpb.2021.07.014

Wan, F., Han, H., Zhong, R., Wang, M., Tang, S., Zhang, S., et al. (2021). Dihydroquercetin supplement alleviates colonic inflammation potentially through improved gut microbiota community in mice. *Food Funct.* 12, 11420–11434. doi:10.1039/d1fo01422f

Wang, J., Wang, H., Zhang, M., Li, X., Zhao, Y., Chen, G., et al. (2020). Sesquiterpene coumarins from Ferula sinkiangensis K.M.Shen and their cytotoxic activities. *Phytochemistry* 180, 112531. doi:10.1016/j.phytochem.2020.112531

Wang, N., Du, N., Peng, Y., Yang, K., Shu, Z., Chang, K., et al. (2020). Network patterns of herbal combinations in traditional Chinese clinical prescriptions. *Front. Pharmacol.* 11, 590824. doi:10.3389/fphar.2020.590824

Wang, Z., Liu, S., Xu, X., Xiao, Y., Yang, M., Zhao, X., et al. (2022). Gut microbiota associated with effectiveness and responsiveness to mindfulness-based cognitive therapy in improving trait anxiety. *Front. Cell. Infect. Microbiol.* 12, 719829. doi:10.3389/fcimb.2022.719829

Weingarden, A. R., and Vaughn, B. P. (2017). Intestinal microbiota, fecal microbiota transplantation, and inflammatory bowel disease. *Gut Microbes* 8, 238–252. doi:10.1080/19490976.2017.1290757

Wishart, D. S., Feunang, Y. D., Guo, A. C., Lo, E. J., Marcu, A., Grant, J. R., et al. (2018). DrugBank 5.0: A major update to the DrugBank database for 2018. *Nucleic Acids Res.* 46, D1074–D1082. doi:10.1093/nar/gkx1037

Wishart, D. S., Feunang, Y. D., Marcu, A., Guo, A. C., Liang, K., Vázquez-Fresno, R., et al. (2018). Hmdb 4.0: The human metabolome database for 2018. *Nucleic Acids Res.* 46, D608–D617. doi:10.1093/nar/gkx1089

Xiao, N., Zhao, Y., He, W., Yao, Y., Wu, N., Xu, M., et al. (2021). Egg yolk oils exert anti-inflammatory effect via regulating Nrf2/NF-κB pathway. *J. Ethnopharmacol.* 274, 114070. doi:10.1016/j.jep.2021.114070

Xie, F., Zhang, H., Zheng, C., and Shen, X. F. (2020). Costunolide improved dextran sulfate sodium-induced acute ulcerative colitis in mice through NF-κB, STAT1/3, and Akt signaling pathways. *Int. Immunopharmacol.* 84, 106567. doi:10.1016/j.intimp.2020.106567

Yang, J., Wang, S., Zhang, T., Sun, Y., Han, L., Banahene, P. O., et al. (2021). Predicting the potential toxicity of 26 components in Cassiae semen using *in silico* and *in vitro* approaches. *Curr. Res. Toxicol.* 2, 237–245. doi:10.1016/j.crtox.2021.06.001

Yoo, H.-S., Chung, K.-H., Lee, K.-J., Kim, D.-H., and An, J. H. (2017). Melanin extract from Gallus gallus domesticus promotes proliferation and differentiation of osteoblastic MG-63 cells via bone morphogenetic protein-2 signaling. *Nutr. Res. Pract.* 11, 190–197. doi:10.4162/nrp.2017.11.3.190

Yu, W., Ou, X., Liu, X., Zhang, S., Gao, X., Cheng, H., et al. (2020). ACE2 contributes to the maintenance of mouse epithelial barrier function. *Biochem. Biophys. Res. Commun.* 533, 1276–1282. doi:10.1016/j.bbrc.2020.10.002

Zhang, H., Lu, J., Zhou, L., Jiang, L., and Zhou, M. (2015). Antioxidant and antitumor effects of ferula sinkiangensis K. M. Shen. *Int. J. Clin. Exp. Med.* 8, 20845–20852.

Zhou, Q., Zhang, W. X., He, Z. Q., Wu, B. S., Shen, Z. F., Shang, H. T., et al. (2020). The possible anti-inflammatory effect of dehydrocostus lactone on DSS-induced colitis in mice. *Evid. Based. Complement. Altern. Med.* 2020, 5659738. doi:10.1155/2020/5659738

frontiers | Frontiers in Pharmacology

TYPE Original Research
PUBLISHED 23 September 2022
DOI 10.3389/fphar.2022.955421

OPEN ACCESS

EDITED BY
Mingyu Sun,
Shanghai University of Traditional Chinese Medicine, China

REVIEWED BY
Jianye Yuan,
Shanghai University of Traditional Chinese Medicine, China
Albert Orock,
University of Oklahoma Health Sciences Center, United States

*CORRESPONDENCE
Gengqing Song,
songgavin2010@gmail.com
Wei Wei,
sxxtyy@sina.com

†These authors have contributed equally to this work

SPECIALTY SECTION
This article was submitted to Gastrointestinal and Hepatic Pharmacology, a section of the journal Frontiers in Pharmacology

RECEIVED 28 May 2022
ACCEPTED 24 August 2022
PUBLISHED 23 September 2022

CITATION
Jiang T, Niu R, Liu Q, Fu Y, Luo X, Zhang T, Wu B, Han J, Yang Y, Su X, Chen JDZ, Song G and Wei W (2022), Wenshen-Jianpi prescription, a Chinese herbal medicine, improves visceral hypersensitivity in a rat model of IBS-D by regulating the MEK/ERK signal pathway.
Front. Pharmacol. 13:955421.
doi: 10.3389/fphar.2022.955421

Wenshen-Jianpi prescription, a Chinese herbal medicine, improves visceral hypersensitivity in a rat model of IBS-D by regulating the MEK/ERK signal pathway

Tianyuan Jiang[1,2†], Ran Niu[1,2†], Qian Liu[1,2†], Yuhan Fu[3], Xiaoying Luo[1,2], Tao Zhang[1,2], Baoqi Wu[1,2], Juan Han[4], Yang Yang[1,2], Xiaolan Su[1,2], Jiande D. Z. Chen[5], Gengqing Song[6]* and Wei Wei[1,2]*

[1]Wangjing Hospital, China Academy of Chinese Medical Sciences, Beijing, China, [2]Laboratory of Functional Gastrointestinal Disorders Diagnosis and Treatment of Traditional Chinese Medicine, Beijing, China, [3]Department of Internal Medicine, MetroHealth Medical Center/Case Western Reserve University, Cleveland, OH, United States, [4]Institute of Acupuncture and Moxibustion, China Academy of Chinese Medical Sciences, Beijing, China, [5]Division of Gastroenterology and Hepatology, Department of Internal Medicine, University of Michigan, Ann Arbor, MI, United States, [6]Department of Gastroenterology and Hepatology, MetroHealth Medical Center/Case Western Reserve University, Cleveland, OH, United States

The goal of the study was to analyze whether WJP can alleviate visceral hypersensitivity in IBS-D model rats. In this study, 36 Sprague–Dawley (SD) rats aged 4 weeks old were randomly divided into two groups: the model group (n = 27) and the control group (n = 9). The rat model of IBS-D was established by modified compound methods for 4 weeks. After the modification, IBS-D rats were randomly divided into three groups, namely, the IBS-D model group (n = 9), the positive drug group (n = 9), and the WJP group (n = 9), with different interventions, respectively. The control group was fed and allowed to drink water routinely. The Bristol stool scale scores were used to assess the severity of diarrhea. Abdominal withdrawal reflex (AWR) scores were used to assess visceral sensitivity. Expression of TNF-α was measured, and histopathological examinations were performed to assess colon inflammation in IBS-D model rats. Key factors of the MEK/ERK signal pathway in the tissue of the colon and hippocampus were measured to analyze the mechanism of WJP. Compared with the control group, the Bristol stool scale scores in the model group were significantly increased ($p < 0.0001$). The scores of the WJP group were significantly decreased compared with the model group ($p = 0.0001$). Compared with the control group, AWR scores in the model group at each pressure level were significantly increased ($p = 0.0003$, $p < 0.0001$, $p = 0.0007$, and $p = 0.0009$). AWR scores of the WJP group were significantly decreased compared with the model group ($p = 0.0003$, $p = 0.0007$, $p = 0.0007$, and $p = 0.0009$). Compared with the control group, the model group had significantly higher expression of TNF-α in the colon tissue ($p < 0.0001$). However, the WJP

group had significantly lower level of TNF-α compared with the model group ($p < 0.0001$). Meanwhile, compared with the control group, the relative expression of the proteins of p-MEK1/2, p-ERK1, and p-ERK2 in the colon tissue was significantly increased in the model group ($p < 0.0001$). Compared with the model group, the relative expression of the proteins in the colon tissue were significantly decreased in the WJP group ($p < 0.0001$, $p = 0.0019$, and $p = 0.0013$). Compared with the control group, the relative expression of the proteins of p-MEK1/2, p-ERK1, and p-ERK2 in the hippocampus tissue were significantly increased in the model group ($p < 0.0001$). Compared with the model group, the relative expression of the proteins in the hippocampus tissue were significantly decreased in the WJP group ($p = 0.0126$, $p = 0.0291$, and $p = 0.0145$). The results indicated that WJP can alleviate visceral hypersensitivity in IBS-D model rats, possibly mediated by downregulating the expression of TNF-α, p-MEK1/2, p-ERK1, and p-ERK2 in the colon tissue. At the same time, WJP also affects downregulating the expression of p-MEK1/2, p-ERK1, and p-ERK2 in the hippocampus tissue.

KEYWORDS

rat model of IBS-D, visceral hypersensitivity, Chinese herbal medicine, colon, hippocampus, MEK/ERK signal pathway

1 Introduction

Irritable bowel syndrome (IBS) is characterized by recurrent abdominal pain associated with disordered defecation (Drossman et al.,2018). IBS can be further classified into four categories based on the predominant stool pattern by the Bristol Stool Form Scale: IBS with constipation (IBS-C), IBS with diarrhea (IBS-D), IBS with mixed stool pattern (IBS-M), and IBS unclassified (IBS-U). IBS-D was the most common subtype based on the Rome IV criteria [reported by 31.5% (95% CI 23.2–40.5; $I^2 = 98.1\%$ 61.6%) of people with IBS, corresponding to 1.4% (0.9%–1.9%) of all included participants having IBS-D] (Oka et al.,2020). The prevalence of IBS is between 5% and 10% in most geographical regions (Ford et al.,2020) and affects patients' quality of life and increases socioeconomic burden (Black et al.,2020). The mechanisms that underlie the disease are complex, and it has a tendency of recurrence, making the development of an effective and safe treatment still a challenging task.

Wenshen-Jianpi prescription (WJP) is a Chinese herbal medicine. It has been shown to be an effective treatment option for IBS-D by alleviating abdominal pain and improving disordered defecation with a good safety profile (Su et al.,2013). Moreover, the results of our previous clinical trials also showed that WJP could decrease the recurrence rates in the treatment group compared to the control group (15.79% vs. 56.86%, $p < 0.01$). However, the therapeutic mechanism of WJP remains unclear.

Visceral hypersensitivity has been proposed to be one of the major pathophysiological mechanisms of IBS. Intestinal inflammation can be seen as one of the triggers, causing visceral hypersensitivity. TNF-α is the main proinflammatory cytokine, and IBS-D patients showed higher levels of TNF-αcompared with healthy controls (Russo et al.,2018). The mitogen-activated extracellular signal–regulated kinase (MEK)/extracellular regulated protein kinases (ERK) signaling pathway plays an important role in the formation and maintenance of visceral hypersensitivity (Sun et al.,2019). The MEK/ERK signaling pathway was recognized as a classical signal pathway with conservative evolution, regulating the basic cellular processes, including proliferation, differentiation, apoptosis, and metabolism, (O'Neill et al.,2004). MEK1/2 usually combines with the nonactivated form of p-ERK1/2, keeping ERK inside the cytoplasm (Wortzel et al.,2011). When MEK1/2 is activated, it can activate p-ERK1/2 by phosphorylating. Once p-ERK1/2 is activated, it detaches from MEK and goes into the nucleus, activating the downstream mediators, such as c-fos (Roskoski,2012), and magnifying the nociceptive stimulation to produce the manifestation of visceral hypersensitivity. Suppressing the expression of ERK can significantly relieve pain perception (Xu et al.,2008).

However, studies in animal post-inflammation models indicated that visceral hypersensitivity to mechanical or chemical stimuli persists after the inflammation has resolved (Coldwell JR et al.,2007; Lyubashina et al.,2022), and it inspired us to explore where the "memory" of the visceral afferent hyperexcitability is stored. Hippocampus is a key structure for cognition and memory. A previous study indicated that it plays an important role in interoceptive signaling driven by memory mechanisms. In addition, the disorders responses to the interoceptive signaling can induce clinically relevant phenotypes, including chronic visceral hypersensitivity (Labrenz et al.,2022). At the same time, adverse life events,

TABLE 1 Constituents of WJP.

Chinese Name	Botanical Name	Genus	Family	Weight (g)	Part Used
Bu Gu Zhi	Cullen corylifolium	Psoralea Linn.	Fabaceae	30	Fruit
Rou Dou Kou	Myristica fragrans	Myristica Gronov.	Myristicaceae	15	Stem
Wu Zhu Yu	Tetradium ruticarpum	Evodia J. R. et G. Forst.	Rutaceae	6	Fruit
Wu Wei Zi	Schisandra chinensis	Schisandra Michx.	Schisandraceae	9	Fruit
Tai Zi Shen	Radix pseudostellariae	Pseudostellaria Pax	Caryophyllaceae	30	Root
Yu Jin	Curcuma aromatica	Curcuma L.	Zingiberaceae	18	Root
Chao Bai Zhu	Atractylodes macrocephala	Atractylodes	Asteraceae	10	Rhizome
Sheng Jiang	Zingiber officinale Roscoe	Zingiber	Suberitidae	10	Rhizome
Hong Zao	Ziziphus jujuba Mill.	Ziziphus Mill.	Rhamnaceae	10	Fruit

Abbreviation: WJP, Wenshen-Jianpi prescription.

TABLE 2 Sequence of gene primers.

Gene official symbol	Forward primer sequence	Reverse primer sequence	Product length (bp)
GAPDH	CAAGTTCAACGGCACAGTCAAG	ACATACTCAGCACCAGCATCAC	123
MEK1	AAGAAGAAGCCGACGCCCA	CCTTCAACTCTCCCACCTTCTG	187
MEK2	CATCAGTGCCACCTCCCAAG	TGAAGGCATGGTTCGTCAGC	129
ERK1	ACCTGCTGGACCGGATGTTA	AGCCACTGGTTCATCTGTCG	113
ERK2	CACCCGCATTGGTAGGAACT	GGATTGATCTGCGGTTGTGC	167

stress, and anxiety/depression can aggravate the degree of abdominal pain (Lyubashina et al.,2022).

Thus, the goal of this study was to explore the therapeutic mechanism of WJP in treating IBS-D model rats and to determine whether it can alleviate visceral hypersensitivity *via* the MEK/ERK signaling pathway in the region of the colon and hippocampus.

2 Experimental materials and methods

2.1 Chemicals and reagents

ELISA Kit for tumor necrosis factor-alpha (TNFa) (BIO EXCELLENCE, SEA133Ra), Kit for TRNzol Universal Reagent (TIANGEN BIOTECH (BEIJING) CO., LTD., DP424), Kit for EasyScrpt One-Step gDNA Removal and cDNA Synthesis SuperMix (TransGen Biotech, AE311-03), Kit for Hieff™ qPCR SYBR® Green Master Mix (No Rox), (Shanghai Yeasen BioTechnologies Co., Ltd., 11201ES08), MEK1/2 antibody (Affinity Biosciences, AF6385), Phospho-MEK1/2 (Ser218 + Ser222/Ser222 + Ser226) antibody (Affinity Biosciences, AF8035), p-ERK1/2 Polyclonal antibody (Cell Signaling Technology, 4695s), and Phospho-ERK1/2 (Thr202/Tyr204) Polyclonal antibody (Cell Signaling Technology, 4695s) were used in this study. Primers to amplify the genes GAPDH, MEK1, MEK2, ERK1, and ERK2 were designed by GENERAL BIOL (Anhui) Co., Ltd. (Anhui, China) (Table 1). Senna leaf and WJP formula granules (Sichuan Neo-Green Pharmaceutical Technology Development Co., Ltd., China) and pinaverium bromide (MYLAN LABORATORIES SAS, France) were used in this study.

2.2 Preparation and high-performance liquid chromatography analysis of WJP

WJP was prepared from nine commonly used herbs (Table 1), purchased from Beijing Sifang traditional Chinese medicine decoction pieces Co., Ltd. The nine ingredients were mixed according to the ratio of 30: 15: 6: 9: 30: 18: 10: 10: 10 (dry weight in grams). All herbs were decocted twice. The decoction of traditional Chinese Medicine was filtered using a 0.22 μm filter membrane, and 10 μl of the supernatant was collected for the test. Caffeoyl quinic acid (isomer of 831, 833, 834) (the representative component of WJP) was determined by HPLC, the Figure 1 showed the molecular structures (https://pubchem.ncbi.nlm.nih.gov/compound/348159). And 83 compounds were detected (the data have not been published).

2.3 Ethics statement

All feeding conditions were in compliance with the Chinese Animal Welfare Law and the relevant regulations of the Chinese Academy of Chinese Medical Sciences Experimental Animal Ethics Committee. Sprague–Dawley (SD) rats from the SiPeiFu (Beijing) Biotechnology Co., Ltd. (Beijing, China) were recruited to establish the model of IBS-D. Animal license Code: SCXK Beijing 2019-0010. Ethics No.: D2021-03-16-3.

2.4 Experimental protocol

A total of 36 male Sprague–Dawley (SD) rats (aged 4 weeks old and weighing 84.11 ± 10.02) were purchased from the SiPeiFu (Beijing) Biotechnology Co., Ltd. (Beijing, China). The rats were housed in an animal room (23 ± 2°C, 60% ± 5% relative humidity) with the setting of a 12 h dark/12 h light cycle. Before the experiment, the rats were given water and fed standard laboratory food for acclimatization for a week. The experiment was divided into two phases. And Figure 2 is a schematic diagram showed the detailed procedures for the experiments and the general conditions.

2.4.1 IBS-D rat model preparation

Rats were randomly divided into two groups: the control group (n = 9) and the model group (n = 27). The control group was fed routinely and only received routine tests but not stimuli or therapies. Meanwhile, the model group was stimulated according to the modified compound methods, including colorectal distention (Al-Chaer et al.,2000), water avoidance stress (Bradesi et al.,2005), load-bearing swimming, and administration of the senna leaf gavage (Li et al.,2017a). Four weeks later, the rats in the model group were randomly divided into the IBS-D model group (n = 9), the positive drug group (n = 9), and the WJP group (n = 9).

To be more specific,

a. Colorectal distention (CRD):

The distention was applied using an apparatus, that is, a latex balloon (length, 20.0 mm; diameter, 3.0 mm) attached to a sphygmomanometer. The balloon was inserted rectally into the descending colon, exerting a pressure of 60 mmHg (as measured with a sphygmomanometer) for 1 min, and then it was deflated and withdrawn. The distention was repeated two times (separated by 30 min) per hour daily for 4 weeks.

b. Water avoidance stress (WAS):

The apparatus consisted of a plastic tank (55 cm length × 35 cm width × 35 cm height) with a block (10 × 8 × 8 cm) affixed to the center of the floor. The tank was filled with fresh room temperature water (25 ± 2)°C to within 1 cm of the top of the block. The rats were placed on the block for the duration of 1 h daily for 4 weeks.

c. Load-bearing swimming:

The apparatus was a plastic bucket (60 cm height, 40 cm diameter). The bucket was filled with fresh room temperature water (25 ± 2)°C with a depth of about 50 cm. The rats were made to swim in the apparatus till they were exhausted, with an iron block of 10% of body weight attached to the tail. The criterion to judge the exhaustion of rats was that their heads did not surface within 7 s after sinking into the water. This process was repeated once every other day for 4 weeks.

d. Administration with Senna leaf:

Senna leaf formula granules dissolved in purified water with a ratio of 1:7, 10 ml/(kg d) were administrated daily for 4 weeks.

2.4.2 Intervention in different groups

The WJP group were administered an aqueous solution of WJP with 0.11 g/ml (WJP formula granules dissolved in purified water), 10 ml/(kg d) (the dosage for the rat = X mg/kg × 70 kg × 0. 018/200 g. X = 12.20 g/70 kg, the dosage for the adult daily). The positive drug group was given an aqueous solution of pinaverium bromide with 2.70 mg/ml (pinaverium bromide tablet dissolved in purified water), 10 ml/(kg d) (the dosage for the rat = X mg/kg × 70 kg × 0. 018/200 g. X = 150 mg/70 kg, the dosage for the adult daily). Meanwhile, the model group was given purified water, 10 ml/(kg d), administered *via* oral gavage daily for 2 weeks. After the assessment of diarrhea and visceral sensitivity at the end of the 7th week, all rats were sacrificed for samples.

2.5 Bristol stool scale score and abdominal withdrawal reflex score

Bristol stool scale was used to measure the symptom of diarrhea. The rats were placed inside a cage mat with filter paper, observed within 4 h (8:00–12:00) of defecation, and the Bristol stool scale scores were recorded according to the Bristol stool scale (Lewis et al.,1997).

Abdominal withdrawal reflex (AWR) was used to measure the visceral sensitivity of rats in each group. The rats were starved for 18 h before the measurement. They were placed on a laboratory table matted with a single-use medical pad sheet. One of the operators, wearing thick gloves, held the rat gently and covered its eyes to restrain it from big movements like turning around. The other operator performed the operation of inserting the balloon. At the beginning of the experiment, it is necessary to

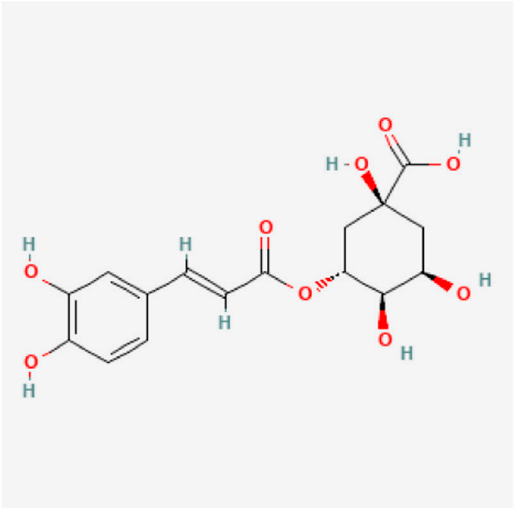

FIGURE 1
Chemical construction of Caffeoyl quinic acid.

touch the anus gently to achieve muscular relaxation. A balloon coated with paraffin oil was inserted 7 cm into the rectum *via* the anus and held in place by taping the tubing to the tail. Then, the rat was placed in a small transparent plastic cubicle (20 cm × 8 cm × 8 cm) (Winston et al.,2007) to restrain it from big movements like turning around. After the rat was completely calm, the balloon was slowly inflated to a pressure of 20, 40, 60, and 80 mmHg incrementally at a duration of 20 s each. AWR was scored as follows (Zhang et al.,2016): 0, no behavioral response to distension; 1, brief head movement followed by immobility; 2, contraction of the abdominal muscle; 3, lifting of the abdomen; or 4, body arching and lifting of the pelvic structure (Figure 3) (Jiajie Zhu,2018). Two blinded investigators conducted the experiments and assessed the scores of the Bristol stool scale and AWR.

2.6 ELISA of the colon tissue

The tissue of the colon was homogenized, mixed with PBS solution (10 ml PBS for 1 g of tissue), and centrifuged at 4,500 rpm for 5 min to obtain the supernatant. The concentrations of TNF-α were measured by ELISA according to the kit instructions.

2.7 Colon histopathology

The colon of rats in each group (3 cm of the colon 5–8 cm distal to the anus) was intercepted, washed with normal saline, and fixed with 10% neutral formalin solution for standby. Paraffin specimens were continuously sectioned at a thickness of 2 μm and stained with hematoxylin–eosin, and the histopathological manifestations of the colon in each group were visualized using Case Viewer 2.1 software.

2.8 Real-time polymerase chain reaction

Total RNA was extracted from tissue samples of the colon and hippocampus using the method of Trizol. The concentration and purity of the sample were determined using a spectrophotometer. The total RNA was then reverse transcribed into cDNA using the EasyScrpt One-Step gDNA Removal and cDNA Synthesis SuperMix kit. PCR primers were designed and synthesized by GENERAL BIOL. The primer sequences are shown in the Table 2. Finally, real-time PCR was performed on target genes, and the data were analyzed using the $2^{-\Delta\Delta Ct}$ method.

2.9 Western blot analysis

The colon and hippocampus tissues were cut into small pieces and mixed with pre-cooled lysis buffer at a ratio of 1:20, respectively. The samples were centrifuged at 10,000 rpm for 5 min to obtain the supernatant. The protein concentration of each sample was determined according to the kit's instructions. 10 μl of the supernatant was separated by 12% SDS-PAGE for 1 h at 150 V. Bands were electrophoretically transferred to 0.22 μm PVDF membranes (Millipore, United States), blocked for nonspecific binding with 5% nonfat dry milk for 1 h, shaken, and washed for 3 min twice. Then, the membranes were incubated with Linked Caprine Anti-Rabbit IgG Polyclonal Antibody and Linked Caprine Anti-Mouse IgG Polyclonal Antibody (Cloud-Clone, China) for 1 h, washed again, and developed with an electrochemiluminescence (ECL) reagent (Yeasen, China). Blots were developed *via* autoradiography. GAPDH (Cloud-Clone, China, 0.03 μg/ml) served as an internal control. Images were analyzed and quantified using ImageJ software. The following primary antibodies were used: MEK1/2 antibody (Affinity Biosciences, United States, 1:1,000), Phospho-MEK1/2 (Ser218 + Ser222/Ser222 + Ser226) antibody (Affinity Biosciences, United States, 1:1,000), p-ERK1/2 Polyclonal antibody (Cell Signaling Technology, United States, 1:1,000), Phospho-ERK1/2 (Thr202/Tyr204) Polyclonal antibody (Cell Signaling Technology, United States, 1:1,000).

2.10 Statistical analysis

Statistical analyses were performed using Graphpad Prism software version 9.2.0. Experiments were repeated at least three times, and results were presented as mean ± standard deviation

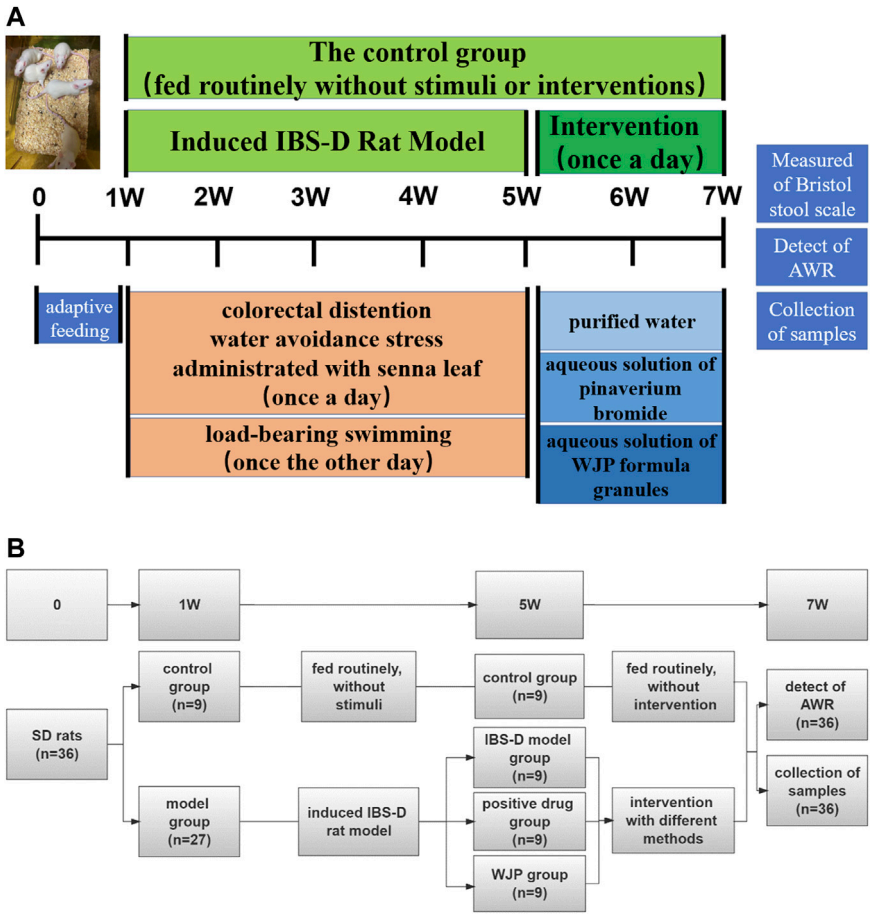

FIGURE 2
Detailed procedures for the experiments and their general conditions. **(A)** Protocol diagram of the time course involved in the experimental procedures of the IBS-D rat model induced and the intervention. **(B)** Specific numbers of animals in each group of the experiment.

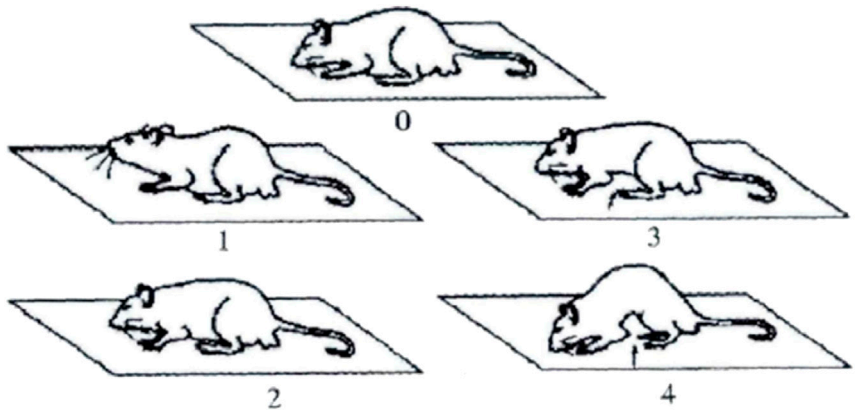

FIGURE 3
AWR diagram.

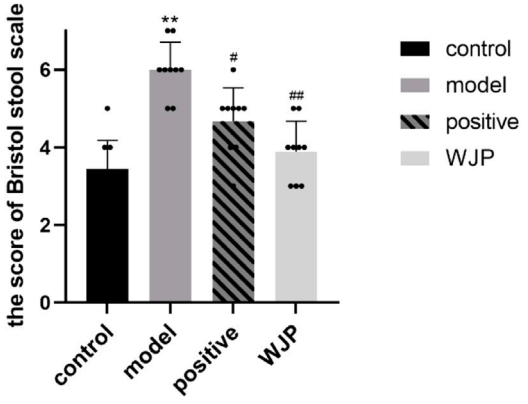

FIGURE 4
Comparison of Bristol stool scale score.

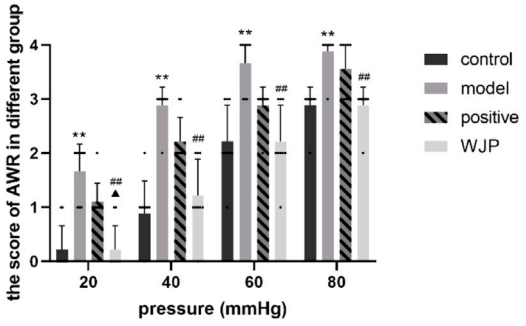

FIGURE 5
Comparison of AWR score. *$p < 0.05$; **$p < 0.01$, versus the control group. $^{\#}p < 0.05$; $^{\#\#}p < 0.01$, versus the model group.

(SD). One-way ANOVA was used to compare the significance of the differences among groups. The Brown–Forsythe and Welch ANOVA tests were applied when the variance was equal among groups, and the Kruskal–Wallis test was performed otherwise. Spearman rank correlation analysis was used to analyze the correlation of data with non-normality and described by correlation coefficient. $p < 0.05$ was considered statistically significant.

3 Results

3.1 WJP ameliorated the symptom of diarrhea of IBS-D rats

Bristol stool scale score was measured to determine whether Wenshen-Jianpi prescription could ameliorate the symptom of diarrhea of IBS-D rats (Figure 4). The Bristol stool scale score of the model group was significantly increased compared with the control group ($p < 0.0001$). It suggested that the IBS-D rats had a variety of fecal patterns, which is consistent with the clinical manifestations of IBS-D patients. Compared with the model group, the Bristol stool scale score of the WJP group was significantly decreased ($p = 0.0001$). These results indicated that Wenshen-Jianpi prescription ameliorated diarrhea in IBS-D models.

3.2 WJP ameliorated visceral hypersensitivity of IBS-D rats

The AWR scores were measured to determine whether Wenshen-Jianpi prescription could ameliorate visceral hypersensitivity of IBS-D rats (Figure 5). Our result showed that the AWR score of the model group increased significantly compared with the control group at each pressure level (20 mmHg, 40 mmHg, 60 mmHg, 80 mmHg) ($p = 0.0003$, $p < 0.0001$, $p = 0.0007$, and $p = 0.0009$). It suggested that the IBS-D rats had visceral hypersensitivity, which is consistent with the clinical manifestations of IBS-D patients. The AWR scores of WJP group were significantly decreased compared with the model group at each pressure level ($p = 0.0003$, $p = 0.0007$, $p = 0.0007$, and $p = 0.0009$). Compared with positive drug group, the AWR scores of WJP group were significantly decreased at the pressure level of 20 mmHg ($p = 0.0403$). These results indicated that Wenshen-Jianpi prescription effectivity ameliorated the visceral hypersensitivity of IBS-D rats and is superior to the positive drug group at the pressure at 20 mmHg. These results indicated that Wenshen-Jianpi prescription ameliorated visceral hypersensitivity in IBS-D models.

3.3 WJP ameliorated the inflammation of IBS-D rats

To determine whether Wenshen-Jianpi prescription could alleviate the inflammation of IBS-D rats, the level of TNF-α in the colon tissues was detected using ELISA, and the colon tissues were stained with HE stain. Compared with the control group, the concentration of TNF-α was significantly increased in the model group ($p < 0.0001$). Compared with the model group, the level of TNF-α in the WJP group was significantly decreased ($p < 0.0001$). Even though there was no significant difference between the positive drug group and the WJP group ($p > 0.05$), the results showed the consistent trend that the level of TNF-α was lower in the WJP group ($p = 0.151$, 0.62 ± 0.072 vs. 0.53 ± 0.086) (Figure 6A).

Immunohistochemistry staining showed that intestinal mucosa and the epithelial cells were intact in the control group without lymphocyte infiltration in the lamina propria.

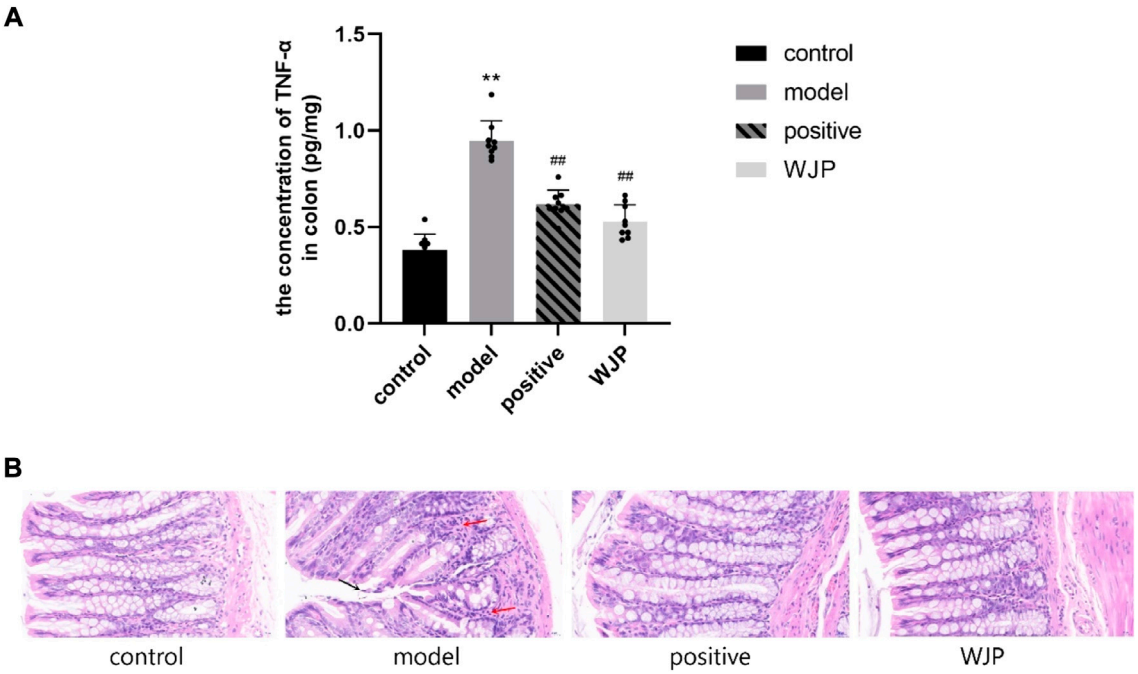

FIGURE 6
Comparison of the concentration of TNF-α in the colon and the histopathological observation of colon tissue. **(A)** Concentration of TNF-α. *p < 0.05; **p < 0.01, versus the control group. $^{\#}p$ < 0.05; $^{\#\#}p$ < 0.01, versus the model group. **(B)** Histological changes in each group observed after HE staining. Magnification ×400. A small amount of epithelial cell shedding can be seen in local mucosa (black arrow). More lymphocyte infiltration can be seen in local lamina propria (red arrow).

However, there was a small amount of epithelial cell shedding in the local mucosa in the model group (Figure 6B, black arrow) and more lymphocyte infiltration in local lamina propria (Figure 6B, red arrow).

3.4 WJP downregulated the expression of pMEK1/2, pERK1, and pERK2 to ameliorate the visceral hypersensitivity of IBS-D rats

The MEK/ERK signaling pathway was also evaluated in the colon tissues. The mRNA levels of MEK1, MEK2, ERK1, and ERK2 in the colon tissues were significantly increased in the model group compared to the control group (p < 0.0001); however, those levels were significantly decreased in the WJP group when compared with the model group (p < 0.0001). There was no significant difference between the positive drug group and the WJP group (p > 0.05) (Figure 7A).

Compared with the control group, the levels of p-MEK1/2 proteins of the colon tissues was significantly increased in the model group (p < 0.0001). Compared with model group, this levels was significantly decreased in the WJP group (p < 0.0001). Compared with the positive drug group, this levels was significantly decreased in the WJP group (p = 0.0390) (Figure 7B).

Compared with the control group, the relative expressions of p-ERK1 and p-ERK2 proteins in the colon tissues were significantly increased in the model group (p < 0.0001); whereas, those expressions were significantly decreased in the WJP group when compared with the model group (p = 0.0019 and p = 0.0013). (Figure 7C). The result of Western blot analysis is shown in Figure 7D.

The MEK/ERK signaling pathway was also evaluated in the hippocampus tissue. The mRNA levels of MEK1, MEK2, ERK1, and ERK2 were significantly increased in the model group compared with the control group (p = 0.0249, p = 0.0018, p = 0.0007, and p < 0.0001). However, the mRNA levels of MEK2, ERK1, and ERK2 were significantly decreased in the WJP group when compared with the model group (p = 0.0215, p = 0.0217, and p = 0.0189). Compared with the positive drug group, the relative mRNA levels of MEK2, ERK1, and ERK2 were significantly increased in the WJP group (p = 0.0198, p = 0.0089, and p < 0.0001) (Figure 8A).

The relative expression of p-MEK1/2 protein was significantly increased in the model group compared with the control group (p < 0.0001); the expression of p-MEK1/2 protein was significantly decreased in the WJP group

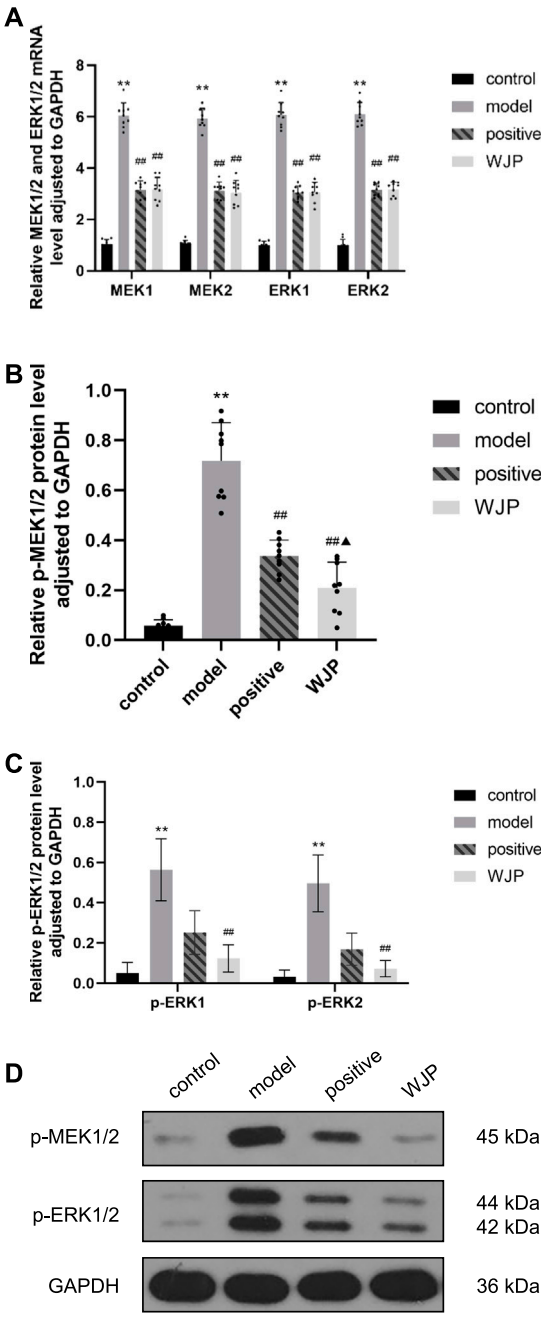

FIGURE 7
Effect of WJP on the relative expression of mRNA of MEK1, MEK2, ERK1, and ERK2 and the relative expression of protein of p-MEK1/2, p-ERK1, and p-ERK2 in the colon in the four groups. **(A)** The relative expression of mRNA of MEK1, MEK2, ERK1, and ERK2. **(B)** The relative expression of protein of p-MEK1/2. **(C)** The relative expression of protein of p-ERK1 and p-ERK2. **(D)** Western blot analysis. $^{*}p < 0.05$; $^{**}p < 0.01$, versus the control group. $^{\#}p < 0.05$; $^{\#\#}p < 0.01$, versus the model group. $^{\blacktriangle}p < 0.05$; $^{\blacktriangle\blacktriangle}p < 0.01$, versus the positive drug group.

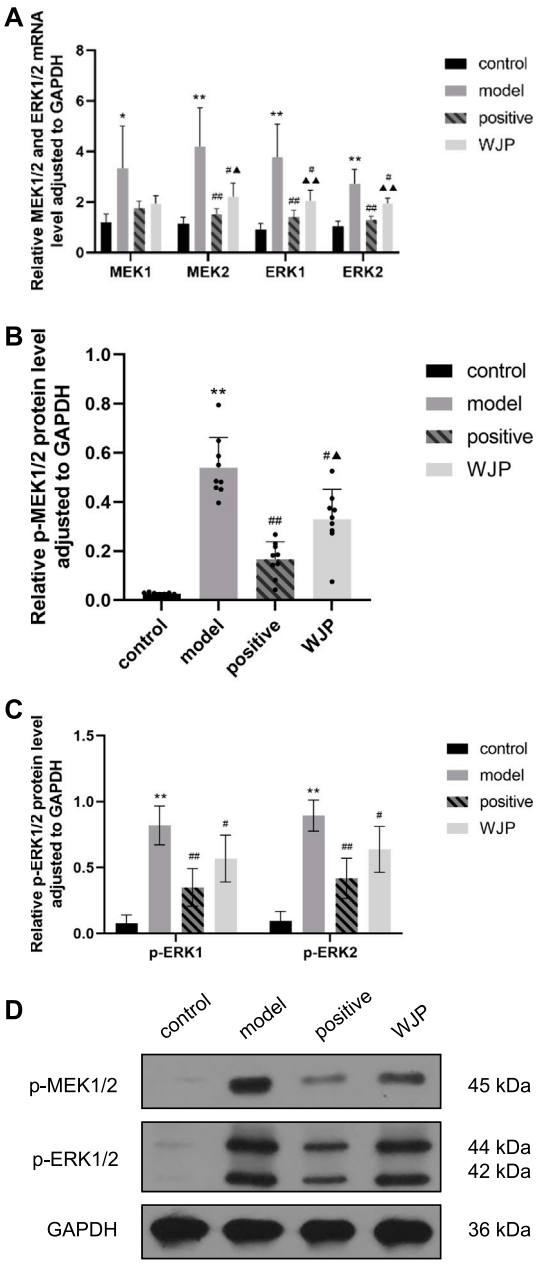

FIGURE 8
Effect of WJP on the relative expression of mRNA of MEK1, MEK2, ERK1, and ERK2 and the relative expression of protein of p-MEK1/2, p-ERK1, and p-ERK2 in the hippocampus in the four groups. **(A)** The relative expression of mRNA of MEK1, MEK2, ERK1, and ERK2. **(B)** The relative expression of protein of p-MEK1/2. **(C)** The relative expression of protein of p-ERK1 and p-ERK2. **(D)** Western blot analysis. $^{*}p < 0.05$; $^{**}p < 0.01$, versus the control group. $^{\#}p < 0.05$; $^{\#\#}p < 0.01$, versus the model group. $^{\blacktriangle}p < 0.05$; $^{\blacktriangle\blacktriangle}p < 0.01$, versus the positive drug group.

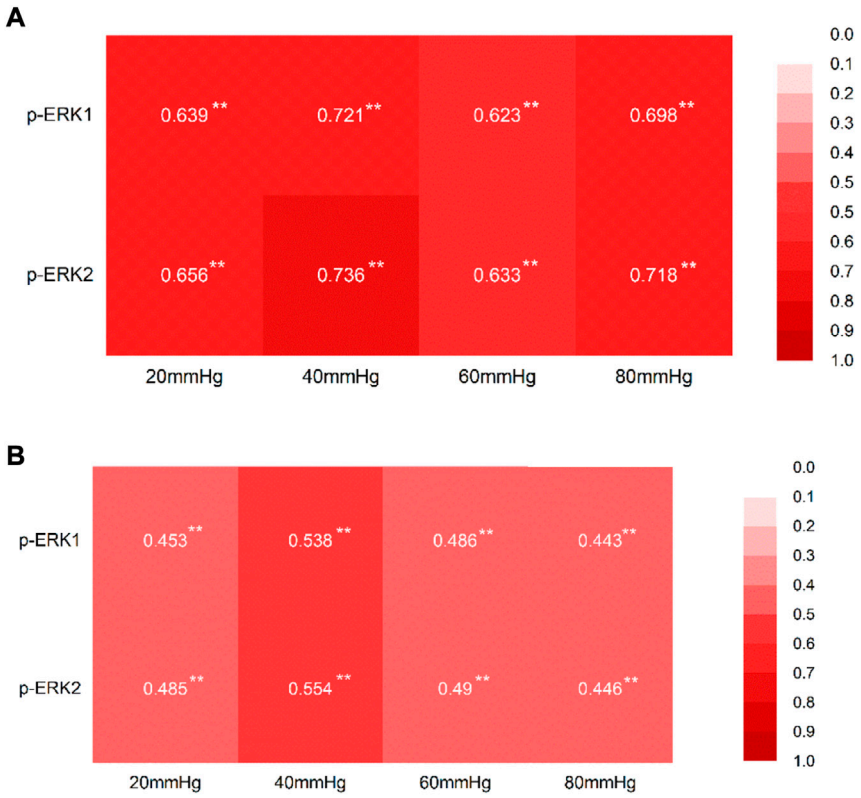

FIGURE 9
Correlation between the AWR score at each pressure level and the expression of p-ERK1/2. **(A)** Correlation between the AWR score at each pressure level and the expression of p-ERK1/2 in the tissue of the colon, with the correlation coefficient. **(B)** Correlation between the AWR score at each pressure level and the expression of p-ERK1/2 in the tissue of the hippocampus, with the correlation coefficient. *$p < 0.05$; **$p < 0.01$.

compared with the model group ($p = 0.0126$). Compared with the positive drug group, the expression of p-MEK1/2 protein was significantly increased in the WJP group ($p = 0.0240$) (Figure 8B). Compared with the control group, the relative expressions of p-ERK1 and p-ERK2 proteins were increased in the model group ($p < 0.0001$). Compared with the model group, the relative expressions of p-ERK1 and p-ERK2 proteins were decreased in the WJP group ($p = 0.0291$ and $p = 0.0145$) (Figure 8C). The result of Western blot analysis is shown in Figure 8D.

3.5 The correlation between the abdominal withdrawal reflex score and the expression of p-p-ERK1/2 in the colon and hippocampus

The AWR scores positively correlated with the expression of p-p-ERK1/2 in both colon tissues and the hippocampus tissues at each pressure level (Figures 9A and B).

4 Discussion

Our study has investigated the Bristol stool scale and AWR scores, inflammatory cytokine, histopathological observation, and the key factors of the MEK/ERK signal pathway among different groups. And Figure 10 is a schematic diagram showed the WJP regulation of the MEK/ERK signal pathway.

The Bristol stool scale was used to measure the symptoms of diarrhea, and AWR was used to evaluate the visceral sensitivity. The findings confirmed that the model rats developed diarrhea and had higher visceral sensitivity at each pressure level compared to the control group, which is consistent with the findings of Zhang et al. (2020). After intervention with the WJP, the Bristol stool scale scores were decreased, and the AWR scores were decreased compared to the model group at each pressure level.

TNF-α is a proinflammatory cytokine, the level of which was increased in IBS patients compared with the healthy controls (Norlin et al.,2021). Our study showed consistent findings that the level of TNF-α is increased in the IBS-D model group. In

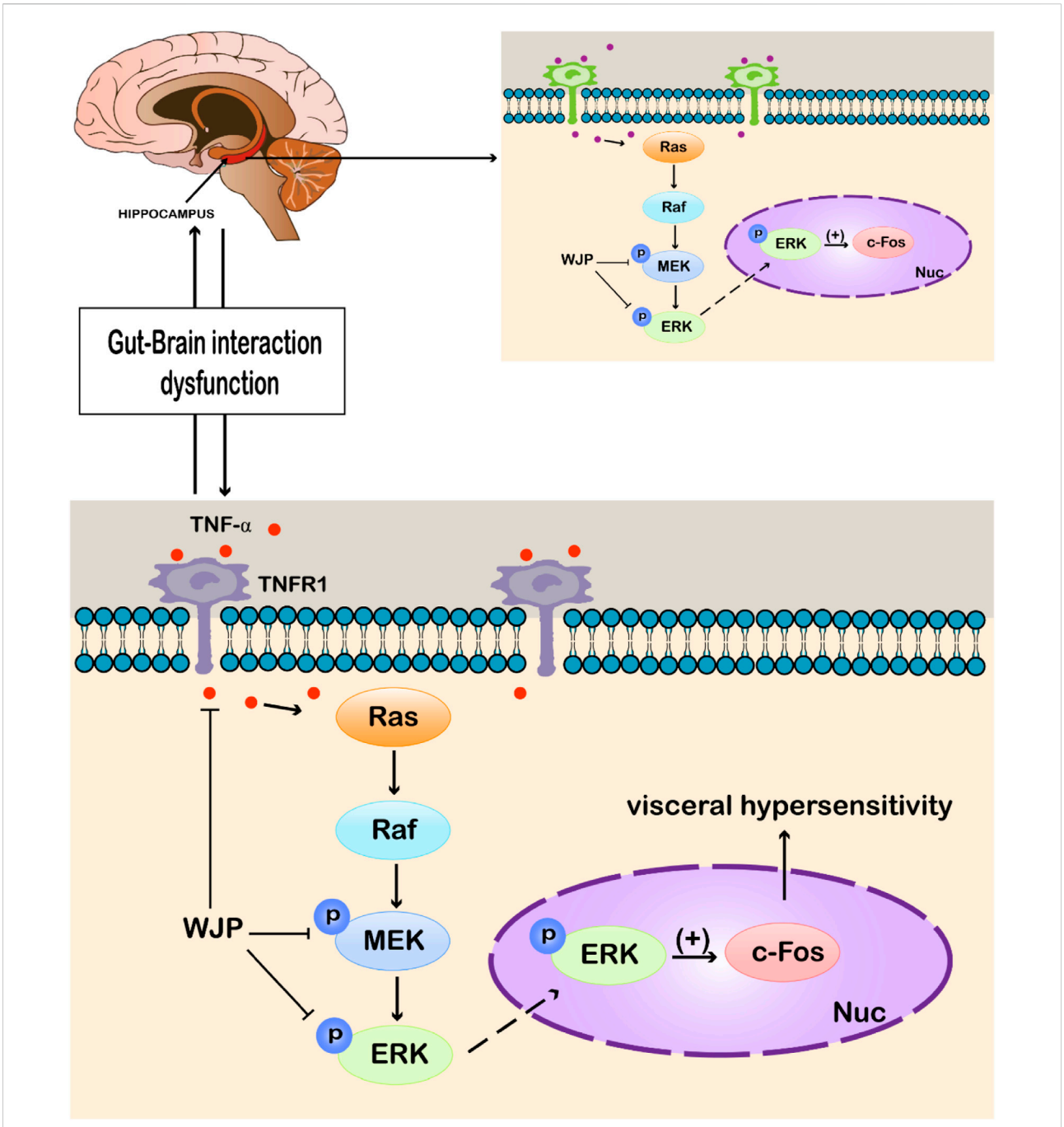

FIGURE 10
WJP regulation of the MEK/ERK signal pathway. Abbreviations: WJP, Wenshen-Jianpi Prescription; TNF-α, tumor necrosis factor-α; TNFR1, tumor necrosis factor receptor-1; MEK, mitogen-activated extracellular signal–regulated kinase; ERK, extracellular regulated protein kinases; p, phosphorylation; Nuc, cell nucleus; (+), activating the expression.

addition, histopathology staining showed that there was more lymphocyte infiltration in local lamina propria in the IBS-D model group compared with the control group.

In their study, Liu et al. (2018) indicated that the expressions of mRNA of MEK1, MEK2, ERK1, and ERK2 were increased in the spinal cord in rats' model of visceral pain. Our study findings confirmed that these parameters were also increased in the colon and hippocampus in the rat model of IBS-D with visceral hypersensitivity compared to the control group. In addition, after the intervention with WJP, the expression of MEK1,

MEK2, ERK1, and ERK2 decreased in the colon, and that of MEK2, ERK1, and ERK2 decreased in the hippocampus.

In their study, Li et al. (2017b) indicated that the expressions of proteins of p-MEK1/2 and p-p-ERK1/2 were increased in the spinal cord in rat's model of visceral pain. Our study findings confirmed that the expressions of proteins of p-MEK1/2, p-ERK1, and p-ERK2 were increased in the colon tissue in the model group compared to the control group. In addition, the expressions of proteins of p-MEK1/2, p-ERK1, and p-ERK2 were also increased in the hippocampus tissue in the model group compared to the control group. The literature research indicated that these proteins are active after phosphorylation (Zhao et al.,2022) and can activate downstream proteins to produce biological effects. Thus, we considered p-MEK1/2, p-ERK1, and p-ERK2 as the key effect parameters and played a significant role in the development of visceral hypersensitivity.

Visceral hypersensitivity has been proposed to be the core pathophysiological mechanism behind IBS (Collaborative group of Gastrointestinal Functional Diseases of Gastroenterology Branch of Chinese Medical Association, 2020), leading to decreased pain threshold and changes in synaptic plasticity (SP) (Greenwood-Van et al., 2017). SP refers to the ability of the nervous system to reconstruct connections in order to adapt to the structural and functional changes in the environment. The changes in synaptic transmission function are mainly regulated by long-term potentiation (LTP) and long-term depression (LTD) (Bennett,2000). LTP strengthens specific synapses, while LTD weakens specific synapses, where LTP is crucial in the formation of visceral sensitization (Ruscheweyh et al.,2011). At the same time, MEK/ERK signaling pathway plays an important role in regulating LTP (Sun et al.,2015). Continuous inflammatory stimulation may activate the MEK/ERK signaling pathway. p-MEK1/2 can activate p-ERK1/2 by phosphorylation. p-ERK1/2 can activate the downstream factors involved in visceral sensitization, such as N-methyl-D-aspartic acid receptor (NMDAR) and c-fos; it also regulates the synaptic plasticity and excitability of cell membrane and amplifies peripheral stimuli (WU Hao-meng et al., 2020). Our previous results are consistent with this conclusion (Shi haixia et al.,2021; Jiang tianyuan et al.,2022). ERK is also the key factor of the mediator of the early-LTP and late-LTP, and the latter period is vital to the maintenance of LTP (Kelly et al.,2007). Visceral hypersensitivity along with the dysfunction of the "brain–gut axis" is thought to be contributing to the IBS-D symptoms (Morreale et al.,2022; Nozu et al.,2022). The "brain–gut axis" is a concept of neuroanatomy. It can be seen as the "connecting line" between the brain and the intestine, transforming the signals, from the emotional center to the cognitive center of the brain, through the neurotransmitters to regulate the function of the surrounding organs, including the intestine (Douglas A. DROSSMAN,2018), and vice versa, which is the biological basis of "gut-brain interaction." Structurally, it is a bidirectional connection between the CNS and visceral smooth muscle and other peripheral organs, which affects the functions of sensation, movement, endocrine, autonomic nerve, immunity, and inflammation. The changes in synaptic plasticity may occur both in the periphery and central. The hippocampus is a key part of memory and cognition, and repeated stress can strengthen the neural connections related to traumatic stimulation in the hippocampus, leading to the persistence of hypersensitivity (Lyubashina et al.,2022b). Therefore, targeting both the colon and hippocampus may be a more effective approach to treat IBS-D and may even alter the natural history of the disease.

In addition, after the intervention with the WJP, the expressions of the proteins of p-MEK1/2, p-ERK1, and p-ERK2 were decreased in the colon and hippocampus compared to the model group. Previous studies suggest that ERK2 may play a more important role in the formation of visceral hypersensitivity (Alter et al.,2010; Xu et al.,2008), whereas in our study, both of the expressions of the p-ERK1 and p-ERK2 were increased in the model group, and decreased after intervention with the decoction of WJP. Thus, further experiments should be performed to research the different functions of p-ERK1 and p-ERK2 and find whether there is a balance between the parameters.

The correlation coefficients, about the AWR score and expression of p-ERK1 and p-ERK2, with a range of 0.44–0.76, indicate that there are correlations between the AWR score and the expression of the p-ERK1and p-ERK2.

There is evidence that p-ERK1/2 is implicated in synaptic plasticity, which is a key mechanism of the formation of visceral hypersensitivity (Zhang et al.,2018). ERK signaling cascade seems essential for neuronal transcription to control long-term memory (Medina et al.,2018), not only in the central never system (CNS) but also in the enteric nervous system (ENS) (Zhang et al.,2018). p-ERK1/2 is implicated in the formation of visceral hypersensitivity. Cold exposure can cause increased visceral pain responses to colorectal distension, accompanied by the activation of the p-ERK1/2 pathway and c-Fos expression in nodose neurons (Chen et al.,2019). Thus, the literature studies were consistent with our findings.

In summary, the MEK/ERK signaling pathway plays an important role in the formation and maintenance of the LTP. Furthermore, it is considered that LTP plays a key role in the formation and maintenance of visceral hypersensitivity. This study may provide another perspective to recognize the mechanism of chronic abdominal pain (one of the main symptoms of IBS-D) and even the recurrence of IBS-D. In addition, Wenshen-Jianpi prescription (WJP), the Chinese herbal medicine, may provide a possible method to promote the normalization of the expression of the MEK/ERK signaling pathway for the treatment of IBS-D. The MEK/ERK signaling pathway has been regulated by WJP both in the region of the colon and hippocampus at the same time. However, the mediators of the interaction between the colon and hippocampus are unclear, which can be explored in further experiments.

5 Conclusion

The Wenshen-Jianpi prescription can downregulate the expression of TNF-α to relieve intestinal inflammation. In addition, it can downregulate the expression of p-MEK1/2, p-ERK1, and p-ERK2 in the colon and hippocampus at the same time to alleviate visceral hypersensitivity in the IBS-D model rats.

Data availability statement

The original contributions presented in the study are included in the article/Supplementary Material; further inquiries can be directed to the corresponding authors.

Ethics statement

The animal study was reviewed and approved by the Chinese Academy of Chinese Medical Sciences Experimental Animal Ethics Committee. Ethics No. D2021-03-16-3.

Author contributions

TJ, RN, and QL contributed equally. TJ and QL performed most of the experiments, and TJ analyzed the data and led the writing of the manuscript draft. QL helped analyze the data. RN conducted the implementation of the experiment and the writing of the manuscript draft. XL, TZ, BW, and JH helped complete animal feeding, behavioral evaluation, and sample collection. JC guided the writing of the manuscript. RN and XS polished the manuscript. YF and GS revised and polished the manuscript. WW monitored the quality of the experiment and the manuscript. All authors read and approved the final manuscript.

Funding

This work was supported by the National Natural Science Foundation of China (Nos. 81904002 and 81774066) and the project of the Chinese Academy of Traditional Chinese Medicine (No. ZZ14-YQ-020).

Conflict of interest

The authors declare that the research was conducted in the absence of any commercial or financial relationships that could be construed as a potential conflict of interest.

Publisher's note

All claims expressed in this article are solely those of the authors and do not necessarily represent those of their affiliated organizations, or those of the publisher, the editors, and the reviewers. Any product that may be evaluated in this article, or claim that may be made by its manufacturer, is not guaranteed or endorsed by the publisher.

Supplementary material

The Supplementary Material for this article can be found online at: https://www.frontiersin.org/articles/10.3389/fphar.2022.955421/full#supplementary-material

References

Al-Chaer, E. D., Kawasaki, M., and Pasricha, P. J. (2000). A new model of chronic visceral hypersensitivity in adult rats induced by colon irritation during postnatal development. *Gastroenterology*. 119(5), 1276–1285. doi: doi:10.1053/gast.2000.19576

Alter, B. J., Zhao, C., Karim, F., Landreth, G. E., and Gereau, R. T. (2010). Genetic targeting of ERK1 suggests a predominant role for ERK2 in murine pain models. *J. Neurosci.* 30(34), 11537-47. doi: doi:10.1523/JNEUROSCI.6103-09.2010

Bennett, M. R. (2000). The concept of long term potentiation of transmission at synapses. *Prog. Neurobiol.* 60(2), 109–137. doi: doi:10.1016/s0301-0082(99)00006-4

Black, C. J., and Ford, A. C. (2020). Global burden of irritable bowel syndrome: Trends, predictions and risk factors. *Nat. Rev. Gastroenterol. Hepatol.* 17(8), 473–486. doi: doi:10.1038/s41575-020-0286-8

Bradesi, S., Schwetz, I., Ennes, H. S., Lamy, C. M., Ohning, G., Fanselow, M., et al. (2005). Repeated exposure to water avoidance stress in rats: A new model for sustained visceral hyperalgesia. *Am. J. Physiol. Gastrointest. Liver Physiol.* 289(1), G42-53. doi: doi:10.1152/ajpgi.00500.2004

Chen, X., Luo, Q., Yan, X., Li, W., and Chen, S. (2019). Vagal transient receptor potential ankyrin 1 mediates stress-exacerbated visceral mechanonociception after antral cold exposure. *J. Neurogastroenterol. Motil.* 25(3), 442–460. doi: doi:10.5056/jnm19014

Coldwell, J. R., Phillis, B. D., Sutherland, K., Howarth, G. S., and Blackshaw, L. A. (2007) Increased responsiveness of rat colonic splanchnic afferents to 5-HT after inflammation and recovery. *J. Physiol.* 579(1):203-579.

Collaborative group of Gastrointestinal Functional Diseases of Gastroenterology Branch of Chinese Medical Association,Gastrointestinal motility Group of Gastroenterology Branch of Chinese Medical Association(2020). Chinese expert consensus of irritable bowel syndrome in 2020. *Chin. J. Dig.*, 40(12): 803–818.

Douglas, A. , 2018, *DROSSMAN. ROME* Ⅳ *functional gastrointestinal disorders-disorders of gut-brain interaction [M]*. Beijing: China Science Publishing &Media Ltd. CSPM.

Ford, A. C., Sperber, A. D., Corsetti, M., and Camilleri, M. (2020). Irritable bowel syndrome. *Lancet.* 396(10263), 1675–1688. doi: doi:10.1016/S0140-6736(20)31548-8

Greenwood-Van Meerveld, M. B., and Johnson, A. C. (2017). Stress-Induced chronic visceral pain of gastrointestinal origin. *Front. Syst. Neurosci.* 11, 86. doi: doi:10.3389/fnsys.2017.00086

Jiang, T, Niu, R, Qian, L, Luo, X, Zhang, T, Yang, Y, et al.(2022) The effect of wenshen-jianpi prescription (WJP) on the changes of visceral sensitivity and expression of C-fos in diarrhea-predominant irritable bowel syndrome rats.*Chin. J. Inf. Traditional Chin. Med.*, 1–7.DOI:doi:10.19879/j.cnki.1005-5304.202202209

Kelly, M. T., Crary, J. F., and Sacktor, T. C. (2007). Regulation of protein kinase Mzeta synthesis by multiple kinases in long-term potentiation. *J. Neurosci.* 27(13), 3439-44. doi: doi:10.1523/JNEUROSCI.5612-06.2007

Labrenz, F., Spisák, T., Ernst, T. M., Gomes, C. A., Quick, H. H., Axmacher, N., et al. (2022). Temporal dynamics of fMRI signal changes during conditioned interoceptive pain-related fear and safety acquisition and extinction. *Behav. Brain Res.* 427, 113868doi:10.1016/j.bbr.2022.113868

Lewis, S. J., and Heaton, K. W. (1997). Stool form scale as a useful guide to intestinal transit time. *Scand. J. Gastroenterol.* 32(9), 920-4. doi: doi:10.3109/00365529709011203

Li, Y. J., Su, X. L., Yang, C. H., Guo, Y. U., Zhu, J. J., Song, Y. L., et al. (2017a). Establishment and evaluation of pi-shen yang deficiency syndrome of diarrhea-predominant irritable bowel syndrome rat model. *Chin. J. Integr. Traditional West. Med.*, 37(08): 950–954.

Li, Z. Y., Huang, Y., Yang, Y. T., Zhang, D., Zhao, Y., Hong, J., et al. (2017b). Moxibustion eases chronic inflammatory visceral pain through regulating MEK, ERK and CREB in rats. *World J. Gastroenterol.* 23(34), 6220–6230. doi: doi:10.3748/wjg.v23.i34.6220

Liu, Y., Liu, W., Wang, X., Wan, Z., Liu, Y., and Leng, Y. (2018). Dexmedetomidine relieves acute inflammatory visceral pain in rats through the ERK pathway, Toll-Like receptor signaling, and TRPV1 channel. *J. Mol. Neurosci.* 66(2), 279–290. doi: doi:10.1007/s12031-018-1172-5

Lyubashina, O. A., Sivachenko, I. B., and Panteleev, S. S. (2022). Supraspinal mechanisms of intestinal hypersensitivity. *Cell. Mol. Neurobiol.* 42(2), 389–417. doi: doi:10.1007/s10571-020-00967-3

Medina, J. H., and Viola, H. (2018). p-ERK1/2: A key cellular component for the formation, retrieval, reconsolidation and persistence of memory. *Front. Mol. Neurosci.* 11, 361. doi: doi:10.3389/fnmol.2018.00361

Morreale, C., Bresesti, I., Bosi, A., Baj, A., Giaroni, C., Agosti, M., et al. (2022). Microbiota and pain: Save your gut feeling. *Cells.* 11, 971(6). doi: doi:10.3390/cells11060971

Norlin, A. K., Walter, S., Icenhour, A., Keita, A. V., Elsenbruch, S., Bednarska, O., et al. (2021). Fatigue in irritable bowel syndrome is associated with plasma levels of TNF-α and mesocorticolimbic connectivity. *Brain Behav. Immun.* 92, 211–222. doi: doi:10.1016/j.bbi.2020.11.035

Nozu, T., and Okumura, T. (2022). Pathophysiological commonality between irritable bowel syndrome and metabolic syndrome: Role of corticotropin-releasing Factor-Toll-like receptor 4-Proinflammatory cytokine signaling. *J. Neurogastroenterol. Motil.* 28(2), 173–184. doi: doi:10.5056/jnm21002

O'Neill, E., and Kolch, W. (2004). Conferring specificity on the ubiquitous Raf/MEK signalling pathway. *Br. J. Cancer*. 90(2), 283-8. doi: doi:10.1038/sj.bjc.6601488

Oka, P., Parr, H., Barberio, B., Black, C. J., Savarino, E. V., and Ford, A. C. (2020). Global prevalence of irritable bowel syndrome according to Rome III or IV criteria: A systematic review and meta-analysis. *Lancet. Gastroenterol. Hepatol.* 5(10), 908–917. doi: doi:10.1016/S2468-1253(20)30217-X

Roskoski, R. J. (2012). MEK1/2 dual-specificity protein kinases: Structure and regulation. *Biochem. Biophys. Res. Commun.* 417(1), 5–10. doi: doi:10.1016/j.bbrc.2011.11.145

Ruscheweyh, R., Wilder-Smith, O., Drdla, R., Liu, X. G., and Sandkühler, J. (2011). Long-term potentiation in spinal nociceptive pathways as a novel target for pain therapy. *Mol. Pain*. 7, 20. doi: doi:10.1186/1744-8069-7-20

Russo, F., Chimienti, G., Riezzo, G., Linsalata, M., D'Attoma, B., Clemente, C., et al. (2018). Adipose Tissue-Derived biomarkers of intestinal barrier functions for the characterization of Diarrhoea-Predominant IBS. *Dis. Markers*. 2018, 1827937doi:10.1155/2018/1827937

Shi, Haixia, Dong, Yongli, Xu, Aili, Yang, Jianqin, Yan, Ningjuan, Yang, Yang, et al. (2021). Effect of kidney warming and spleen strengthening on NMDA receptor and its phosphorylation expression in dorsal root ganglion of diarrhoeal irritable bowel syndrome rats. *World J. Integr. Traditional West. Med.*, 16(12): 2220–2225.

Su, X., Tang, Y., Zhang, J., Dong, Y., Wei, W., Bai, Y., et al. (2013). Curative effect of warming kidney and fortifying spleen recipe on diarrhea-predominant irritable bowel syndrome. *J. Tradit. Chin. Med.* 33(5), 615-9. doi: doi:10.1016/s0254-6272(14)60030-3

Sun, L., Zhou, J., and Sun, C. (2019). MicroRNA-211-5p enhances analgesic effect of dexmedetomidine on inflammatory visceral pain in rats by suppressing ERK signaling. *J. Mol. Neurosci.* 68(1), 19–28. doi: doi:10.1007/s12031-019-01278-z

Sun, Y., Liu, W. Z., Liu, T., Feng, X., Yang, N., and Zhou, H. F. (2015). Signaling pathway of MAPK/ERK in cell proliferation, differentiation, migration, senescence and apoptosis. *J. Recept. Signal Transduct. Res.* 35(6), 600-4. doi: doi:10.3109/10799893.2015.1030412

Winston, J., Shenoy, M., Medley, D., Naniwadekar, A., and Pasricha, P. J. (2007). The vanilloid receptor initiates and maintains colonic hypersensitivity induced by neonatal colon irritation in rats. *Gastroenterology*. 132(2):615-27. doi: doi:10.1053/j.gastro.2006.11.014

Wortzel, I., and Seger, R. (2011). The ERK cascade: Distinct functions within various subcellular organelles. *Genes Cancer*. 2(3), 195–209. doi: doi:10.1177/1947601911407328

Wu, H, Xu-dong, T. A. N. G., Wang, Feng-yun, and Huang, Shaogang. (2020). Mechanism of autophagy on the formation of visceral hypersensitivity in diarrhea-predominant irritable bowel syndrome. *China J. Traditional Chin. Med. Pharm.*, 35(12):6261–6264.

Xu, Q., Garraway, S. M., Weyerbacher, A. R., Shin, S. J., and Inturrisi, C. E. (2008). Activation of the neuronal extracellular signal-regulated kinase 2 in the spinal cord dorsal horn is required for complete Freund's adjuvant-induced pain hypersensitivity. *J. Neurosci.* 28(52), 14087-96. doi: doi:10.1523/JNEUROSCI.2406-08.2008

Zhang, G., Yu, L., Chen, Z. Y., Zhu, J. S., Hua, R., Qin, X., et al. (2016). Activation of corticotropin-releasing factor neurons and microglia in paraventricular nucleus precipitates visceral hypersensitivity induced by colorectal distension in rats. *Brain Behav. Immun.* 55, 93–104. doi: doi:10.1016/j.bbi.2015.12.022

Zhang, L., Song, J., Bai, T., Wang, R., and Hou, X. (2018). Sustained pain hypersensitivity in the stressed colon: Role of mast cell-derived nerve growth factor-mediated enteric synaptic plasticity. *Neurogastroenterol. Motil.* 30(9), e13430doi:10.1111/nmo.13430

Zhang, Y., Zhang, H., Zhang, W., Zhang, Y., Wang, W., and Nie, L. (2020). LncRNA XIST modulates 5-hydroxytrytophan-induced visceral hypersensitivity by epigenetic silencing of the SERT gene in mice with diarrhea-predominant IBS. *Cell. Signal.* 73, 109674doi:10.1016/j.cellsig.2020.109674

Zhao, J., and Luo, Z. (2022). Discovery of raf family is a milestone in deciphering the Ras-Mediated intracellular signaling pathway. *Int. J. Mol. Sci.* 23, 5158(9). doi: doi:10.3390/ijms23095158

Zhu, J. (2018). *Study of Establishment of IBS-D rat model of spleen-kidney-Yang deficiency and the therapeutic mechanism of Wenshen-Jianpi Prescription[D]*. Beijing, china: Beijing University of Chinese Medicine.

Advantages of publishing in Frontiers

OPEN ACCESS
Articles are free to read for greatest visibility and readership

FAST PUBLICATION
Around 90 days from submission to decision

HIGH QUALITY PEER-REVIEW
Rigorous, collaborative, and constructive peer-review

TRANSPARENT PEER-REVIEW
Editors and reviewers acknowledged by name on published articles

Frontiers
Avenue du Tribunal-Fédéral 34
1005 Lausanne | Switzerland

Visit us: www.frontiersin.org
Contact us: frontiersin.org/about/contact

REPRODUCIBILITY OF RESEARCH
Support open data and methods to enhance research reproducibility

DIGITAL PUBLISHING
Articles designed for optimal readership across devices

FOLLOW US
@frontiersin

IMPACT METRICS
Advanced article metrics track visibility across digital media

EXTENSIVE PROMOTION
Marketing and promotion of impactful research

LOOP RESEARCH NETWORK
Our network increases your article's readership